NIMA ZAERPOUR

Efficient Management of Compact Storage Systems

EFFICIENT MANAGEMENT OF COMPACT STORAGE SYSTEMS

Efficient Management of Compact Storage Systems

Het efficiënt managen van compact opslag systemen

Thesis

to obtain the degree of Doctor from the
Erasmus University Rotterdam
by command of the
rector magnificus

Prof.dr. H.G. Schmidt

and in accordance with the decision of the Doctorate Board.

The public defense shall be held on
Friday 22 February 2013 at 11:30 hours

by

Nima Zaerpour
born in Gorgan, Iran

ERASMUS UNIVERSITEIT ROTTERDAM

Doctoral Committee

Promoter: Prof.dr. M.B.M. de Koster

Other members: Prof.dr. J.J. Bartholdi III

Prof.dr. L.G. Kroon

Prof.dr. K.J. Roodbergen

Co-promoter: Dr. Yugang Yu

Acknowledgements

This dissertation would not have been possible without the guidance and the help of several individuals who in one way or another contributed and extended their valuable assistance in the preparation and completion of this study.

First and foremost, I owe sincere and earnest thanks to my promoter René de Koster whose presence and encouragement I will never forget. He has given me guidance and advice on a personal and professional level that has been instrumental in my growth as a student preparing to be an academician. René has been my inspiration as I hurdle all the obstacles in the completion this dissertation. Besides I am sincerely and heartily grateful to my daily supervisor, Yugang Yu, for the support and guidance he showed me throughout my Ph.D. Yugang always provided me with different points of view and my weekly discussions with him were always fun and sincere on Friday afternoons.

I am also truly thankful to John Bartholdi who hosted me at Industrial and System Engineering School at Georgia Tech in 2012. The result of my collaboration with John is a work in progress on order picking in mobile-robotic order fulfillment systems. This research visit has been an invaluable experience for me. It is a special honor to me that he agreed to be part of my doctoral committee. Similarly, I would like to thank the other members of the inner committee, Leo Kroon, and Kees Jan Roodbergen. I am grateful for all the time and effort both Leo and Kees Jan put into this work and for their comments and feedback on the earlier version of this dissertation. I also would like to extend my thanks to other members of doctoral committee, Kai Furmans from Karlsruhe Institute of Technology, Liang Liang from University of Science and Technology of China, Albert Wagelmans, and Rob Zuidwijk who kindly agreed to be a part of defense committee and gave valuable feedbacks.

I would like to show my gratitude to ERIM's office staff, including Marisa van Iperen, Miho Iizuka, and Tineke van der Vhee. I am obliged to many of my current or former colleagues in the Department of Management of Technology and Innovation. I thank Carmen Meesters-Mirasol, who has always been helpful and made my visits to her office enjoyable. Special thanks go to Amir Hossein and Sandra for accepting to be my paranimfen. I would also like to thank José for always being open to any research related discussion, Jordan, Melek, Jelmer, Yeming, Irma, Basak, Dirk, Lameez, Mashiho, Oguz, Stefanie, Merlijn, Murat and many others of the department and ERIM community. I would like to extend my thanks to Morteza and Sepideh for helping me to settle especially in my first days in Rotterdam and Javad for his helps in Atlanta.

Finally, I am extremely thankful and indebted to my family. My brothers, Masoud and Farzad, who were always supporting me and encouraging me with their best wishes. The greatest words of thanks are owed to my lovely wife, voice of reason, counselor, and life raft, Sholeh. She was always there cheering me up and stood by me through the good times and bad. Last but not least, for the inspiration behind my years of academic pursuit, I am exceedingly grateful to my parents, Ahmad and Safoura. They have always supported, encouraged, and believed in me, and who so lovingly and unselfishly cared for me.

Nima Zaerpour
Novemebr 28 2012, Rotterdam

Contents

Chapter 1

Introduction

1.1. Recent trends in warehousing

Warehouses are important nodes in supply chains. They decouple supply from demand in time, assortment, quantity, and space. By doing so, economies of scale can be achieved in transport, as warehouses allow to regroup transport flows leading to lower cost. They also allow postponement of value addition, increasing service levels at lower inventory levels. This is why all physical supply chains contain warehouses at multiple points, either insourced or outsourced: at suppliers, manufacturers, wholesalers, retailers and stores.

Warehouses are particularly needed in densely populated areas, close to where demand is generated and where the labor is available. Modern warehouses require large space to realize economies of scale: road (sometimes rail and water) infrastructure around and at the facility, space for parking trucks and trailers, space for docking trucks, and space within the facility itself. Warehouse buildings are often quite large, more than 10,000 m^2 built space is common (De Koster and Balk, 2008). Unfortunately, in many of the urbanized areas, space for such large facilities has become short. In such facilities, order picking - the process of collecting items in specified quantities in a warehouse or distribution center (DC) in response to a customer order - is one of the most critical activities (De Koster et al., 2007). It has been identified as

a labor-intensive process in manual systems (Goetschalckx and Ashayeri, 1989; Drury, 1988; De Koster et al., 2007; Tompkins et al., 2010). The cost of order picking in a typical warehouse is estimated to be as much as 55% of the total warehouse operating expense (Tompkins et al., 2010). In addition, according to Bureau of Labor Statistics, by 2014, the number of workers over 55 will grow to 20% of the labor force, up from the 15% in 2004 (BLS 2004 report).

There is an emerging consensus that traditional storage systems do not address these issues. Therefore, enterprises are moving toward a next generation storage systems, namely "3D compact storage systems". These systems are designed in order to save labor costs and floor space, increase the reliability of the order picking process, reduce error rates, and shorten the response times. Moreover, while the costs of labor and building are lower, these systems require high investment in automation. This thesis focuses on these new types of storage systems and this chapter presents an overview of different types and their potential applications.

1.2. 3D compact storage systems

Traditional automated storage/retrieval systems (known as 2-dimensional, or 2D, AS/RSs) have been widely used in distribution and production environments since their introduction in the 1950s. An AS/R system is capable of automatically handling unit loads (e.g. pallets, totes). Automated storage/retrieval systems contain aisles, storage racks, storage/retrieval (S/R) machines, and I/O-points as their main components (Roodbergen and Vis, 2009). S/R machines can autonomously move in *x*- and *y*- directions, pick up, and drop off unit loads. They operate in aisles between the racks. Every machine has one or more input/output points (I/O point or depot) to drop off retrieved unit loads or to pick up incoming unit loads for storage. In such systems, unit loads are usually stored in single-deep racks (i.e. with a depth of only one unit load). In a traditional AS/R system, the aisles between the racks occupy a significant percentage of the floor space (Yu and De Koster, 2009a).

Shortage of land for warehouses has driven companies to come up with 3D compact storage systems for unit-loads (e.g. pallets, totes, containers), saving much footprint and reducing the building size. A smaller storage system leads to lower investment and operational costs (Gue and Kim, 2007). Compact storage systems have become increasingly popular for storing products (Hu et al., 2005). In compact storage systems, unit loads are stored multiple-deep, requiring less space than 2D systems. Figure 1.1

illustrates that 3D compact systems require less footprint compared to 2D traditional systems. In sum, compared with the 2D system (an AS/R system), 3D compact systems have two main advantages:

- The load throughput time is often short due to prepositioning of the unit-loads, the compactness, and full automation of the system. Some 3D systems have multiple depth movement mechanisms (DMM) which can operate independently and simultaneously for prepositioning open locations (i.e., empty storage locations) and retrieval loads while the horizontal and vertical movement mechanisms (an S/R machine or conveyors and lifts) work on other jobs. Moreover, compared with a 2D system, unit-loads are closer to the depot on average, which also contributes to the reduction of the travel time.

- Much warehouse space can be saved because most aisles are eliminated by storing unit-loads multi-deep. Depending on the configuration, in a compact storage system about 40-50% less footprint is required compared to traditional storage systems to accommodate the same number of unit loads (Hyundai Elevator, 2011).

(a) 2D storage system   (b) 3D storage system
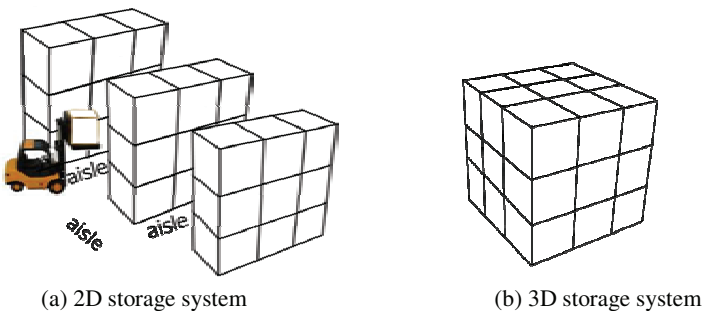
Figure 1.1. Comparison of 2D and 3D storage systems

Several types of 3D compact storage systems exist with different handling systems (like S/R machine, conveyors, shuttles, or elevators) taking care of the horizontal, vertical and depth movements. In the simplest multi-deep compact storage system, a conveyor system takes care of the depth movement of unit loads. There are at least two conveyor variants: gravity and powered conveyors. Another possible variation of the basic compact storage system is when a satellite machine (shuttle) handles the depth movement. The satellite is attached to the S/R machine and can move in the depth dimension to store or retrieve loads stored multi-deep. The S/R machine waits in front of the deep lane while the satellite

machine stores or retrieves a pallet. Typically, S/R machines can move in horizontal and vertical directions simultaneously. Autonomous vehicle storage and retrieval systems (AVS/RS) represent a relatively new technology for automated unit load storage systems. Within the storage rack, the key distinction of AVS/R systems is the movement patterns of the handling system (Fukunari and Malmborg, 2007). In an AVS/R system, vehicles share a fixed number of lifts for vertical movement and follow rectilinear flow paths in two dimensions for horizontal movement. The last group of compact storage systems studied in this thesis are live-cube storage systems. In such systems, each load is stored on an autonomous shuttle, which can move in x- and y- directions at each level. Lift(s) take care of the movements across levels. Table 1.1 gives an overview of different compact storage system types.

Table 1.1. Overview of different types of compact storage system

Type	x- direction transport system	y- direction transport system	z- direction transport system	Travel time function for retrieval from location (X,Y,Z)	Reference
Conveyor-based system	S/R machine	S/R machine	Power or gravity conveyor	$max\{max\{X,Y\},Z\}+max\{X,Y\}$	Yu and De Koster, 2009b; De Koster et al., 2008
Satellite-based system	S/R machine	S/R machine	Satellite	$2(max\{X,Y\}+Z)$	Chapter 3
Live-cube system	Shuttle	Lift	Shuttle	$max\{X+Y,Z\}+Z$ (if multiple empty locations are available per level)	Chapters 4, 5, 6
AVS/R system	Autonomous vehicle	Lift	Autonomous vehicle	Dependent on the location of vehicles	Malmborg, 2002; Kuo et al., 2007

Below, we discuss the compact storage system types which are studied in this thesis in more detail.

1.2.1. Satellite-based compact storage systems

The most common type of compact storage system, is a multi-deep satellite-based compact storage system. This system consists of a compact storage rack, an S/R machine with an attached satellite, and an I/O point (or depot). The S/R machine moves in both vertical and horizontal directions simultaneously. The satellite attached to the S/R machine can move inside the lane to store or retrieve unit loads multi-deep while the S/R machine waits in front of the lane. All storage and retrieval movements start with the S/R machine at the I/O point (located at the lower left-hand corner of the rack). Unit loads retrieved are

dropped off by the S/R machine at the I/O point on an outgoing conveyor for further transport. The main difficulty with these systems is that the unit loads need to be reshuffled if multiple products are stored per lane. This is the process of removing unit loads stored in front of a unit load that needs retrieval. Figure 1.2 illustrates such a satellite-based compact storage system.

Satellite-based compact storage systems are particularly used for refrigerated storage, as cooling cost is directly related to storage space. A larger conditioned storage space yields higher cooling cost. As a result, these systems are widely used in fresh produce distribution systems. In addition, the fully automated process facilitates storage and retrieval avoiding quality loss of the products.
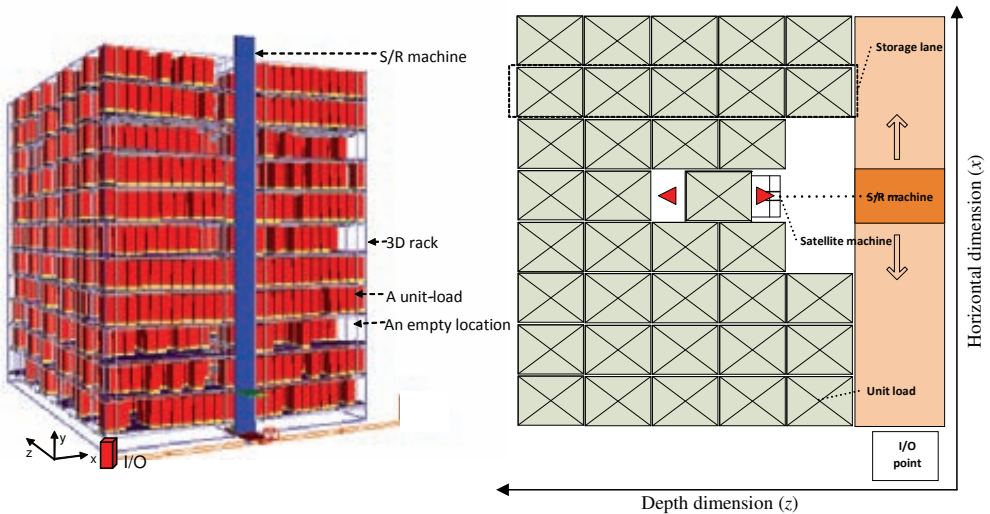
Figure 1.2. 3D view (left) and top view (right) of a satellite-based compact storage system

1.2.2. Live-cube compact storage systems

Live-cube compact storage systems have recently been introduced. They can achieve a very high storage density paired with short response times. Live-cube compact storage systems contain multiple levels of storage grids, shuttles, a lift, and a depot, or an Input/Output (I/O) point. At each level, all unit loads are stored on shuttles which can move in x- and y- directions (as long as there is an empty space). A lift takes

care of movements across different levels in the *z*- direction (see Figure 1.3). We assume the I/O point is located at the lower left corner of the system. When idle, the lift waits at the I/O point.

Compared to other types of compact storage systems, a live-cube system has a major advantage which is the independency of movements in 3-dimensional space. The lift moves independent of the shuttles. Shuttles at different levels move independently. Multiple shuttles on a level may even move simultaneously in a coordinated fashion as long as an empty space is present. In this respect, moving a given load on a shuttle to a certain position is comparable to solving a Sam Loyd's 15-puzzle game. This makes the system flexible yielding a short response time to retrieve requests. In addition, a very high storage density can be achieved as virtually no aisle is required.

   Live-cube systems have found several applications, although several are in the pilot phase, like in parking systems (e.g. "Park, Swipe, Leave" parking systems (Automotion Parking Systems, 2011), "Space Parking Optimization Technology" or SPOT (Eweco, 2011), "Hyundai Integrated Parking" or HIP Systems (Hyundai Elevator, 2011), "Wohr Parksafe" (Wohr, 2011)). They are also applied in warehouses and cross-dock systems (e.g. "Magic Black Box" (ODTH, 2011)), container yards (e.g. "Ultra-high Container Warehouse" or UCW systems (EZ-Indus, 2011)), and healthcare management (e.g. "pharmacy storage and retrieval systems" (Swisslog, 2011)).
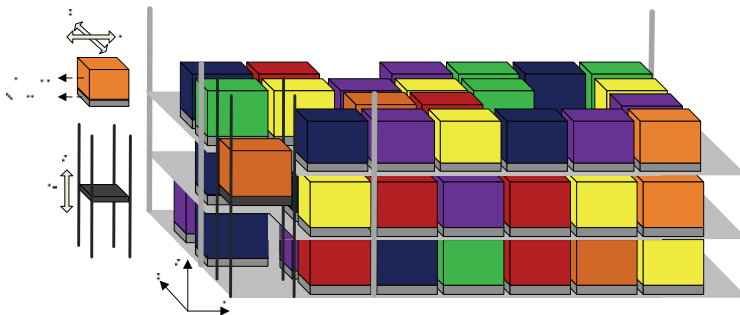
Figure 1.3. A live-cube compact storage system

1.3. Contribution and outline of the dissertation

Storage and retrieval are main activities in a warehouse. Automated storage and retrieval systems are widely used in warehouses to enhance response to customer orders. Increased shortage of land and space has led companies to come up with new 3D compact automated storage and retrieval systems. A large number of papers focuses on performance evaluation of 2D AS/R systems whereas few studies analyze

the performance of 3D compact systems. In this thesis, we analyze these systems at two levels. At the tactical (design) decision level, we focus on the rack-dimensioning problem to reduce the response time of the system. At the operational decision level, we investigate storage assignment and retrieval sequencing problems to shorten the response time. We summarize each chapter as follows.

Chapter 2. Storage Policies and Optimal Shape of a Storage System

Three main decisions can significantly influence the response time of a storage system: the storage system shape (configuration), the storage assignment policy, and the location of the Input/Output points. In chapter 2, we show that the optimal shape of a storage system, which minimizes the response time, is independent of the storage policy being used and the location of an Input/Output point. Decoupling the decisions on the shape of the storage system and the storage policy helps the warehouse managers to design a storage system. When little information of customer demand is available, a storage system can be designed for optimality under a random storage policy. Such a system optimally accommodates other time-saving storage policies such as class-based or full-turnover-based storage without requiring configuration correction. This chapter is based on Zaerpour et al., 2012c.

Chapter 3. Storing Fresh Produce for Fast Retrieval in an Automated Compact Cross-dock System

In chapter 3, we study temporary storage of fresh produce in a cross-dock center. This study is inspired by a major fresh produce distributor in the Netherlands. In order to minimize cooling cost, compact, satellite-based storage systems are used. A disadvantage of these systems is that additional retrieval time is needed, caused by necessary reshuffles due to the improper storage sequence of unit loads. In practice therefore, a dedicated storage policy is used in which every storage lane in the system accommodates only one product. However, this policy requires much space and results in long retrieval times compared to shared storage. In this chapter, we propose a shared storage strategy which considers the planned arrival time information of the outbound trucks to avoid reshuffling. This chapter proposes a mathematical model for a shared storage policy that minimizes the total retrieval time. The policy allows different products to share the same lane. In order to solve real-sized problems, an effective and efficient heuristic is proposed, based on a greedy construction and an improvement part, which provides near optimal solutions, and which is generally robust against disturbances in arrival or departure times. The gaps between the results of the heuristic and the lower bound are often zero and mostly less than 1%. Our results, tested for a

major distributor of fresh produce, show that compared to the dedicated storage policy, the shared storage policy can reduce retrieval time by an average of 16%. This chapter is based on Zaerpour et al., 2010.

Chapter 4. Optimal Configuration of a Live-cube Compact Storage System

Chapter 4 studies live-cube compact storage systems storing and handling unit loads. We assume multiple empty locations are available on each level. The shuttles can then cooperate to create a virtual aisle for fast retrieval of a desired unit load. First, we derive closed-form formulas for the expected retrieval time of an arbitrary unit load for a live-cube system under random storage. Although the system needs to be decomposed in several cases and sub-cases, eventually four simple closed-form expressions are obtained corresponding to four complementary configurations. Second, we propose and solve a mixed-integer nonlinear model to optimize system dimensions by minimizing the retrieval time. Even though the procedure of finding the optimal configuration of a live-cube storage system is relatively complex, we can derive closed-form expressions which are simple to apply in practice. This chapter is based on Zaerpour et al., 2011.

Chapter 5. Response Time Analysis of a Live-Cube Compact Storage System with Two Storage Classes

Chapter 5 extends the previous chapter by considering a two-class-based storage policy in a live-cube compact storage system. We derive closed-form formulas for the expected retrieval time. Although the system needs to be decomposed into several cases and sub-cases, we eventually obtain simple to use closed-form formulas to evaluate the performance of such systems with any configuration and first zone boundary. The resulting closed-form formulas, which are obtained under the assumption of continuous space, are shown to be very precise for a discrete system through a Monte Carlo simulation. Compared to a simulation approach, closed-form formulas can instantly evaluate the performance of a live-cube system with any given configuration and first zone boundary. The closed-form formulas can be used as a reference for further research on live-cube systems such as optimizing system configurations and first zone boundaries. This chapter is based on Zaerpour et al., 2012a.

Chapter 6. Optimal Two-Class-Based Storage in a Live-Cube Compact Storage System

Chapter 6 also studies live-cube compact storage systems with two storage classes. An optimal class-based storage policy where high turnover products are stored at locations closer to the Input/Output point

reduces the response time significantly. This chapter uses the closed-form formulas obtained in the previous chapter to optimize the system configuration and zone boundary leading to minimum response time. We propose a mixed-integer nonlinear model. The model consists of 36 sub-cases each representing a specific configuration and zone boundary yielding a complex mathematical model. Some properties of the optimal solution are used to simplify the model without losing optimality. The overall optimal solutions are then obtained by solving the remaining sub-cases. Although the solution procedure is tedious, we eventually obtain two sets of closed-form expressions for the optimal solutions of the model. The results show that up to 50% reduction in the response time may be gained by using an optimal two-class storage policy compared to a random storage policy. This chapter is based on Zaerpour et al., 2012b.

Chapter 7. Summary and Conclusion

Chapter 7 summarizes the results of previous chapters and provides potential future research questions. In addition, this chapter looks at factors affecting the performance of compact storage systems at operational and design decision levels and investigates methodological challenges in analyzing such systems. Chapter 7 also discusses the potential impacts of automation in material handling systems on different aspects of society such as aging and shortage of labor force, energy and sustainability, etc.

Chapter 2

Storage Policies and Optimal Shape of a Storage System

2.1. Introduction

Warehouse and distribution centers play an important role in the supply chain. Minimizing the response time is a key objective, as response time determines responsiveness and system throughput capacity. In a warehouse, four main design decisions influence the response time of a unit load automated storage system (Roodbergen and Vis, 2009):

- storage system dimensions,
- storage assignment policy,
- retrieval policy, and
- location of Input/Output (I/O) point.

Several methods exist for assigning products to storage locations in a unit load storage system. Commonly used storage assignment policies in practice include:

- random storage assignment,
- class-based storage assignment, and

- full-turnover storage assignment.

For a random storage policy, every empty storage location has an equal chance of accommodating an incoming unit load. However, by assigning more popular unit loads to the locations closer to the I/O point, the response time of the system can be reduced. In a full-turnover storage policy, the storage location of a unit load is based on its demand frequency. The unit loads are individually ranked based on decreasing demand frequencies and assigned to the storage locations which are arranged according to travel distance to the I/O point in an ascending order. Fast-moving unit loads are stored closer to the I/O point and slow-moving unit loads are located farther away from the I/O point. In a full-turnover storage policy, however, any change to the demand frequencies or addition to the product assortments leads to repositioning of all the unit loads. As an alternative, class-based storage can be used where the storage locations and the unit loads are partitioned into C ($C \geq 2$) classes according to travel distances of the locations and turnover frequencies, respectively. The unit loads of the highest turnover frequency class are then assigned to the storage locations of the class closest to the I/O point. Within each class, unit loads are assigned randomly to storage locations. Class-based storage can simply be implemented in practice with a performance comparable to a full-turnover-based storage policy. For class-based storage, the decisions are the number of classes, and the size of each storage class or zone. In practice, a two or three-class-based storage policy is commonly used due to the low complexity, while a significant reduction in travel time (in fact close to optimal, see Yu and De Koster, 2012) can yet be achieved.

Jointly optimizing the system dimensions and storage class sizes of a storage system is closely related to the storage policy being used. As an example, for a system shaped as a rectangular cuboid and under the random storage policy, the decision variables are the dimensions of the storage system while for a C-class-based storage policy ($C \geq 2$) in addition to the dimensions, the boundaries of these C classes (at least C-1 variables) are also decision variables.

Hausman et al. (1976) appear to be the first who study storage policies in a two-dimensional (2D) automated storage and retrieval (AS/R) system. They derive travel time formulas for random and two-class-based storage policies and obtain the optimal zone boundaries for two-class and three-class-based storage policies, numerically. Since then, many researchers have studied the optimization of 2D storage systems under different storage policies (e.g. Rosenblatt and Eynan, 1989; Eynan and Rosenblatt, 1994; Kouvelis and Papanicolaou, 1995; Van den Berg, 1996; Thonemann and Brandeau, 1998; Ashayeri et al., 2002; Park, 2006). Roodbergen and Vis (2009) review different methods that have been used to obtain the optimal zone boundaries in a class-based storage policy. Hausman et al. (1976) use a grid search method

to minimize the one-way travel time in a Square-In-Time (SIT) AS/R system. Rosenblatt and Eynan (1989) propose a recursive procedure to determine the optimal boundaries for any desired number of zones in an AS/R system. Eynan and Rosenblatt (1994) develop a one-dimensional search procedure to establish zones of a *C*-class-based storage policy in a Non-Square-In-Time (NSIT) AS/R system. Kouvelis and Papanicolaou (1995) propose a closed-form formula for optimal zone boundary of a two-class-based NSIT AS/R system. Van den Berg (1996) proposes a dynamic programming to obtain optimal zone boundary for a NSIT AS/R system. Thonemann and Brandeau (1998) extend the work of Hausman et al. (1976) by considering stochastic demands. Ashayeri et al. (2002) develop an analytical model to compute the expected travel time of SIT and NSIT class-based AS/R system with different zone layouts. Park (2006) determines the mean and variance of a NSIT AS/R system and numerically obtains the travel time of selected shape factors and skewness parameters. Yu and De Koster (2012) show that the small number of storage classes is (nearly) optimal.

These papers only address the optimization of storage class boundaries and compare the percentage of improvement with an optimal random storage policy as a benchmark. In a traditional 2D AS/R system, the S/R machine is capable of moving in *x*- and *y*- directions simultaneously (Chebyshev distance metric). Since the movements in x- and y- directions are symmetric, it is trivial that the optimal dimensions of the system will be SIT. Therefore, optimizing the system dimensions of an AS/R system has not been a concern for researchers.

Three-dimensional (3D), or compact, storage systems with different internal movement systems have recently been introduced aiming at higher storage density and shorter response times. These systems are becoming increasingly popular due to full-automation, high storage density and short response times. In such systems, different components of the system can move in three-dimensional space. Different types of 3D compact storage systems with different internal movement systems already exist in practice while several system types with new movement systems are being introduced.

De Koster et al. (2008) study a 3D compact storage system where a conveyor takes care of the depth movement. They optimize the dimensions of such a storage system under random storage leading to minimum response times. Yu and De Koster (2009b) study a similar 3D compact storage system with a two-class-based storage policy. They optimize the system configuration together with the first class boundary leading to minimum response time. For two-class-based storage, the derivation of the travel time formula is more complex than that of random storage. Considering the ABC curve and including the first class boundaries in addition to system dimensions results in a more complex objective function (i.e.

travel time formula) and a larger number of constraints and variables. However, model optimization eventually shows that the optimal dimensions (or, more precisely the length/width/height ratios) of the system are identical to the ones from random storage. Zaerpour et al. (2011) study a live-cube compact storage system where shuttles take care of the movements in *x*- and *y*- directions at each level and a lift moves unit loads across different levels in *z*- direction. They optimize the system dimensions under a random storage policy by using a decomposition process leading to four different complementary cases. Zaerpour et al. (2012b) extend their work by considering a two-class-based storage policy for a live-cube compact storage policy. Adding the first class boundary as a decision variable to the problem makes the travel time derivation procedure much more complex yielding 36 cases for the two-class-based storage compared to four cases for the random storage. This leads to a mathematical model with larger number of variables and constraints. However, the results show that the optimal dimensions of a system with two-class-based storage is identical to those for random storage.

In this chapter, we simply generalize this property to any storage system with any internal movement system, Pareto-demand curve (ABC curve), and zoning scheme. We prove that the optimal dimensions and even more generally the optimal shapes (in case the system is not in a shape of a cuboid) of any storage system with a given capacity are identical for random storage, full-turnover-based storage and *C*-class-based storage. This finding affects the research in the area of warehousing since it decouples the system sizing decisions at the design phase from the storage-class sizing decisions at the operational phase.

It implies that, first, at the design phase, any storage system with a given capacity can optimally be designed for a random storage policy. Designing an optimal storage system under random storage is more straightforward than under class-based or full-turnover-based storage strategies due to 1) less complexity in travel time derivation and 2) a smaller number of variables and constraints in the mathematical model. In addition, detailed information on customer demand is not required to optimally design a storage system under random storage.

Second, at the operational phase, an optimally designed system with a given capacity under a random storage policy (i.e. the simplest case), can optimally accommodate full-turnover or *C*-class-based storage without any configuration modification. In addition, for *C*-class-based storage, the optimal class boundaries can be obtained more simply. In previous studies, in order to design an optimal *C*-class-based storage policy, system dimensions and class boundaries have been considered as the decision variables in the mathematical model. Now, as optimal system dimensions are already known from random storage

optimization, the corresponding decision variables can be replaced by their optimal values. Therefore, the new mathematical model needs only to be solved for the class boundaries, yielding a smaller number of constraints and decision variables.

The remainder of this chapter is organized as follows. Section 2.2 compares storage policies in terms of the complexity in modeling. Section 2.3 proves the claimed property for a general case. Section 2.4 discusses the results and concludes the chapter.

2.2. General model formulation

We consider a storage system with only four basic assumptions as follows: 1) The system storage capacity is given (however, note that a system of a given capacity can accommodate a smaller number of unit loads per product under class-based or full-turnover storage than a system of the same capacity under random storage; in random storage all empty locations can be pooled to accommodate a stochastic number of storage and retrieval jobs), 2) all storage locations are equal in size and each location accommodates only one type of product, 3) within each storage class unit loads are stored randomly (i.e., unit loads within one class are treated equally although they might have different turnover rates), and 4) a single command policy is assumed (in a single command policy either a storage or retrieval request is processed per cycle; this assumption is required to derive closed-form formulas for travel times). The assumptions are not overly restrictive and can commonly be found in the literature (e.g. Hausman et al., 1976; Bozer and White, 1984; Rosenblatt and Eynan, 1989; Eynan and Rosenblatt, 1994; Kouvelis and Papanicolaou, 1995; De Koster et al, 2008; Yu and De Koster, 2009b; Zaerpour et al., 2011, 2012b).

Similar to Hausman et al. (1976), let

N = number of storage locations in the storage system;

t_i = the one-way travel time to move a unit load from location i to the I/O point or vice versa, $i = 1,...,N$; locations are ranked in an ascending order so that $t_i \leq t_{i+1}$ $\forall i < N$;

λ_j = the turnover of unit load j, that is the number of times the product on unit load j is stored or retrieved per time unit; λ_j are ranked in a descending order so that $\lambda_j \geq \lambda_{j+1}$ $\forall j < N$.

Under random storage the expected one-way travel time for a unit load equals,

$$E[T_R] = \bar{t} = \frac{\sum_{i=1}^{N} t_i}{N} .$$

(2.1)

In a full-turnover storage policy, the highest-turnover unit load is assigned to the location closest to the I/O point, while next unit loads are assigned to the locations in a similar fashion (i.e., unit load 1 with turnover λ_1 assigned to location 1 with travel time t_1, unit load 2 with turnover λ_2 assigned to location 2 with travel time t_2, etc). Therefore, the expected one-way travel time for an arbitrary unit load under full-turnover storage is (Hausman et al., 1976)

$$E[T_F] = \frac{\sum_{i=1}^{N} t_i \lambda_i}{\lambda} ,$$

(2.2)

where, $\lambda = \sum_{i=1}^{N} \lambda_i$.

In a class-based storage policy, the storage system and products are partitioned into C zones and product classes respectively and the class with the highest turnover is assigned to the zone closest to the I/O point, etc. The products within each class are not distinguished in terms of turnover rates and therefore the unit loads of any product can be assigned randomly to any storage location within the dedicated zone. The expected one-way travel time for a unit load under two-class based storage is

$$E[T_C] = \frac{\sum_{i \in R_1} \lambda_i \bar{t}_I + \sum_{i \in R_2} \lambda_i \bar{t}_{II}}{\lambda} ,$$

(2.3)

where, R_1 and R_2 are the set of locations belonging to the first and second zones respectively; λ_i is the turnover of unit load at location i ($\lambda_i \geq \lambda_j$, $\forall i \in R_1$ & $\forall j \in R_2$); $\bar{t}_I$ and $\bar{t}_{II}$ are the average travel times from locations in R_1 and R_2 respectively to the I/O point ($\bar{t}_I = \frac{\sum_{i \in R_1} t_i}{|R_1|}$ and $\bar{t}_{II} = \frac{\sum_{i \in R_2} t_i}{|R_2|}$).

In order to compare the complexity of analysis (travel time derivation and the configuration optimization) for different storage policies we give a simple illustrative example. Figure 2.1 shows a two-class-based storage system with a rectangular cuboid shaped for both the system and the first zone (R_1). b_i and x_i ($i = 1, 2, 3$) represent the dimensions (in time units) of the first zone and the system, respectively.

The internal movement system defines the travel time model and this defines the shape of the first zone. In our illustrative example, the time to reach a load at location (X,Y,Z) is given by $\max\{\max\{t_X,t_Y\},t_Z\}$. This time corresponds to an S/R machine moving in *x*- and *y*- directions simultaneously, with an independent depth travel handling system in *z*- direction starting simultaneously with the S/R machine such as a conveyor (see Yu and De Koster, 2009b). This travel time expression leads to a rectangular cubic shape for the first zone (t_X and t_Y represent the travel time of S/R machine from the I/O point to the location $(X,Y,0)$ (i.e. the front face of the rack) in *x*- and *y*- directions, respectively; and t_Z represents the travel time of depth handling system form depth Z to the front face of the rack in *z*- direction). Apparently, any different travel time model can result in a different shape for the first zone.
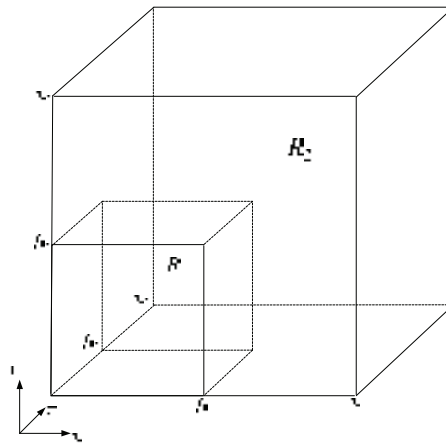
Figure 2.1. A schematic view of our illustrative two-class-based storage system

In the literature, the storage locations and turnover are often represented in continuous forms. These representations considerably reduce the difficulty of analysis while the results are sufficiently close to discrete systems (Hausman et al., 1976; Graves et al., 1977; Rosenblatt and Eynan, 1989; Eynan and Rosenblatt, 1994; Kouvelis and Papanicolaou, 1995). For the case where the turnovers of unit loads are represented by the well-known ABC curve, modeled for example by

$$A(i) = i^s \text{ for } 0 < s \leq 1, \tag{2.4}$$

where s is the skewness parameter and where the economic order quantity (EOQ) policy is used for replenishment of each product, the expected one-way travel time of an arbitrary unit load under two-class-based storage can be expressed by (Hausman et al., 1976; Rosenblatt and Eynan, 1989; Eynan and Rosenblatt, 1994)

$$E[T_C] = G^{2s/(1+s)}E[T_1] + (1 - G^{2s/(1+s)})E[T_2] \; , \tag{2.5}$$

where G is the volume of the first zone divided by the volume of the system (V_1/V) and $E[T_1]$ and $E[T_2]$ are the expected travel times of the first and the second zones, respectively. In order to derive $E[T_C]$, $E[T_1]$ and $E[T_2]$ must be obtained separately. In addition, for our illustrative example, six variables need to be considered in the derivation process of $E[T_C]$ (b_i and $x_i, i = 1, 2, 3$). On the other hand, the derivation of the expected travel time of the same system under random storage ($E[T_R]$) is more straightforward as it only deals with three variables which are the dimensions of the system ($x_i, i = 1, 2, 3$). For a two-class system with shape of the first zone different from a cuboid, the complexity of derivation even increases.

The optimization process of a system under random storage is also less complex than the one under two-class storage. In our illustrative example, a mathematical model which optimizes two-class storage system configuration and first zone boundaries leading to a minimum expected travel time, can be formulated as follows (the system capacity is normalized to one),

$$\min E[T_C], \tag{2.6}$$

subject to:

$$b_i \le x_i \; , \qquad\qquad \text{for } i = 1, 2, 3 \tag{2.7}$$

$$b_1 b_2 b_3 = G \; , \tag{2.8}$$

$$x_1 x_2 x_3 = 1 \; , \tag{2.9}$$

decision variables: x_1, x_2, x_3 and b_1, b_2, b_3 .

Constraints (2.7) state that the first zone boundaries (b_i) are closer to the I/O point than the system dimensions (x_i). Constraints (2.8) and (2.9) show that the volume of the first zone accounts for $100G\%$ of the total system volume, and the volume of the second zone accounts for $100(1 - G)\%$ of the total system volume.

However, for a similar storage system under a random storage policy, the mathematical model which optimizes the system configuration leading to a minimum expected travel time, can be formulated as follows,

$$\min E[T_R],\tag{2.10}$$

subject to:

$$x_1 x_2 x_3 = 1,\tag{2.11}$$

decision variables: $\quad x_1, x_2, x_3$.

For this example, it is not trivial that the optimal configurations for both mathematical models are identical as the model for the class-based storage consists of more decision variables and constraints.

In the next section, we show that the optimal configuration of the any storage system is independent of the storage policy being used. Therefore, regardless of the storage policy, the configuration, which minimizes the expected travel time, remains the same.

2.3. Analysis

In this section, we prove that the optimal shape of a storage system, which minimizes the expected travel time, is the same for random storage, full-turnover storage, and class-based storage.

***Theorem* 1**. *The optimal shape of a storage system, which minimizes the expected travel time, is the same under random storage and full-turnover storage policies.*

Proof. Consider a storage system with an optimal shape for random storage with the total capacity of N storage locations. Assume the N storage locations have travel times $t_1, t_2,\ldots, t_N$ to the I/O point where $t_i \le t_j, \forall 1 \le i < j \le N$. An optimal storage system with random storage is formed by the N storage locations closest to the I/O point as this minimizes Equation (2.1). Now, consider a storage system of the same capacity N and with a similar movement system, but with a full-turnover storage policy. Assume N storage locations have travel times $t'_1, t'_2,\ldots, t'_N$ to the I/O point where $t'_i \le t'_j, \forall 1 \le i < j \le N$.

Assume the system with full-turnover storage does not have a shape identical to the one with random storage. Thus, there exists at least one storage location in the system with full-turnover storage which causes the difference in shapes. If this is the ith closest location to the I/O point, find its corresponding location (ith closest location to the I/O point) in the system with random storage. Then, we have either $t_i > t'_i$ or $t_i \le t'_i$. The first case $t_i > t'_i$ cannot occur since the system with the random storage is assumed to be optimal which means it includes the N closest storage locations to the I/O point ($E[T_R] = \bar{t} = \sum_{i=1}^{N} t_i \Big/ N$). In the second case, $t_i \le t'_i$, we can write $\lambda_i t_i \le \lambda_i t'_i$. As a result, moving the ith

storage location (with travel time t_i') in the system under full-turnover storage to the corresponding *i*th storage location (with travel time t_i) in the system with optimal shape for random storage, leads to a shorter or equal average travel time for full-turnover storage (see Equation (2.2)). By repeating this procedure for all such locations, the shape of a full-turnover storage system will eventually be transformed to a shape identical to the one for optimal random storage system. This new full-turnover system has a minimum average travel time.   □

Theorem 2. *The optimal shape of a storage system, which minimizes the expected travel time, is the same under random storage and C-class-based storage policies.*

Proof. We demonstrate the theorem for two-class storage. Consider a storage system with an optimal shape for random storage with a total capacity of *N* storage locations. Assume these *N* storage locations have travel times t_1, t_2,…, t_N to the I/O point where $t_i \leq t_j, \forall 1 \leq i < j \leq N$. An optimal storage system with random storage is formed by the *N* storage locations closest to the I/O point as Equation (2.1) is minimized. Now, consider a storage system of the same capacity *N* and with a similar movement system, but with a two-class-based storage policy. Assume, b ($1 \leq b < N$) storage locations (not necessarily closest ones to the I/O point) form the first zone (R_1) and *N-b* remaining storage locations form the second zone (R_2). b storage locations of R_1 have travel times $t_1', t_2',...,t_b'$ to the I/O point, which can be ordered such that $t_i' \leq t_j', \forall 1 \leq i < j \leq b$. In addition, assume *N-b* storage locations of R_2 have travel times $t_{b+1}',...,t_N'$ to the I/O point where $t_k' \leq t_l', \forall b+1 \leq k < l \leq N$. We consider two situations:

Assume the system with two-class storage does not have a shape identical to the one with random storage. Thus, there exists at least one storage location in the system with class-based storage which causes the difference in shapes. If this is the *i*th closest location to the I/O point, find its corresponding location (*i*th closest location to the I/O point) in the system with random storage. The location *i* belongs to either R_1 or R_2. Hence, we consider two cases as follows:

- Location $i \in R_1$: in this case either $t_i > t_i'$ or $t_i \leq t_i'$ ($1 \leq i \leq b$). The first case $t_i > t_i'$ cannot occur since the system with random storage is assumed to be optimal which means it includes the *N* closest storage locations to the I/O point ($E[T_R] = \bar{t} = \sum_{i=1}^{N} t_i \Big/ N$). In the second case $t_i \leq t_i'$, according to Equation (2.3), the expected (average) weighted travel time of the first zone (R_1) of a two-class-based storage system can be calculated by

$$\sum_{j=1}^{b} \lambda_j \vec{t_I} \Big/ \lambda \,, \tag{2.12}$$

where $\vec{t_I} = \sum_{k=1}^{b} t'_k \Big/ b$. Therefore, Equation (2.12) can be reformulated as follows,

$$\sum_{k=1}^{b} (t'_k \sum_{j=1}^{b} \lambda_j) \Big/ (b\lambda) \,. \tag{2.13}$$

For location i we can write $t_i \sum_{j=1}^{b} \lambda_j \le t'_i \sum_{j=1}^{b} \lambda_j$. As a result, moving the ith storage location (with travel

time t'_i) in the system under two-class storage to the corresponding ith location (with travel time t_i) in the system under optimal random storage leads to a shorter or equal average travel time for two-class storage (see Equation (2.13)). By repeating this procedure for all such locations, the shape of the first zone R_1 will eventually be transformed to a shape identical to the b closest storage locations of an optimal random storage system. This new first zone has a minimum average weighted travel time.

- Location $i \in R_2$: in this case, again either $t_i > t'_i$ or $t_i \le t'_i$ ($b+1 \le i \le N$). The first case $t_i > t'_i$ cannot occur since the system with the random storage is assumed to be optimal which means it includes

  the N closest storage locations to the I/O point ($E[T_R] = \bar{t} = \sum_{i=1}^{N} t_i \Big/ N$). In the second case $t_i \le t'_i$,

  according to Equation (2.3), the expected (average) weighted travel time of the second zone (R_2) of a two-class-based storage system can be calculated by

$$\sum_{j=b+1}^{N} \lambda_j \vec{t_{II}} \Big/ \lambda \,, \tag{2.14}$$

where $\vec{t_{II}} = \sum_{k=b+1}^{N} t'_k \Big/ (N-b)$. Therefore, Equation (2.14) can be reformulated as follows,

$$\sum_{k=b+1}^{N} (t'_k \sum_{j=b+1}^{N} \lambda_j) \Big/ (N-b)\lambda \,. \tag{2.15}$$

For location i we can write $t_i \sum_{j=b+1}^{N} \lambda_j \leq t_i' \sum_{j=b+1}^{N} \lambda_j$. As a result, moving the ith storage location (with travel time t_i') in the system under two-class storage to the corresponding ith location (with travel time t_i) in the system under optimal random storage leads to a shorter or equal average travel time for two-class storage (see Equation (2.15)). By repeating this procedure for all such locations, the shape of the second zone R_2 will eventually be transformed to a shape identical to the one of the optimal random storage system excluding the b closest storage locations. This new second zone has a minimum average weighted travel time.   □

This proof can simply be generalized to a C-class-based storage system.

Corollary 1. *An optimal C-class-based storage system with a given capacity and minimum expected travel time can be designed using a hierarchical procedure as follows:*

Step 1. Obtain the optimal system configuration assuming a random storage.

Step 2. Obtain the optimal zone boundaries for a C-class-based system with configuration obtained at Step 1.

This hierarchical procedure decouples the configuration optimization from zone boundary optimization reducing the analysis complexity.

2.4. Discussion

In this chapter, we have shown that the optimal shape of a storage system with a given capacity is independent of the storage policy being used. We prove that minimizing the response time (for single-command cycles) of a storage system with any internal movement system and any location of the I/O point, under random storage, full-turnover storage, or C-class-based storage (for any Pareto-demand curve) leads to an identical system shape or configuration. This result may influence current warehouse design practice as the storage system can optimally be designed for a random storage policy, minimizing the response time. This leads to a much simpler optimization model. In addition, little information of customer demand is necessary in the design phase. At the operational phase, the system designed for optimal random storage can be used to accommodate full-turnover and C-class-based storage, without losing optimality.

Chapter 3

Storing Fresh Produce for Fast Retrieval in an Automated Compact Cross-dock System

3.1. Introduction

Many companies use cross-dock processes to decouple outbound from inbound transport. In a cross-dock system, the arriving supply has already been allocated to demand. Compared to warehousing the products, cross-docking leads to lower handling and inventory costs, while it shares the benefit of having high truck load factors.

This chapter studies temporary storage in cross-dock facilities, using a compact automated storage system. Our study is inspired by a cross-dock center storing fresh produce (vegetables and fruits) which is harvested on demand partly from greenhouses. Products are temporarily stored in a refrigerated warehouse and, at the planned truck arrival times, retrieved to fill customer orders. The company has several main performance measures:

- serving the outbound trucks within their planned arrival and departure times,

- preventing quality loss by minimizing the time during which the unit loads to be shipped are outside the conditioned (i.e. refrigerated, humidity and air-controlled) storage lanes,

- increasing the throughput and system utilization.

Minimizing total retrieval time is a good proxy for all measures. When an outbound truck arrives at the dock door, fast retrieval of unit loads of customer orders reduces the truck's waiting time. Therefore,

the truck can more likely be served within its planned arrival and departure times. The risk of quality loss is also reduced as the products spend the minimum time outside the conditioned area. Reducing the waiting time of each truck potentially provides the opportunity to serve more trucks within a shift, leading to higher throughput and system utilization. Cross-docking has been implemented widely in many supply chain networks by companies such as Wal-Mart (United States), Albert Heijn (Netherlands), Tesco (UK) and Carrefour (France). The cross-dock operates in a shift-based mode: products are harvested in the evening, arrive during the night, are stored temporarily, and are retrieved and shipped the next morning. Short lead times are possible due to the use of automated storage and handling systems.

These cross-dock systems often use satellite-based compact storage systems (also known as multi-deep storage systems) in order to minimize the cooling cost as cooling cost is directly related to storage space. Chapter 1 illustrates such a satellite-based compact storage system and its work mechanism (see section 1.2.1).

The main difficulty with multi-deep systems is that the unit loads need to be reshuffled. This is the process of removing unit loads stored in front of a unit load that needs storage or retrieval. In a system which operates automatically, in a shift-based mode, outbound reshuffles (the reshuffles required during the outbound process) are more critical than inbound reshuffles. Unit loads of inbound trucks can be assigned temporarily to the conditioned storage lanes while minimizing the total storage time and so the time that products spend in the unconditioned area. While waiting inside the conditioned area, the products can be reshuffled automatically and relocated to their proper storage locations without quality loss. There is ample time for such reshuffles during the night shift. Therefore, storage allocation decisions, taken during the inbound process, can be decoupled from outbound sequencing decisions to minimize the total retrieval time. Hence, unlike the outbound process, the inbound process is not a bottleneck in our cross-dock operation. In addition, since the truck loading process is much faster than the retrieval process, the bottleneck of the outbound process is the retrieval process. Minimizing the total retrieval time during the outbound process is therefore the company's prime objective.

The current solution to avoid outbound reshuffles, incrementing the total retrieval time in compact storage systems, is to use the dedicated storage policy in which every lane is dedicated to only one product, originating from one production batch. Hence, if a unit load of a product is requested, the load located at the rack's front face can be retrieved without any reshuffles. However, this policy does not use the known order information, and results in low space utilization ('honeycombing') due to partially filled lanes (Tompkins et al., 2010). As a consequence, additional lanes have to be used for the same number of

unit loads to be stored, leading to longer S/R machine travel time and potentially longer lead time. Our sample company is no exception. It uses different storage lanes in the racks for each batch of a product, leading to partially filled lanes. However, the major advantage is that no reshuffles are required when trucks have to be loaded.

In this chapter, we propose a shared storage policy which allows unit loads of different products to share the same storage lane, while avoiding reshuffles during the outbound process. We make use of customer order information to condense the storage system and minimize the response time simultaneously. By making use of a time window to realistically capture the arrival time instant of each truck the shared storage is robust to changes in outbound truck arrival times. We formulate the problem as a mixed-integer model to determine where to store unit loads in the compact storage system in order to minimize total retrieval time, assuming trucks arrive within the time window. The mathematical model is proven to be strongly NP-complete and so we propose an efficient heuristic to solve the problem. The results show that the shared storage policy can reduce total retrieval time by up to 30% compared to the dedicated storage policy. We test the robustness of the shared-storage policy to changes in outbound truck time windows and expose our heuristic to different levels of uncertainty. Shared storage seems better than dedicated storage in most scenarios. Therefore, warehouse managers should preferably use shared, rather than dedicated, storage in a fast-turnover automated compact cross-dock system in order to serve the customer faster, to avoid quality loss, and to increase throughput and system utilization. Only when the available outbound information is very uncertain, dedicated storage yields shorter response times.

In the next section, we review previous studies on different storage policies in compact storage systems and assignment policies in cross-docks. In section 3.3, we give an overview of the configuration of the system under study. Furthermore, we develop a mathematical model to optimize the storage operation by minimizing the total retrieval time. A solution algorithm is proposed in section 3.4. In section 3.5, we introduce an approach to obtain a lower bound to measure the performance of the solution algorithm. Section 3.6 illustrates the numerical results for our reference company for problems of different sizes. We test the robustness of our heuristic in section 3.7. Finally, section 3.8 concludes the chapter and proposes further research.

3.2. Literature review

Different decision problems of cross-dock systems have been studied in the literature. For a comprehensive review on cross-dock systems we refer to a paper by Boysen and Fliedner (2010). The

problem of locating single or multiple cross-dock systems in a distribution network is studied in the literature on hub location problems, e.g., by Klose and Drexl (2005) and Chen (2007). Bartholdi and Gue (2004) investigate the layout and the shape of a cross-dock system. Many papers study operational-level decision problems in cross-dock systems. A commonly studied problem is the assignment of destinations (mid-term horizon decision) and trucks (short-term horizon decision) to dock doors (e.g. Tsui and Chang, 1992, Gue, 1999, Bartholdi and Gue, 2000, Lim et al., 2005, Lee et al., 2006, Bozer and Carlo, 2008, and Miao et al., 2009). However, few papers focus on minimizing the total retrieval time of a block of retrievals stored in a cross-dock system. Stadtler (1996) introduces a five-module storage and retrieval assignment concept for a deep lane storage system where a lift takes care of vertical movement. He assumes a cross-dock process where the expected retrieval instant is known at the time of storage. He also assumes that retrieval as well as storage requests consist of a number of unit loads of the same product and that they are therefore stored together in a storage lane of the rack.

Several papers have analyzed the performance of different storage systems and policies. De Koster et al. (2008) and Roodbergen and Vis (2009) provide a comprehensive literature review on AS/RSs. We here only review papers on storage policies and compact storage systems.

Four main classes of storage policies can be distinguished (Francis et al. 1991): random, dedicated, class-based, and shared storage policy based on the duration of stay (DOS). With a *random storage policy*, each unit load has an equal chance of being stored in any of the storage locations. The random storage policy is studied broadly in the literature (Hausman et al., 1976, Bozer and White, 1984, Lee and Elsayed, 2005 and De Koster et al., 2008). Random storage requires the fewest data since no product information is used in determining storage assignment (Goetschalckx and Ratliff, 1990). On the other hand, the optimal dedicated storage and class-based storage policies require historical information of the turnover rates for each product. A *dedicated storage policy* in a 2D system involves the assignment of specific storage locations to each product. In a compact storage system, this means each lane accommodates unit loads of only one product. The dedicated storage policy in 2D systems has been studied extensively in the literature (e.g. Montulet et al., 1998, Malmborg, 1996). An early study of a dedicated storage policy is on the cube-per-order index (COI) rule by Heskett (1963). As a compromise between dedicated and random storage, a *class-based* dedicated storage policy is frequently used in which the unit loads are partitioned into a small number of classes based on their turnover rates. The class of unit loads with the highest turnover rate is assigned to locations closest to the I/O point. Storage is random within a class. Using product turnover frequency, class-based and dedicated storage policies may reduce

S/R machine travel time substantially compared to a random storage policy (e.g. Hausman et al., 1976, Graves et al., 1977, Rosenblatt and Eynan, 1989, Eynan and Rosenblatt, 1994, Kouvelis and Papanicolaou 1995, Kulturel et al., 1999, Van den Berg and Gademann, 2000, Foley et al., 2004). Park and Webster (1989b) present a class-based storage policy in a compact system where total travel time is minimized.

With a *shared storage policy* based on DOS, different products can share a common storage location over time if their DOS does not overlap, which allows more flexible use of space than allowed by a dedicated storage policy. This provides the opportunity to reduce the maximum effective storage area and to better utilize the more desirable storage locations (Chen et al., 2010). Goetschalckx and Ratliff (1990) show that, for single-command storage and retrieval, a DOS-based shared storage policy potentially decreases S/R machine travel time compared to dedicated storage, random storage, and class-based storage policies. Chen et al. (2010) address the combined location assignment and interleaving problem in an AS/RS with a shared storage policy based on DOS. Their objective is to minimize the travel time of an S/R machine considering storage assignment and interleaving at the same time. The authors provide an integer-programming model to solve the model optimally.

Compact storage systems have not yet been widely studied in the academic literature. Although Park and Webster (1989a, 1989b) appear to be the first to study compact storage systems, they actually study 2D pallet storage systems with multiple aisles. Gue (2006) develops models for very high-density storage systems, in which interfering unit loads have to be moved to gain access to desired unit loads. Gue and Kim (2007) study a "puzzle-based" compact storage system where a unit load can move in x and y-directions as long as an empty slot is available next to it. Sari et al. (2005) study a flow rack compact storage system where the pallets are stored and retrieved at different rack sides by two S/R machines responsible for storage and retrieval respectively. De Koster et al. (2008) and Yu and De Koster (2009b, 2012) study a compact storage system with built-in multi-deep circular conveyors. The system is fully automated, and every pallet stored is accessible individually by rotating conveyors.

The previous papers study cross-dock processes, compact storage systems and policies in isolation. However, as many cross-docks apply temporary (compact) storage in order to partly decouple inbound and outbound flows, it is necessary to integrate these systems and policies in system optimization decisions, which is the purpose of this chapter. Different from Goetschalckx and Ratliff (1990), shared storage is now defined as a storage policy which simultaneously accommodates different products in a single multi-deep lane. We focus on overall performance, integrating the storage, retrieval, and shipping processes in such a cross-dock.

3.3. Problem description, assumptions, and general model

The compact storage system studied in this chapter consists of a compact storage rack, an I/O point (or depot) and an S/R machine (an automated crane) with an attached satellite. The storage rack has R rows, C columns, and I depth tiers. $J = R \times C$ is the number of lanes in the rack. The S/R machine is capable of moving in both vertical and horizontal directions simultaneously. Therefore, its travel time is determined by the Chebyshev metric. While the S/R machine waits in front of the lane, the satellite attached to the S/R machine can move inside the lane to store or retrieve unit loads multi-deep. The S/R machine's pick-up or drop-off time of a unit load at the I/O point or a storage location is assumed to be constant. All storage and retrieval movements start with the S/R machine at the I/O point (located at the lower left-hand corner of the rack). Unit loads retrieved are dropped off by the S/R machine at the I/O point on an outgoing conveyor for further transport.

We are interested in cross-docking situations where orders are known at product receipt. The system operates in a shift-based mode: products received during the night shift have to be buffered and will be shipped during the next day shift according to appointment. Upon storage of a unit load, the exact arrival time of its departure truck is not yet known. Instead, a time window is used which captures all possible arrival time instants. The truck is allowed to arrive anywhere within this time window without imposing any reshuffling to the system. This makes our model robust to deviations from the truck's appointment time.

Therefore a time window is defined as follows:

Definition 1 (**time window**). The time window of an outbound truck refers to a time interval which captures all possible arrival time instants of the truck.

We start with the assumptions and then present the travel-time model for storage assignment. Most of our assumptions are rather standard in AS/RS literature. When the S/R machine is idle, it stops at the depot. The pick-up and deposit time of a unit load is constant; therefore, it is omitted from the minimization model. In addition, since the system operates in a shift-based mode, the S/R machine only uses single command (SC) cycles with only product storages during the night shift and product retrievals during the day shift. Moreover, we assume a cross-dock concept, i.e. all customer orders are known at product receipt. Outbound trucks are assigned to the dock doors in first come, first served (FCFS) sequence. In addition, the S/R machine serves the retrieval requests of an outbound truck according to the FCFS rule. Reshuffling is avoided.

The main notations are:

Objective

TRT The total retrieval time of a given block of retrieval requests. A block includes all the unit loads which have to be retrieved during the day shift.

Decision variables

x_{ijk} $x_{ijk} = 1$ if the unit load k is assigned to lane j and depth i during the night shift, otherwise $x_{ijk} = 0$.

Sets and indices

i Depth tier index of a storage lane in the rack $1 \le i \le I$; the smaller the index of a tier is, the closer it is to the rack's front face.

j Lane index $1 \le j \le J$; the smaller index of lane, the closer it is to the I/O point.

k Index of unit load to be retrieved, $1 \le k \le K$.

$S(k)$ Set of unit loads that cannot be stored in front of unit load k to avoid reshuffling.

Parameters

$X_j, Y_j,$ Travel time of the S/R machine from the depot to lane j and then back to the depot in horizontal and vertical directions, respectively.

Z_i Travel time of the satellite machine to transport a unit load from the front face of the lane to depth tier i without interference and then back to the front face of the lane.

We obtain the total retrieval travel time given by Equation (3.1) and the model of the storage assignment problem as below (Model P):

Model P:

$$\min \quad TRT = \sum_{i=1}^{I} \sum_{j=1}^{J} \sum_{k=1}^{K} x_{ijk} [Max\{X_j, Y_j\} + Z_i] \qquad (3.1)$$

Subject to

$$\sum_{k=1}^{K} x_{ijk} \le 1 \qquad for \qquad i = 1,...,I, j = 1,...,J, \qquad (3.2)$$

$$\sum_{i=1}^{I}\sum_{j=1}^{J} x_{ijk} = 1 \qquad for \qquad k = 1,...,K, \qquad\qquad (3.3)$$

$$x_{ijk} + \sum_{m \in S(k)} x_{ojm} \le 1 \qquad for \qquad i = 2,...,I, j = 1,...,J, k = 1,...,K, o = 1,...,i-1, \qquad (3.4)$$

$$x_{ijk} \in \{0,1\} \qquad for \qquad i = 1,...,I, j = 1,...,J, k = 1,...,K, \qquad\qquad (3.5)$$

where x_{ijk} represents the assignment of unit load k to lane j and depth i. Since the S/R machine can move in horizontal and vertical directions simultaneously, the time needed to go from the I/O point to the front face of lane j in Equation (3.1) is $Max\{X_j, Y_j\}$. Furthermore, the satellite machine cannot move in the depth dimension until the S/R machine is positioned at the lane's front face. Therefore, the satellite machine's travel time (Z_i) is added to the S/R machine's travel time. Constraints (3.2) ensure that every storage location can accommodate at most one unit load. Constraints (3.3) make sure that every unit load is assigned to exactly one storage location. Constraints (3.4) ensure that reshuffling is prevented by defining an appropriate set S for each unit load. In order to define set S for a unit load, we consider the outbound truck in which it is contained. Assume trucks A and B arrive at the outbound area with time windows $[i_A, j_A]$ and $[i_B, j_B]$, respectively. Then we might have two situations:

a) If $j_A < i_B$ or $j_B < i_A$:

In this case, the unit loads a and b of the two trucks A and B, respectively, can be assigned to the same lane. If $j_A < i_B$, truck A arrives earlier than truck B. Therefore, the unit loads of truck A should be assigned to the positions in front of unit loads of truck B to avoid reshuffling, if products are not identical. Hence, $b \in S(a)$ and $a \notin S(b)$. If $j_B < i_A$, truck B arrives earlier than truck A. Therefore, unit loads of truck B should be stored in front of unit loads of truck A to avoid reshuffling, if the products are not identical. Hence, $a \in S(b)$ and $b \notin S(a)$. If unit loads a and b contain the same product, they can be assigned to any locations of the same lane without any reshuffles, i.e. $a \notin S(b)$ and $b \notin S(a)$.

b) If $i_A < i_B < j_A$ or $i_A < j_B < j_A$ or $i_B < i_A < j_B$ or $i_B < j_A < j_B$:

In this situation, the time windows of trucks A and B overlap and so the arrival sequence of trucks A and B cannot be determined. Thus, reshuffling cannot be avoided if the unit loads (of different products) of trucks A and B are assigned to the same lane. Therefore, two unit loads of different products of trucks A and B cannot be stored in the same lane. If a and b are two unit loads of different products of trucks A and B respectively, then set S for unit loads a and b can be defined as $b \in S(a)$ and $a \in S(b)$. If no information

of arrival times of outbound trucks is available, the model will automatically assign unit loads of the same product to each lane (dedicated-storage policy). Having more accurate information of truck arrival times results in more narrow time windows with smaller chance of overlap, and hence more unit loads of different products can share the same lane.

The most difficult constraints are constraints (3.4). In Appendix 3A, we prove the problem is strongly NP-complete. Exact algorithms fail to solve the model optimally even for relatively small problem sizes. For real-life problems, the number of variables and constraints might be very large. Therefore, heuristic methods have to be developed to find solutions.

3.4. Solution construction and improvement (C&I) algorithm

Our C&I algorithm includes three main steps, which results in a shared storage policy. Step 1 defines an 'Ideal' storage area used to benchmark feasible solutions of Model P. Step 2 constructs a feasible solution that can be improved later to a near optimal solution. Step 3 consists of local improvements of the feasible solution and finds a near optimal solution.

To further explain the steps, we use illustrative example 1. Appendix 3B refers to the input parameters of example 1.

Step 1. Ideal boundary construction

We drop constraints (3.4) in Model P and then obtain Model R. Model R is a simple assignment problem that can be solved easily in polynomial time (Munkres, 1957). Its optimal solution provides a lower bound of the objective value of Model P.

Optimally solving Model R gives a solution for assigning K unit loads into a storage area in the rack. Obviously, the optimal solution of Model R results in the Ideal storage area and boundary defined below.

Definition 2 (the Ideal storage area). The Ideal storage area is the area consisting of the K closest storage locations to the I/O point.

Definition 3 (the Ideal boundary). The Ideal boundary is the boundary of the Ideal storage area.

By solving example 1, we obtain the Ideal storage area and boundary shown in Figure 3.1(a). Figure 3.1(a) illustrates the top view of a one-level rack (for every number d or $d(b)$ in each cell of Figures 3.1(a-e), d represents the distance from the cell location to the I/O point and b represents the truck index). The storage locations within the bold lines form the Ideal storage area and the border of the Ideal storage area forms the Ideal boundary. In case of a sufficiently large continuous rack, the top-viewed shape of the Ideal storage area equals a quarter circle.

If we can locate the *K* unit loads within the Ideal boundary such that constraints (3.4) are satisfied, then an optimal solution of Model P is obtained. However, in most cases unit loads will be shipped by different trucks with overlapping time windows, and relocations of unit loads cannot possibly satisfy constraints (3.4) without violating the Ideal boundary. Steps 2 and 3 below aim to find a storage area for feasibly assigning the *K* unit loads which violates the Ideal boundary as little as possible. As a result, these steps may provide a near optimal solution for Model P.
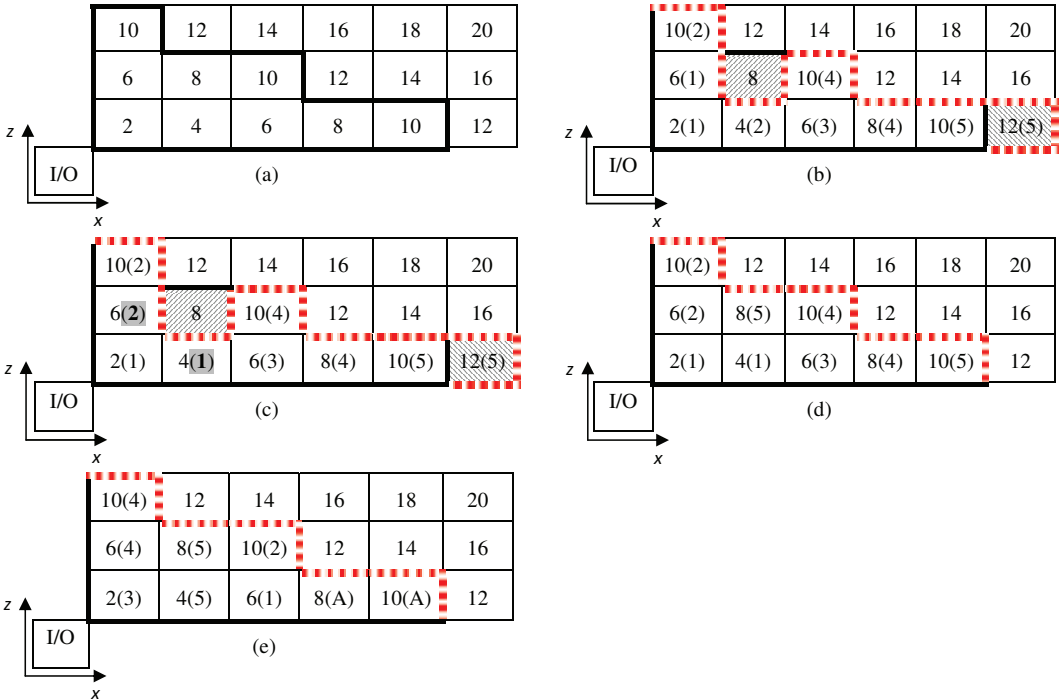
Notes. (1) The bold line forms the Ideal boundary.
(2) The dotted line gives the boundary from an actual feasible unit load assignment.
(3) ▨ represents an empty storage location within the Ideal boundary.
(4) ▧ represents an occupied storage location outside the Ideal boundary.
(5) The highlighted numbers represent the swapped unit loads in Figure 3.1(c).

**Figure 3.1.** Improvement of storage assignment over different steps

Step 2. Feasible solution construction

This step aims to find a feasible solution of Model P by using a graph representation approach. In Step 2.1, we represent the time windows of all the unit loads in a directed graph. Step 2.2 assigns unit loads to the storage rack without violating constraints (3.4).

Step 2.1. Graph representation

Because all the unit loads stored during a night shift will be shipped by trucks during the next day shift, the time window of each unit load is determined by the time window of its shipping truck. Hence, all the unit loads of one truck have the same time window. To represent the time windows of the unit loads, we group the K unit loads by truck and define the directed graph $G = (V, E)$. V is the set of vertices corresponding to the earliest and latest arrival times of all outbound trucks in the day shift. $V = \{0, 1, 2, ..., T\}$, where 0 and T represent the starting and ending times in the day shift. E is the set of directed arcs, where an arc represents the time window of all unit loads that will be shipped by the same truck. Each arc starts from a time node corresponding to the earliest arrival time of a truck (starting point of its time window) at the warehouse and ends at a time node corresponding to the latest arrival time of the truck (ending point of its time window). Each arc is weighted with the number of unit loads to be shipped by the truck which is called the length of the arc in the rest of chapter.

In example 1, $V = \{0, 1, 2, 3, 4\}$ as shown in Figure 3.2. The arc $T1(2)$, for example, represents the time windows of 2 unit loads to be shipped by truck 1.
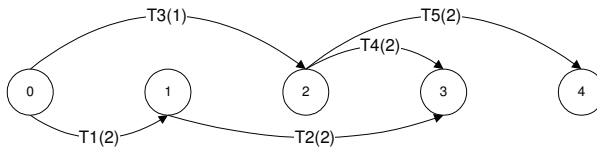
Note. *Ta(b)* represents the arc for truck *a* that ships *b* unit loads.

Figure 3.2. Truck time window graph

We aim to identify paths in this graph that connect unit loads of different trucks which can share the same storage lanes in the rack without reshuffling upon retrieval. We first define a partition set:

Definition 4 (a lane-sharing set). A lane-sharing set is a partition of all arcs into subsets with the following properties:

1) The time windows of any two arcs within each of the subsets do not overlap.

2) The subsets are 'maximal', i.e., any arc of a subset of a lane-sharing set cannot be added to another subset containing arcs with more unit loads, without violating property 1.

3) If an arc of a subset of a lane-sharing set is swapped with an arc of another subset containing arcs with more unit loads, it cannot increase the number of unit loads in the latter subset without violating property 1.

4) Given the subsets are maximal, they have minimal time window length; i.e. if two arcs of two different subsets of the partition have the same number of unit loads and they can be swapped without violating property 1, the arc belonging to the subset with more unit loads has a shorter time window.

Now, a lane sharing path can be defined as follows:

Definition 5 (a lane-sharing path). A lane-sharing path is a partition subset of a lane-sharing set.

Obviously, the unit loads in a path can be assigned to the same storage lanes without reshuffling if the unit loads of a truck arriving earlier are stored closer to the rack's front face than those arriving later. Any directed graph can be decomposed into a group of such paths.

Figure 3.3 shows a partition of the graph of Figure 3.2 into three lane-sharing paths which form a lane-sharing set with all four properties in Definition 4.
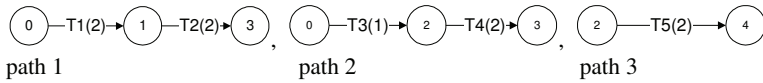
Figure 3.3. A set of lane-sharing paths for the above example

Step 2.2 addresses how to select lane-sharing paths and thereby to construct a feasible solution.

Step 2.2. Initial feasible solution construction

In this step, the C&I heuristic tries to obtain an initial feasible solution by selecting lane-sharing paths from a graph and assigning the unit loads based on the selected paths.

We first select a longest path in terms of the number of unit loads included in it. If there is a tie, we select the path with the shortest time window length (i.e. the time window between the earliest arrival time of the earliest truck in the path and the latest arrival of the latest truck in the path). To select a second path, we first remove the previous one from the graph and then select the longest one in the remaining part of the graph. The above process terminates when all the arcs have been removed. Eventually, an array of paths is obtained with non-increasing path lengths.

In Figure 3.2, the first path consists of arcs $T1(2)$ and $T2(2)$ with a length of 4 (=2+2) unit loads. By removing the longest path from Figure 3.2, we obtain Figure 3.4. The second path consisting of arcs $T3(1)$ and $T4(2)$ is selected from Figure 3.4. Figure 3.3 gives the result which consists of ordered paths 1, 2, and 3 for example 1.

Figure 3.4. The graph obtained by removing the longest path in Figure 3.2

The unit loads of the trucks, corresponding to the paths are now assigned to the storage locations within the Ideal boundary, in sequence. Note that a storage lane closer to the I/O point has a larger number of storage loc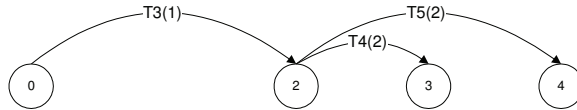ations within the Ideal boundary (see Step 1). Hence, in order to find a good initial feasible solution for Model P, the unit loads in a longer path are assigned to storage lanes closer to the I/O point. Within a path, the unit loads of a truck with earlier arrival time are assigned to storage locations closer to the rack's front face in a lane, or to a lane closer to the I/O point if multiple lanes are used for the path. As unit loads of a truck all have the same time window, they can be assigned arbitrarily to storage locations in a rack lane. However, when the assignment process continues, some unit loads may not fit in the Ideal storage area. In this case, the locations closest to I/O point but outside the Ideal boundary are attached to the Ideal boundary.

As shown in Figure 3.1(b), unit loads in the first path are assigned to the storage locations of the first two lanes closest to the I/O point without violating the Ideal boundary and constraints (3.4). The unit loads of truck 1 arriving earlier than those of truck 2 are assigned to the storage locations closer to the rack's front face in the first lane. Unit loads of the second path are assigned to the 3rd and 4th lanes without violating the Ideal boundary and constraints (3.4). A unit load of truck 5 is stored in a location in the rightmost lane that is outside the Ideal area.

Theorem 1. *The output of Step 2 is a feasible solution of Model P.*

Proof. In Step 2, if a unit load is assigned to a location, no other unit load can be assigned to the same location, therefore constraints (3.2) are satisfied. If a unit load is assigned to a location, it will be removed from the graph and therefore it will not be assigned to any other location. The process repeats until all arcs are removed and therefore constraints (3.3) are also satisfied. Since unit loads from a truck with an

earlier arrival time window are assigned to locations closer to the rack's front face, constraints (3.4) are satisfied and the output of Step 2 is a feasible solution of Model P.   □

The results of the assignment produce an *actual assigned storage area*. If the area is the same as the Ideal storage area, the optimal solution of Model P has been found. Otherwise, we improve the solution in Step 3, in four sub-steps.

Step 3. Improvement of a feasible solution

If the actual assigned storage area is not the same as the Ideal storage area, the relocation of a unit load from outside the Ideal storage area into an empty location in the Ideal storage area will reduce total retrieval time (see Steps 3.1-3.3). However, this kind of relocation cannot always be achieved without violating constraints (3.4). Therefore, Step 3.4 consists of relocating unit loads to reduce the distance of the boundary of the actual storage area (see Step 3.4).

Step 3.1. Rearrange each path independently for future improvement

In the feasible solution of Step 2, unit loads in a path may be assigned to multiple lanes, so that some unit loads of a late arriving truck will occupy storage locations close to the front face of the rack in a lane. Empty locations behind these unit loads but within the Ideal boundary are difficult to use without violating constraints (3.4). Therefore, if these unit loads are swapped with unit loads of earlier arriving trucks in the same path without violating constraints (3.4), the empty locations behind can potentially accommodate more unit loads in next steps.

This step swaps a unit load assigned to a storage location with empty locations behind it with a unit load in the same path but of an earlier arriving truck and assigned to a deeper storage location without violating constraints (3.4). In example 1, path1 consists of arcs representing trucks 1 and 2 where truck 1 arrives earlier than truck 2. Figure 3.1(b) shows that there is an empty storage location within the Ideal boundary behind the unit load of truck 2 in the second lane. Therefore, this unit load will be swapped with the unit load of truck 1 located at the second depth tier of the first lane. Figure 3.1(c) illustrates the result of Step 3.1.

Step 3.2. Improve the solution by letting different paths share the same lane

After rearranging each path independently, this step tries to improve the solution by combining different paths of a graph. Unit loads of different paths can be assigned to empty locations of one of their lanes if their time windows do not overlap. To do so, select a longest path from the array of paths obtained in Step 2.2 (in our example, path 1 in Figure 3.3). If its storage lanes contain an empty location, check if any unit load of a shortest path in the array can be assigned to that empty location without

violating constraints (3.4). Otherwise, select the second shortest path from the array. The process sequentially selects all shorter paths and then proceeds with the second longest path and repeats until there is no path to be selected.

In example 1, the storage location at the second depth tier of the second lane (Figure 3.1(c)), located within the Ideal boundary, is empty. Therefore, the objective value can be reduced by relocating the unit load located at the front face of the sixth lane, which is outside the Ideal boundary, to the empty storage location. This relocation reduces the objective value by eight units (the travel time is the time it takes to move from the I/O point to the point and then back to the I/O point; $2 \times (12 - 8) = 8$). The final output of Step 3.2 is shown in Figure 3.1(d). As the Ideal boundary and the actual storage assignment boundary coincide, the result of this step is optimal for the example.

Step 3.3. Improve the solution by considering products

Different unit loads of the same product can be swapped even if they have overlapping time windows. The first product to be selected is the one with the most unit loads. The graph is updated by adding a path representing unit loads of the selected product and adjusting the weights of the other arcs. This step then tries to reduce the objective value by grouping unit loads of the selected product and repeating the previous steps (Step 2.2 onward) for the updated graph. The new storage assignment is accepted if the objective value is reduced. Next, the product with the second most unit loads is selected. The process repeats until all products have been selected.

An updated graph for example 1 considering product "A" is shown in Figure 3.5. Each of the trucks 1 and 2 ships one unit load of "A". Therefore, the weights of the arcs representing trucks 1 and 2 have been reduced by one unit load and the new path "A" has a length of 2 unit loads. The time windows of the unit loads in path "A" determine the starting point and ending point of path "A".
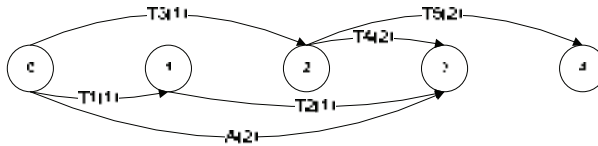

Figure 3.5. Updated graph considering product "A"

The result of Step 3.3 is shown in Figure 3.1(e). The total retrieval time of the assignment in Figure 3.1(e) is still identical to the total retrieval time of the result of the previous step and so it is still optimal.

Step 3.4. Improve the solution by swapping two different lanes

In the final solution of Step 3.3, some lanes close to the I/O point may store a smaller number of unit loads than remote lanes. The solution may be improved by swapping lanes as follows: The more unit loads assigned to a lane, the closer the lane should be to the I/O point.

The final solution of the C&I heuristic is shown in Figure 3.6(a); comparing the result of the heuristic with its equivalent dedicated storage policy (Figure 3.6(b)) shows approximately 9% reduction in total retrieval time.

In order to test the quality of the C&I heuristic, we provide a tight lower-bound in the next section.

Since Step 3.2 is the most complicated step, it determines the computational complexity of our C&I algorithm. In this step, unit loads of different paths can share the same lane if their trucks' time windows do not overlap. In the worst case, all unit loads need to be compared pairwise. In addition, based on Step 3.3, the previous steps should be replicated based on the number of product types which equals the total number of unit loads in the worst case. Therefore, our C&I algorithm has a polynomial time complexity of $O(n^3)$ where n is total number of unit loads.

10(4)	12	14	16	18	20	22
6(4)	8(5)	10(2)	12	14	16	18
2(3)	4(5)	6(1)	8(A)	10(A)	12	14

10	12	14	16	18	20	22
6(A)	8(B)	10	12	14	16	18
2(A)	4(B)	6(C)	8(D)	10(E)	12(F)	14(G)

Note. Products are denoted by capital letters

(a)   (b)
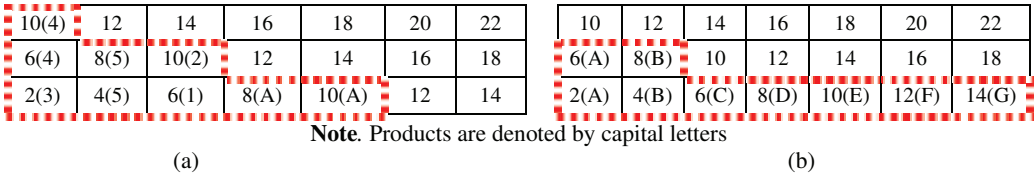
Figure 3.6. (a) Solution of the shared-storage heuristic, (b) Solution of the dedicated-storage policy

3.5. Lagrangean relaxation approach

This section provides a tight lower bound of the minimum objective value of Model P by using a Lagrangean relaxation approach. The lower bound can be used to evaluate the performance of the feasible solution found in Section 3.4; the feasible solution gives an upper bound of the minimum objective value of Model P. If the gap (i.e., ((the upper bound - the lower bound)/the lower bound)×100%) is small, the feasible solution is a good near optimal solution.

The constraints that complicate the solution of Model P are constraints (3.4), which ensure that reshuffling is avoided. We relax the constraints by introducing a set of non-negative Lagrange multipliers $\lambda = (\lambda_{ijko})_{(I-1)\times J \times K \times (i-1)}$ and then obtain a Lagrangean relaxed model as follows:

Model RP:

$$\min \quad TRT_\lambda = \sum_{i=1}^{I}\sum_{j=1}^{J}\sum_{k=1}^{K} x_{ijk}[Max\{X_j, Y_j\} + Z_i] + \sum_{i=2}^{I}\sum_{j=1}^{J}\sum_{k=1}^{K}\sum_{o=1}^{i-1}\lambda_{ijko}(x_{ijk} + \sum_{m\in S(k)} x_{ojm} - 1), \quad (3.6)$$

subject to Constraints (3.2), (3.3) and (3.5).

Let $D(\lambda)$ be the minimum objective value of Model RP for any Lagrange multipliers $(\lambda_{ijko})_{(I-1)\times J\times K\times(i-1)} \geq 0$. The Lagrangean dual problem of Model RP, denoted by DP, can be formulated as:

Model DP:

$$\max_{\lambda\geq 0} D(\lambda),$$

where λ is the vector of decision variables of Model DP.

According to the theory of Fisher (1981), for any given $(\lambda_{ijko})_{(I-1)\times J\times K\times(i-1)} \geq 0$,

$$D(\lambda) = TRT_\lambda^* \leq TRT^*,$$

where TRT_λ^* and TRT^* are the minimum objective values of Models RP and P. Therefore, the larger $D(\lambda)$ is, the better lower bound it provides for TRT^*. Model RP is a simple assignment problem that can be solved in polynomial time. The question is how to find good $(\lambda_{ijko})_{(I-1)\times J\times K\times(i-1)} \geq 0$ that can provide a larger $D(\lambda)$. The sub-gradient method is used here to update $(\lambda_{ijko})_{(I-1)\times J\times K\times(i-1)} \geq 0$. The procedure of the approach, based on the paper by Yu et al. (2008), is as follows:

Step 0: Initialize λ^t and θ^t at $t = 0$ where t is the iteration step ($\lambda^0 = 0, \theta^0 = 1$).

Step 1: Solve the relaxed Model RP to obtain TRT^t (i.e., $D(\lambda)$) that is the current dual value with a given λ^t (a lower bound).

Step 2: Set the step size s^t in iteration t by

$$s^t = \beta\frac{TRT^* - TRT^{[t]}}{\left\|g^t\right\|^2},$$

where β is a parameter with $0 < \beta < 1$, TRT^* of Model P is estimated by $\left(1 + \omega/\theta^\rho\right)TRT^{[t]}$. $TRT^{[t]}$ is the best dual value obtained prior to iteration *t,* parameters ω and ρ are random numbers within the their

intervals where $\omega \in [0.1,1.0]$, $\rho \in [1.1,1.5]$. The value of θ in iteration $t+1$ is given by $\theta^{t+1} = \max(1, \theta^t - 1)$ if $TRT^t > TRT^{[l]}$, otherwise $\theta^{t+1} = \theta^t + 1$ and

$$\left\| g^t \right\|^2 = \sum_{i=2}^{I} \sum_{j=1}^{J} \sum_{k=1}^{K} \sum_{o=1}^{i-1} \left(x_{ijk} + \sum_{m \in S(k)} x_{ojm} - 1 \right)^2 .$$

Note that $s^t \geq 0$.

Step 3: Update the Lagrange multipliers in iteration $t+1$

$$\lambda_{ijko}^{t+1} = \max \left\{ \lambda_{ijko}^t + s^t \left(x_{ijk} + \sum_{m \in S(k)} x_{ojm} - 1 \right), 0 \right\} .$$

Step 4: Check the stop criterion, which is given by either 1) The dual value TRT^t has not improved for a given number of iterations, or 2) A given maximum number of iterations has been reached. If the criterion is met, stop and output the results, otherwise set $t = t+1$ and go to Step 1.

3.6. Numerical results

In this section, we test the quality of our C&I heuristic. In addition, we compare the performance of the C&I heuristic with a dedicated storage policy. Our base example is based on data from a company in the Netherlands which distributes fresh vegetables and fruits to retail customers in Europe in a shift-based cross-dock operation. The company has a refrigerated compact storage system consisting of five identical modules, each with an S/R machine and satellite using dedicated storage. Products with a larger inventory are stored in the lanes closer to the I/O point.

Input parameters describing orders placed by customers and parameters describing a single module of the storage system are shown in Table 3.1. The starting point of the time window of a truck arrival is randomly generated within the eight-hour day shift. The lengths of the time windows are varied. In the next step, the C&I heuristic is evaluated.

First, we present the results of the base example. Then, to test the robustness of our C&I heuristic to different sources of variation in the inputs of our model, a sensitivity analysis is performed. In each experiment, we vary one of the parameters of the base example over five different alternative values while the other parameters are fixed.

Table 3.1. Parameters related to orders and storage system

Parameters	Base example	Range for scenarios	Fixed parameters of storage system
Time window length (hours)	1	[0.001, 8]	
Number of orders	36	[1, 60]	
Order size (number of unit loads)	10	[1, 15]	
Number of products (PT)	10	[1, 40]	
Number of depth tiers	5	[1, 11]	
Duration of shift (hours)			8
Size of pallet (centimeters)			width=120, height=260, depth=80
Size of storage location (centimeters)			width=150, height=300, depth=100
Size of rack (No. of tiers)			level=3, depth tier=5, lanes/level=24
Size of rack (meters)			width=36, height=6.4, depth=5
S/R machine horizontal speed (v_x) (m/s)			2
S/R machine vertical speed (v_y) (m/s)			0.5
Satellite speed (v_z) (m/s)			0.25
Nominal capacity of S/R machine (No. of unit loads/hour)			60

All test problems have been solved using MATLAB software on a portable computer Intel(R) Pentium(R) M1.86GHz with 512MB RAM and MS Windows XP professional. For each instance, including the base example, the results in the tables are the average of ten runs of simulated orders with corresponding time windows. Table 3.2 compares the solutions of the C&I heuristic and the dedicated storage policy for the base example. A one-tailed paired t-test ($H_1 : \mu_H < \mu_D$) shows the results of the C&I heuristic and the dedicated-storage policy differ significantly at a 5% level ($p < 0.0001$ for nearly all instances tested).

Table 3.2. Comparison of solutions of C&I heuristic and dedicated storage policy for the base example

No. of orders	Order size	PT	TRT_D	TRT_H	Imp (%)	P-value	CT_H	TRT_{LR}	Gap (%)	# runs Gap=0	CT_{LR}
36	U[1,10]	10	6373.9	5513.1	13.6%	<0.0001	0.9	5490.1	0.4%	4	73.9

Note: (1) *PT*, *Gap* and #runs Gap=0 are the total number of products, gap between C&I heuristic and LR (Lagrangean relaxation) and the number of runs out of 10 runs with gap=0, respectively.
(2) TRT_x is the total average retrieval time for method *x* (in seconds), where *x* = D (dedicated storage), H (C&I heuristic), LR (Lagrangean relaxation).

(3) CT_x is the average computational time per instance for method x (in seconds), where $x = $ H (C&I heuristic), LR (Lagrangean relaxation).

(4) $\text{Imp} = (\dfrac{TRT_D - TRT_H}{TRT_D}) \times 100\%$.

The results of the C&I heuristic for a varying number of depth tiers are shown in Table 3.3. In order to make a fair comparison, the rack's capacity and the number of levels of the rack are assumed to be identical to those in the base example for all instances in Table 3.3 (the rack's capacity for each scenario is the closest possible integer value to the capacity of rack in the base example). In subsequent examples, we vary the time window lengths (Table 3.4), the number of orders (Table 3.5), the order size (Table 3.6), and the number of products (Table 3.7).

Table 3.3. Sensitivity analysis for a varying number of depth tiers

Depth tiers	TRT_D	TRT_H	Imp (%)	P-value	CT_H	TRT_{LR}	Gap (%)	# runs Gap=0	CT_{LR}
1	11384.0	11384.0	0.0%	_	0.2	11384.0	0.0%	10	44.1
3	5529.0	5355.9	3.1%	<.0001	0.5	5341.9	0.3%	3	66.7
7	7178.2	5636.0	21.6%	<.0001	0.9	5614.8	0.4%	6	72.2
9	7847.2	5997.5	23.7%	<.0001	0.8	5969.8	0.4%	8	100.1
11	9445.6	7097.6	25.1%	<.0001	1.1	7057.4	0.6%	6	126.0

Table 3.4. Sensitivity analysis for varying time windows

Time window length (hour)	TRT_D	TRT_H	Imp (%)	P-value	CT_H	TRT_{LR}	Gap (%)	# runs Gap=0	CT_{LR}
0.001	6395.3	5538.4	13.5%	<.0001	0.3	5520.8	0.3%	6	65.2
0.5	6339.4	5489.8	13.7%	<.0001	1.0	5468.1	0.4%	5	74.4
2	5998.4	5125.8	14.6%	<.0001	0.7	5115.4	0.2%	5	64.5
4	6282.0	5432.7	13.6%	<.0001	1.0	5413.8	0.4%	4	67.3
8	6446.2	5592.9	13.5%	<.0001	0.8	5581.8	0.2%	4	80.5

Table 3.5. Sensitivity analysis for a varying number of orders

No. of orders	TRT_D	TRT_H	Imp (%)	P-value	CT_H	TRT_{LR}	Gap (%)	# runs Gap=0	CT_{LR}
1	36.2	30.8	16.9%	.0125	0.5	30.8	0.0%	10	3.4
10	1130.0	816.2	28.0%	<.0001	0.1	806.3	1.2%	3	276.1
20	3015.6	2422.2	19.9%	<.0001	0.4	2410.9	0.5%	5	78.2
50	9479.9	8816.5	7.1%	<.0001	1.1	8792.7	0.3%	5	95.3
60	10532.9	9960.8	5.4%	<.0001	1.4	9944.2	0.2%	5	84.9

Table 3.6. Sensitivity analysis for varying order sizes

Order size	TRT_D	TRT_H	Imp (%)	P-value	CT_H	TRT_{LR}	Gap (%)	# runs Gap=0	CT_{LR}
U[1, 1]	685.2	469.5	31.4%	<.0001	0.2	462.4	1.5%	3	251.2
U[1, 3]	1717.8	1315.5	23.4%	<.0001	0.5	1305.8	0.8%	5	94.0
U[1, 5]	2955.8	2369.0	20.0%	<.0001	0.5	2354.2	0.6%	5	67.2
U[1, 8]	4930.4	4119.5	16.6%	<.0001	0.8	4097.6	0.5%	4	75.7
U[1, 15]	9282.1	8588.0	7.6%	<.0001	1.0	8567.2	0.2%	6	83.9

Table 3.7. Sensitivity analysis for a varying number of products (PT)

PT	TRT_D	TRT_H	Imp (%)	P-value	CT_H	TRT_{LR}	Gap (%)	# runs Gap=0	CT_{LR}
1	6453.2	5551.3	14.0%	<.0001	0.2	5551.3	0.0%	10	54.5
5	6393.9	5510.4	14.0%	<.0001	0.4	5493.2	0.3%	6	66.8
20	5979.1	5196.0	13.2%	<.0001	1.8	5168.3	0.6%	3	75.6
30	5924.6	5212.9	12.1%	<.0001	4.7	5197.2	0.3%	6	65.6
40	6160.8	5468.9	11.4%	<.0001	6.7	5457.1	0.2%	7	77.1

From the results in Tables 3.2-3.7 we make the following observations.

Observation 1. The C&I heuristic outperforms the dedicated storage policy in our experiment. The total retrieval time can be reduced by up to 31.4% depending on the input parameters, and the average reduction in total retrieval time is about 16%. As p-values in Tables 3.2-3.7 illustrate, the difference between the total retrieval times of the C&I heuristic and the dedicated storage is statistically significant, except for a single-deep rack where the results of both policies are identical.

The C&I heuristic performs very well, as the gaps between the results of the C&I heuristic and the lower bound are often zero and mostly less than 1%. For those solutions with zero gap, the best solution of the Lagrangean relaxation is obtained at $\lambda = 0$, i.e. it equals the optimal solution of Model R. Simultaneously, the C&I heuristic yields a solution within the Ideal boundary without any infeasibility. Therefore the objective value of the Lagrangean relaxation equals the objective value of the solution of the C&I heuristic and the gap becomes zero. The gap between the result of the C&I heuristic and the optimal objective value is always less than or equal to the gap between the result of the C&I heuristic and the lower bound of the optimal objective value. Therefore, it can be inferred that the results of the C&I heuristic are near optimal or optimal. However, the C&I heuristic cannot provide the optimal solution for every case (see Appendix 3C). The C&I algorithm finds near optimal solutions very fast; normally in less than one second.

Observation 2. The total retrieval time of the C&I heuristic (TRT_H) and dedicated storage policy (TRT_D) are convex functions of the number of depth tiers (see Table 3.3). This observation indicates that an optimal number of depth tiers can be found for a given storage capacity. This result is consistent with the findings of De Koster et al. (2008). Here the rack with three depth tiers has the shortest total retrieval time for both policies (see Table 3.2 and 3.3). Two elements affect total retrieval time: depth-movement travel time and horizontal and vertical movement travel times. When the number of depth tiers is small, the rack has a large number of lanes. Hence, although the depth-movement part of total retrieval time is small, the horizontal and vertical movement part of total retrieval time becomes large. In contrast, when the number of depth tiers is large, the rack has a small number of lanes. Consequently, the depth movement plays a significant role in total retrieval time compared to horizontal and vertical movements. This trade-off indicates that optimal rack dimensions exist.

Observation 3. With an increasing number of depth tiers the relative improvement of the C&I heuristic compared to the dedicated storage policy ($(TRT_D - TRT_H)/TRT_D$) increases (see Table 3.3). In both policies, the total retrieval time for a single-deep rack is the same, while the relative improvement is 25% for an eleven-deep rack.

Observation 4. When time window lengths increase (this also implies more overlaps), the C&I heuristic can still reduce the retrieval time compared to the dedicated storage policy (see Table 3.4). This is because the C&I heuristic is capable of assigning unit loads belonging to every truck to the same lane (unit loads of a truck have the same time window) while least violating the Ideal boundary.

Observation 5. The relative improvement of the C&I heuristic compared to the dedicated storage policy decreases with an increasing number of orders and order sizes. This follows from the increase of the rack utilization with an increasing number of orders and order sizes (see Tables 3.5 and 3.6). A higher rack utilization generally means fewer empty storage locations and less space for improvement.

3.7. Robustness testing

In our model formulation, the time window of an outbound truck is defined as a time interval which captures all possible arrival time instants of the truck. However, in real life an outbound truck might arrive outside its allocated time window because of inaccurate information. In order to evaluate the performance of the shared-storage policy, we expose our C&I heuristic to higher levels of uncertainty using a Monte Carlo simulation.

We assume the actual arrival time of each outbound truck is normally distributed with known mean μ and standard deviation σ. However, the actual arrival time can fall outside the time window. Although in practice, very early arriving trucks might be asked to wait until their scheduled arrival, in our experiments they are assumed to be served in a first come, first served sequence, potentially leading to more reshuffles (worst-case scenario). By increasing the level of uncertainty, the preset time window becomes less accurate. A given time window can capture $\mu \pm 3\sigma$, $\mu \pm 2.5\sigma$, …, $\mu \pm 0.5\sigma$ percentile of the actual arrival time instants depending on the level of uncertainty. For instance, an outbound truck with a time window that captures $\mu \pm 3\sigma$ of the actual arrival time distribution, arrives within its time window with a probability of 0.997.

If a truck arrives outside its time window, reshuffling might be required. For this purpose, buffer lanes are used; empty lanes closest to the ones that are occupied. For our experiments, we take the base example shown in Table 3.1. Each of the input parameters (number of depth tiers, time window length, number of orders, order size, number of products) is varied under different levels of uncertainty. The means of the arrival times of outbound trucks are uniformly distributed within the eight-hour shift period (from 6 a.m. to 2 p.m.). For each scenario, we randomly generate 10 instances (truck arrivals) and calculate the average number of required reshuffles and average reshuffling time for the C&I heuristic under different levels of uncertainty.

Table 3.8. Comparison of the C&I heuristic and dedicated storage in real application

Variable	Range	TRT_D [1]	TRT_H [1]	$\mu \pm 3\sigma$		$\mu \pm 2.5\sigma$		$\mu \pm 2\sigma$		$\mu \pm 1.5\sigma$		$\mu \pm \sigma$		$\mu \pm 0.5\sigma$	
				NRes [2]	ResT [3]	NRes	ResT	NRes	ResT	NRes	ResT	NRes	ResT	NRes	ResT
# depth tiers	3	5627.8	5456.4	0.3	30	0.4	37.8	0.5	40.4	0.5	44.5	1.7	165.8	*2.5*	*243.8* [4]
	9	8273.6	6438.4	3.2	135.6	3.6	152.6	3.6	153	4.9	206.2	7.4	303.2	18.2	749.9
	11	10047.0	7704.2	3.8	210.2	4.5	221.9	5.1	242.2	5.8	304.4	13.6	681.8	27.4	1231.2
Time window length (hour)	0.5	6205.6	5306.1	0.0	0.0	0.0	0.0	0.2	8.0	0.5	17.0	0.6	28.5	3.0	194.3
	1	6150.5	5345.3	0.3	13.9	0.5	30.9	0.7	41.0	1.2	63.7	2.0	129.6	4.5	272.0
	1.5	6195.3	5388.9	0.5	17.1	1.5	78.8	2.0	121.6	2.5	148.2	3.8	219.2	7.2	430.1
# orders	20	2968.2	2379.8	0.1	6.7	0.2	13.6	0.2	13.6	0.2	13.6	0.3	21.3	1.2	79.1
	50	9325.8	8614.8	0.5	19.1	1.4	63.7	1.4	70.0	1.6	71.4	6.7	378.7	11.4	610.1
	60	10520.0	9792.0	1.7	72.5	3.5	215.5	3.6	223.4	3.8	234.8	9.2	566.5	*25.2*	*1588.0*

Order size	[1, 3]	1714.8	1288.0	0.0	0.0	0.2	11.9	0.3	18.3	0.3	18.3	0.3	21.8	1.6	115.0
	[1, 8]	4758.4	3952.8	0.2	14.4	0.2	14.8	0.2	14.8	0.3	21.2	0.7	34.3	4.6	304.8
	[1,15]	10138.0	9525.4	1.3	74.3	2.3	115.2	2.2	101.9	3.1	187.1	4.6	233.5	9.5	501.2
# products	5	6219.9	5354.6	0.5	20.4	0.7	36.2	0.9	45.1	0.9	43.6	1.9	99.6	3.5	186.6
	20	6424.1	5662.1	0.7	28.5	0.8	32.4	1.0	46.1	1.3	77.2	2.4	114.2	5.7	338.9
	40	5753.9	5083.8	0.4	20.5	0.4	26.3	0.4	26.3	1.0	65.1	1.0	44.3	2.7	167.4

(1) TRT_x is the total average retrieval time for method x (in seconds), where $x =$ D (dedicated storage), H (C&I heuristic), excluding reshuffling time.

(2) $NRes$ is the average number of reshuffles for C&I heuristic.

(3) $ResT$ is the average reshuffling time for C&I heuristic (in seconds).

(4) Bold and italic numbers represent situations where $TRT_D < TRT_H + ResT$

Table 3.8 gives both the total retrieval time of the C&I heuristic excluding reshuffling time (TRT_H) and the reshuffling time ($ResT$). The table shows that inaccurate arrival information of outbound trucks adds more reshuffling time to the shared-storage policy (see right-hand side columns of Table 3.8). On the other hand, more accurate arrival information of outbound trucks avoids imposing reshuffling costs to the shared-storage policy (see left-hand side columns of Table 3.8). Still, a shared storage appears to be more beneficial than a dedicated storage in nearly all scenarios. We next discuss the impact of different levels of uncertainty on each input parameter.

For a given number of depth tiers, a higher level of uncertainty increases the number of required reshuffles and the average reshuffling time. This increase is more significant for a system with deeper lanes. However, shared storage still appears to provide shorter total retrieval times than dedicated storage even for an eleven-deep storage system, and very inaccurate information. By increasing the number of depth tiers, the improvement of shared storage over a dedicated storage policy increases significantly, which can still compensate the time of additional reshuffles caused by inaccurate information.

For a given time window length, a higher level of uncertainty increases reshuffling time. This increase is more significant for a wider time window. Violation of wider time windows is more likely to cause reshuffling, as the expected arrival sequence of outbound trucks is more likely to change.

For a given number of orders, or order size, a higher level of uncertainty increases the average reshuffling time accordingly. By increasing the number of orders, system utilization will also increase as the system capacity is given. Therefore, the system becomes more vulnerable to inaccurate information, leading to a higher risk of reshuffling. If a very large number of orders has to be processed during a shift and the available information is very uncertain, dedicated storage seems to have a shorter total retrieval

time than shared storage. For example, with sixty orders in one shift and a confidence level of 68% ($\mu \pm \sigma$) or lower, dedicated storage provides solutions with shorter total retrieval times.

Finally, a large order size and a higher level of uncertainty will increase reshuffling time. The explanation is similar to the one above for an increasing number of orders.

3.8. Conclusion

Compact storage systems are often used for temporarily storing refrigerated products in cross-dock environments. To retrieve a unit load stored multi-deep in such a system, the unit loads in front of it have to be removed first. This reshuffling increases the complexity of the storage and retrieval process and also increases the retrieval time of the unit loads. In practice, the dedicated storage policy is used to avoid reshuffling. Since an exact lane-sharing model is strongly NP-complete, we introduce a C&I heuristic based on a greedy construction and an improvement part leading to a shared storage policy. The gap between the C&I heuristic and Lagrangean relaxation of the exact model appears to be very small indicating the C&I heuristic gives near optimal solutions, normally within a second computation time. Our results show that, compared to the dedicated storage policy, the shared storage policy using the C&I heuristic reduces total retrieval time by an average of 16% for the instances tested. For the reference system we studied, management can achieve a total retrieval time reduction of 13.6%. In addition, with an increasing number of depth tiers, the C&I heuristic outperforms the dedicated storage policy. The reason is that the C&I heuristic fills the lanes closer to the I/O point fully with unit loads of different products, whereas the dedicated storage policy fills each lane only partially with single-product unit loads. In order to test the robustness of the C&I heuristic, we consider a range of scenarios by varying the level of uncertainty in arrival information of outbound trucks. A greater level of uncertainty results in an increase in the number of required reshuffles and thus an increase in reshuffling time. Shared storage, however, remains the better storage policy in most scenarios. Therefore, warehouse managers should preferably use shared storage in fast-turnover automated compact cross-dock systems as this yields shorter response times. In addition, the shared storage policy is virtually insensitive to disturbances. The reason is that the C&I heuristic takes any potential overlap between time windows of different trucks into account and optimizes within their constraint. Only when the available information is very uncertain, dedicated storage might result in shorter response times.

Appendix 3A: NP-completeness proof

In order to show our problem is strongly NP-complete we consider a special case of the problem. Our problem will be proven to be strongly NP-complete if our problem in this special case is strongly NP-complete.

To construct the special case we assume

$$Z_i << \max\{X_j, Y_j\} \qquad for\, i = 1...I, J = 1...J\,, \tag{3.7}$$

indicating the depth movement travel time is negligible compared to horizontal and vertical movement travel times. This holds when the satellite machine moves much faster than the S/R crane does. It implies that K unit loads should be stored in the smallest number of lanes closest to the I/O point without violating Constraints (3.4) in order to minimize (3.1).

Hence, with the assumption given by Equation (3.7), Model P is equivalent to the following model: Model SP:

$$\min \quad TRT = \sum_{k=1}^{K} \sum_{i=1}^{I} \sum_{j=1}^{J} x_{ijk} [Max\{X_j, Y_j\}]\,, \tag{3.8}$$

subject to constraints (3.2), (3.3), (3.4) and (3.5).

As a solution of Model SP, we must know how to assign the K unit loads into the smallest number of lanes. Model SP is equivalent to minimizing the required number of storage lanes for storing K unit loads subject to constraints (3.2), (3.3), (3.4), and (3.5) (denoted by Model TP). Therefore, an optimal solution of Model TP is also an optimal solution of Model SP. If we can prove Model TP is strongly NP-complete, we then know Model SP, which is a special case of Model P, is strongly NP-complete.

In the following, we transform the problem defined by Model TP to be the Graph C-colorability problem.

Definition (Graph C-colorability (Chromatic number) problem): Define a graph where V and E are the sets of vertices and undirected edges. A positive integer C, $C \le |V|$, represents the total number of colors. Each vertex must be colored with only one color of $\{1, 2,..., C\}$ and any two vertices on the same edge have to be colored differently. The question is: Is G C-colorable, i.e. is there a function $f : V \to \{1, 2,..., C\}$ such that $f(u) \ne f(v)$ whenever $(u, v) \in E$?

Suppose each truck has one unit load and there are no two unit loads of the same product. Each vertex of the graph represents a shipping truck and if trucks u and v have overlapping time windows, vertices u and v are connected by an edge. A color can then correspond to a storage lane.

We need to make two steps:

1. Show that the problem belongs to NP.

2. Show that a strongly NP-complete problem reduces to our problem.

To demonstrate (1) it suffices to remark that a nondeterministic algorithm can check in polynomial time whether a given solution is feasible (i.e. $f(u) \neq f(v)$ whenever $(u,v) \in E$).

To demonstrate (2) we remark the formulation of Model TP exactly matches the Graph C-colorability (Chromatic number) problem which is proven to be strongly NP-complete by Garey and Johnson (1979). Hence, we can conclude that Model SP and then Model P are strongly NP-complete.

Appendix 3B: Illustrative example 1

Consider a single-level compact storage system with a rack configuration as given in Table 3.9. Figure 3.7 illustrates a top view of the rack. In each storage slot the travel distance to the I/O point is given. The time windows of unit loads are shown in Table 3.10.

Table 3.9. Rack configuration and system parameters

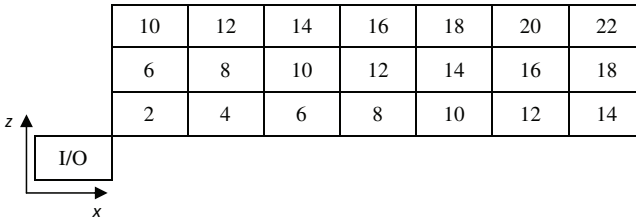| Parameter	value
Number of levels	1
Number of lanes	7
Number of depth tiers	3

Figure 3.7. Travel distance of each storage location to the I/O point

Table 3.10. Earliest and latest arrival times of trucks

Truck index	Earliest arrival time	Latest arrival time	Latest - Earliest(hours)	Number of unit loads	Indices of unit loads	Products
1	0	1	1	2	{1,2}	{A, C}
2	1	3	2	2	{3,4}	{A, D}
3	0	2	2	1	{5}	{B}
4	2	3	1	2	{6,7}	{E, F}
5	2	4	2	2	{8,9}	{B, G}

Appendix 3C: The optimality of the C&I heuristic

In order to investigate the optimality of the C&I heuristic, we searched for a counterexample in small size problems. We obtained a counterexample that the C&I heuristic cannot provide the optimal solution and a gap exists between the optimal solution and the heuristic solution.

Consider a rack with 5 lanes and 2 depth tiers. Figure 3.8 shows a top view of the rack. I/O point is located at lower left of the rack. The numbers in storage locations indicate the distance of the storage locations to the I/O point in time units.

2.1	3.1	4.1	5.1	6.1
1	2	3	4	5

I/O
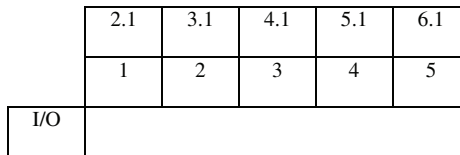
Figure 3.8. Travel time distance of storage locations from I/O point

Table 3.11 shows the orders that have to be shipped to customers in the next shift.

Table 3.11. Orders placed by five different customers in a shift

Order	Order size	Product	Time window $(a<b<c<d)$
O_1	1	A	$[a, b]$
O_2	1	A	$[a, b]$
O_3	1	A	$[a, b]$
O_4	1	B	$[a, b]$
O_5	1	C	$[c, d]$

Figure 3.9(a) shows the results of the C&I heuristic and Figure 3.9(b) shows the optimal solution for the proposed example. The 8% gap between the total retrieval times of the solution provided by the C&I heuristic and the optimal solution proves that the C&I heuristic cannot guarantee the optimal solution for every instance.
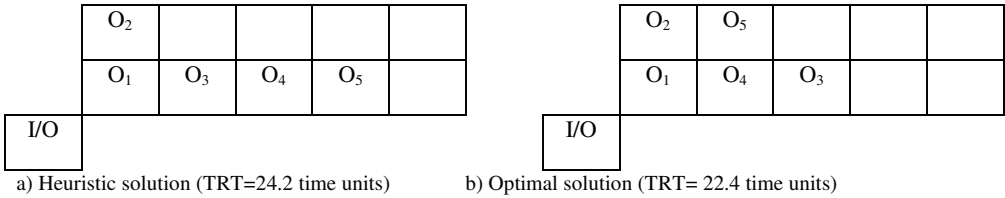
O_2				
O_1	O_3	O_4	O_5	

I/O

O_2	O_5			
O_1	O_4	O_3		

I/O

a) Heuristic solution (TRT=24.2 time units)   b) Optimal solution (TRT= 22.4 time units)

Figure 3.9. (a) Solution of the heuristic, (b) optimal solution for the counterexample

Chapter 4

Optimal Configuration of a Live-cube Compact Storage System

4.1. Introduction

In traditional storage systems, vehicles transporting unit loads needing storage or retrieval require transport aisles. These aisles occupy much space that could otherwise be used to store unit loads. Compact storage systems have been introduced to increase the storage density. The higher storage density results in a smaller storage system leading to lower investment and operational costs (Gue and Kim, 2007). As a result, a new generation of storage systems is emerging; 'live-cube' compact storage systems. In a live-cube compact storage system, the highest possible storage density can be achieved as virtually no empty moving space is needed. Saving storage space is particularly important in places where land or space is scarce. Live-cube systems can respond fast to customer requests due to simultaneous and

collaborative movements of different components. However, this high storage density might also lead to long response times due to interfering unit loads.

Due to the novelty and complexity of live-cube storage systems, research is still scarce with many unanswered fundamental questions including:

1. What is the performance of a live-cube compact storage system?
2. What is the impact of the system dimensions on the system performance?

This chapter aims to answer the above two questions. Chapter 1 illustrates the main components and work mechanism of a live-cube compact storage system (see Figure 1.3). Shuttles can move in x and y directions while carrying a unit load. Each unit load holds only one product type. All storage locations and unit loads are standard and have the same size. Therefore, all storage locations can be used for storing any unit load. Shuttles simultaneously move unit loads into the empty locations (at least one empty location needed on each level) to maneuver the desired unit load to the lift at the unit load's storage level. A lift facilitates the movements of the unit loads across different levels in z direction. The shuttles can move independently of the lift. We assume the I/O point is located at the lower left corner of the system (at the ground level) and we furthermore assume a random storage policy is used, which implies that each location is equally likely to contain a requested unit load. The random storage policy is broadly studied in the literature (e.g. Hausman et al., 1976, Bozer and White, 1984, Lee and Elsayed, 2005, De Koster et al., 2008). Random storage requires the least data since no product information is used in determining storage assignment (Goetschalckx and Ratliff, 1990). In addition, random storage is frequently used as a benchmark in comparison for system response time with other storage policies (e.g. by Hausman et al., 1976, and Lee and Elsayed, 2005).

Our first contribution is the derivation of expected retrieval time formulas for an arbitrary retrieval corresponding to all possible (16 in total) system configurations through a rather complex decomposition procedure. Our second contribution is deriving closed-form expressions for the optimal dimensions of a live-cube compact storage system minimizing the expected retrieval time. To obtain these dimensions, we propose a mixed-integer nonlinear model. We split the model into several solvable sub-models such that the optimal solution for each sub-model can be obtained. The global optimal solution can be found by comparing the optimal solutions of all the sub-models. Although the procedure for determining the optimal solutions is tedious, the results are simple.

Traditional automated material handling systems have been studied extensively in the literature over the past thirty years. For a general review on the design and control of automated material handling

systems, we refer to Johnson and Brandeau (1996) and Roodbergen and Vis (2009). However, compact storage systems have not yet been widely studied in the academic literature (Stadtler, 1996, Sari et al., 2005, De Koster et al., 2008, Yu and De Koster, 2009b, Zaerpour et al., 2010). De Koster et al. (2008) and Yu and De Koster (2009b) study the optimal design of a compact storage system where conveyors take care of the movement of unit loads in depth direction. To access a unit load, other unit loads also need to be moved by the rotating conveyor. They optimally solve the problem by decomposing it into three cases.

Stadtler (1996), Sari et al. (2005), and Zaerpour et al. (2010) study unit load storage assignment in compact storage systems using different horizontal movement mechanisms (e.g. satellite-based and conveyor-based compact storage systems). Gue and Kim (2007) study a single-level live-cube (which they call a 'puzzle-based' storage system). For systems with a single empty location, they develop a method to maneuver unit loads to the I/O point minimizing the retrieval time of an arbitrary unit load. In addition, for systems with multiple empty locations, they propose a heuristic retrieval method yielding short retrieval times. To our knowledge, this is the first study on multi-level live-cube compact storage systems. Our study differs from Gue and Kim's work in two respects. First, this study considers a multi-level live-cube system. Second, while they develop methods to move unit loads, we focus on the optimal design of the live-cube system, using a simple method to maneuver unit loads to the I/O point. This simple method enables us to derive closed-form expressions for the expected retrieval time.

The remainder of this chapter is organized as follows. Section 4.2 describes the problem and gives the notations and model assumptions. Section 4.3 derives the expected retrieval time for single-level and multi-level systems. Section 4.4 proposes the mathematical model and obtains the optimal system dimensions for single-level and multi-level systems. Section 4.5 discusses results and further extensions. Section 4.6 concludes the chapter.

4.2. Problem description and assumptions

Consider a system with length l (in travel time units), width or depth w (in travel time units) and height h (in travel time units). For the sake of convenience and without loss of generality, we suppose that the travel time in length direction of the system is not less than the travel time in the depth direction; i.e. $l \geq w$ (see also Bozer and White (1984) and Eynan and Rosenblatt (1994)).

The retrieval time of a unit load at a given level depends on its (x,y) position, and the distribution of empty locations on its trajectory to the lift. In case only one empty location is available Gue and Kim

(2007) show it equals $4x + 2y - 8$ (if $x > y$). However, in practice utilizations of not more than 95% are common in systems containing 1000 unit loads or more. This implies that at one level sufficient empty locations are commonly available to create a virtual aisle to maneuver a requested unit load the lift at the same level without interfering with other unit loads (a sufficient condition for this is that the number of empty locations on a level equals at least the maximum of the number of rows and the number of columns. For more details about the properties of such a system, see Appendix 4A). This assumption does not prohibit a potentially high utilization of the system while it reduces the retrieval time of any unit load significantly compared to results of Gue and Kim (2007). Figure 4.1 shows an example situation where a car needs to be moved out of a single-level live-cube parking system. Block movement is possible; i.e. moving multiple unit loads simultaneously if the movement path is a straight line. Therefore, a virtual aisle can be created immediately by simultaneously moving interfering cars. The desired car can then be moved to the I/O point without any further interference.

| Retrieval request | A solution by creating a virtual aisle |
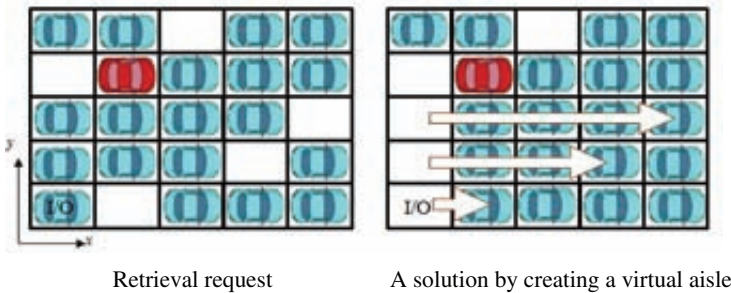
Note. The requested car is shown by a dark color

Figure 4.1. A virtual aisle in a single-level live-cube parking system

For a system where the I/O point is at the left-lower corner the retrieval time of a unit load at location (x,y) of a single-level live-cube storage system, $t(x, y)$, can be calculated by

$$t(x, y) = x + y.$$ (4.1)

In Equation (4.1) we neglect the small (constant) time needed to create the virtual aisle (see Appendix 4A) and assume the coordinates of the system to be continuous. The assumption of continuous dimensions is commonly made in other papers (e.g. Hausman et al., 1976, Yu and De Koster, 2009b). It considerably simplifies the problem analysis while the results are normally sufficiently close to those of

real world discrete rack systems, as long as the system size is not too small and there is a sufficiently high number of levels.

In a multi-level live-cube system, (x,y,z) is a location (in travel time units) where z refers to the level coordinate (in travel time units) in vertical direction. When idle, the lift waits at the ground level (this assumption will be relaxed in section 4.5.2).

The retrieval time of a unit load consists of the following two components:

1. The time needed to bring the unit load to the lift. Since the movements in x and y directions are independent of movement in z direction, this time equals $\max\{x+y,z\}$ where $x+y$ is from Equation (4.1) and z is the time needed for the lift to go from the I/O point to level z.

2. The time needed for the lift to return to the I/O point from level z.

Thus, the retrieval time of a unit load located at (x,y,z) to the I/O point for a multi-level system can be calculated by

$$t(x,y,z) = \max\{x+y,z\} + z .$$
(4.2)

Equation (4.2) gives an estimate for the retrieval time of a given unit load. In order to evaluate the performance of the system the expected value of the retrieval time of an arbitrary unit load must be derived. This expression can then be used to optimize the dimensions of the system leading to minimum expected retrieval time.

4.3. Derivation of the expected retrieval time of an arbitrary unit load

In order to calculate the expected retrieval time of an arbitrary unit load, the probability density function of the retrieval time must be obtained. This is done by splitting the system into several cases and then obtaining the probability density function for each case individually. Section 4.3.1 explains the procedure for single-level systems while section 4.3.2 extends the procedure to multi-level systems.

4.3.1. Expected retrieval time for the single-level system

The retrieval time of a unit load in a single-level system at position (x,y) is calculated by $x+y$. Let $T=X+Y$, where X and Y are random variables representing the length and depth coordinates of the system, respectively. The cumulative distribution function of T is denoted by $F(t)$ and the probability density function of T is denoted by $f(t)$. We have $F(t) = P(T \le t) = P(X + Y \le t)$. The set $\{(x,y) \mid x + y \le t\}$

includes all the locations with coordinates (x,y) where $x + y \leq t$. Since under random storage all locations have the same probability of being requested, the probability that the retrieval time is less than or equal to t equals the area of $T \leq t$ divided by the area of the whole system (lw). The corresponding shapes are illustrated in Figures 4.2(a), 4.2(b) and 4.2(c) for increasing t values.

The cumulative distribution function of the retrieval time can be calculated as follows:

One of the three below cases is possible:

- When $0 \leq t \leq w$, according to Figure 4.2(a) we have:

$F_{0 \leq t \leq w}(t) = P(T \leq t) = P(X + Y \leq t) = (t^2 / 2) / (lw)$. Hence, $f_{0 \leq t \leq w}(t) = t / (lw)$.

- When $w < t \leq l$, according to Figure 4.2(b) we have:

$F_{w < t \leq l}(t) = P(T \leq t) = P(X + Y \leq t) = (2tw - w^2) / (2lw)$. Hence, $f_{w < t \leq l}(t) = 1 / l$.

- When $l < t \leq l+w$, according to Figure 4.2(c) we have:

$F_{l < t \leq l+w}(t) = P(T \leq t) = P(X + Y \leq t) = (2wt + 2lt - t^2 - w^2 - l^2) / (2lw)$. Hence, $f_{l < t \leq l+w}(t) = (w + l - t) / (lw)$.
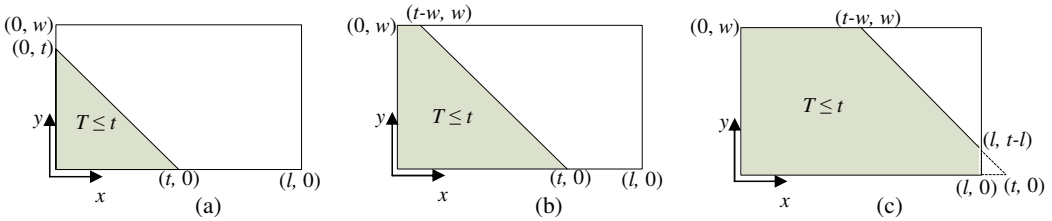
Figure 4.2. Area of $T \leq t$ if (a) $0 \leq t \leq w$ (b) $w < t \leq l$ (c) $l < t \leq l+w$

Therefore, $f(t)$ can be written as follows:

$$f(t) = \begin{cases} t / (lw) & \text{if } t \leq w, \\ 1 / l & \text{if } w < t \leq l, \\ (w + l - t) / (lw) & \text{if } l < t \leq l + w. \end{cases}$$

Consequently, the expected retrieval time $E[T]$ can be calculated:

$$E[T] = \int_{(x,y)} f(t)t(x,y)\,dxdy = \int_{t=0}^{w} t f_{0 \leq t \leq w}(t)dt + \int_{t=w}^{l} t f_{w < t \leq l}(t)dt + \int_{t=l}^{l+w} t f_{l < t \leq l+w}(t)dt = \frac{l + w}{2}.$$

This result is quite intuitive in view of the random storage policy and the fact that movements in x and y directions are carried out sequentially.

4.3.2. Expected retrieval time for the multi-level system

The expected retrieval time of an arbitrary unit load in a multi-level live-cube storage system with a given capacity can be calculated as:

$$E[T] = \int_{t=0}^{\max\{w+l,h\}+h} t f(t) dt ,$$

where t represents the retrieval time for retrieval location (x, y, z). $f(t)$ represents the probability density function of retrieval time, t, $0 \leq t \leq \max\{w+l,h\}+h$. The cumulative distribution function of retrieval time $F(t)$ can be calculated as:

$$F(t) = P(T \leq t) = P(\max\{X+Y,Z\}+Z \leq t) = P(X+Y+Z \leq t \cap 2Z \leq t) .$$

The two conditions, $X+Y+Z \leq t$ and $2Z \leq t$ are not independent. Therefore, we have to consider both conditions simultaneously which increases the complexity of calculations. The two following inequalities form the shape which includes all the locations with retrieval time less than or equal to t: $x+y+z \leq t$ and $2z \leq t$ where $x, y, z \geq 0$. Figure 4.3(a) illustrates the shape which includes all the locations with retrieval time less than or equal to t. Therefore, for any value of retrieval time t, the probability that the random variable T is less than or equal to t is given by Equation (4.3),

$$F(t) = P(T \leq t) = \frac{\text{volume of the region } T \leq t \text{ in the system}}{\text{volume of the system}} . \qquad (4.3)$$

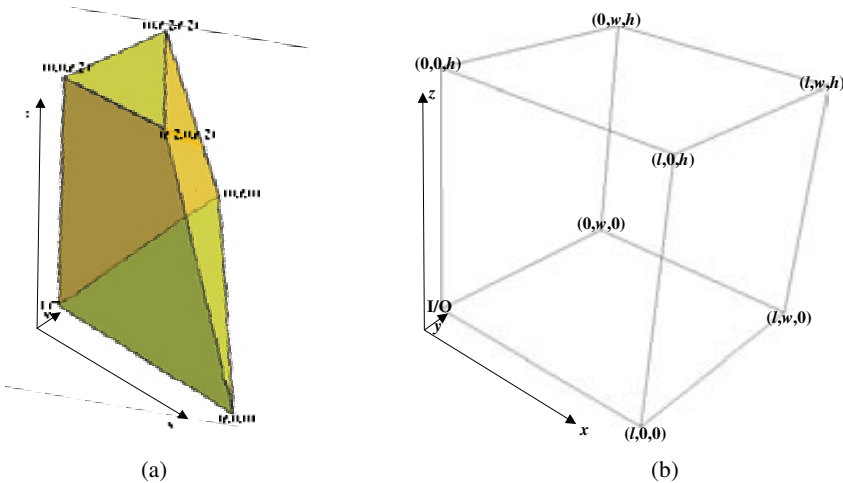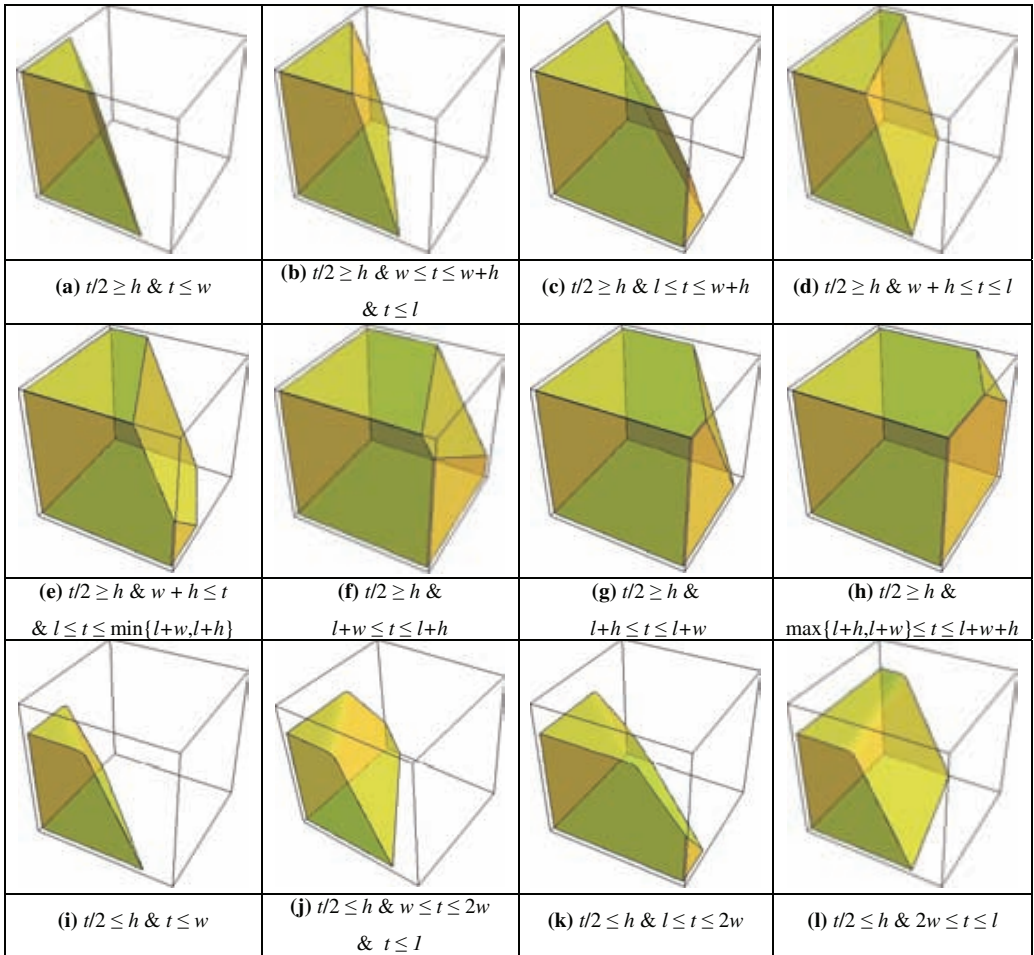
(a)   (b)

Figure 4.3. (a) The region formed by $x+y+z \leq t$ and $2z \leq t$ (b) cubic shape of a multi-level system with its corner points

In Figure 4.3(a), two planes, $x + y + z = t$ and $2z = t$ are contour planes where the retrieval time of locations located on these two planes equals t. However, the region in Figure 4.3(a) is also restricted by the system as illustrated in Figure 4.3(b). Therefore, the shape in Figure 4.3(a) can be truncated in different ways depending on the system dimensions and retrieval time t. Figure 4.4 illustrates all possible shapes for different system sizes and retrieval times t. The probability density function can be derived for each shape separately by using Equation (4.3).

(a) $t/2 \geq h$ & $t \leq w$	**(b)** $t/2 \geq h$ & $w \leq t \leq w+h$ & $t \leq l$	**(c)** $t/2 \geq h$ & $l \leq t \leq w+h$	**(d)** $t/2 \geq h$ & $w + h \leq t \leq l$
(e) $t/2 \geq h$ & $w + h \leq t$ & $l \leq t \leq \min\{l+w, l+h\}$	**(f)** $t/2 \geq h$ & $l+w \leq t \leq l+h$	**(g)** $t/2 \geq h$ & $l+h \leq t \leq l+w$	**(h)** $t/2 \geq h$ & $\max\{l+h, l+w\} \leq t \leq l+w+h$
(i) $t/2 \leq h$ & $t \leq w$	**(j)** $t/2 \leq h$ & $w \leq t \leq 2w$ & $t \leq l$	**(k)** $t/2 \leq h$ & $l \leq t \leq 2w$	**(l)** $t/2 \leq h$ & $2w \leq t \leq l$

(m) $t/2 \leq h$ & $2w \leq t$	**(n)** $t/2 \leq h$ &	**(o)** $t/2 \leq h$ &	**(p)** $t/2 \leq h$ &
& $l \leq t \leq l+w$	$l+w \leq t \leq 2l$	$2l \leq t \leq 2(l+w)$	$2(l+w) \leq t \leq 2h$
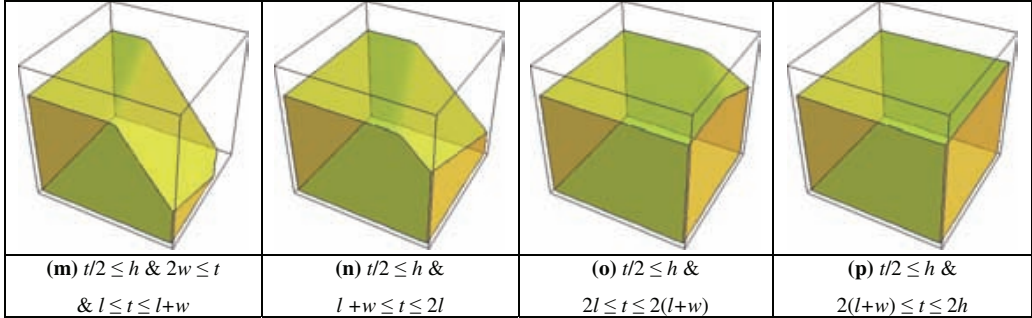
Figure 4.4. All possible shapes of the region $T \leq t$ in the system

It turns out that calculation of $E[T]$ can be classified into four different complementary cases, each referring to a specific configuration of the system. The four cases of system configuration are:

- Case A. $h \leq w$,
- Case B. $w \leq h \leq l$,
- Case C. $l \leq h \leq l+w$, and
- Case D. $l+w \leq h$.

These cases can again be split in several sub-cases. As an illustration, in section 4.3.2.1 the calculation of $E[T]$ for one sub-case of case A (sub-case A.1) is explained. Section 4.3.2.2 gives the formulas of $E[T]$ for all the other cases.

4.3.2.1. Computation of expected retrieval time of an arbitrary unit load for case A

In this section, we give the detailed procedure of calculating $E[T]$ for one of the sub-cases of case A (sub-case A.1: $l \leq 2h$). Given the configuration of sub-case A.1, Figures 4.5(a-g) show how the region $T \leq t$ changes with increasing retrieval time t.

Definition 1 (Critical retrieval time). The critical retrieval time is a time instant t at which the region $T \leq t$ changes shape, resulting in a different volume formula.

It can be shown that for case A, the region $T \leq t$ changes at the following values for t:

$$w, l, 2h, w+h, l+h, w+l, l+w+h. \tag{4.4}$$

For sub-case A.1, we can arrange the critical retrieval times as follows,

$$w \leq l \leq 2h \leq h+w \leq h+l \leq l+w \leq l+w+h. \tag{4.5}$$

Equation (4.5) gives seven different possible positions of the retrieval time $t: 0 \leq t < w$; $w \leq t < l$ ... $l+w \leq t \leq l+w+h$ each corresponding to one of the figures in Figure 4.5.

For Figure 4.5(a), we have $0 \leq t < w$. Since $t < w$ the shape does not touch the $y = w$ plane of the cube. In addition, since $w \leq l$, the shape also does not touch the $x = l$ plane of the cube. Furthermore, $z = t/2$ represents the top surface of the shape. However, $t < w$ and also $w < 2h$ (see Equation (4.5)) and therefore $t < 2h$. Hence, the plane $z = t/2$ of the shape does not touch the plane $z = h$ of the cube.

For Figure 4.5(b), $w \leq t < l$. Since $w \leq t$ the shape touches the $y = w$ plane of the cube. The point ($t-w,w,0$) in the $y = w$ plane has a retrieval time equal to t ($t-w+w$) which is greater than w. The explanation of the shape of the polytope in x and z directions is similar to the previous shape.

In Figure 4.5(c), $l \leq t < 2h$. Since $l \leq t$, the shape touches the $x = l$ plane of the cube. The retrieval time of the corner point ($l,t-l,0$) of the shape has retrieval time t ($t-l+l$) which is greater than l. The explanation in of the shape in y and z directions is similar to the previous shape.

The other shapes of the Figure 4.5 can be explained similarly.

| **(a)** $0 \leq t < w$ | **(b)** $w \leq t < l$ | **(c)** $l \leq t < 2h$ |
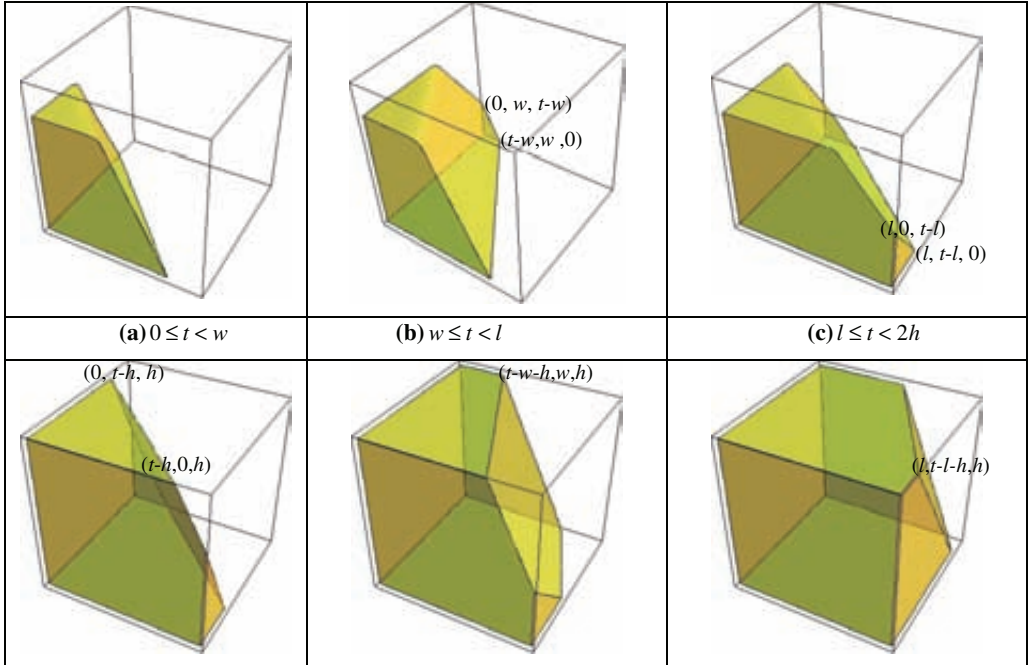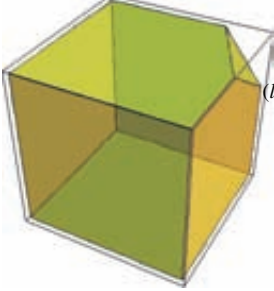
(d) $2h \le t < h+w$	**(e)** $h+w \le t < h+l$	**(f)** $h+l \le t < l+w$
$(l,w,t\text{-}l\text{-}w)$		
(g) $l+w \le t \le l+w+h$		

Figure 4.5. Region of $T \le t$ for sub-case A.1 ($l \le 2h$) with increasing t

We now derive the volumes of the first three shapes in Figure 4.5. To derive the volumes of the first three shapes we consider the base of the shape to be in the $y\,z$-plane.

For Figure 4.5(a), y and z are bounded: $0 \le y \le t-z$ and $0 \le z \le t/2$. The volume of the shape can be obtained by integrating the function $\min\{l,t-y-z\}$ over the mentioned boundaries. In this case $\min\{l,t-y-z\}$ always equals $t-y-z$. Therefore, the volume of Figure 4.5(a) is given by

$$\int_{z=0}^{t/2}\int_{y=0}^{t-z}(t-y-z)\,dy\,dz = 7t^3/48\,.$$

In Figure 4.5(b) y and z are bounded as follows: $0 \le y \le \min\{w,t-z\}$, $0 \le z \le t/2$. The volume is given by

$$\int_{z=0}^{t/2}\int_{y=0}^{\min\{w,t-z\}}(t-y-z)\,dy\,dz\,.$$

Figure 4.5(b) shows the line $y = t-z$ intersects $y = w$ plane at point $(0,w,t\text{-}w)$. For any $z \le t\text{-}w$, $\min\{w,t-z\} = w$ and for any $z > t\text{-}w$, $\min\{w,t-z\} = t-z$. Therefore, the volume of Figure 4.5(b), where $w \le t < l$, is given by

$$\int_{z=0}^{t-w}\int_{y=0}^{w}(t-y-z)\,dy\,dz + \int_{z=t-w}^{t/2}\int_{y=0}^{t-z}(t-y-z)\,dy\,dz = \frac{1}{48}\left(-t^3 + 24t(t-w)w + 8w^3\right).$$

In Figure 4.5(c), y and z are bounded as follows: $0 \leq y \leq \min\{w, t-z\}$, $0 \leq z \leq t/2$. Figure 4.5(c) is a truncated version of Figure 4.5(b); the plane $x = l$ has removed a pyramid shaped top in x direction. Therefore, volume (third shape) = volume (second shape) - volume (removed pyramid).

The height of the removed pyramid equals t-l, and the base of pyramid is a right triangle with both legs equaling t-l. Therefore, the volume of the removed pyramid equals $(t-l)^3/6$. The resulting volume of Figure 4.5(c) is given by

$$\int_{z=0}^{t-w}\int_{y=0}^{w}(t-y-z)dydz + \int_{z=t-w}^{t/2}\int_{y=0}^{t-z}(t-y-z)dydz - \frac{1}{6}(t-l)^3 = \frac{1}{48}\left(-t^3 - 8(t-l)^3 + 24t(t-w)w + 8w^3\right).$$

The volumes of the other figures can be derived similarly. The formulas representing the volumes of Figures 4.4(a-p) are given in Appendix 4B.

The cumulative distribution function for each boundary in Figure 4.5 can be derived by dividing its volume by the volume of the cube: $V_{cube} = w\,l\,h$. By taking the derivative, the probability density function is obtained. Corresponding to Figures 4.5(a-c), the cumulative and density functions are given by

$$F_{t<w}(t) = \left(7t^3/48\right)/(wlh),$$

$$f_{t<w}(t) = \frac{dF_{t<w}}{dt} = \left(21t^2/48\right)/(wlh),$$

$$F_{w\leq t<l}(t) = (\frac{1}{48}\left(-t^3 + 24t(t-w)w + 8w^3\right))/(wlh),$$

$$f_{w\leq t<l}(t) = \frac{dF_{w\leq t<l}}{dt} = \frac{-3t^2 + 24tw + 24(t-w)w}{48hlw},$$

$$F_{l\leq t<2h}(t) = (\frac{1}{48}\left(-t^3 - 8(t-l)^3 + 24t(t-w)w + 8w^3\right))/(wlh),$$

$$f_{l\leq t<2h}(t) = \frac{dF_{l\leq t<2h}}{dt} = \frac{-24(l-t)^2 - 3t^2 + 24tw + 24(t-w)w}{48hlw}.$$

The probability density function for other boundaries in Figure 4.5 can be calculated similarly. This results in:

$$f(t) = \begin{cases} \left(21t^2/48\right)/\left(wlh\right) & \text{if } 0 \leq t < w, \\[2mm] \dfrac{-3t^2 + 24tw + 24(t-w)w}{48hlw} & \text{if } w \leq t < l, \\[3mm] \dfrac{-24(l-t)^2 - 3t^2 + 24tw + 24(t-w)w}{48hlw} & \text{if } l \leq t < 2h, \\[3mm] \dfrac{-3h^2 - 3(l-t)^2 + 6ht - 3t^2 + 3tw + 3(t-w)w}{6hlw} & \text{if } 2h \leq t < w+h, \\[3mm] \dfrac{-\dfrac{1}{2}(l-t)^2 + hw}{hlw} & \text{if } w+h \leq t < l+h, \\[3mm] \dfrac{h + 2(l-t+w)}{2lw} & \text{if } l+h \leq t < l+w, \\[3mm] \dfrac{(h+l-t+w)^2}{2hlw} & \text{if } l+w \leq t \leq l+w+h, \\[3mm] 0 & \text{otherwise.} \end{cases} \tag{4.6}$$

From this the total expected retrieval time of an arbitrary unit load for sub-case A.1 can be calculated, as

$$\begin{aligned} \mathrm{E}[\mathrm{T}_{A1}] = &\int_0^w \left(\left(21t^3\right)/48\right)/\left(wlh\right) dt + \int_w^l \left(t\left(-\frac{t^2}{16} + \frac{tw}{2} + \frac{1}{2}(t-w)w\right)\right)/\left(wlh\right) dt \\ &+ \int_l^{2h} \left(t\left(-\frac{t^2}{16} - \frac{1}{2}(-l+t)^2 + \frac{tw}{2} + \frac{1}{2}(t-w)w\right)\right)/\left(wlh\right) dt \\ &+ \int_{2h}^{w+h} \left(t\left(-\frac{1}{2}(-l+t)^2 + \frac{1}{6}\left(-3h^2 + 6ht - 3t^2\right) + \frac{tw}{2} + \frac{1}{2}(t-w)w\right)\right)/\left(wlh\right) dt \\ &+ \int_{w+h}^{l+h} \left(t\left(-\frac{1}{2}(-l+t)^2 + hw\right)\right)/\left(wlh\right) dt \\ &+ \int_{l+h}^{l+w} \left(t\left(-\frac{1}{2}(l-t+w)^2 + \frac{1}{2}(h+l-t+w)^2\right)\right)/\left(wlh\right) dt + \int_{l+w}^{l+w+h} \left(t\left(\frac{(h+l-t+w)^2}{2(wlh)}\right)\right) dt \\ = &\frac{h^3 + 12hlw + 12lw(l+w)}{24lw}. \end{aligned}$$

This expression is only valid for sub-case A.1 ($l \leq 2h$). However, case A can be divided in 5 different sub-cases due to 5 different possible arrangements of the critical retrieval times (see Equation (4.4)).

- Sub-case A.1. $l \leq 2h$,
- Sub-case A.2. $w \leq 2h$ and $2h < l \leq w+h$,

- Sub-case A.3. $w \leq 2h$ and $l > w + h$,

- Sub-case A.4. $w > 2h$ and $2h < l \leq w + h$, and

- Sub-case A.5. $w > 2h$ and $l > w + h$.

$E[T]$ can be calculated in a similar way for sub-cases A.2-A.5. The results are summarized in Theorem 1.

Theorem 1. *The expected retrieval times ($E[T]$) for all sub-cases of case A ($h \leq w$) can be formulated as Equation* (4.7),

$$E[T_A] = E[T_{A1}] = E[T_{A2}] = E[T_{A3}] = E[T_{A4}] = E[T_{A5}] = \frac{h^3 + 12hlw + 12lw(l + w)}{24lw} \qquad \text{if } h \leq w. \quad (4.7)$$

Proof. See Appendix 4C.

4.3.2.2. Expected retrieval time of an arbitrary unit load for cases B, C and D

The expected retrieval time $E[T]$ for cases B,C, and D can be derived in a similar fashion to case A. Theorems 2-4 summarize the results. All the proofs can be found in Appendix 4D.

Theorem 2. *The expected retrieval time ($E[T]$)of an arbitrary unit load for case B ($w \leq h \leq l$) is given by Equation* (4.8),

$$E[T_B] = \frac{4h^3 + 6h^2(2l - w) - w^3 + 4h(3l^2 + 3lw + w^2)}{24hl} \qquad \text{if } w \leq h \leq l. \qquad (4.8)$$

Theorem 3. *The expected retrieval time ($E[T]$) of an arbitrary unit load for case C ($l \leq h \leq l + w$) is given by Equation* (4.9),

$$E[T_C] = -\frac{h^4 + l^4 + 6h^2(l - w)^2 + w^4 - 4h^3(l + w) - 4h(l + w)^3}{24hlw} \quad \text{if } l \leq h \leq l + w. \qquad (4.9)$$

Theorem 4. *The expected retrieval time ($E[T]$) of an arbitrary unit load for case D ($l + w \leq h$) is given by Equation* (4.10),

$$E[T_D] = \frac{12h^2 + 2l^2 + 3lw + 2w^2}{12h} \qquad \text{if } l + w \leq h. \qquad (4.10)$$

4.4. General model and optimization

The results obtained in the previous section can be used to optimize the system dimension by minimizing the expected retrieval time. Section 4.4.1 gives the mathematical model for a single-level system and

obtains the optimal solutions. Section 4.4.2 gives the mathematical model for a multi-level system and solves it optimally.

4.4.1. Optimizing the single-level system

To optimize the dimensions of the single-level storage system, Model SGM can be formulated:

Model SGM

$$\min E[T],\tag{4.11}$$

subject to:

$$lw = A,\tag{4.12}$$

$$l - w \geq 0,\tag{4.13}$$

decision variables: $l > 0,$ and $w > 0$.

Equation (4.11) minimizes the expected retrieval time of an arbitrary unit load. Constraint (4.12) ensures the given storage capacity A is achieved. Constraint (4.13) ensures the length equals at least the width of the system.

The optimal length (l^*) and width (w^*) of the system can be obtained from this model. To find the optimal values of decision variables the expression for $E[T]$ is derived in section 4.3.1.

If unit loads are stored according to the random storage policy, the optimal dimensions of the system are given by Theorem 5.

Theorem 5. *For a single-level live-cube storage system, the optimal system dimensions, minimizing the expected retrieval time under a random storage policy, are given by*

$$l^* = w^* = \sqrt{A}.$$

Proof. If a random storage policy is used, model SGM can be rewritten as follows:

$$\min E[T] = \frac{l + w}{2},\tag{4.14}$$

subject to

$$lw = A,$$

$$l - w \geq 0,$$

decision variables: $l > 0,$ and $w > 0$.

From constraint (12), we have:

$$w = A / l.\tag{4.15}$$

Substituting Equation (4.15) into Equation (4.14), we have $E[T] = \dfrac{l^2 + A}{2l}$.

Because $\dfrac{d^2 E[T]}{dl^2} = \dfrac{A}{4l^4} > 0$, $E[T]$ is a convex function of l. Let $\dfrac{dE[T]}{dl} = \dfrac{l^2 - A}{2l^2} = 0$, only one minimum

can be obtained at $l^* = \sqrt{A}$ and thus $w^* = \sqrt{A}$ resulting in $E[T^*] = \sqrt{A}$.   □

4.4.2. Optimizing the multi-level system

To optimize the dimensions of storage system in a multi-level system, we propose the following mixed-integer model (Model MGM):

Model MGM

$$\min \sum_{i \in \{A,B,C,D\}} u_i E[T_i] , \tag{4.16}$$

subject to:

$$lwh = V , \tag{4.17}$$

$$l - w \geq 0 , \tag{4.18}$$

$$\sum_{i \in \{A,B,C,D\}} u_i = 1 , \tag{4.19}$$

$$u_A(w - h) \geq 0 , \tag{4.20}$$

$$u_B(h - w) \geq 0 , \tag{4.21}$$

$$u_B(l - h) \geq 0 , \tag{4.22}$$

$$u_C(h - l) \geq 0 , \tag{4.23}$$

$$u_C(l + w - h) \geq 0 , \tag{4.24}$$

$$u_D(h - l - w) \geq 0 , \tag{4.25}$$

Decision variables: $l > 0, w > 0, h > 0$, and $u_i \in \{0,1\}$ for $i \in \{A, B, C, D\}$.

Equation (4.16) minimizes the expected retrieval time $E[T]$. Constraint (4.17) makes sure that the given capacity is achieved. Constraint (4.18) ensures the length is at least equal to the width of the

system. Constraint (4.19) guarantees exactly one of the cases is considered in the objective function. Constraints (4.20)-(4.25) take care of the feasibility of the solutions of each case.

In order to solve Model MGM, we first solve each case individually and obtain the optimal solution in each case. Next, by comparing the optimal solutions obtained from the four cases the optimal solution of Model MGM can be found.

Optimizing the dimensions in case A ($h \leq w$)

For this case, the following theorem shows that in the optimal solution, the optimal values of the length and the width of the system are equal ($w^* = l^*$).

Theorem 6. *In the optimal solution of case A, the optimal values of the length and width of the system are equal ($w^* = l^*$).*

Proof. See Appendix 4E.

Since $w^* = l^*$, w can be replaced with l in the model. Furthermore, since $w l h = V$ we can replace l with $(V / h)^{1/2}$. Thus, the objective function can be written as a function of h,

$$E[T_A(h)] = \frac{h(h^3 + 12V + 24(V/h)^{3/2})}{24V}.$$

The optimal value of h, minimizing the objective function can be obtained by the first order condition,

$$\frac{dE[T_A]}{dh} = \frac{h^4 + 3hV - 3V\sqrt{V}}{6hV} = 0.$$

The following equations give the optimal values of l, w and h, which satisfy the condition $0 < h \leq w$,

$$h^*(V) = \left(-2 + \left(\frac{1}{2}(11 - 3\sqrt{13}) \right)^{1/3} + \left(\frac{1}{2}(11 + 3\sqrt{13}) \right)^{1/3} \right)^{1/3} V^{1/3} = 0.874 V^{1/3}, \tag{4.26}$$

$$w^*(V) = l^*(V) = \left(\left(-2 + \left(\frac{1}{2}(11 - 3\sqrt{13}) \right)^{1/3} + \left(\frac{1}{2}(11 + 3\sqrt{13}) \right)^{1/3} \right)^{1/3} \right)^{-1/2} V^{1/3} = 1.069 \ V^{1/3}. \tag{4.27}$$

The second derivative test proves that the objective function is a convex function and therefore the optimal dimension values give the minimum objective value,

$$\frac{d^2 E[T_A]}{dh^2} = \frac{h^2}{2V} + \frac{3\sqrt{V/h}}{4h^2} \geq 0.$$

Optimizing the dimensions in cases B, C and D

The following equations give the optimal values of h, w and l for case B ($w \le h \le l$) as a function of the volume of the system. The detailed calculation is given in Appendix 4F.

$$h^*(V) = w^*(V) = (-3+\sqrt{15})^{1/3} \ V^{1/3} = 0.955V^{1/3}$$

$$l^*(V) = \frac{V^{1/3}}{\left(-3+\sqrt{15}\right)^{2/3}} = 1.094 \ V^{1/3}$$

For case C ($l \le h \le l+w$) the optimal values of h and w and l as a function of the volume of the system are

$$h^*(V) = w^*(V) = l^*(V) = \ V^{1/3}.$$

For case D ($l+w \le h$) the optimal values of h, w and l as a function of the volume of the system are

$$w^*(V) = l^*(V) = \frac{V^{1/3}}{2^{1/3}} = 0.793V^{1/3},$$

$$h^*(V) = 2^{2/3}V^{1/3} = 1.587 \ V^{1/3}.$$

4.4.3. Optimal solution of Model MGM

By substituting the results of section 4.4.2 in the objective function, the optimal values of $E[T_A]$, $E[T_B]$, $E[T_C]$, and $E[T_D]$ as a function of volume of the system, V can be obtained

$$E[T_A^*] = \frac{3}{8}(\frac{68+2^{2/3}(9947-429\sqrt{13})^{1/3}+2^{2/3}(9947+429\sqrt{13})^{1/3}}{2})^{1/3}V^{1/3} = 1.531V^{1/3}, \quad (4.28)$$

$$E[T_B^*] = \frac{3^{2/3}}{4}(\frac{13}{2}+5\sqrt{15})^{1/3} \ V^{1/3} = 1.538V^{1/3}, \tag{4.29}$$

$$E[T_C^*] = \frac{37V^{1/3}}{24} = 1.542V^{1/3}, \tag{4.30}$$

$$E[T_D^*] = \frac{55}{24}(\frac{V}{2})^{1/3} = 1.819V^{1/3}. \tag{4.31}$$

Figure 4.6 illustrates the minimum $E[T]$ of four cases for varying system volumes.
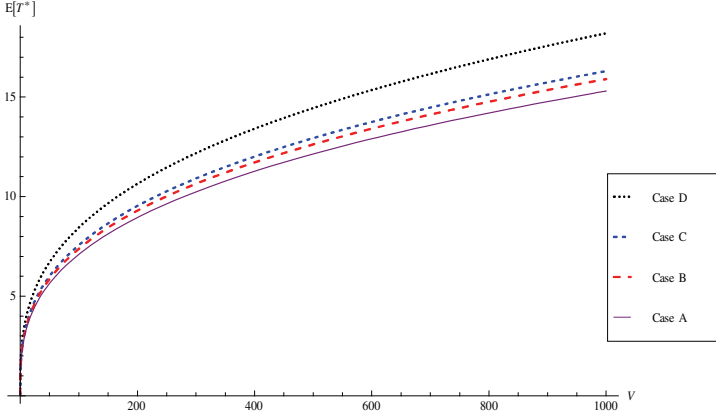
Figure 4.6. Optimal $E[T]$ for cases A, B, C, and D versus system volume

As it can be seen from Equations (4.28-4.31), the optimal solution of case A gives the minimum $E[T]$ for Model MGM. Therefore, for any given volume of the system, the following dimensions give the minimum expected retrieval time (See Equations (4.26) and (4.27)).

$$h^*(V) = \left(-2 + \left(\frac{1}{2}\left(11 - 3\sqrt{13}\right) \right)^{1/3} + \left(\frac{1}{2}\left(11 + 3\sqrt{13}\right) \right)^{1/3} \right)^{1/3} V^{1/3},$$

$$w^*(V) = l^*(V) = \left(\left(-2 + \left(\frac{1}{2}\left(11 - 3\sqrt{13}\right) \right)^{1/3} + \left(\frac{1}{2}\left(11 + 3\sqrt{13}\right) \right)^{1/3} \right)^{1/3} \right)^{-1/2} V^{1/3}, \text{ and}$$

$$u_A^* = 1, \ u_B^* = u_C^* = u_D^* = 0.$$

4.5. Further discussion and extension

The results obtained in the previous sections are summarized in section 4.5.1. In addition, section 4.5.1 investigates how the expected retrieval time changes by departing from optimal dimensions. Section 4.5.2 discusses extensions of our model.

4.5.1. Further discussion

Section 4.3 derives four closed-form expressions for the optimal expected retrieval time for a live-cube system, by dividing the space in four regions. Figure 4.7(a) illustrates which case has to be considered for any volume, height and shape factor (*w/l*). As the shape factor decreases, case B becomes the dominant feasible region. Moreover, by increasing the height of the system, the feasible region moves from case A to case B, to case C, and finally to case D. For any given volume *v*, a projection of Figure 4.7(a) on the plane $V = v$ gives all possible values of height and shape factor for each case. For example Figure 4.7(b) shows the projection of 3D plot on the plane $V = 10^6$. For $V = 10^6$, A^* ($h = 87.44$, *w/l* = 1), B^* (95.57, 0.8728), C^* (100, 1) and D^* (158.74, 1) are the optimal solutions of cases A, B, C and D with the objective values 153.097, 153.789, 154.167 and 181.889 respectively that can be obtained from section 4.4. The arrows in Figure 4.7(b) illustrates that, starting from a random feasible point a global optimum (A^*) can always be obtained.

(a)   (b)
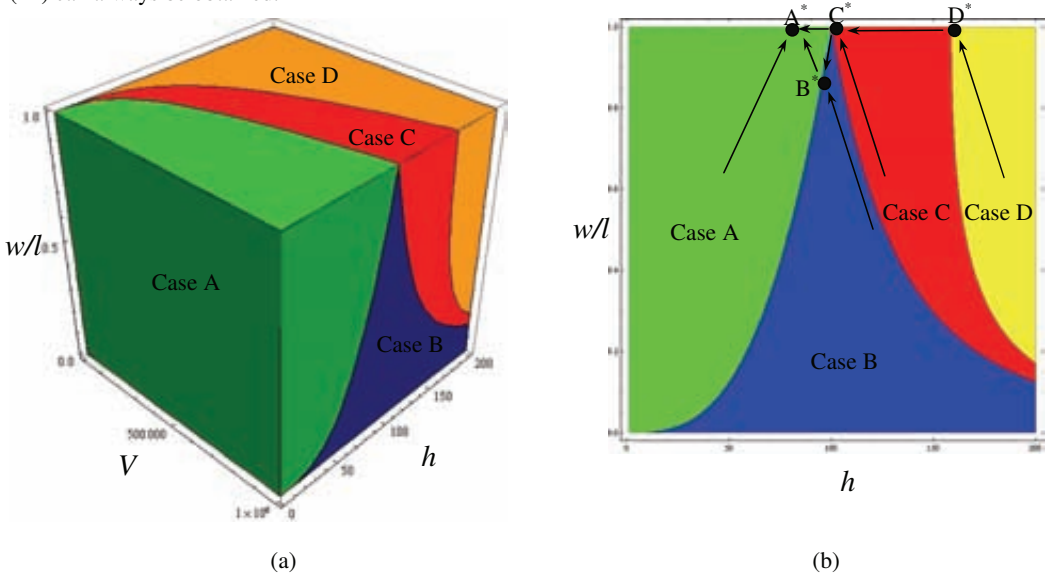
Figure 4.7.(a) Cases A, B, C and D for varying volume, height and shape factor (b) projection of 3D plot on the plane $V = 10^6$

    Table 4.1 summarizes the obtained results from sections 4.3 and 4.4, including the closed-form formulas for the expected retrieval time and optimal dimensions for each case individually.

Table 4.1. Optimal retrieval times and system dimensions for each case

Case	$E[T]$ formula	Optimal dimensions
A*	$\dfrac{h^3 + 12hlw + 12lw(l+w)}{24lw}$	$h^*(V) = 0.87446\,V^{1/3}$ $w^*(V) = l^*(V) = 1.06937V^{1/3}$ $E[T_A^*] = 1.53097V^{1/3}$
B	$\dfrac{4h^3 + 6h^2(2l-w) - w^3 + 4h(3l^2 + 3lw + w^2)}{24hl}$	$h^*(V) = w^*(V) = 0.95573V^{1/3}$ $l^*(V) = 1.09479\,V^{1/3}$ $E[T_B^*] = 1.53789V^{1/3}$
C	$-\dfrac{h^4 + l^4 + 6h^2(l-w)^2 + w^4 - 4h^3(l+w) - 4h(l+w)^3}{24hlw}$	$h^*(V) = w^*(V) = l^*(V) = V^{1/3}$ $E[T_C^*] = 1.54167V^{1/3}$
D	$\dfrac{12h^2 + 2l^2 + 3lw + 2w^2}{12h}$	$w^*(V) = l^*(V) = 0.793701V^{1/3}$ $h^*(V) = 1.58740\,V^{1/3}$ $E[T_D^*] = 1.81889V^{1/3}$

* The overall optimal solution is obtained in case A according to section 4.3.

As it can be seen from Table 4.1, the optimal dimensions in case A, lead to the minimum expected retrieval time. However, the optimal dimensions in cases B and C also result in a very close to optimal (less than 1% gap) expected retrieval time. This means if the company is willing to have a taller system with a smaller footprint, the optimal dimensions of case B or C can be used which give a gap of less than 1% from the optimal expected retrieval time. A cubic in time system ($l = w = h$) appears to be not optimal, but has a gap of only 1% from the optimal solution.

In order to check how the configuration of a live-cube storage system affects the expected retrieval time we have varied h for a fixed volume of the system. The gap is determined by Equation (4.32). The right-hand side of Equation (4.32) should be evaluated at $w = l$. In Equation (4.32), boundaries are calculated according to the conditions of the cases. If the condition of more than one case is satisfied, the case with minimum objective value is considered.

$$Gap_h = \frac{E[T(h)] - E[T^*]}{E[T^*]} = \begin{cases} (E[T_A(h)] - E[T^*]) \,/\; E[T^*] & \text{if } h \leq V^{1/3}, \\ (E[T_C(h)] - E[T^*]) \,/\; E[T^*] & \text{if } V^{1/3} < h \leq 2^{2/3}V^{1/3}, \\ (E[T_D(h)] - E[T^*]) \,/\; E[T^*] & \text{if } h > 2^{2/3}V^{1/3}. \end{cases} \quad (4.32)$$

Figure 4.8 illustrates the gap for different values of h and V. Figure 4.8(a) illustrates Equation (4.32) for a relatively large range of V ($V \in (0,10^6]$). Figure 4.8(b) presents the contour plot of Equation (4.32) for different values of h and V. Figure 4.8 illustrates that for any given volume, the gap increases with an increasing height of the system. However, for smaller values of the volume, the increase is more dramatic.

(a)   (b)
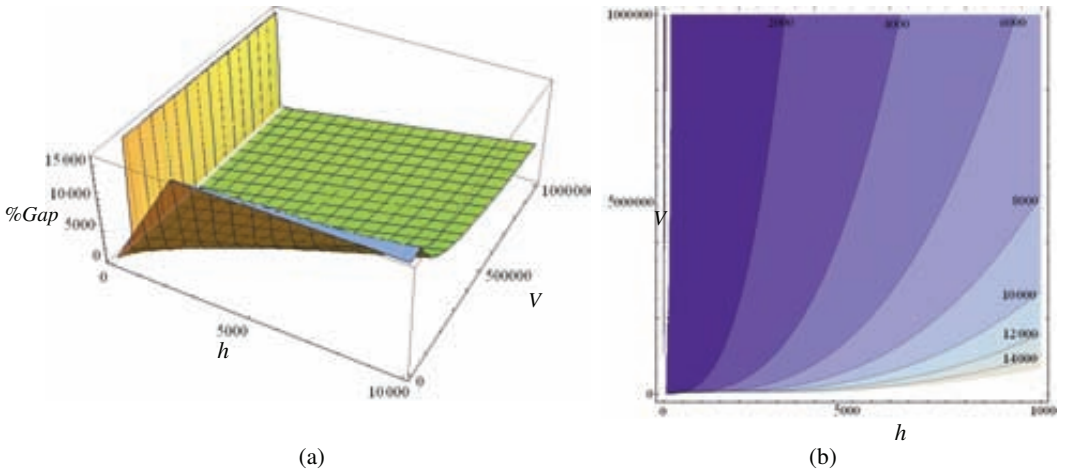
Figure 4.8. (a) 3D plot (b) contour plot of the gap (%) between $E[T(h)]$ and $E[T^*]$ for varying h and $V \in$ $(0,10^6]$

We also investigate how the shape factor (w/l) affects the expected retrieval time of a live-cube storage system. Since it was assumed that $w \leq l$, the shape factor can obtain any value in $(0,1]$. Equation

(4.33) determines the gap between the expected retrieval time of varying w/l and optimal expected retrieval time given the volume is fixed ($V=10^6$),

$$Gap_{w/l} = \frac{E[T(w,l,h)] - E[T^*]}{E[T^*]} = \begin{cases} (E[T_A(w,l,h)] - E[T^*]) / E[T^*] & \text{if } h \leq ((w/l)V)^{1/3}, \\ (E[T_B(w,l,h)] - E[T^*]) / E[T^*] & \text{if } ((w/l)V)^{1/3} < h \leq ((l/w)V)^{1/3}, \\ (E[T_C(w,l,h)] - E[T^*]) / E[T^*] & \text{if } ((l/w)V)^{1/3} < h \leq (((l/w)+(w/l)+2)V)^{1/3}, \quad (4.33) \\ (E[T_D(w,l,h)] - E[T^*]) / E[T^*] & \text{if } h > (((l/w)+(w/l)+2)V)^{1/3}. \end{cases}$$

Figure 4.9 illustrates the 3-dimension and contour plots of Equation (4.33) for varying values of shape factor (w/l) and h for $V=10^6$. Figure 4.9(a) illustrates that for a decreasing shape factor (w/l) for any given h, the gap increases. The increase is more dramatic for smaller values of h (see Figure 4.9(b)).

(a)   (b)
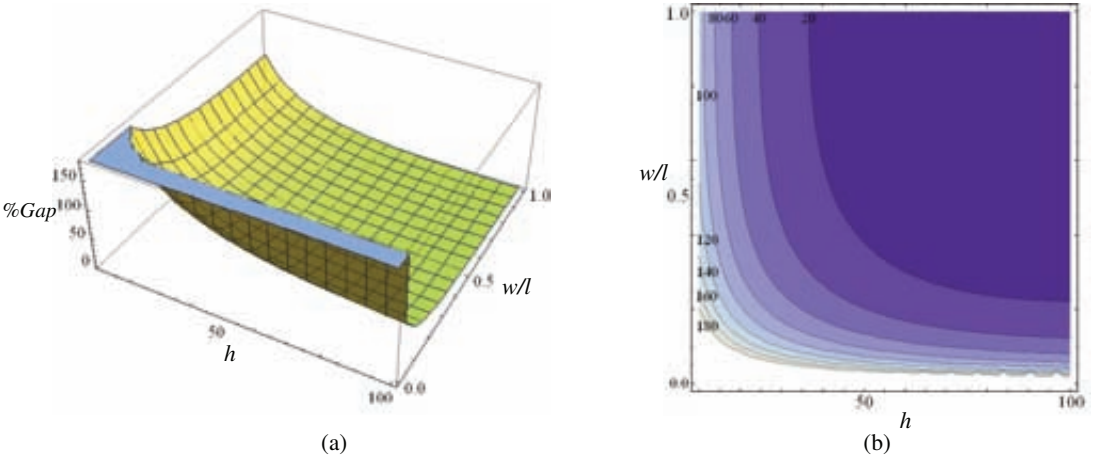
Figure 4.9. (a) 3D plot (b) contour plot of the gap (%) between $E[T(w,l,h)]$ and $E[T^*]$ for varying w/l and h and $V = 10^6$

4.5.2. Extensions

In this section, we propose some extensions of our problem and discuss the possible solution approaches.

Minimizing the maximum response time

The objective of the Model MGM is to minimize the expected retrieval time. However, it is also possible to minimize the maximum response time of a live-cube compact storage system. The maximum response

time of live-cube system is the retrieval time of the unit load located on the location farthest from the I/O point. Therefore, the maximum response time is $\max\{l+w,h\}+h$.

The corresponding mathematical model can be constructed as follows (Model MRT):

$$\min\{\max\{l+w,h\}+h\},$$

subject to

$$lwh=V,$$

Decision variables: $l>0, w>0, \text{and } h>0$.

The model can be solved optimally by decomposing it into two sub-models and using Lagrange multipliers for each sub-model.

- If $l+w>h$ then the objective function becomes $l+w+h$ and therefore the optimal dimension sizes and objective value for this case are $l^*(V)=w^*(V)=h^*(V)=V^{1/3}$ and $3V^{1/3}$ respectively.

- If $l+w\leq h$ then the objective function becomes $2h$ and therefore the objective function is minimized when $h=l+w$. Thus the optimal dimension sizes and objective value are $l^*(V)=w^*(V)=(V/2)^{1/3}$, $h^*(V)=2(V/2)^{1/3}$ and $4(V/2)^{1/3}$ respectively.

By comparing two above objective values, it is obvious that the optimal dimensions which minimize the maximum response time of a live-cube system are $l^*(V)=w^*(V)=h^*(V)=V^{1/3}$ that is a cubic in time system. Moreover, the optimal solution of Model MGM ($l^*(V)=w^*(V)=1.069V^{1/3}$, $h^*(V)=0.874V^{1/3}$) has a gap of only 1% from this optimal solution. In conclusion, the optimal solution of Model MGM has a gap of only 1% from the optimal solution of Model MRT and vice versa.

Location of the lift

In our problem, the lift is assumed to be located at the left corner of the system and when idle it waits at the ground floor. However, by changing the location of the lift the retrieval time can be calculated differently. For example if the lift is located at the middle of the front face of the system, then the travel time in x direction of any arbitrary unit load to the lift at the same level can be halved at most. To solve such a problem, the travel time formula and the expected retrieval time should be derived and then the same model as Model MGM can be constructed. However, it is also possible to consider the system as two similar sub-systems where the lift is located at the corner of each sub-system and then results of our model can still be applied. The volume of each sub-system will be the half volume of the system. Thus, the optimal dimensions and expected retrieval time of a live-cube system with a lift at the middle position

are $h^*(V) = 0.69406 \ V^{1/3}$, $w^*(V) = 0.84876 \ V^{1/3}$, $l^*(V) = 1.69753 \ V^{1/3}$ and $E[T^*] = 1.21513 V^{1/3}$. Results show that a lift at the middle position leads to 20% reduction in expected retrieval time.

We also assume that the lift waits at the ground level. Alternatively, if the lift waits at the middle floor the travel time of the lift in z direction to pick up a unit load can be halved at most. However, in such a case the lift needs to travel $h/2$ to the ground floor if a unit load needs to be stored. In general, our studied problem can provide the basic analysis for any other live-cube compact storage systems (e.g. live-cube systems with multiple lifts).

4.6. Conclusion

In this study, we derive the expected retrieval time of an arbitrary unit load in a live-cube compact storage system under a random storage policy. We propose a mathematical model to optimize the dimensions of such a system minimizing the response time. The model can be solved optimally by splitting it into several solvable cases without losing the optimal solution. In total, 4 cases have to be distinguished, each with at most 5 sub-cases. Although the solution procedure is tedious, closed-from expressions for the expected retrieval time can be obtained which can be used to compare the performance of a live-cube compact storage system with other types of compact storage systems. Our results show that the optimal configuration of the system provides a significant reduction in expected retrieval time compared to any arbitrary configuration. The sensitivity analysis shows that any deviation from the optimal system height can substantially increase the expected retrieval time for a given volume of the system. In addition, unequal length and width of the system may also bring significant increase in expected retrieval time depending on the volume and height of the system.

Appendix 4A. Virtual aisle conditions

Consider a live-cube storage system with $|I|$ columns and $|J|$ rows where the number of columns is assumed to be larger than or equal to the number of rows ($|I| \geq |J|$). It is easy to understand if there are $|I|$ +$|J|$ empty locations in the system, then for any arbitrary retrieval location a virtual aisle can be created in one unit of time and then the desired unit load can be easily moved to the I/O point. Having created the virtual aisle, the desired unit load can be removed without any interference. Consequently, the retrieval

time is only the Manhattan distance in time between the retrieval location and the I/O point. Therefore for any retrieval location (x,y) the retrieval time can be approximated by $x+y$.

Even stronger, if there are at least $\max\{|I|, |J|\}$ empty locations in the system (excluding the location of the lift) it can be proven that in one unit of time the system can be repositioned to a system where there is at least one empty location in each row and each column (see the proof). Then, the system can create a virtual aisle in one unit of time and consequently the retrieval time can be approximated by $x+y$ for any retrieval location (x,y). In most of the cases, it is possible to move the desired unit load toward I/O point while the other unit loads are moving to create a virtual aisle. However, in the worst case we need two units of time to create a virtual aisle. Since the constant maximum time does not influence the optimization results, the required time to create the virtual aisle can be ignored.

Proof.

For any unit load in the system located at (i,j) one of the following situations is possible:

- If the number of empty locations in column i and row j is at least 1 then the proof is complete.

- If there is no empty location in column i, then there is at least one column ($k \in I - i$) with at least 1 empty location at row $l \in J - j$. Therefore in one unit of time, an empty location can be created at location (i,l) and then the proof is complete. The proof is analogous for the case if there is no empty location in row j.

- If there is no empty location in column i and row j, then there is at least one column ($k \in I - i$) and at least one row ($l \in J - j$) both with at least 1 empty location. Therefore in one unit of time, two empty locations can be created at locations (i,l) and (k,j) and then the proof is complete. □

Appendix 4B. Volume formulas of Figures 4.4(a-p)

Table 4.2. Volume formulas of Figures 4.4(a-p)

Figure	Volume Derivation	Volume Formula
5(a)	$\int\limits_{0}^{h}\int\limits_{0}^{t-z}(t-y-z)dydz$	$\frac{1}{6}h(3t^2-3th+h^2)$

5(b)

$$\int_0^{t-w}\int_0^w (t-y-z)dydz + \int_{b-w}^h \int_0^{t-z}(t-y-z)dydz$$

$$\frac{1}{6}(-t^3 + h^3 + w^3 + 3t^2(h+w) - 3t(h^2+w^2))$$

5(c)

$$\int_0^{t-w}\int_0^w (t-y-z)dydz + \int_{t-w}^h \int_0^{t-z}(t-y-z)dydz - ((t-l)^3/6)$$

$$\frac{1}{6}(-2t^3 + h^3 + l^3 + w^3 + 3t^2(h+l+w)$$
$$-3t(h^2 + l^2 + w^2))$$

5(d)

$$\int_0^h\int_0^w (t-y-z)dydz$$

$$-\frac{1}{2}hw(-2t+h+w)$$

5(e)

$$\int_0^h\int_0^w (t-y-z)dydz - \int_0^{t-l}\int_0^{t-l-z}\int_l^{t-y-z} dxdydz$$

$$-\frac{1}{6}(t-l)^3 - \frac{1}{2}hw(-2t+h+w)$$

5(f)

$$\int_0^{t-l-w}\int_0^w l\,dydz + \int_{t-l-w}^h\int_0^w (t-y-z)dydz - \int_{t-l-w}^{t-l}\int_0^{t-l-z}\int_l^{t-y-z} dxdydz$$

$$-\frac{1}{6}w(3t^2 + 3h^2 + 3l^2 + 3hw$$
$$+3lw + w^2 - 3t(2h+2l+w))$$

5(g)

$$lwh - (((l-(t-h-w))(w-(t-l-h))(h+l+w-t))/6)$$
$$+(((l-(t-w))(w-(t-l))(l+w-t))/6)$$

$$\frac{1}{6}(6hlw + (-t+l+w)^3 - (-t+h+l+w)^3)$$

5(h)

$$lwh - (((l-(t-w-h))(w-(t-l-h))(h-(t-l-w)))/6)$$

$$hlw - \frac{1}{6}(-t+h+l+w)^3$$

5(i)

$$\int_0^{t/2}\int_0^{t-z} (t-y-z)dydz$$

$$\frac{7t^3}{48}$$

5(j)

$$\int_0^{t-w}\int_0^w (t-y-z)dydz + \int_{t-w}^{t/2}\int_0^{t-z}(t-y-z)dydz$$

$$\frac{1}{48}(-t^3 + 24t(t-w)w + 8w^3)$$

5(k)

$$\int_0^{t-w}\int_0^w (t-y-z)dydz + \int_{t-w}^{t/2}\int_0^{t-z}(t-y-z)dydz - \frac{1}{6}(t-l)^3$$

$$\frac{1}{48}(-t^3 - 8(t-l)^3 + 24t(t-w)w + 8w^3)$$

5(l)	$\int\limits_0^{t/2}\int\limits_0^w (t-y-z)dydz$	$\dfrac{1}{8}t(3t-2w)w$
5(m)	$\int\limits_0^{t/2}\int\limits_0^w (t-y-z)dydz - ((t-l)^3/6)$	$-\dfrac{1}{6}(t-l)^3 + \dfrac{1}{8}t(3t-2w)w$
5(n)	$\int\limits_0^{t-l-w}\int\limits_0^w ldydz + \int\limits_{t-l-w}^{t/2}\int\limits_0^w (t-y-z)dydz - \int\limits_{t-l-w}^{t-l}\int\limits_0^{t-l-z}\int\limits_l^{t-y-z} dxdydz$	$-\dfrac{1}{24}w(3t^2 - 6t(4l+w) + 4(3l^2 + 3lw + w^2))$
5(o)	$((lwt)/2) - (((l-((t/2)-w))$ $(w-((t/2)-l))((t/2)-(t-l-w)))/6)$	$\dfrac{1}{48}(24tlw + (t-2(l+w))^3)$
5(p)	$\dfrac{tlw}{2}$	$\dfrac{tlw}{2}$

Appendix 4C. Proof of Theorem 1

We prove that the expected retrieval times for sub-cases A.1 and A.2 are the same. The proof for the rest of sub-cases in each case is analogous.

The expected retrieval time for sub-cases A.1 and A.2 can be calculated as follows:

$E[T_{A1}]=$

$$\int_0^w \frac{tf_1'(t)}{wlh}dt + \int_w^l \frac{tf_2'(t)}{wlh}dt + \int_l^{2h} \frac{tf_3'(t)}{wlh}dt + \int_{2h}^{w+h} \frac{tf_4'(t)}{wlh}dt + \int_{w+h}^{l+h} \frac{tf_5'(t)}{wlh}dt + \int_{l+h}^{w+l} \frac{tf_6'(t)}{wlh}dt + \int_{w+l}^{w+l+h} \frac{tf_7'(t)}{wlh}dt , \tag{4.34}$$

$E[T_{A2}]=$

$$\int_0^w \frac{tf_1'(t)}{wlh}dt + \int_w^{2h} \frac{tf_2'(t)}{wlh}dt + \int_{2h}^l \frac{tf_3^{*'}(t)}{wlh}dt + \int_l^{w+h} \frac{tf_4'(t)}{wlh}dt + \int_{w+h}^{l+h} \frac{tf_5'(t)}{wlh}dt + \int_{l+h}^{w+l} \frac{tf_6'(t)}{wlh}dt + \int_{w+l}^{w+l+h} \frac{tf_7'(t)}{wlh}dt , \tag{4.35}$$

where f_i ($i=1,\ldots,7$) are functions of retrieval time (t) representing the volumes of Figures 4.5(a-g) respectively. f_3^* is a function of retrieval time (t) representing the volume of Figure 4.4(b). Derivative and primitive of function f are represented b f' and F respectively.

Integrals including f_1, f_5, f_6 and f_7 can be removed from both Equations (4.34) and (4.35) since they are equal. The volume of the system which has a constant value (i.e. *wlh*) can also be removed from both equations. Therefore, Equations (4.34) and (4.35) can be simplified which are represented by Equations (4.36) and (4.37) respectively,

$$PE[T_{A\,1}] = \int_w^l tf_2'(t)dt + \int_l^{2h} tf_3'(t)dt + \int_{2h}^{w+h} tf_4'(t)dt , \qquad (4.36)$$

$$PE[T_{A\,2}] = \int_w^{2h} tf_2'(t)dt + \int_{2h}^l tf_3^{*'}(t)dt + \int_l^{w+h} tf_4'(t)dt . \qquad (4.37)$$

By knowing the formula for integration by parts, we have:

$$\int tf'(t)dt = tf(t) - \int f(t)dt .$$

We can also write (Since for example volume of Figure 4.5(b) equals the volume of Figure 4.5(c) at the boundary *l*):

$f_2(l) = f_3(l), f_3(2h) = f_4(2h), f_2(2h) = f_3^*(2h)$ and $f_3^*(l) = f_4(l)$.

Therefore, $PE[RT_{A\,1}]$ and $PE[RT_{A\,2}]$ can be rewritten as follows:

$PE[T_{A\,1}] = F_4(2h) - F_3(2h) + F_3(l) - F_2(l)$ and $PE[T_{A2}] = F_3^*(2h) - F_2(2h) + F_4(l) - F_3^*(l)$.

On the other hand, from the calculation of volumes we know that:

$f_4(t) - f_3(t) = f_3^*(t) - f_2(t)$ and $f_i(0) = 0$.

Therefore,

$F_4(2h) - F_3(2h) = F_3^*(2h) - F_2(2h)$ and $F_3(l) - F_2(l) = F_4(l) - F_3^*(l)$. □

Appendix 4D. Derivation of $E[T]$ of cases B, C, and D

Derivation of density functions and $E[T]$ of sub-cases of case B

Under such a configuration, the critical retrieval times are as follows:

$l, w, 2h, 2w, l+h, w+l, l+w+h$. $\qquad (4.38)$

In order to arrange the critical retrieval times based on their values we can split the case B to five sub-cases as follows:

- *Sub-case B*.1. $2h \le l+w$ and $l \le 2w$,

- *Sub-case B*.2. $2h \le l+w$ and $2w < l \le 2h$,

- *Sub-case B*.3. $2h \le l + w$ and $l > 2h$,

- *Sub-case B*.4. $2h > l + w$ and $l \le 2w$,

- *Sub-case B*.5. $2h > l + w$ and $l > 2w$.

Each sub-case corresponds to an arrangement of critical retrieval times different from other sub-cases in case B. We give the derivation of the probability density function for one sub-case of case B. The density functions of other sub-cases can be obtained in a similar fashion.

- **Sub-case B.1.** $2h \le l + w$ and $l \le 2w$

Under such a configuration, Equation (4.39) gives the arrangement of critical retrieval times and Equation (4.40) gives the probability density function. $2w$ is the only critical retrieval time in case B, which does not belong to critical retrieval times of case A. Figure 4.10 shows how the region $T \le t$ changes at $t = 2w$.

$$w \le l \le 2w \le 2h \le l + w \le h + l \le h + l + w. \tag{4.39}$$

$$
f(t) =
\begin{cases}
\left(21t^2 / 48\right) / \left(wlh\right) & \text{if } t < w, \\[2ex]
\dfrac{-3t^2 + 24tw + 24(t-w)w}{48hlw} & \text{if } w \le t < l, \\[2ex]
\dfrac{-24(l-t)^2 - 3t^2 + 24tw + 24(t-w)w}{48hlw} & \text{if } l \le t < 2w, \\[2ex]
-\dfrac{2l^2 - 4lt + 2t^2 - 3tw + w^2}{4hlw} & \text{if } 2w \le t < 2h, \\[2ex]
\dfrac{-\dfrac{1}{2}(l-t)^2 + hw}{hlw} & \text{if } 2h \le t < l + w, \\[2ex]
\dfrac{2h + 2l - 2t + w}{2hl} & \text{if } l + w \le t < l + h,
\end{cases}
\tag{4.40}
$$

$$\frac{(h+l-t+w)^2}{2hlw} \qquad\qquad\qquad if\ l+h \le t < l+w+h.$$

| Retrieval time (t) boundary	Figure
$l \le t < 2w$	
$2w \le t < 2h$	
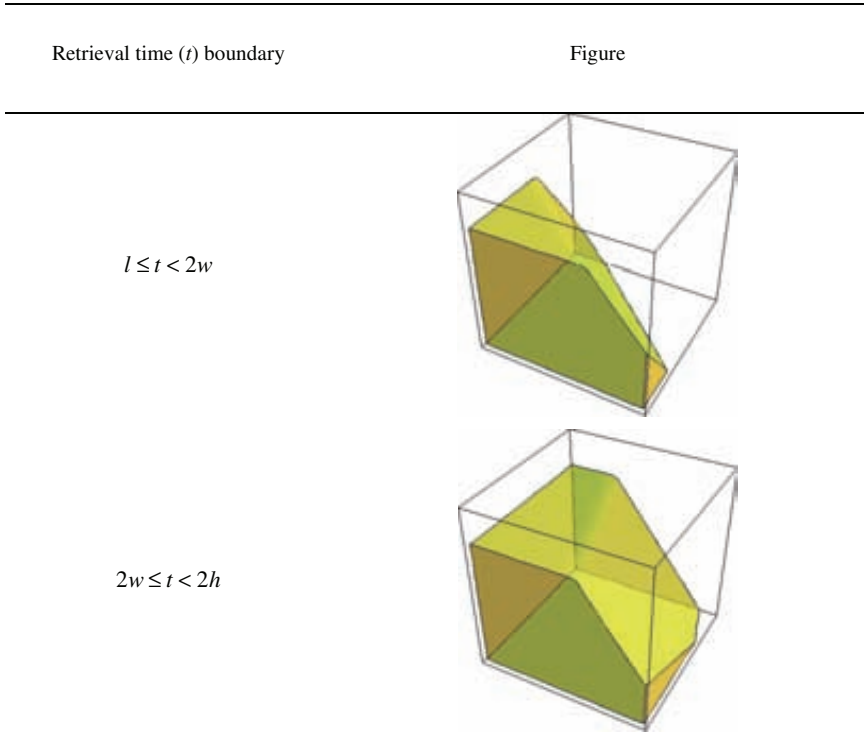
Figure 4.10. Region $T \le t$ if $t < 2w$ and $t \ge 2w$ in sub-case B.1

Eventually, the total expected retrieval time for sub-case B.1can be calculated as follows:

$$E[T_{B1}] = \int_0^w ((21t^3)/48)/(hlw)dt + \int_w^l (t(-\frac{t^2}{16} + \frac{tw}{2} + \frac{1}{2}(t-w)w))/(hlw)dt$$

$$+ \int_l^{2w} (t(-\frac{t^2}{16} - \frac{1}{2}(-l+t)^2 + \frac{tw}{2} + \frac{1}{2}(t-w)w))/(hlw)dt$$

$$+ \int_{2w}^{2h} (t(-\frac{1}{2}(-l+t)^2 + \frac{3tw}{8} + \frac{1}{8}(3t-2w)w))/(hlw)dt$$

$$+ \int_{2h}^{l+w} (t(-\frac{1}{2}(-l+t)^2 + hw))/(hlw)dt$$

$$+ \int_{l+w}^{l+h} (t(lw - \frac{1}{2}(-h+l+u)w - \frac{1}{2}(-h-l+t-w)w))/(hlw)dt$$

$$+ \int_{l+h}^{l+w+h} (u(\frac{(h+l-t+w)^2}{2(hlw)}))dt$$

$$= \frac{4h^3 + 6h^2(2l-w) - w^3 + 4h(3l^2 + 3lw + w^2)}{24hl}.$$

Derivation of density functions and $E[T]$ of sub-cases of case C

Under such a configuration, the critical retrieval times are as follows:

$$l, w, 2h, 2w, 2l, w+l, l+w+h.$$
<div style="text-align: right;">(4.41)</div>

In order to arrange the critical retrieval times based on their values we can split the case C to two sub-cases as follows:

- *Sub-case C.*1. $l \le 2w$,

- *Sub-case C.*2. $l > 2w$.

Each sub-case corresponds to an arrangement of critical retrieval times different from the other sub-case in case C. We give the derivation of the probability density function for one sub-case of case C. The density function of the other sub-case can be obtained in a similar fashion.

- **Sub-case C.1.** $l \le 2w$

Under such a configuration, Equation (4.42) gives the arrangement of critical retrieval times and Equation (4.43) gives the probability density function. $2l$ is the only critical retrieval time in case C, which does not belong to critical retrieval times of case B. Figure 4.11 shows how the region $T \le t$ changes at $t = 2l$.

$$w \le l \le 2w \le l+w \le 2l \le 2h \le h+l+w.$$
<div style="text-align: right;">(4.42)</div>

$$f(t) = \begin{cases} \left(21t^2 / 48\right) / \left(wlh\right) & \text{if } t < w, \\[2em] \dfrac{-3t^2 + 24tw + 24\left(t - w\right)w}{48hlw} & \text{if } w \le t < l, \\[2em] \dfrac{-24\left(l - t\right)^2 - 3t^2 + 24tw + 24\left(t - w\right)w}{48hlw} & \text{if } l \le t < 2w, \\[2em] -\dfrac{2l^2 - 4lt + 2t^2 - 3tw + w^2}{4hlw} & \text{if } 2w \le t < l + w, \\[2em] \dfrac{4l - t + w}{4hl} & \text{if } l + w \le t < 2l, \\[2em] \dfrac{2lw + (l - \dfrac{t}{2} + w)^2}{4hlw} & \text{if } 2l \le t < 2h, \\[2em] \dfrac{(h + l - t + w)^2}{2hlw} & \text{if } 2h \le t < l + w + h. \end{cases} \qquad (4.43)$$

Retrieval time (t) boundary	Figure
$l + w \le t < 2l$	
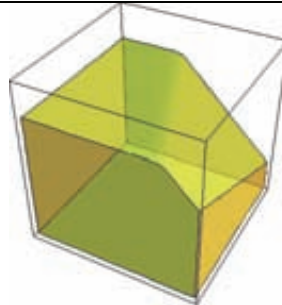
$$2l \leq t < 2h$$
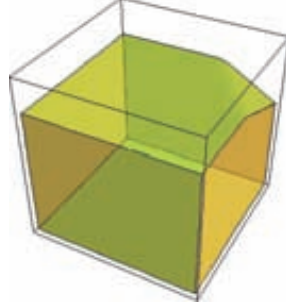
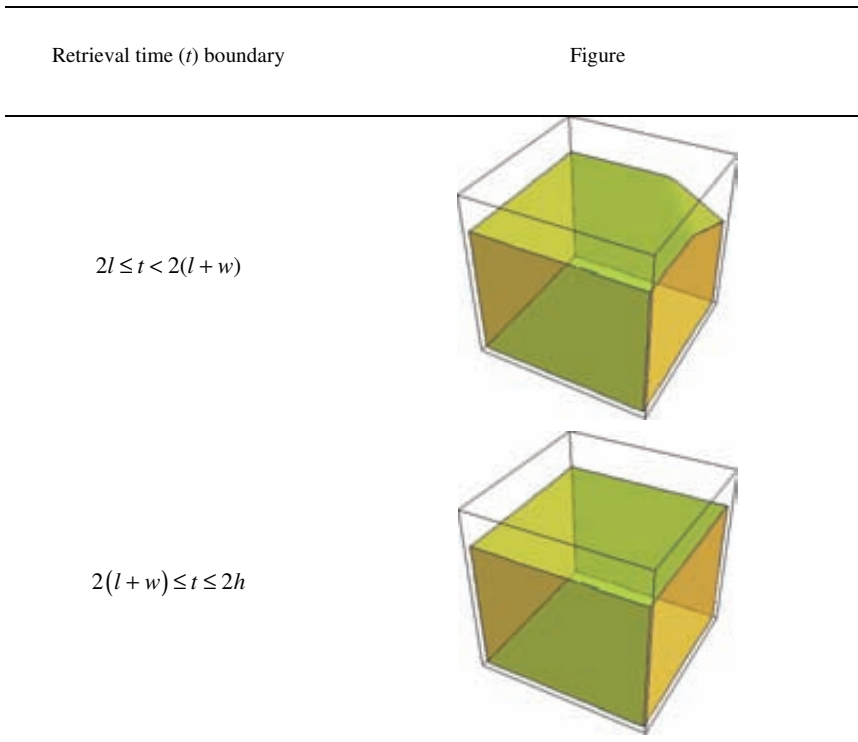**Figure 4.11.** Region $T \leq t$ if $t < 2l$ and $t \geq 2l$ in sub-case C.1

Eventually, the total expected retrieval time for sub-case C.1can be calculated as follows:

$$E[T_{C1}] = \int_0^w ((21t^3)/48)/(hlw)dt + \int_w^l (t(-\frac{t^2}{16} + \frac{tw}{2} + \frac{1}{2}(t-w)w))/(hlw)dt$$

$$+ \int_l^{2w} (t(-\frac{t^2}{16} - \frac{1}{2}(-l+t)^2 + \frac{tw}{2} + \frac{1}{2}(t-w)w))/(hlw)dt$$

$$+ \int_{2w}^{l+w} (t(-\frac{1}{2}(-l+t)^2 + \frac{3tw}{8} + \frac{1}{8}(3t-2w)w))/(hlw)dt$$

$$+ \int_{l+w}^{2l} (t(lw - \frac{1}{8}(2l+t)w - \frac{1}{8}w(t-2(l+w))))/(hlw)dt$$

$$+ \int_{2l}^{2h} (t(\frac{lw}{2} + \frac{1}{4}(l - \frac{t}{2} + w)^2))/(hlw)dt + \int_{2h}^{l+w+h} (t(\frac{(h+l-t+w)^2}{2(hlw)}))dt$$

$$= -\frac{h^4 + l^4 + 6h^2(l-w)^2 + w^4 - 4h^3(l+w) - 4h(l+w)^3}{24hlw}.$$

Derivation of density functions and $E[T]$ of sub-cases of case D

Under such a configuration, the critical retrieval times are as follows:

$$l, w, 2h, 2w, 2l, w+l, 2(l+w), 2h.$$ (4.44)

In order to arrange the critical retrieval times based on their values we can split the case D to two sub-cases as follows:

- *Sub-case D.1.* $l \leq 2w$,
- *Sub-case D.2.* $l > 2w$.

Each sub-case corresponds to an arrangement of critical retrieval times different from the other sub-case in case D. We give the derivation of the probability density function for one sub-case of case D. The density function of the other sub-case can be obtained in a similar fashion.

- **Sub-case D.1.** $l \le 2w$

Under such a configuration, Equation (4.45) gives the arrangement of critical retrieval times and Equation (4.46) gives the probability density function. $2(l+w)$ is the only critical retrieval time in case D, which does not belong to critical retrieval times of case C. Figure 4.12 shows how the region $T \le t$ changes at $t = 2(l+w)$.

$$w \le l \le 2w \le l+w \le 2l \le 2(l+w) \le 2h. \tag{4.45}$$

$$f(t) = \begin{cases} \left(21t^2/48\right)/\left(wlh\right) & \text{if } t < w, \\[2ex] \dfrac{-3t^2 + 24tw + 24(t-w)w}{48hlw} & \text{if } w \le t < l, \\[2ex] \dfrac{-24(l-t)^2 - 3t^2 + 24tw + 24(t-w)w}{48hlw} & \text{if } l \le t < 2w, \\[2ex] -\dfrac{2l^2 - 4lt + 2t^2 - 3tw + w^2}{4hlw} & \text{if } 2w \le t < l+w, \\[2ex] \dfrac{4l - t + w}{4hl} & \text{if } l+w \le t < 2l, \\[2ex] \dfrac{2lw + (l - \frac{t}{2} + w)^2}{4hlw} & \text{if } 2l \le t < 2(l+w), \\[2ex] \dfrac{1}{2h} & \text{if } 2(l+w) \le t < 2h. \end{cases} \tag{4.46}$$

Retrieval time (t) boundary	Figure
$2l \leq t < 2(l + w)$	
$2(l + w) \leq t \leq 2h$	

Figure 4.12. Region $T \leq t$ if $t < 2(l + w)$ and $t \geq 2(l + w)$ in sub-case D.1

Eventually, the total expected retrieval time for sub-case D.1can be calculated as follows:

$$E[T_{D1}] = \int_0^w ((21t^3)/48)/(hlw)dt + \int_w^l (t(-\frac{t^2}{16} + \frac{tw}{2} + \frac{1}{2}(t-w)w))/(hlw)dt$$

$$+ \int_l^{2w} (t(-\frac{t^2}{16} - \frac{1}{2}(-l+t)^2 + \frac{tw}{2} + \frac{1}{2}(t-w)w))/(hlw)dt$$

$$+ \int_{2w}^{l+w} (t(-\frac{1}{2}(-l+t)^2 + \frac{3tw}{8} + \frac{1}{8}(3t-2w)w))/(hlw)dt$$

$$+ \int_{l+w}^{2l} (t(lw - \frac{1}{8}(2l+t)w - \frac{1}{8}w(t-2(l+w))))/(hlw)dt$$

$$+ \int_{2l}^{2(l+w)} (t(\frac{lw}{2} + \frac{1}{4}(l - \frac{t}{2} + w)^2))/(hlw)dt + \int_{2(l+w)}^{2h} (t(\frac{1}{2h}))dt$$

$$= \frac{12h^2 + 2l^2 + 3lw + 2w^2}{12h}.$$

Appendix 4E: Proof of Theorem 6

The following, is the function of expected retrieval time for case A:

$$E[T_A(w,l,h)] = \frac{h^3 + 12hlw + 12lw(l+w)}{24lw}.$$

Assuming $l = d\,w$, the theorem can be proven if the optimal $d^* = 1$. Substituting $l = d\,w$ into above equation we obtain:

$$E[T_A(w,h,d)] = \frac{h^3 + 12dhw^2 + 12dw^2(w+dw)}{24dw^2}.$$

In order to find the optimal value of d which minimizes the objective function we have to solve the following equation:

$$\frac{dE[T_A]}{dd} = -\frac{h^3}{24d^2w^2} + \frac{w}{2} = 0.$$

The values for d obtained by solving the first derivative equation are:

$$\{\{d \rightarrow -\frac{h^{3/2}}{2\sqrt{3}w^{3/2}}\},\{d \rightarrow \frac{h^{3/2}}{2\sqrt{3}w^{3/2}}\}\}.$$

However, since $0 < h < w$ none of the obtained values of d satisfies the condition $d \geq 1$. Therefore, the optimal value of d is a boundary extremum if the objective function is monotonically increasing. We have,

$$\frac{dE[T_A]}{dd} = -\frac{h^3}{24d^2w^2} + \frac{w}{2} \geq 0 \qquad \forall\, 0 < h \leq w \text{ and } d \geq 1.$$

So, the optimal d which minimizes the objective function is at $d^* = 1$ and therefore $w^* = l^*$.   □

Appendix 4F. Optimization of cases B, C, and D

Optimizing the dimensions in case B ($w < h \leq l$)

In order to find the optimal solution of the mathematical model in case where the height of the system is no larger than the length of the system ($h \leq l$) while it is larger than or equal to the width of the system ($w \leq h$), first we give the following theorem which shows that in the optimal solution, the optimal values of the width and the height of the system are equal ($w^* = h^*$).

Theorem I. *In optimal solution of case B ($w \leq h \leq l$), the optimal values of the width and height of the system are equal ($w^* = h^*$).*

Proof. The following, is the function of expected retrieval time for case B:

$$E[T_B(w,l,h)] = \frac{4h^3 + 6h^2(2l - w) - w^3 + 4h(3l^2 + 3lw + w^2)}{24hl}.$$

Assuming $h = d\,w$, the theorem can be proven if the optimal $d^* = 1$. Substituting $h = d\,w$ into $E[T_B]$ we obtain Equation (4.47),

$$E[T_B(l,w,d)] = \frac{6d^2(2l - w)w^2 - w^3 + 4d^3w^3 + 4dw(3l^2 + 3lw + w^2)}{24dlw}. \tag{4.47}$$

In order to find the optimal value of d which minimizes the objective function we have to solve the following equation,

$$\frac{dE[T_B]}{dd} = \frac{w(6d^2(2l - w) + w + 8d^3w)}{24d^2l} = 0. \tag{4.48}$$

However, since the objective function is a monotonically increasing function of d (See Equation (4.49)) Therefore, the optimal d which minimizes the objective function locates at $d^* = 1$. So, $h^* = w^*$ and the proof is complete, □

$$\frac{dE[T_B]}{dd} = \frac{w(6d^2(2l-w)+w+8d^3w)}{24d^2l} > 0 \qquad \forall w \le h < l \text{ and } d \ge 1. \tag{4.49}$$

Since $d^* = 1$, now we can replace w with h. Furthermore, since $w\,l\,h = v$ we can replace l with $(V/h)^{1/2}$. Thus, the objective function can be written as a function of h,

$$E[T_B(h)] = h + \frac{h^4}{24V} + \frac{V}{2h^2}. \tag{4.50}$$

We can obtain the optimal value of h, which minimizes the objective function by solving the first derivative of objective function over h,

$$\frac{dE[T_B]}{dh} = 1 + \frac{h^3}{6v} - \frac{V}{h^3} = 0. \tag{4.51}$$

The following Equation gives the optimal value of h and w ($h^* = w^*$) which satisfies the condition $w \le h \le l$ as a function of the volume of the system,

$$h^*(V) = w^*(V) = (-3V + \sqrt{15V})^{1/3}. \tag{4.52}$$

The following Equation gives the optimal value of l,

$$l^*(V) = \frac{V}{\left(-3V + \sqrt{15V}\right)^{2/3}}. \tag{4.53}$$

We have to check that the optimal values h, w, l satisfy the condition $w \le h \le l$. By comparing the values of dimensions, we observe that the condition holds:

$$h^*(V) = w^*(V) = 0.95573V^{1/3} \text{ and } l^*(V) = 1.09479\,V^{1/3}. \tag{4.54}$$

In order to make sure that the optimal values of dimensions result in minimal objective value we need to check whether the objective function is convex. Therefore, we derive the second derivative of the objective function to check whether it is positive or not. The second derivative test proves that the objective function is a convex function and then the optimal values of dimensions lead to minimum objective value,

$$\frac{d^2 E[T_B]}{dh^2} = \frac{h^2}{2V} + \frac{3V}{h^4} \geq 0. \tag{4.55}$$

Optimizing the dimensions in case C ($l \leq h \leq l + w$)

In order to find the optimal solution of the mathematical model in case where the height of the system is no larger than the length plus width ($h \leq l + w$) while it is larger than or equal to the length of the system ($l \leq h$), first we give the following theorem which shows that in the optimal solution, the optimal values of the length and the width of the system are equal ($w^* = l^*$).

Theorem II. *In optimal solution of case C ($l \leq h \leq l + w$), the optimal values of the width and length of the system are equal ($w^* = l^*$).*

Proof. The following, is the function of expected retrieval time for case C,

$$E[T_C(w,l,h)] = -\frac{h^4 + l^4 + 6h^2(l-w)^2 + w^4 - 4h^3(l+w) - 4h(l+w)^3}{24hlw}.$$

Assuming $l = d\,w$, the theorem can be proven if the optimal $d^* = 1$. Substituting $l = d\,w$ into $E[T_C]$ we obtain Equation (4.56),

$$E[T_C(w,h,d)] = -\frac{h^4 + w^4 + d^4 w^4 + 6h^2(-w+dw)^2 - 4h^3(w+dw) - 4h(w+dw)^3}{24dhw^2}. \tag{4.56}$$

In order to find the optimal value of d which minimizes the objective function we have to solve the following equation,

$$\frac{dE[T_C]}{dd} = \frac{h^4 - 4h^3 w - 6(-1+d^2)h^2 w^2 + 4(1+d)^2(-1+2d)hw^3 + (1-3d^4)w^4}{24d^2 hw^2} = 0. \tag{4.57}$$

However, since the objective function is a monotonically increasing function of d (See Equation (4.58)) Therefore, the optimal d which minimizes the objective function locates at $d^* = 1$. So, $l^* = w^*$ and the proof is complete,   □

$$\frac{dE[T_C]}{dd} = \frac{h^4 - 4h^3 w - 6(-1+d^2)h^2 w^2 + 4(1+d)^2(-1+2d)hw^3 + (1-3d^4)w^4}{24d^2 hw^2} > 0 \tag{4.58}$$
$$\forall l \leq h \leq l + w \text{ and } d \geq 1.$$

Since $d^* = 1$, now we can replace l with w. Furthermore, since $w\,l\,h = V$ we can replace w with $(V/h)^{1/2}$. Thus, the objective function can be written as a function of h,

$$E[T_C(h)] = -\frac{h^4 + \dfrac{2V^2}{h^2} - 8h^3\sqrt{V/h} - 32V\sqrt{V/h}}{24V}.$$ (4.59)

We can obtain the optimal value of h, which minimizes the objective function by solving the first derivative of objective function over h,

$$\frac{dE[T_C]}{dh} = \frac{5h^3V - 4V^2 - h^5\sqrt{V/h} + V(V/h)^{3/2}}{6h^3(V/h)^{3/2}} = 0.$$ (4.60)

Solving Equation (4.60) returns no real value solution which satisfies the condition $l \le h \le l+w$ considering $w\,l\,h = V$ for any $V > 0$. If the objective function is a convex function of h, then the optimal solution is located at the boundaries: $h = l = w$.

Therefore, we derive the second derivative of the objective function to check whether it is positive or not. The second derivative test proves that the objective function is a convex function,

$$\frac{d^2E[T_C]}{dh^2} = \frac{-2h^6 - 2V^2 + 5h^5\sqrt{V/h} + 4h^3(V/h)^{3/2}}{4h^4V} > 0 \qquad \forall l \le h \le l+w.$$ (4.61)

Therefore, the following equation gives the optimal values of l, w and h for case C,

$$h^*(V) = w^*(V) = l^*(V) = V^{1/3}.$$ (4.62)

We have to check that the optimal values h, w and l satisfy the condition $l \le h \le l+w$. By comparing the values of dimensions, we observe that the condition holds.

Optimizing the dimensions in case D ($l+w \le h$)

In order to find the optimal solution of the mathematical model in case where the height of the system is larger than the length plus width ($l+w \le h$), first we give the following theorem which shows that in the optimal solution, the optimal values of the length and the width of the system are equal ($w^* = l^*$).

Theorem III. *In optimal solution of case D ($l+w \le h$), the optimal values of the width and length of the system are equal ($w^* = l^*$).*

Proof. The following, is the function of expected retrieval time for case D,

$$E[T_D(w,l,h)] = \frac{12h^2 + 2l^2 + 3lw + 2w^2}{12h}.$$

Assuming $l = d\,w$, the theorem can be proven if the optimal $d^* = 1$. Substituting $l = d\,w$ into $E[T_D]$ we obtain Equation (4.63),

$$E[T_D(w,h,d)] = \frac{12h^2 + 2w^2 + 3dw^2 + 2d^2w^2}{12h}. \tag{4.63}$$

In order to find the optimal value of d which minimizes the objective function we have to solve the following equation:

$$\frac{dE[T_D]}{dd} = \frac{3w^2 + 4dw^2}{12h} = 0. \tag{4.64}$$

However, since the objective function is a monotonically increasing function of d (See Equation (4.65)) Therefore, the optimal d which minimizes the objective function locates at $d^* = 1$. So, $l^* = w^*$ and the proof is complete,   □

$$\frac{dE[T_D]}{dd} = \frac{3w^2 + 4dw^2}{12h} > 0 \qquad \forall l + w \leq h \text{ and } d \geq 1. \tag{4.65}$$

Since $d^*=1$, now we can replace l with w. Furthermore, since $w\,l\,h = V$ we can replace w with $(V/h)^{1/2}$. Thus, the objective function can be written as a function of h,

$$E[T_D(h)] = h + \frac{7V}{12h^2}. \tag{4.66}$$

We can obtain the optimal value of h, which minimizes the objective function by solving the first derivative of objective function over h,

$$\frac{dE[T_D]}{dh} = 1 - \frac{7V}{6h^3} = 0. \tag{4.67}$$

Solving Equation (4.67) returns no real value solution which satisfies the condition $l + w \leq h$ considering $w\,l\,h = V$ for any $V > 0$. Therefore, if the objective function is a convex function of h, then the optimal solution is located at the boundaries: $l + w = h$. Since it is proven $l^* = w^*$ then $h^* = 2l^* = 2w^*$.

Therefore, we derive the second derivative of the objective function to check whether it is positive or not. The second derivative test proves that the objective function is a convex function,

$$\frac{d^2E[T_D]}{dh^2} = \frac{7V}{2h^4} > 0 \qquad \forall l + w \leq h. \tag{4.68}$$

Therefore, the following equations give the optimal values of l, w and h for case D,

$$w^*(V) = l^*(V) = \frac{V^{1/3}}{2^{1/3}}, \tag{4.69}$$

$$h^*(V) = 2^{2/3}V^{1/3}. \tag{4.70}$$

We have to check that the optimal values h, w, l satisfy the condition $l + w \leq h$. By comparing the values of dimensions, we observe that the condition holds:

$$w^* (V) = l^* (V) = 0.793701V^{1/3},$$ (4.71)

$$h^* (V) = 1.5874 \ V^{1/3}.$$ (4.72)

Chapter 5

Response Time Analysis of a Live-Cube Compact Storage System with Two Storage Classes

5.1. Introduction

Live-cube compact storage systems are recently introduced automated storage systems which can achieve high storage density together with short response times. In live-cube compact storage systems, the highest storage density can be achieved while unit loads can individually move in a 3-dimensional space. Such storage systems operate with electrically powered shuttles and lifts, which lead to significantly reduced fossil fuel and energy consumption, and CO_2 emissions. Table 5.1 compares the energy consumption and CO_2 emission of a typical live-cube and a traditional multi-storey car parking system of the same capacity (192 cars), and for different types of power plants generating the energy needed for operation (lighting,

ventilation, moving the cars). Parameters describing both storage systems and detailed calculations are given in Appendix 5A.

Table 5.1. Energy consumption and CO2 emissions of live-cube parking system and traditional multi-storey car park[*]

Generated by	Fossil-fuel power plant		Nuclear power plant		Biomass-fuel power plant	
Parking type	Live-cube parking	Traditional car park	Live-cube parking	Traditional car park	Live-cube parking	Traditional car park
Average CO2 emission (gram/car)	96	4369	1	200	0	184
Average S/R energy consumption (kWh/car)	0.12	4.94	0.12	4.94	0.12	4.94
Average lighting energy consumption (kWh/car)	0.00	0.25	0.00	0.25	0.00	0.25
Average ventilation energy consumption (kWh/car)	0.00	5.00	0.00	5.00	0.00	5.00
Total (kWh/car)	0.12	10.19	0.12	10.19	0.12	10.19

[*]Input data retrieved from Hyundai Elevator Co. Ltd. (2011) and multi-storey car park (2011).

As Table 5.1 shows, a live-cube parking system significantly reduces the energy consumption and CO2 emissions compared to the traditional multi-storey car park. This saving is even more significant for CO2 emissions if electricity is provided by a fossil-fuel power plant. Chapter 1 illustrates the main components and work mechanism of a live-cube compact storage system (see Figure 1.3).

The performance of a compact storage system in service industries is often measured in terms of its response time. It has been shown that class-based storage can reduce the response time of a storage system of up to 50% compared to random storage (Hausman et al., 1976; Eynan and Rosenblatt, 1994; Kouvelis and Papanicolaou, 1995; Ruben and Jacobs, 1999; Park, 2006; Yu and De Koster, 2009b). Two-class-based storage can simply be implemented in practice by classifying unit loads in high turnover and low turnover classes. The high-turnover unit loads are then assigned to locations closer to the I/O point. Therefore, shorter response times can be realized since a major portion of customer requests can be retrieved from locations closer to the I/O point.

In this chapter, we study the performance of a two-class-based storage policy in a live-cube compact storage system. We derive closed-form formulas for the expected retrieval time of an arbitrary unit load for any system size and first zone boundary. To obtain closed-form formulas, the system needs to be decomposed into several cases, sub-cases, and even sub-sub-cases. Although, the decomposition procedure is complicated, it can be condensed to 36 complementary cases each corresponding to a unique closed-form formula for the expected retrieval time. Each case represents a specific system configuration and a first zone boundary range. The closed-form formulas can be used to instantaneously evaluate the performance of a two-class-based live-cube system with any configuration and first zone boundary. In addition, the impact of different sizes of the first zone can be investigated for a fixed system configuration. Systems with different configurations can also be compared in terms of their performance. We compare the closed-form formulas (which are based on a continuous space approximation) with the results of simulation in a real life setting. The results show that the gaps between the results of closed-form formulas and simulation are mostly less than 2%.

Hausman et al. (1976) appear to be the first to study travel time models for an automated storage and retrieval (AS/R) system. They propose closed-form expressions for the travel time in a square-in-time (SIT) continuous rack under different storage policies. Graves et al. (1977) extend their work by considering interleaving times in their travel time model. Bozer and White (1984) develop closed-form expressions for the expected travel time for a non-SIT (NSIT) rack and random storage. Based on simulation results, they show that the model is quite accurate. Since then, researchers have mainly continued studies in different directions, such as derivation of closed-form expressions for travel time (Kim and Seidmann, 1990; Sarker et al., 1991) and system optimization based on closed-from expressions obtained in previous studies (Rosenblatt and Eynan, 1989; Eynan and Rosenblatt, 1994; Kouvelis and Papanicolaou, 1995). In addition, several authors study travel time models for other types of storage and retrieval systems such as multi-shuttle AS/R systems (Sarker et al., 1991; Keserla and Peters, 1994; Malmborg, 2000), miniload AS/R system (Park et al., 2003, 2006), and compact storage systems (De Koster et al., 2008; Yu and De Koster, 2009b; Zaerpour et al., 2010).

Gue and Kim (2007) study a single-level live-cube system or a so-called "puzzle-based" system. They investigate the travel time (expressed in number of movements) of any unit load to the I/O point. They derive closed-form formulas for a single-level system with one empty location and also develop a method to maneuver unit loads to the I/O point, minimizing the retrieval time of an arbitrary unit load. In addition, they propose a heuristic retrieval method yielding short retrieval times for systems with multiple

empty locations. Zaerpour et al. (2011) study travel time in a multi-level live-cube compact storage system considering a random storage policy. Through a decomposition procedure, they derive four closed-form travel-time formulas corresponding to four complementary system configurations. We study a multi-level live-cube system with class-based storage. Deriving closed-form travel-time formulas for a multi-level live-cube system with random storage is already complex. However, applying a storage zone boundary increases the complexity of the problem significantly, leading to 36 cases in the decomposition process compared to four cases for the random storage problem.

The remainder of this chapter is organized as follows. Section 5.2 describes the problem and assumptions. Section 5.3 derives the closed-form formulas for expected retrieval times of the first and second zones of the single-level and multi-level rectangular live-cube systems. For a rectangular single-level system, three cases can be distinguished. For a rectangular multi-level system, 36 cases need to be distinguished. Section 5.4 evaluates the quality of the closed-form formulas by comparing them with results from a Monte Carlo simulation. Section 5.5 concludes the chapter.

5.2. Problem description and assumptions

In this section, we first describe the two-class based storage policy and the general procedure to derive the expected retrieval time. Then we explain the work mechanism of a live-cube storage system under a two-class-based storage policy.

The system and storage coordinates are assumed to be continuous. This assumption is commonly used in the literature (see Hausman et al. (1976), Bozer and White (1984), Rosenblatt and Eynan (1989), Yu and De Koster (2009b)) and significantly reduces the complexity of analysis. The product and unit load turnover distribution can be derived from the Pareto-demand curve (ABC curve) and assuming EOQ product replenishment model. The ABC curve represents the percentage of cumulative demand in number of unit loads versus the fraction of ranked inventoried products. Equation (5.1) gives a representation of the ABC curve function where p is the percentage of inventoried products (which are ranked in descending order based on their demand) and s is the skewness parameter. A smaller s means a more skewed curve (see Hausman et al. (1976)).

$$A(p) = p^s , \ 0 < s \leq 1 \tag{5.1}$$

$\lambda(j)$ represents the turnover of the product on unit load j (j is normalized between 0 and 1) or, briefly, the turnover of unit load j in the system. Based on Hausman et al. (1976), using the EOQ policy, we find

$$\lambda(j) = (2s/K)^{0.5} j^{\frac{s-1}{s+1}}, 0 < j \leq 1,$$ (5.2)

where K is the ratio of order cost to holding cost and is assumed to be identical for all items. For a two-class-based system, the expected retrieval time of the system can be expressed as follows,

$$E[T] = \frac{\int_{j \in R_1} \lambda(j) E[T^1] dj + \int_{j \in R_2} \lambda(j) E[T^2] dj}{\int_{j=0}^{1} \lambda(j) dj},$$ (5.3)

where $j \in R_i$ represents the unit loads assigned to zone R_i ($i = 1,2$) and $E[T^i]$ is the expected retrieval time of a unit load in zone i. Let B represent the boundary of the first zone which is the set of all locations with travel time distance b to the I/O point. Therefore, all locations with travel time distance less than or equal to the boundary parameter b form the first zone and the remaining locations of the system form the second zone. In Equation (5.3), $\lambda(j)$ can be replaced by the expression given in Equation (5.2). Since $2s/K$ is a constant that appears in both the numerator and denominator, it can be removed from the expression. The remaining part is equivalent to Equation (5.4) as follows,

$$E[T] = G_1^{2s/(s+1)} E[T^1] + (1 - G_1^{2s/(s+1)}) E[T^2],$$ (5.4)

where G_1 is the volume of the first zone divided by the volume of the system (V^1/V).

A system has length l (shuttle travel time from/to the I/O point to/from the farthest location in x-direction in an empty lane), width or depth w (shuttle travel time from/to the I/O point to/from the farthest location in y-direction in an empty lane) and height h (lift travel time from/to the I/O point to/from the farthest level in z-direction). For sake of convenience and without loss of generality, we suppose that the length of the system is not less than the width of the system; i.e. $l \geq w$ (see also Bozer and White (1984), Eynan and Rosenblatt (1994) and Yu and De Koster, (2009b)). The system capacity is constant.

The travel time of a unit load to the lift location at a given level depends on its (x,y) position, and the distribution of empty locations on its path to the lift. In case only one empty location is available, Gue and Kim (2007) show it equals $4x + 2y - 8$ (if $x > y$). However, in practice utilizations of not more than 95% are common in systems containing 1000 unit loads or more. This implies there are sufficient empty locations at each level to create a virtual aisle for any desired unit load. By creating a virtual aisle, the requested unit load can move to the lift location without interfering with other unit loads. A sufficient condition to create such a virtual aisle is that the number of empty locations on a level equals at least the maximum of the number of rows and the number of columns. For more details about the properties of

such a system, see Zaerpour et al. (2011). Figure 5.1(a) shows a situation where a unit load needs to be moved out of a live-cube system. In this case, a virtual aisle can be created by simultaneously moving some interfering unit loads (Figure 5.1(b)). The desired unit load can then be moved to the I/O point without any interference.
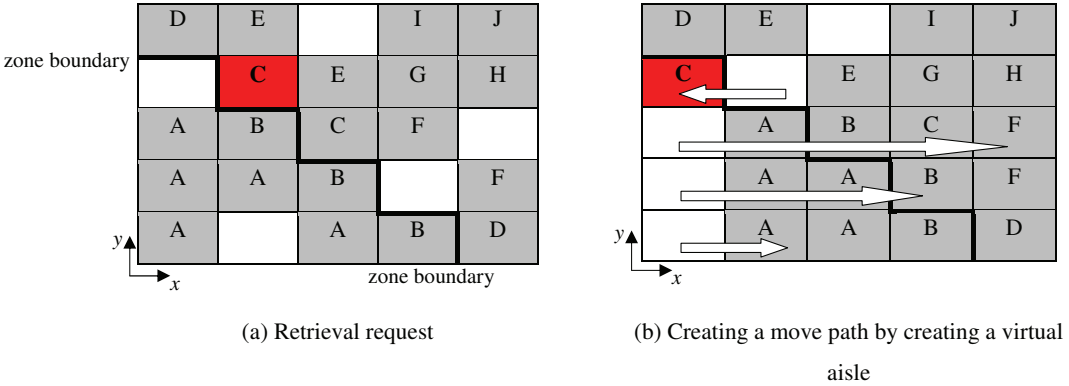
(a) Retrieval request

(b) Creating a move path by creating a virtual aisle

Notes. (1) Requested unit load is in red

(2) Bold line represents first zone boundary

(3) I/O point is located at lower left corner

Figure 5.1. A virtual aisle in a single-level live-cube system

For a system where the I/O point is at the left-lower corner, the retrieval time of a unit load at location (x,y) of a single-level live-cube storage system can be approximated by

$$t(x, y) = x + y. \tag{5.5}$$

We assume x and y to be continuous. While creating the virtual aisle, the desired unit load can usually move toward the I/O point at the same time. In the worst case, the virtual aisle can usually be created in one time unit and then the desired unit load can immediately move toward the I/O point. With an increasing system size, the effect of this constant time to create a virtual aisle disappears. Therefore, in Equation (5.5) we neglect the (constant) time needed to create the virtual aisle. Based on the retrieval time function (Equation (5.5)), a triangular-in-time (TIT) shape appears to be optimal for a live-cube system for any given capacity. However, such a system is not very practical and much more costly (for a given storage capacity) than a rectangular system. Therefore, we consider rectangular systems only.

In a multi-level live-cube storage system, a lift takes care of the vertical movement. When idle, the lift waits at the lower left corner of the system (i.e. I/O point). Assume (x,y,z) represents a location (in units of time) where z refers to the coordinate of each level (in units of time) in height direction.

The retrieval time of a unit load consists of the following two components:

1) The time needed to bring the unit load to the lift. Since the movements of shuttles at each level are independent of the movement of the lift, this time equals the maximum of the time to move the unit load to the lift at the same level ($x+y$) and the time needed for the lift to go from the I/O point to the unit load's level (z).

2) The time needed for the lift to return to the I/O point when it has the unit load (z).

Thus, the retrieval time of a unit load located at (x,y,z) for a multi-level system can be estimated by Equation (5.6),

$$t(x, y, z) = \max\{x + y, z\} + z .$$

(5.6)

In order to evaluate the performance of a live-cube system with two classes, the expected value of the retrieval time of an arbitrary unit load in the first and second zones must be derived. Figure 5.2 shows a top-view of a two-class single-level live-cube system with a first zone boundary. For the sake of illustration, we assume shuttle speeds in x and y directions are equal and normalized. Then boundary B divides the system into two zones; the first zone R_1 includes locations with retrieval time less than or equal to b and the second zone R_2 includes locations with retrieval time greater than b. In other words, $R_1 = \{(x, y) \mid x + y \le b\}$ and $R_2 = \{(x, y) \mid x + y > b\}$. Since there is at least one empty location at each row and each column of the system, a virtual aisle can be created for any requested unit load. Although the empty locations are evenly distributed within the system, the number of empty locations at each zone can vary from time to time. For instance, to retrieve the highlighted unit load in the second zone, the empty locations in the first zone also need to be used to create a horizontal virtual aisle for the unit load's leftward movement. This leads to more empty locations in the second zone and fewer open locations in the first zone. In a next step, the locations in the second zone can be used to create a virtual aisle in the left-most column of the system for downward movement of the highlighted unit load toward the I/O point. In creating these virtual aisles to move a unit load, empty locations can temporarily be transferred from one zone to another. After the unit load has been retrieved, the system can again be transformed to a system with at least one empty location at each row and each column in a maximum of one unit of time (see Zaerpour et al. (2011)). In the next section, closed-form formulas for single-level and multi-level live-cube systems are derived.
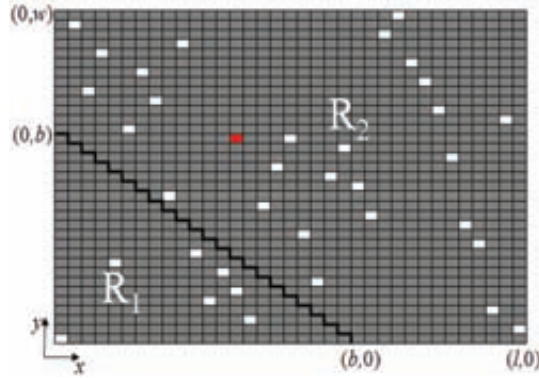
Figure 5.2. A two-class single-level live-cube system with a first zone boundary

5.3. Analytical model for the expected retrieval time of a live-cube system

In this section, we analytically derive the expected retrieval times for the first and second zones of a two-class live-cube system. Sections 5.3.1 and 5.3.2 derive the expected retrieval times for the first and second zones of rectangular single-level and rectangular multi-level systems, respectively. The first step is to locate the first zone boundary within a specific configuration of a live-cube system. Several cases can be distinguished, each with a different shape of the first or the second zone compared to other cases. In total, three cases for a single-level live-cube system and 36 cases for a multi-level live-cube system can be obtained. The next step is to divide each case into necessary sub-cases to calculate the expected retrieval time for each sub-case.

5.3.1. Single-level live-cube compact storage system

In this section, we derive the expected retrieval time for the first and second zones of a rectangular single-level live-cube system. First, we need to obtain the possible shapes of the first and second zones. All locations (x, y) which satisfy $t(x, y) = x + y = b$ form the boundary. Therefore, the inequalities $x + y \leq b$ and $x, y \geq 0$ include all locations belonging to the first zone. They form a triangular shaped area which includes all the locations with retrieval time less than or equal to b (see Figure 5.3(a)). However, this triangle can be bounded by the rectangular shaped system (see Figure 5.3(b)) depending on first zone boundary parameter and system configuration.
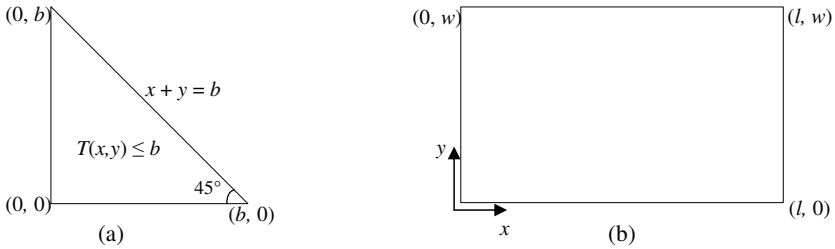
Figure 5.3. (a) The region formed by $t(x, y) \leq b$ and $x, y \geq 0$ (b) a rectangular single-level system

One of the three following cases can be distinguished depending on the first zone boundary parameter and system configuration for a rectangular single-level live-cube system.

1. Case $b \leq w$
2. Case $w < b \leq l$
3. Case $l < b \leq l + w$

Figure 5.4 shows the shapes of the first and second zones for each of these three cases.

    (a) $b \leq w$ (b) $w < b \leq l$ (c) $l < b \leq l + w$
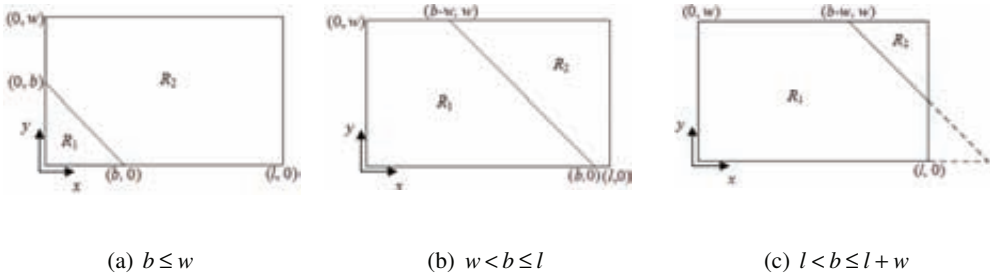
Figure 5.4. Three complementary cases for a single-level live-cube system

Each of the above cases needs to be split into several sub-cases. The sub-cases can be used to derive the expected retrieval times of the first and second zones for each case. The expected retrieval time of an arbitrary unit load in the first ($E[T^1]$) and second ($E[T^2]$) zones of a single-level live-cube storage system can be calculated by Equations (5.7) and (5.8), respectively:

$$E[T^1] = \int_{t=0}^{b} t f^1(t) dt, \tag{5.7}$$

$$E[T^2] = \int_{t=b}^{l+w} tf^2(t)dt \,, \tag{5.8}$$

where t represents the retrieval time of a unit load at location (x, y). b represents the boundary parameter of the first zone. $f^i(t)$ represents the probability density function of the retrieval time t for zone i ($i =1, 2$). Equation (5.5) gives the retrieval time of any location (x, y) in a single-level system. Within each zone, unit loads are stored randomly. Thus, any storage location has an equal chance of accommodating a requested unit load. Therefore, the cumulative distribution function $F^i(t)$ for $i =1$ and 2 can be calculated by Equations (5.9) and (5.10), respectively:

$$F^1(t) = P(T(X,Y) \le t) = \frac{\text{area of } \{(x,y)|\ t(x, y) \le t, t \le b\}}{\text{area of the first zone}} \,, \tag{5.9}$$

$$F^2(t) = P(b \le T(X,Y) \le t) = \frac{\text{area of } \{(x,y)\ |\ b \le t(x, y) \le t\}}{\text{area of the second zone}}. \tag{5.10}$$

As an example, consider the case $w < b \le l$. The area of the first zone can be calculated by integrating the function $b - y$ over $0 \le y \le w$ which equals $(2bw - w^2)/2$ ($y = 0$ is considered as the base). Therefore, G_1 which is the area of the first zone divided by the area of the system can be calculated by $G_1 = (2bw - w^2)/(2lw)$. $F^1(t), F^2(t), f^1(t),$ and $f^2(t)$ for case $w < b \le l$ can now be calculated by

$$F^1_{w<b\le l} = \begin{cases} t^2/(2wb - w^2) & \text{if } t \le w \\ (2wt - w^2)/(2wb - w^2) & \text{if } w \le t \le b \end{cases},$$

$$F^2_{w<b\le l} = \begin{cases} (2wt - 2wb)/(w^2 + 2wl - 2wb) & \text{if } b \le t \le l \\ (2wt + 2lt - t^2 - 2wb - l^2)/(w^2 + 2lw - 2wb) & \text{if } l \le t \le l + w \end{cases},$$

$$f^1_{w<b\le l} = \begin{cases} (2t)/(2wb - w^2) & \text{if } t \le w \\ (2w)/(2wb - w^2) & \text{if } w \le t \le b \end{cases},$$

$$f^2_{w<b\le l} = \begin{cases} (2w)/(w^2 + 2wl - 2wb) & \text{if } b \le t \le l \\ (2w + 2l - 2t)/(w^2 + 2lw - 2wb) & \text{if } l \le t \le l + w \end{cases}.$$

Consequently, $E[T^1]$ and $E[T^2]$ for the case $w < b \le l$ can be calculated by using Equations (5.11) and (5.12),

$$E[T^1_{w<b\le l}] = \int_0^w (2t^2/(2wb - w^2))dt + \int_w^b (2wt/(2wb - w^2))dt = \frac{(3b^2 - w^2)}{3(2b - w)}, \tag{5.11}$$

$$E[T_{w<b\leq l}^2] = \int_b^l 2wt/(w^2 + 2lw - 2wb)dt + \int_l^{l+w} (2wt + 2lt - 2t^2)/(w^2 + 2lw - 2wb)dt$$

$$= \frac{-3b^2 + 3l^2 + 3lw + w^2}{3(2l + w) - 6b}. \tag{5.12}$$

By replacing $E[T^1]$, $E[T^2]$ and G_1 in Equation (5.4), $E[T]$ for the case $w < b \leq l$ can be obtained by using Equation (5.13),

$$E[T_{w<b\leq l}] = (\frac{2b-w}{2l})^{\frac{2s}{s+1}} \frac{(3b^2 - w^2)}{3(2b-w)} + (1 - (\frac{2b-w}{2l})^{\frac{2s}{s+1}}) \frac{-3b^2 + 3l^2 + 3lw + w^2}{3(2l+w) - 6b}. \tag{5.13}$$

$E[T]$ for other two cases can be calculated similarly (for detailed calculation we refer to our working paper),

$$E[T_{b\leq w}] = (\frac{b^2}{2lw})^{\frac{2s}{s+1}} \frac{2b}{3} + (1 - \frac{b^2}{2lw}) \frac{2b^3 - 3lw(l+w)}{3(b^2 - 2lw)},$$

$$E[T_{l<b\leq l+w}] = (\frac{2bw + 2bl - b^2 - w^2 - l^2}{2lw})^{\frac{2s}{s+1}} \frac{3b^2w + 3b^2l - 2b^3 - w^3 - l^3}{3(2bw + 2bl - b^2 - w^2 - l^2)} +$$

$$(1 - (\frac{2bw + 2bl - b^2 - w^2 - l^2}{2lw})^{\frac{2s}{s+1}}) \frac{1}{3}(2b + l + w).$$

5.3.2. Multi-level live-cube compact storage system

In this section, we derive the expected retrieval time formulas for any possible configuration of a multi-level live-cube system and any first zone boundary. The first step is to obtain all possible shapes of the first and second zones. The boundary B is a set of locations which can be defined as $B = \{(x, y, z) \mid \max\{x + y, z\} + z = b\}$. Therefore, the first zone is a set of locations which can be defined as $R_1 = \{(x, y, z) \mid \max\{x + y, z\} + z \leq b \ \& \ x, y, z \geq 0\}$. However, $\max\{x + y, z\} + z \leq b$ can be split into two inequalities as follows:

$x + y + z \leq b$ if $x + y \geq z$,

$2z \leq b$ if $x + y < z$.

The above inequalities together with $x, y, z \geq 0$ form a truncated pyramid-shaped polytope as shown in Figure 5.5(a). This polytope again has to be truncated from different angles by system planes (Figure 5.5(b)), depending on the position of the parameters, l, w, h, and b. Therefore, several different shapes for

the first and second zones can be obtained depending on the position of the first zone boundary and system dimensions.
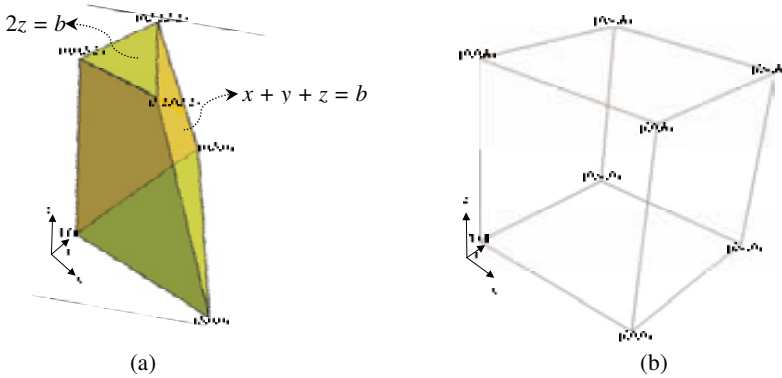

Figure 5.5. (a) The first zone formed by $x + y + z \leq b$ and $2z \leq b$ (b) cubic shape of a multi-level system
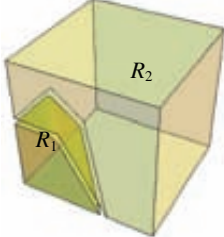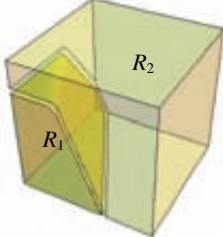
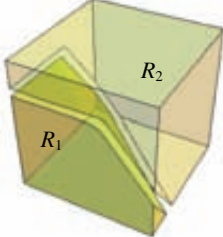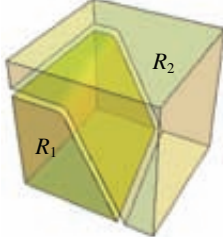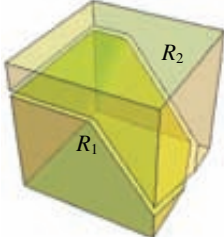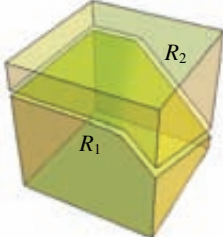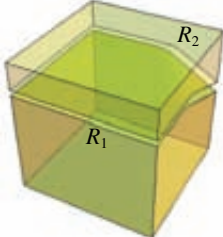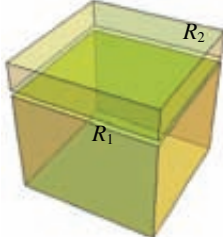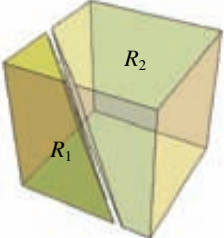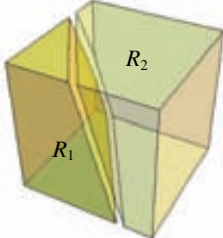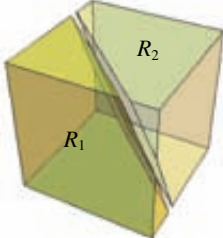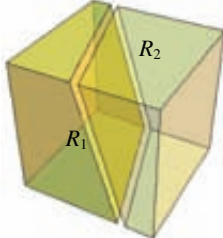In section 5.3.2.1, we explain the general procedure for obtaining all possible shapes. For the lengthy detailed procedure, we refer to our working paper.

5.3.2.1. Hierarchical decomposition procedure for shapes with differently shaped R_1 or R_2

On one side we have the planes $z = b/2$ and $x + y + z = b$ in Figure 5.5(a), while on the other side we have the planes $z = h$, $y = w$ and $x = l$ in Figure 5.5(b). Following a hierarchical procedure, we first consider both horizontal planes in z-direction (i.e. $z = b/2$ and $z = h$). Two situations are possible depending on the values of b and h: $b/2 \leq h$ and $b/2 > h$. Assuming constraints defined by the other planes in Figure 5.5(b) are not effective, we obtain two different shapes for the second zone shown in Figure 5.6(a) and 5.6(i) corresponding to $b/2 \leq h$ and $b/2 > h$, respectively. Now let us only consider Figure 5.6(a). In y-direction, the shape has two corner points: $(0, b/2, b/2)$ and $(0, b, 0)$. The plane $y = w$ can be positioned differently depending on the value of w and b as follows: $w > b$ (still Figure 5.6(a)), $b/2 < w \leq b$ (Figure 5.6(b)), $w \leq b/2$ (Figure 5.6(d)). The next step is to consider the plane $x = l$ in x-direction. Let us consider only one of the possibilities obtained so far which is $b/2 \leq h$ and $w > b$ (still Figure 5.6(a)). Figure 5.6(a) has two corner points in x-direction: $(b/2, 0, b/2)$ and $(b, 0, 0)$. The plane $x = l$ can be positioned differently depending on the value of l and b as follows: $l > b$ (still Figure

5.6(a)), $b/2 < l \leq b$ (not feasible since we have $w > b$ and also $l \geq w$), $l \leq b/2$ (not feasible for a similar reason). This hierarchical analysis leads to a tree with each node representing a specific configuration and first zone boundary while some nodes are infeasible (see Appendix 5C. In the illustrative example, only one feasible case ($b/2 \leq h$, $w > b$, $l > b$: Figure 5.6(a)) is eventually obtained.

In total 16 different cases can be obtained with differently shaped R_1 or R_2 (see Figure 5.6).

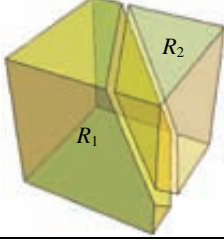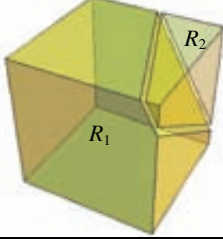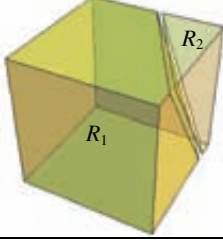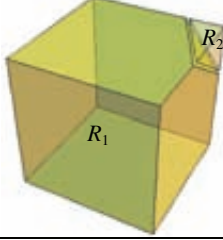|			
(A) $b/2 \leq h$ & $b \leq w$	**(B)** $b/2 \leq h$ & $w \leq b \leq 2w$ & $b \leq l$	**(C)** $b/2 \leq h$ & $l \leq b \leq 2w$	**(D)** $b/2 \leq h$ & $2w \leq b \leq l$
(E) $b/2 \leq h$ & $2w \leq b$ & $l \leq b \leq l+w$	**(F)** $b/2 \leq h$ & $l+w \leq b \leq 2l$	**(G)** $b/2 \leq h$ & $2l \leq b \leq 2(l+w)$	**(H)** $b/2 \leq h$ & $2(l+w) \leq b \leq 2h$
(I) $b/2 \geq h$ & $b \leq w$	**(J)** $b/2 \geq h$ & $w \leq b \leq w+h$ & $b \leq l$	**(K)** $b/2 \geq h$ & $l \leq b \leq w+h$	**(L)** $b/2 \geq h$ & $w+h \leq b \leq l$

(M) $b/2 \geq h$ & $w+h \leq b$ & $l \leq b \leq \min\{l+w, l+h\}$	**(N)** $b/2 \geq h$ & $l+w \leq b \leq l+h$	**(O)** $b/2 \geq h$ & $l+h \leq b \leq l+w$	**(P)** $b/2 \geq h$ & $\max\{l+h, l+w\} \leq b \leq l+w+h$

Figure 5.6. Cases A-P with their corresponding shapes of first and second zones

Different shapes of the first and second zones lead to different volume formulas and so according to Equations (5.9) and (5.10) different cumulative distribution functions will be obtained. We denote these 16 cases in an alphabetical order by cases A, B, C,…, P.

In order to calculate the volume of the first zone in each case, we consider the base of the solid to be in yz-plane. Then the function $\min\{l, b-y-z\}$ can be integrated over these boundaries: $0 \leq y \leq w$, $0 \leq z \leq h$, $y+z \leq b$, $z \leq b/2$. Depending on the shape of the first zone in each case, every boundary might need to be split into several boundaries.

The expected retrieval time of an arbitrary unit load in the first ($E[T^1]$) and second ($E[T^2]$) zones of a multi-level live-cube storage system can be calculated by using Equations (5.14) and (5.15), respectively:

$$E[T^1] = \int_{t=0}^{b} t f^1(t) dt, \tag{5.14}$$

$$E[T^2] = \int_{t=b}^{\max\{l+w,h\}+h} t f^2(t) dt, \tag{5.15}$$

where, b represents the zone boundary parameter. $f^i(t)$ represents the probability density function of retrieval time t for zone i ($i = 1, 2$). The cumulative distribution function $F^i(t)$ for $i = 1$ and 2 can be calculated by Equations (16) and (17), respectively:

$$F^1(t) = P(T(X,Y,Z) \leq t) = \frac{\text{volume of } \{(x,y,z) | t(x,y,z) \leq t, t \leq b\}}{\text{volume of the first zone}}, \tag{5.16}$$

$$F^2(t) = P(b \leq T(X,Y,Z) \leq t) = \frac{\text{volume of } \{(x,y,z) | b \leq t(x,y,z) \leq t\}}{\text{volume of the second zone}}. \tag{5.17}$$

In order to calculate $E[T^1]$ and $E[T^2]$, each of 16 cases again needs to be split into at most four sub-cases depending on the system configuration. In total 36 complementary sub-cases can be considered, each corresponding to a unique $E[T]$ formula. In section 5.3.2.2, we explain the detailed procedure to derive $E[T^1]$ and $E[T^2]$ where case A ($b/2 \leq h$ and $b \leq w$) and configuration $h \leq w$ is considered (i.e. sub-case A1). Then, in section 5.3.2.3 we give all other 35 complementary sub-cases and we discuss all the sub-cases generally.

5.3.2.2. Computation of $E[T]$ for sub-case A1

In this section, we give the detailed procedure of calculating $E[T]$ for one of the sub-cases of case A (sub-case A1: $b \leq 2h$, $b \leq w$ and $h \leq w$). Based on Equation (5.4), $E[T_{A1}]$ can be calculated as follows:

$$E[T_{A1}] = \left(\frac{7b^3}{48hlw}\right)^{\frac{2s}{1+s}} \frac{3b}{4} + \left(1 - \left(\frac{7b^3}{48hlw}\right)^{\frac{2s}{1+s}}\right) \frac{21lb^4 - 8h\left(h^3 + 12hlw + 12lw(l+w)\right)}{4\left(7b^3 - 48hlw\right)}, \tag{5.18}$$

where, $G_1 = \frac{7b^3}{48hlw}$, $E[T^1_{A1}] = \frac{3b}{4}$ and $E[T^2_{A1}] = \frac{21lb^4 - 8h\left(h^3 + 12hlw + 12lw(l+w)\right)}{4\left(7b^3 - 48hlw\right)}$. Now, the derivation

of all components, G_1, $E[T^1_{A1}]$, and $E[T^2_{A1}]$ can be explained. Figure 5.7 shows the shape of the first and second zones for sub-case A1.

According to Equations (5.16) and (5.17), we first need to calculate the volume of the first and second zones. The volume of the first zone (V^1) can be obtained by integrating the function $\min\{l, b-y-z\}$ over the boundaries $0 \leq y \leq b-z$ and $0 \leq z \leq b/2$. In this case $\min\{l, b-y-z\}$ always equals $b-y-z$. Therefore, the volume of the first zone (V^1) is given by

$$V^1_{A1}(b) = \int_{z=0}^{b/2} \int_{y=0}^{b-z} (b-y-z)dydz = 7b^3/48. \tag{5.19}$$

The second zone includes the locations of the system which have not been assigned to the first zone. Therefore, the volume of the second zone (V^2) is the volume of the system subtracted by the volume of the first zone, i.e.

$$V^2_{A1}(b, l, w, h) = wlh - 7b^3/48. \tag{5.20}$$

(a)   (b)
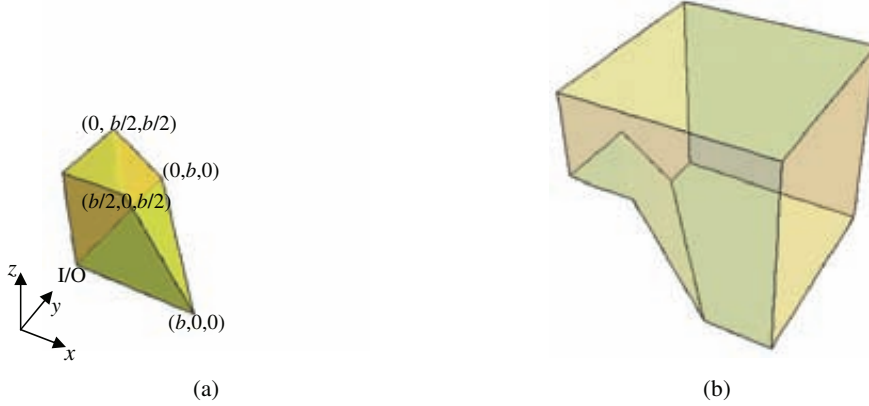
Figure 5.7. (a) The first zone (b) the second zone of sub-case A1

G_1 can be obtained by dividing the volume of the first zone ($\dfrac{7b^3}{48}$) by the volume of the system (lwh),

i.e. $G_1 = \dfrac{7b^3}{48lwh}$.

In order to calculate $E[T^1_{A1}]$ and $E[T^2_{A1}]$, we first give the following definition:

Definition 1 (Critical retrieval time). The critical retrieval time is a time instant t at which the region $T \leq t$ in the first zone or the region $b \leq T \leq t$ in the second zone changes shape, resulting in a different volume formula.

It can be shown that for sub-case A1 the following values are the critical retrieval times:

$$w, l, 2h, w+h, l+h, w+l, l+w+h. \qquad\qquad\qquad (5.21)$$

However, conditions of sub-case A1 ($b/2 \leq h$, $b \leq w$, $h \leq w$) are not sufficient to arrange these critical retrieval times. In order to be able to arrange critical retrieval times, sub-case A1 needs again to be split into five different sub-sub-cases as follows:

- sub-sub-case A11: sub-case A1 ($b/2 \leq h$, $b \leq w$, $h \leq w$) plus $l \leq 2h$,

- sub-sub-case A12: sub-case A1 ($b/2 \leq h$, $b \leq w$, $h \leq w$) plus $w \leq 2h$ and $2h < l \leq w+h$,

- sub-sub-case A13: sub-case A1 ($b/2 \leq h$, $b \leq w$, $h \leq w$) plus $w \leq 2h$ and $l > w+h$,

- sub-sub-case A14: sub-case A1 ($b/2 \leq h$, $b \leq w$, $h \leq w$) plus $w > 2h$ and $2h < l \leq w+h$, and

- sub-sub-case A15: sub-case A1 ($b/2 \leq h$, $b \leq w$, $h \leq w$) plus $w > 2h$ and $l > w+h$.

Now it is possible to arrange the critical retrieval times for each of these five sub-sub-cases. One possibility for sub-case A1 is when $l \leq 2h$ (sub-sub-case A11). Therefore, we can arrange the critical retrieval times as follows:

$$w \leq l \leq 2h \leq h + w \leq h + l \leq l + w \leq l + w + h. \qquad (5.22)$$

Now we can calculate $E[T^1]$ and $E[T^2]$ for sub-sub-case A11($b/2 \leq h,\ b \leq w,\ h \leq w,\ l \leq 2h$).

Computation of $E[T^1_{A11}]$

In order to calculate $E[T^1_{A11}]$ we first need to derive the cumulative distribution function of the random variable T by using Equation (5.16). Based on Equation (5.22), we have $w \leq 2h$ and so $0 \leq b \leq w$. Therefore, the only possible situation for retrieval time t in the first zone is when $0 \leq t \leq b$. Figure 5.8 shows the shape of the region $T \leq t$ in the first zone.
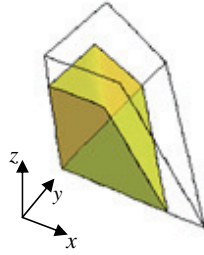
Figure 5.8. Region $T \leq t$ in the first zone of sub-sub-case A11

In this case, the shape of region $T \leq t$ is exactly similar to the shape of the first zone. Therefore, the volume of region $T \leq t$ is given by

$$\int_{z=0}^{t/2} \int_{y=0}^{t-z} (t - y - z)\,dy\,dz = 7t^3 / 48.$$

The cumulative distribution function for the first zone can now be derived by using Equation (5.16). By taking the derivative, the probability density function is obtained. Therefore, we have

$$F^1_{A11}(t) = t^3 / b^3,$$

$$f^1_{A11}(t) = \frac{dF^1_{A11}(t)}{dt} = 3t^2 / b^3.$$

Consequently, $E[T^1_{A11}]$ is given by

$$E[T_{A11}^1] = \int_0^b (3t^3/b^3)dt = \frac{3b}{4}.$$

(5.23)

In fact, $E[T_{A1}^1] = E[T_{A11}^1] = E[T_{A12}^1] = E[T_{A13}^1] = E[T_{A14}^1] = E[T_{A15}^1]$, since it can be shown that the other four sub-sub-cases (A12,…, A15) lead to a similar closed-form formula as Equation (5.23). For the proof, we refer to our working paper.

Computation of $E[T^2_{A11}]$

According to Equation (5.22), seven different positions for the retrieval time t in sub-sub-case A11 are possible which are: $b \le t < w$; $w \le t < l \ldots l+w \le t \le l+w+h$. Each of these seven boundaries corresponds to one of the regions $b \le T \le t$ in Figure 5.9. Figure 5.9 shows the region $b \le T \le t$ changes shape from one to another boundary. Therefore, the volume formula and correspondingly the cumulative distribution and density function for each shape need to be calculated. We here explain the procedure for Figures 5.9(a), 5.9(b) and 5.9(c).

In Figure 5.9(a), we have $b \le t < w$. Since $t < w$, the shape does not touch the $y = w$ plane of the cube. In addition, since $w \le l$, the shape also does not touch the $x = l$ plane of the cube. Furthermore, $z = t/2$ represents the top surface of the shape. However, $t < w$ and also $w < 2h$ (see Equation (5.22)) and therefore $t < 2h$. Hence, the plane $z = t/2$ of the shape does not touch the plane $z = h$ of the cube.

In Figure 5.9(b), $w \le t < l$. Since $w \le t$, the shape touches the $y = w$ plane of the cube. The point $(t-w,w,0)$ in the $y = w$ plane has a retrieval time equal to t $(t-w+w)$ which is greater than w. The explanation for the shape of the polytope in x- and z- directions is similar to the previous shape.

In Figure 5.9(c), $l \le t < 2h$. Since $l \le t$, the shape touches the $x = l$ plane of the cube. The corner point $(l,t-l,0)$ of the shape has retrieval time t $(t-l+l)$ which is greater than l. The explanation for the shape of polytope in y- and z- directions is similar to the previous shape.

The other shapes in Figure 5.9 can be explained similarly.
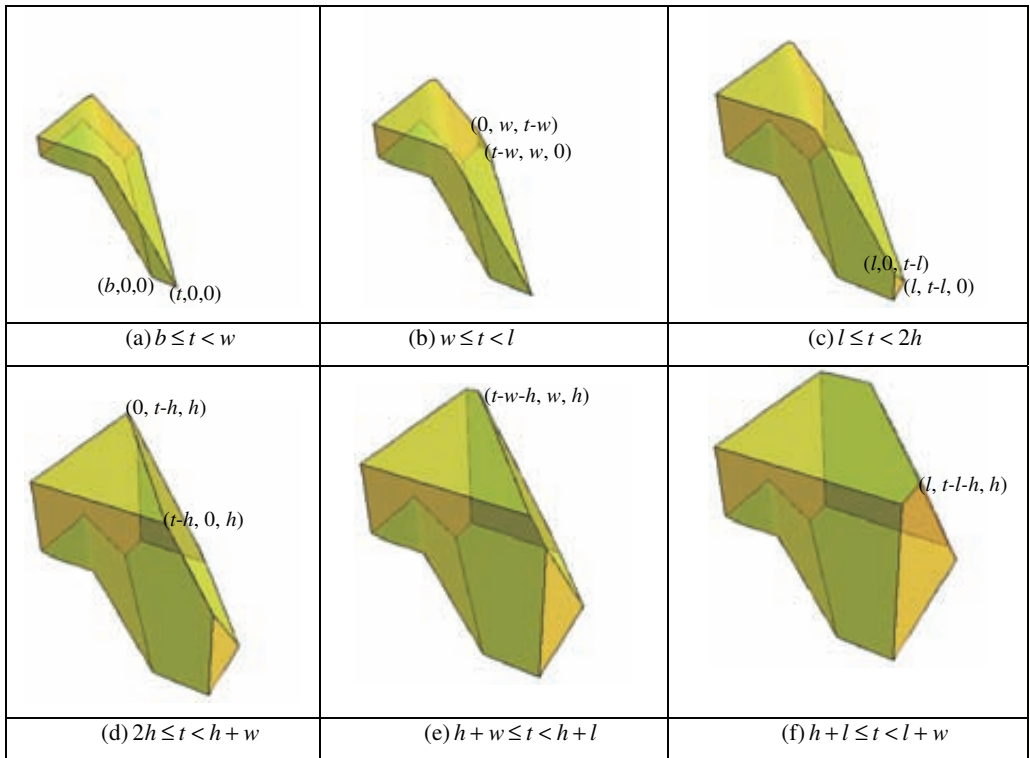
We now derive the volumes of the first three shapes in Figure 5.9 by considering the base of the shape to be in the yz-plane. In Figure 5.9(a), the region $b \le T \le t$ can be formed by removing the first zone from the region $0 \le T \le t$. The volume of the region $0 \le T \le t$ is $7t^3/48$ and therefore the volume of region $b \le T \le t$ can be calculated by

$$\int\limits_{z=0}^{t/2}\int\limits_{y=0}^{t-z}(t-y-z)dydz-7b^3/48=7(t^3-b^3)/48.$$

In Figure 5.9(b), we derive the volume of the region $0\le T\le t$ and then subtract the volume of the first zone. For the region $0\le T\le t$, y and z are bounded as follows: $0\le y\le \min\{w,t-z\}$, $0\le z\le t/2$. The volume of the region $0\le T\le t$ is given by

$$\int\limits_{z=0}^{t/2}\int\limits_{y=0}^{\min\{w,t-z\}}(t-y-z)dydz.$$

$(b,0,0)$ $(t,0,0)$	$(0, w, t\text{-}w)$ $(t\text{-}w, w, 0)$	$(l,0, t\text{-}l)$ $(l, t\text{-}l, 0)$
(a) $b\le t<w$	(b) $w\le t<l$	(c) $l\le t<2h$
$(0, t\text{-}h, h)$ $(t\text{-}h, 0, h)$	$(t\text{-}w\text{-}h, w, h)$	$(l, t\text{-}l\text{-}h, h)$
(d) $2h\le t<h+w$	(e) $h+w\le t<h+l$	(f) $h+l\le t<l+w$

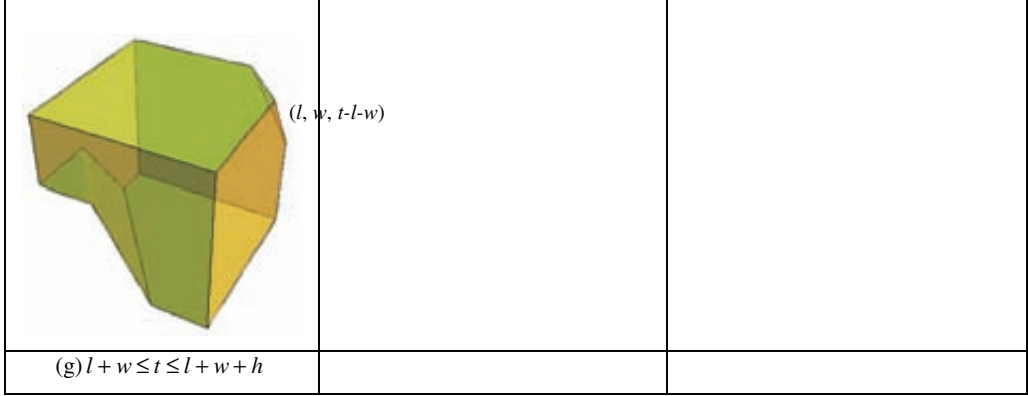|		
$(l, w, t\text{-}l\text{-}w)$		
(g) $l + w \le t \le l + w + h$		

Figure 5.9. Region of $b \le T \le t$ for the second zone of sub-sub-case A11

Figure 5.9(b) shows the line $y = t - z$ intersects $y = w$ plane at point $(0,w,t\text{-}w)$. For any $z \le t\text{-}w$, $\min\{w, t - z\} = w$ and for any $z > t\text{-}w$, $\min\{w, t - z\} = t - z$. Therefore, the volume of the Figure 5.9(b), where $w \le t < l$, is given by

$$\int_{z=0}^{t-w}\int_{y=0}^{w}(t - y - z)\,dydz + \int_{z=t-w}^{t/2}\int_{y=0}^{t-z}(t - y - z)\,dydz - 7b^3 / 48 = \frac{1}{48}\left(-b^3 - t^3 + 24t(t - w)w + 8w^3\right).$$

Figure 5.9(c) is a truncated version of Figure 5.9(b); the plane $x = l$ has removed a pyramid shaped top in x-direction. Therefore, the volume (5.9c) = volume (5.9b) – volume (truncated pyramid). The height of the removed pyramid equals $t\text{-}l$, and the base of pyramid is a right triangle with both legs equaling $t\text{-}l$. Therefore, the volume of the removed pyramid equals $(t - l)^3 / 6$. The resulting volume of Figure 5.9(c) is given by

$$\int_{z=0}^{t-w}\int_{y=0}^{w}(t - y - z)\,dydz + \int_{z=t-w}^{t/2}\int_{y=0}^{t-z}(t - y - z)\,dydz - \frac{1}{6}(t - l)^3 - 7b^3 / 48 = \frac{1}{48}\left(-b^3 - t^3 - 8(t - l)^3 + 24t(t - w)w + 8w^3\right).$$

The cumulative distribution function of the second zone for each shape in Figure 5.9 can be derived by using Equation (5.17). By taking the derivative, the probability density function is obtained. Corresponding to Figures 5.9(a-c), the cumulative distribution and density functions are given by

$$F^2(t) = \left(7(t^3 - b^3) / 48\right) / \left(wlh - 7b^3 / 48\right) \qquad\qquad \text{if } b \le t < w,$$

$$f^2(t) = \frac{d(F^2)}{dt} = (21t^2) / (48hlw - 7b^3) \qquad\qquad \text{if } b \le t < w,$$

$$F^2(t) = (\frac{1}{48}(-b^3 - t^3 + 24t(t-w)w + 8w^3)) / (wlh - 7b^3 / 48) \qquad\qquad \text{if } w \le t < l,$$

$$f^2(t) = \frac{d(F^2)}{dt} = \frac{-3t^2 + 48wt - 24w^2}{48hlw - 7b^3} \qquad\qquad \text{if } w \le t < l,$$

$$F^2(t) = \frac{1}{48}(-b^3 - t^3 - 8(t-l)^3 + 24t(t-w)w + 8w^3) / (wlh - 7b^3 / 48) \qquad\qquad \text{if } l \le t < 2h,$$

$$f^2(t) = \frac{d(F^2)}{dt} = \frac{-3t^2 - 24(t-l)^2 + 48wt - 24w^2}{48hlw - 7b^3} \qquad\qquad \text{if } l \le t < 2h.$$

The probability density function for other boundaries in Figure 5.9 can be calculated similarly. This results in:

$$f^2_{A11} = \begin{cases} (21t^2) / (48hlw - 7b^3) & \text{if } b \le t < w, \\[2mm] \dfrac{-3t^2 + 48wt - 24w^2}{48hlw - 7b^3} & \text{if } w \le t < l, \\[2mm] \dfrac{-3t^2 - 24(t-l)^2 + 48wt - 24w^2}{48hlw - 7b^3} & \text{if } l \le t < 2h, \\[2mm] \dfrac{-3h^2 - 3(l-t)^2 + 6ht - 3t^2 + 3wt + 3(t-w)w}{6(wlh - 7b^3 / 48)} & \text{if } 2h \le t < w + h, \\[2mm] \dfrac{-\frac{1}{2}(l-t)^2 + hw}{wlh - 7b^3 / 48} & \text{if } w + h \le t < l + h, \\[2mm] \dfrac{h^2 + 2h(l-t+w)}{2(wlh - 7b^3 / 48)} & \text{if } l + h \le t < l + w, \\[2mm] \dfrac{(h+l-t+w)^2}{2(wlh - 7b^3 / 48)} & \text{if } l + w \le t \le l + w + h, \\[2mm] 0 & \text{Otherwise.} \end{cases} \qquad (5.24)$$

Consequently, $E[T^2_{A11}]$ can be calculated by

$$E[T_{A11}^2] = \left(\frac{48}{48lwh - 7b^3}\right)\left(\begin{array}{l} \int\limits_b^w \left(t\left(\frac{21t^2}{48}\right)\right)dt + \int\limits_w^l \left(t\left(\frac{-3t^2 + 48wt - 24w^2}{48}\right)\right)dt \\[2ex] + \int\limits_l^{2h} \left(t\left(\frac{-3t^2 - 24(t-l)^2 + 48wt - 24w^2}{48}\right)\right)dt \\[2ex] + \int\limits_{2h}^{w+h} \left(t\left(-\frac{1}{2}(t-l)^2 + \frac{1}{6}\left(-3h^2 + 6ht - 3t^2\right) + \frac{tw}{2} + \frac{1}{2}(t-w)w\right)\right)dt \\[2ex] + \int\limits_{w+h}^{l+h} \left(t\left(-\frac{1}{2}(t-l)^2 + hw\right)\right)dt \\[2ex] + \int\limits_{l+h}^{l+w} \left(t\left(\frac{h^2 + 2h(l-t+w)}{2}\right)\right)dt \\[2ex] + \int\limits_{l+w}^{l+w+h} \left(t\left(\frac{(h+l-t+w)^2}{2}\right)\right)dt \end{array}\right) \tag{5.25}$$

$$= \frac{21b^4 - 8h(h^3 + 12hlw + 12lw(l+w))}{4(7b^3 - 48lwh)}.$$

In fact, $E[T_{A1}^2] = E[T_{A11}^2] = E[T_{A12}^2] = E[T_{A13}^2] = E[T_{A14}^2] = E[T_{A15}^2]$, since it can be shown that the other 4 sub-sub-cases (A12,…, A15) lead to similar closed-form formula as Equation (5.25). For the proof, we refer to our working paper.

5.3.3. Discussion on computation of *E[T]* for other sub-cases

Sixteen different cases (cases A,…,P) have been considered according to the shapes of the first and second zones, which are illustrated in Figure 5.6. However, it is necessary to decompose each case into at most four sub-cases based on system configurations as follows:

- Configuration 1. $h < w$,
- Configuration 2. $w \leq h < l$,
- Configuration 3. $l \leq h < l + w$, and
- Configuration 4. $l + w \leq h$.

Therefore, in total 36 sub-cases can be obtained (e.g. sub-case A1 discussed in section 5.3.2.1) each corresponding to a specific closed-form formula for *E[T]*. Table 5.2 gives all 36 possible sub-cases. Any

sub-case XY corresponds to case X and configuration Y (e.g. case A and configuration 1 result in sub-case A1).

Table 5.2. All sub-cases each corresponding to a specific $E[T]$ formula[*]

Case \ Configuration	Configuration 1. $h < w$	Configuration 2. $w \leq h < l$	Configuration 3. $l \leq h < l + w$	Configuration 4. $l + w \leq h$
A	A1	A2	A3	A4
B	B1	B2	B3	B4
C	C1	C2	C3	C4
D	–	D2	D3	D4
E	–	E2	E3	E4
F	–	F2	F3	F4
G	–	–	G3	G4
H	–	–	–	H4
I	I1	–	–	–
J	J1	–	–	–
K	K1	–	–	–
L	L1	L2	–	–
M	M1	M2	–	–
N	–	N2	–	–
O	O1	–	–	–
P	P1	P2	P3	–

[*]The closed-form formulas for sub-cases A1,…,P3 can be found in Appendix 5B, Tables 5.11, 5.12, 5.13.

We now explain the reason of decomposing each case into at most four sub-cases through an illustrative example. We consider sub-case A1 ($b/2 \leq h$, $b \leq w$, $h \leq w$) described in section 5.3.2.1 and sub-case A2 ($b/2 \leq h$, $b \leq w$, $w \leq h < l$). The shapes of the first and second zones for both sub-cases are similar. Therefore, it is expected they both lead to the same closed-form formula. However, the closed-

form formulas for these two sub-cases are different. It is necessary to look again at the critical retrieval times. Critical retrieval times for sub-case A1 are given in Equation (5.21). Equation (5.26) gives the critical retrieval times for sub-case A2,

$$l, w, 2h, 2w, l+h, w+l, l+w+h .$$ (5.26)

Comparing Equations (5.21) and (5.26) shows that even though the shapes of the first and second zones in sub-cases A1 and A2 are similar, they have different critical retrieval times (e.g. $w + h$ in sub-case A1 and $2w$ in sub-case A2). Different critical retrieval times lead to different volume formulas in the derivation process. Therefore, different cumulative distribution functions, different density functions and consequently different closed-form formulas for $E[T]$ are obtained. Comparing sub-cases A1 and A2, identical expressions for $E[T^1]$ are obtained for both sub-cases, however $E[T^2]$ and consequently $E[T]$ will be different.

In addition, the four configurations are not always feasible for the cases A,…,P. Consider, for example, case D ($b/2 \leq h$, $w \leq b/2$, $b \leq l$) together with configuration 1 ($h < w$). In case D, $b/2 \leq h$ and $w \leq b/2$ which means $h \geq w$. This is inconsistent with configuration 1 which is $h < w$. As it can be seen from Table 5.2, sub-case D1 is not feasible and is left blank. Similar to sub-case A1 in section 5.3.2.1, each sub-case is decomposed into a maximum of 5 sub-sub-cases to derive the closed-form formulas. However, similar to sub-case A1, the obtained closed-form formulas are the same for all sub-sub-cases. The derivation procedure for all 36 sub-cases appears to be very tedious and exhaustive. However, the results obtained are simple to use.

The volume of the first zone (V_1), $E[T^1]$ and $E[T^2]$ for each sub-case is given in Appendix 5B, Tables 5.11, 5.12 and 5.13, respectively. Tables 5.11, 5.12 and 5.13 can be used as a reference to instantly evaluate the performance of any two-class-based live-cube compact storage system with any configuration and first zone boundary. According to Equation (4), the expected retrieval time for each sub-case can be calculated by

$$E[T] = G_1^{2s/(s+1)} E[T^1] + (1 - G_1^{2s/(s+1)}) E[T^2] .$$

For example, for case B2, G_1, $E[T^1]$, $E[T^2]$ and $E[T]$ are as follows:

$$G_{B2} = \frac{1}{48lwh}(-b^3 + 24b(b-w)w + 8w^3)$$

$$E[T_{B2}^1] = \frac{3b^4 - 64b^3w + 48b^2w^2 - 8w^4}{4b^3 - 96b^2w + 96bw^2 - 32w^3}$$

$$E[T_{B2}^2] = \frac{3b^4 - 64b^3w + 48b^2w^2 + 16w(2h^3 + h^2(6l - 3w) - w^3 + 2h(3l^2 + 3lw + w^2))}{4(b^3 - 24b^2w + 48hlw + 24bw^2 - 8w^3)}$$

$$E[T_{B2}] = \left(\frac{1}{48lwh}\left(-b^3 + 24b(b-w)w + 8w^3\right)\right)^{\frac{2s}{s+1}}\left(\frac{3b^4 - 64b^3w + 48b^2w^2 - 8w^4}{4b^3 - 96b^2w + 96bw^2 - 32w^3}\right) +$$

$$\left(1 - \left(\frac{1}{48lwh}\left(-b^3 + 24b(b-w)w + 8w^3\right)\right)^{\frac{2s}{s+1}}\right)\left(\frac{3b^4 - 64b^3w + 48b^2w^2 + 16w(2h^3 + h^2(6l - 3w) - w^3 + 2h(3l^2 + 3lw + w^2))}{4(b^3 - 24b^2w + 48hlw + 24bw^2 - 8w^3)}\right)$$

For any configuration (l, w, h) and zone boundary (b) corresponding sub-case can be found in Table 5.2 and the closed-form formula can be constructed similarly.

5.4. Evaluation and sensitivity analysis

To obtain the closed-form formulas, a continuous system is assumed while in reality the systems are discrete. Therefore, we test the accuracy of the closed-form formulas for estimating the response time of a discrete system. As it can be expected that the continuous approximation is better for large-scale systems, we also include small-size systems. Our base example is based on a live-cube system from a South-Korean company which produces live-cube parking systems. Compared to conventional parking systems, live-cube parking systems take 40%-50% less footprint area for the same number of parking slots (Hyundai Elevator, 2011). Therefore, this system reduces the cost per unit as it maximizes the usage of allowable parking lot space. Although the system can be designed in any desired size by the customer, we here focus on a medium-sized live-cube parking system. Input parameters describing the live-cube storage system are shown in Table 5.3. We consider a typical moderate ABC curve in practice which is 20%-80% (20% of inventoried products represent 80% of total demand in number of unit loads).The corresponding skewness parameter s can be calculated by using Equation (5.1). Thirty percent of the closest storage locations to the I/O point are dedicated to the first zone and the remaining 70% locations accommodate the vehicles that belong to the second class and stay in the system for a longer period. In order to calculate the expected retrieval time by using closed-form formulas, the corresponding sub-case has to be

considered. For any given configuration and any volume of the first zone, the boundary parameter b can be obtained by using the volume formula of the first zone, i.e. $V^1(b)/V = G_1$. Since the sub-cases are complementary, exactly one case can be considered for any configuration and first zone size.

First, we present the results for the base example. Then, we perform a sensitivity analysis (SA) to test the quality of closed-form formulas for different sources of variation in the input parameters. In each experiment, we vary one of the parameters of the base example over five different alternative values.

Table 5.3. Parameters describing storage system and storage policy

Fixed parameters	Data	
Size of a standard vehicle (mm)	Height=1550, Width =5160, Length=2100[*]	
Size of a storage location (mm)	Height=2925, Width=6400, Length=3250	
Shuttle speed in x-direction (v_x) (m/min)	45	
Shuttle speed in y-direction (v_y) (m/min)	100	
Lift speed (v_z) (m/min)	90	
Size of storage location (sec)	Height=1.95, Width=3.80, Length=4.33	
Varying parameters	Base example data	Range for scenarios
Size of system (sec)	Height=13.65, Width=15.2, Length=21.65	
Size of system (m)	Height=23.4, Width=32, Length=19.5	
First zone size (percentage of system size)	30%	[20%,100%]
ABC curve (percentage)	20%-80%	[20%-20%,20%-90%]
Capacity of the system (no. of parking slots)[**]	192	[100, 4000]
Length/Width (no. of tiers)	1.2	[0.25,4]
Height (no. of tiers)	8	[6,30]

[*]Length and Width denote the size in *x*- and *y*-directions, respectively.

[**]capacity of the system = total slots (Length × Width × Height =6×5×8=240 (in number of tiers)) – empty slots required to create virtual aisles (empty slots per level × Height in number of tiers = 6×8)

All instances have been simulated using MATLAB software on a portable computer Intel(R) Pentium(R) M1.86GHz with 512MB RAM and MS Windows XP professional. The results for the base example are shown in Table 5.4. Expected retrieval time for each instance of simulation is the average of 1000 randomly generated retrieval requests. The confidence intervals are given at a 95% confidence level.

Table 5.4. Comparison of the expected retrieval times obtained from the closed-form formula and simulation for the base example

1st zone size (%)	ABC curve (%)	Corresponding sub-case	Boundary (*b*) (sec)	$E[T_D]$ from derivation (sec)	$E[T_S]$ from simulation (sec)	% Gap*
30	20%-80%	B1	21.17	19.34	18.97±0.33	1.91%

$$* Gap = \frac{|E[T_S] - E[T_D]|}{E[T_D]} \times 100\%$$

In subsequent tables, we vary system capacity (Table 5.5), first zone size (Table 5.6), the skewness parameter or ABC curve (Table 5.7), Height (Table 5.8) and shape factor of the system i.e. *L/W* (in number of tiers) (Table 5.9) while the other parameters stay the same. In Table 5.5, when varying the capacity, the number of tiers in *x*-direction and *y*-direction are equal i.e. *L/W*=1. In Table 5.9, when varying the shape factor, the capacity of the system changes correspondingly.

Table 5.5. Results of sensitivity analysis when varying system capacity

System capacity (No. of slots)	Corresponding sub-case	Boundary (*b*) (sec)	$E[T_D]$ from derivation (sec)	$E[T_S]$ from simulation (sec)	% Gap
100	J1	15.38	14.11	13.65±0.25	3.23%
500	I1	32.09	29.13	28.75±0.51	1.29%
1000	J1	36.60	33.92	33.59±0.56	0.99%
2000	C2	47.13	42.94	42.65±0.65	0.68%
4000	C3	63.23	61.10	60.80±1.05	0.49%

Table 5.6. Results of sensitivity analysis when varying first zone size

1st zone size (%)	Corresponding sub-case	Boundary (*b*) (sec)	$E[T_D]$ from derivation (sec)	$E[T_S]$ from simulation (sec)	% Gap
20%	B1	18.37	18.55	18.15±0.33	2.17%

40%	C1	23.50	20.14	19.80±0.34	1.71%
60%	K1	27.58	21.73	21.43±0.40	1.38%
80%	M1	32.88	23.41	23.25±0.55	0.68%
100%	_	_	25.57	25.45±0.40	0.48%

Note. "_" means any sub-case or any value for b

Table 5.7. Results of sensitivity analysis when varying skewness parameter

ABC curve (%)	Corresponding sub-case	Boundary (b) (sec)	$E[T_D]$ from derivation (sec)	$E[T_S]$ from simulation (sec)	% Gap
20%-90%	B1	21.17	17.69	17.17±0.30	2.93%
20%-70%	B1	21.17	20.70	20.32±0.33	1.86%
20%-50%	B1	21.17	22.99	22.68±0.36	1.33%
20%-30%	B1	21.17	24.78	24.53±0.33	1.03%
20%-20%	_	_	25.57	25.45±0.40	0.48%

Table 5.8. Results of sensitivity analysis when varying Height

Height (No. of tiers)	Corresponding sub-case	Boundary (b) (sec)	$E[T_D]$ from derivation (sec)	$E[T_S]$ from simulation (sec)	% Gap
6	B1	18.81	17.47	16.97±0.30	2.88%
12	C2	25.01	22.80	22.38±0.38	1.85%
18	C3	29.89	28.18	27.71±0.48	1.68%
24	E4	34.46	33.45	33.11±0.50	1.02%
30	F4	39.15	39.00	38.78±0.75	0.57%

Table 5.9. Results of sensitivity analysis when varying shape factor (Length and Width in number of tiers)

Shape factor (L/W)	Corresponding sub-case	Boundary (b) (sec)	$E[T_D]$ from derivation (sec)	$E[T_S]$ from simulation (sec)	% Gap
0.25	L1	43.87	41.36	40.80±0.70	1.36%
0.5	J1	30.11	28.15	27.49±0.48	2.35%

1	C1	22.64	20.76	19.98±0.35	3.77%
2	B1	26.30	24.72	24.01±0.43	2.89%
4	L1	39.11	37.00	36.27±0.70	1.98%

Table 5.4 shows that for our base example the closed-form formula gives a very precise approximation of the expected retrieval time of a medium-sized discrete real system. Tables 5.5-5.9 show that the closed-form formulas give a very precise approximation of the expected retrieval times of real discrete systems, with errors often less than 2%. In addition, the sensitivity analysis proves that by varying the system parameters, the closed-form formulas can still give very good approximations of the expected retrieval times of real discrete systems even for extreme cases such as very small-size systems (100 storage locations), very steep ABC curves (e.g. 20%-90%) or small sizes of the first zone. Moreover, we observe the following:

Observation 1. The gap between the results of the closed-form formula and simulation decreases with an increase in capacity of the system, (see Table 5.5). This is due to the fact that we have assumed a continuous system in the derivation procedure while the simulation is based on a discrete system. The continuity assumption becomes more accurate if the size of the system divided by the size of a storage location is sufficiently large.

Observation 2. The gap between the results of the closed-form formula and simulation decreases with an increase in size of the first zone (see Table 5.6). According to observation 1, the results of the closed-form formulas are more accurate for a larger system. Therefore, with an increase in size of the first zone, the formula for the first zone gives a result closer to reality. Since we consider a 20%-80% ABC curve, the expected retrieval time for the first zone has a higher impact on the total expected retrieval time. Therefore, for a larger first zone, the expected retrieval time of the first zone and consequently the expected retrieval time of the system is closer to the one obtained from simulation.

Observation 3. The gap between the results of the closed-form formula and simulation decreases with a decreasing skewness of the ABC curve (see Table 5.7). We considered a fixed size (30% of the system size) for the first zone in every instance of Table 5.7, which means the closed-form formula of the second zone leads to more accurate results. In addition, if the skewness of the ABC curve decreases, the turnover of the unit loads in the second zone will relatively increase. This increases the weight of the expected retrieval time of the second zone in the total expected retrieval time.

Observation 4. The gap between the results of the closed-form formula and simulation decreases by increasing the Height and departing from an equal Length and Width ratio (shape factor equal to 1) (see Tables 5.8 and 5.9). This is due to the fact that in both cases, the capacity of the system increases, leading to more precise results from closed-form formulas.

5.5. Conclusion

We study a next generation of storage systems: live-cube compact storage systems. These systems are increasingly used, particularly in service industries such as automated parking systems, warehouses and cross-docks and healthcare management systems. One of the most important performance measures is the customer response time. We consider a two-class-based storage policy, which reduces response times compared to random storage. We derive closed-form formulas to calculate the expected retrieval time of a two-class-based live-cube system for any system configuration and zone boundary. In order to obtain the closed-form formulas, the system needs to be decomposed into multiple cases. However, eventually they can be summarized in simple closed-form formulas, which can be used to evaluate the performance of any two-class-based live-cube system. In order to evaluate the quality of these closed-form formulas (obtained using a continuous-space approximation), a Monte Carlo simulation is performed based on a real case application. The results show that the closed-form formulas approximate the expected retrieval time of a discrete system with high precision; errors are usually less than 2%, and below 4% even in extreme cases. With increasing system capacity, skewness parameter, and first zone size, the approximation becomes more precise. Compared to a simulation approach, closed-form formulas can instantly evaluate the performance of a live-cube system with any given configuration and first zone boundary. The closed-form formulas can be used as a reference for further research on live-cube systems such as optimizing system configurations and first zone boundaries.

Appendix 5A. Parameters describing a traditional multi-storey car park and a live-cube parking system

Table 5.10 presents the parameters describing a multi-storey car park and a live-cube parking system. We consider a typical multi-storey car park with an efficient layout without external ramps (for the layout see Multi-Storey Car Park, 2011). In addition, to make a fair comparison we assume both alternatives have

the same capacity per level (24 cars). The building dimensions can be calculated based on parking slot dimensions, system capacity, and aisle width in traditional car parks. Consequently, the average storage and retrieval time of a car can be obtained based on building dimensions, shuttles and lift speeds (in live-cube systems), and maximum allowed driving speed (in car parks). By using average storage and retrieval time and engine power, the average energy consumption for each alternative can be calculated (considering the average energy consumption to create virtual aisles in a live-cube system). In addition, for a multi-storey car park lighting and ventilation energy consumptions have to be considered. To obtain the average lighting and ventilation energy consumptions per car, we assume a 16-hour shift and (on average) a four-hour duration of stay of a car. Input data for a live-cube system and a multi-storey car park are retrieved from Hyundai Elevator Co. Ltd. (2011) and Multi-Storey Car Park (2011), respectively. CO_2 emissions of both alternatives can be obtained by using life cycle analysis for different types of power plants (see Manicore, 2011).

Table 5.10. Parameters describing a traditional multi-storey car park and a live-cube parking system

Parking system	Capacity (# of cars)	Parking slot dimensions (mm)	Building dimensions (m)	Engine power (kW)	Speed (m/min)	Average travel time per S/R (sec)
Live-cube parking	192	Width=3250 Length=6400 Height=2925	Width=19.5 Length=32.0 Height=23.4	1.5 (per level for x-movement), 3 (per level for y-movement), 22 (per lift for z-movement)	Shuttle speed in x-direction (v_x)=45, Shuttle speed in y-direction (v_y)=100, Lift speed (v_z) =90	61
Traditional car park	192	Width=3500 Length=6500 Height=3300	Width=25.0 Length=51.0 Height=26.4	100 (average engine power of a car), 30 (ventilation per level), 1.5 (lighting per level)	Driving speed= 300	178

Appendix 5B. V^1, $E[T^1]$ and $E[T^2]$ for all sub-cases

In Appendix 5B, we give closed-form formulas of the volume of the first zone (V^1), $E[T^1]$ and $E[T^2]$ for all sub-cases A1,…, P3.

Table 5.11. Volume formulas for first zones of sub-cases A1,…,P3

Sub-case	Volume formula (V^1)
A1, A2, A3, A4	$\dfrac{7b^3}{48}$
B1, B2, B3, B4	$\dfrac{1}{48}(-b^3 + 24b(b-w)w + 8w^3)$
C1, C2, C3, C4	$\dfrac{1}{48}(-b^3 - 8(b-l)^3 + 24b(b-w)w + 8w^3)$
D2, D3, D4	$\dfrac{1}{8}b(3b - 2w)w$
E2, E3, E4	$-\dfrac{1}{6}(b-l)^3 + \dfrac{1}{8}b(3b - 2w)w$
F2, F3, F4	$-\dfrac{1}{24}w(3b^2 - 6b(4l + w) + 4(3l^2 + 3lw + w^2))$
G3, G4	$\dfrac{1}{48}(24blw + (b - 2(l + w))^3)$
H4	$\dfrac{blw}{2}$
I1	$\dfrac{1}{6}h(3b^2 - 3bh + h^2)$
J1	$\dfrac{1}{6}(-b^3 + h^3 + w^3 + 3b^2(h + w) - 3b(h^2 + w^2))$
K1	$\dfrac{1}{6}(-2b^3 + h^3 + l^3 + w^3 + 3b^2(h + l + w) - 3b(h^2 + l^2 + w^2))$

L1, L2	$-\dfrac{1}{2}hw(-2b+h+w)$
M1, M2	$-\dfrac{1}{6}(b-l)^3 - \dfrac{1}{2}hw(-2b+h+w)$
N2	$-\dfrac{1}{6}w(3b^2 + 3h^2 + 3l^2 + 3hw + 3lw + w^2 - 3b(2h+2l+w))$
O1	$\dfrac{1}{6}(6hlw + (-b+l+w)^3 - (-b+h+l+w)^3)$
P1, P2, P3	$hlw - \dfrac{1}{6}(-b+h+l+w)^3$

Table 5.12. $E[T^1]$ of all sub-cases

Sub-case	$E[T^1]$ closed-form formula
A1, A2, A3, A4	$\dfrac{3b}{4}$
B1, B2, B3, B4	$\dfrac{3b^4 - 64b^3w + 48b^2w^2 - 8w^4}{4b^3 - 96b^2w + 96bw^2 - 32w^3}$
C1, C2, C3, C4	$\dfrac{27b^4 - 64b^3(l+w) + 48b^2(l^2+w^2) - 8(l^4+w^4)}{4(9b^3 - 24b^2(l+w) + 24b(l^2+w^2) - 8(l^3+w^3))}$
D2, D3, D4	$-\dfrac{-6b^3 + 3b^2w + w^3}{9b^2 - 6bw}$
E2, E3, E4	$\dfrac{3b^4 - l^4 + w^4 - 2b^3(4l+3w) + 3b^2(2l^2+w^2)}{4b^3 - 4l^3 - 3b^2(4l+3w) + 6b(2l^2+w^2)}$

F2, F3, F4	$$\frac{2b^3 - 3b^2(4l+w) + 2(2l^3 + 3l^2w + 2lw^2 + w^3)}{3b^2 - 6b(4l+w) + 4(3l^2 + 3lw + w^2)}$$
G3, G4	$$\frac{3b^4 - 16b^3(l+w) - 16(l^2 + lw + w^2)^2 + 24b^2(l^2 + 4lw + w^2)}{4(b^3 - 6b^2(l+w) - 8(l+w)^3 + 12b(l^2 + 4lw + w^2))}$$
H4	$$\frac{3b^2 + 2l^2 + 3lw + 2w^2}{6b}$$
I1	$$\frac{4b^3 - 3b^2h + h^3}{6b^2 - 6bh + 2h^2}$$
J1	$$-\frac{-3b^4 + 2h^4 + w^4 + 8b^3(h+w) - 6b^2(h^2 + w^2)}{4(b^3 - h^3 - w^3 - 3b^2(h+w) + 3b(h^2 + w^2))}$$
K1	$$-\frac{6b^4 - 2h^4 - l^4 - w^4 - 8b^3(h+l+w) + 6b^2(h^2 + l^2 + w^2)}{4(-2b^3 + h^3 + l^3 + w^3 + 3b^2(h+l+w) - 3b(h^2 + l^2 + w^2))}$$
L1	$$\frac{-h^3 + 4h^2w + 6hw^2 + 4w(-3b^2 + w^2)}{12w(-2b + h + w)}$$
L2	$$\frac{-12b^2h + 12h^2w + w^3}{12h(-2b + h + w)}$$
M1	$$-\frac{-3b^4 + h^4 + 8b^3l + l^4 - 4h^3w - 6h^2w^2 - 4hw^3 - 6b^2(l^2 - 2hw)}{4(b^3 - 3b^2l - l^3 + 3hw(h+w) + 3b(l^2 - 2hw))}$$
M2	$$\frac{3b^4 - 8b^3l - l^4 + 12h^2w^2 + w^4 + 6b^2(l^2 - 2hw)}{4(b^3 - 3b^2l - l^3 + 3hw(h+w) + 3b(l^2 - 2hw))}$$
N2	$$\frac{4b^3 + 2l^3 + 6h^2w + 3l^2w + 2lw^2 + w^3 - 3b^2(2h + 2l + w)}{2(3b^2 + 3h^2 + 3l^2 + 3hw + 3lw + w^2 - 3b(2h + 2l + w))}$$

O1	$$\frac{4b^3 + 2h^2(l+w) + 3h(l^2+w^2) + 2(l^3+w^3) - 3b^2(h+2(l+w))}{2(3b^2 + h^2 + 3h(l+w) + 3(l^2+w^2) - 3b(h+2(l+w)))}$$
P1	$$-\frac{3b^4 - 4h^3(l+w) - (l+w)^4 - 8b^3(h+l+w) + 6b^2(h+l+w)^2 - 6h^2(l^2+w^2) - 4h(l^3+w^3)}{4(-b^3 + h^3 + 3h^2(l+w) + (l+w)^3 + 3b^2(h+l+w) - 3b(h+l+w)^2 + 3h(l^2+w^2))}$$
P2	$$-\frac{3b^4 - h^4 - 4h^3l - 6h^2l^2 - 4hl^3 - l^4 - 4l^3w - 12h^2w^2 - 6l^2w^2 - 4lw^3 - 2w^4 - 8b^3(h+l+w) + 6b^2(h+l+w)^2}{4(-b^3 + h^3 + 3h^2(l+w) + (l+w)^3 + 3b^2(h+l+w) - 3b(h+l+w)^2 + 3h(l^2+w^2))}$$
P3	$$-\frac{3b^4 - 8b^3(h+l+w) + 6b^2(h+l+w)^2 - 2(h^4 + 6h^2(l^2+w^2) + (l^2+lw+w^2)^2)}{4(-b^3 + h^3 + 3h^2(l+w) + (l+w)^3 + 3b^2(h+l+w) - 3b(h+l+w)^2 + 3h(l^2+w^2))}$$

Table 5.13. $E[T^2]$ of all sub-cases
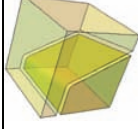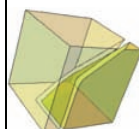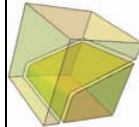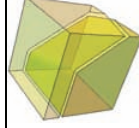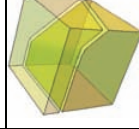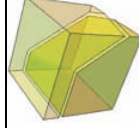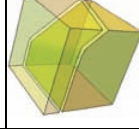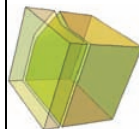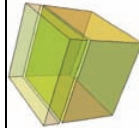
Sub-case	$E[T^2]$ closed-form formula
A1	$$\frac{21b^4 - 8h(h^3 + 12hlw + 12lw(l+w))}{4(7b^3 - 48hlw)}$$
A2	$$\frac{21b^4 - 8w(4h^3 + 6h^2(2l-w) - w^3 + 4h(3l^2 + 3lw + w^2))}{4(7b^3 - 48hlw)}$$
A3	$$\frac{21b^4 + 8(h^4 + l^4 + 6h^2(l-w)^2 + w^4 - 4h^3(l+w) - 4h(l+w)^3)}{4(7b^3 - 48hlw)}$$
A4	$$\frac{21b^4 - 16lw(12h^2 + 2l^2 + 3lw + 2w^2)}{4(7b^3 - 48hlw)}$$
B1	$$\frac{3b^4 - 64b^3w + 48b^2w^2 + 8(h^4 + 12h^2lw - w^4 + 12hlw(l+w))}{4(b^3 - 24b^2w + 48hlw + 24bw^2 - 8w^3)}$$

B2
$$\frac{3b^4 - 64b^3w + 48b^2w^2 + 16w(2h^3 + h^2(6l - 3w) - w^3 + 2h(3l^2 + 3lw + w^2))}{4(b^3 - 24b^2w + 48hlw + 24bw^2 - 8w^3)}$$

B3
$$\frac{3b^4 - 64b^3w + 48b^2w^2 - 8(h^4 + l^4 + 6h^2(l - w)^2 + 2w^4 - 4h^3(l + w) - 4h(l + w)^3)}{4(b^3 - 24b^2w + 48hlw + 24bw^2 - 8w^3)}$$

B4
$$\frac{3b^4 - 64b^3w + 48b^2w^2 + 8w(24h^2l + 4l^3 + 6l^2w + 4lw^2 - w^3)}{4(b^3 - 24b^2w + 48hlw + 24bw^2 - 8w^3)}$$

C1
$$\frac{27b^4 - 64b^3(l + w) + 48b^2(l^2 + w^2) + 8(h^4 - l^4 + 12h^2lw - w^4 + 12hlw(l + w))}{4(9b^3 - 24b^2(l + w) + 24b(l^2 + w^2) - 8(l^3 - 6hlw + w^3))}$$

C2
$$\frac{27b^4 - 64b^3(l + w) + 48b^2(l^2 + w^2) + 8(-l^4 + 12hl^2w + 12hlw(h + w) - 2w(-2h^3 + 3h^2w - 2hw^2 + w^3))}{4(9b^3 - 24b^2(l + w) + 24b(l^2 + w^2) - 8(l^3 - 6hlw + w^3))}$$

C3
$$\frac{27b^4 - 64b^3(l + w) + 48b^2(l^2 + w^2) - 8(h^4 + 6h^2(l - w)^2 - 4h^3(l + w) - 4h(l + w)^3 + 2(l^4 + w^4))}{4(9b^3 - 24b^2(l + w) + 24b(l^2 + w^2) - 8(l^3 - 6hlw + w^3))}$$

C4
$$\frac{27b^4 - 64b^3(l + w) + 48b^2(l^2 + w^2) - 8(l^4 - 4l^3w - 6l^2w^2 + w^4 - 4l(6h^2w + w^3))}{4(9b^3 - 24b^2(l + w) + 24b(l^2 + w^2) - 8(l^3 - 6hlw + w^3))}$$

D2
$$\frac{6b^3 - 3b^2w - 2h(2h^2 + 6hl + 6l^2 - 3hw + 6lw + 2w^2)}{9b^2 - 24hl - 6bw}$$

D3
$$-\frac{h^4 + l^4 + 6h^2(l - w)^2 + 3b^2(2b - w)w - 4h^3(l + w) - 4h(l + w)^3}{3w(-3b^2 + 8hl + 2bw)}$$

D4
$$-\frac{-6b^3 + 24h^2l + 4l^3 + 3b^2w + 6l^2w + 4lw^2 + w^3}{3(3b^2 - 8hl - 2bw)}$$

E2
$$\frac{3b^4 - l^4 + 12hl^2w + 12hlw(h + w) - 2b^3(4l + 3w) + 3b^2(2l^2 + w^2) + 2hw(2h^2 - 3hw + 2w^2)}{4b^3 - 3b^2(4l + 3w) - 4l(l^2 - 6hw) + 6b(2l^2 + w^2)}$$

E3
$$\frac{3b^4 - h^4 - 2l^4 - 6h^2(l-w)^2 + 4h^3(l+w) + 4h(l+w)^3 - 2b^3(4l+3w) + 3b^2(2l^2+w^2)}{4b^3 - 3b^2(4l+3w) - 4l(l^2-6hw) + 6b(2l^2+w^2)}$$

E4
$$\frac{3b^4 - l^4 + 4l^3w + 6l^2w^2 + w^4 - 2b^3(4l+3w) + 3b^2(2l^2+w^2) + 4l(6h^2w+w^3)}{4b^3 - 3b^2(4l+3w) - 4l(l^2-6hw) + 6b(2l^2+w^2)}$$

F2
$$\frac{2b^3 + 4h^3 + 4l^3 + 6h^2(2l-w) + 6l^2w + 4lw^2 + w^3 - 3b^2(4l+w) + 4h(3l^2+3lw+w^2)}{3b^2 - 6b(4l+w) + 4(6hl+3l^2+3lw+w^2)}$$

F3
$$\frac{-h^4 - l^4 - 6h^2(l-w)^2 + 4l^3w + 6l^2w^2 + (b-w)^2w(2b+w) + 4h^3(l+w) + 4h(l+w)^3 + 4lw(-3b^2+w^2)}{w(3b^2 - 6b(4l+w) + 4(6hl+3l^2+3lw+w^2))}$$

F4
$$\frac{2b^3 - 3b^2(4l+w) + 2(12h^2l + 4l^3 + 6l^2w + 4lw^2 + w^3)}{3b^2 - 6b(4l+w) + 4(6hl+3l^2+3lw+w^2)}$$

G3
$$\frac{3b^4 - 16b^3(l+w) + 24b^2(l^2+4lw+w^2) + 8(h^4 + 6h^2(l-w)^2 - 4h^3(l+w) - 4h(l+w)^3 - (l+w)^4)}{4(b^3 - 6b^2(l+w) + 12b(l^2+4lw+w^2) - 8(l^3+3l^2w+w^3+3lw(2h+w)))}$$

G4
$$\frac{-3b^4 + 16b^3(l+w) - 24b^2(l^2+4lw+w^2) + 16(l^4+4l^3w+6l^2w^2+w^4+4l(3h^2w+w^3))}{32(-3blw + 6hlw + (-\frac{b}{2}+l+w)^3)}$$

H4
$$\frac{b}{2} + h$$

I1
$$\frac{8b^3 - 6b^2h + h^3 - 12hlw - 12lw(l+w)}{4(3b^2 - 3bh + h^2 - 6lw)}$$

J1
$$-\frac{-3b^4 + h^4 - 12h^2lw + w^4 + 8b^3(h+w) - 12hlw(l+w) - 6b^2(h^2+w^2)}{4(b^3 - h^3 + 6hlw - w^3 - 3b^2(h+w) + 3b(h^2+w^2))}$$

K1
$$-\frac{6b^4 - h^4 - l^4 + 12h^2lw - w^4 + 12hlw(l+w) - 8b^3(h+l+w) + 6b^2(h^2+l^2+w^2)}{4(-2b^3 + h^3 + l^3 - 6hlw + w^3 + 3b^2(h+l+w) - 3b(h^2+l^2+w^2))}$$

L1, L2	$$-\frac{6b^2 - 2h^2 - 6hl - 6l^2 - 3hw - 6lw - 2w^2}{6(-2b + h + 2l + w)}$$
M1, M2	$$\frac{3b^4 - 8b^3l - l^4 + 12hl^2w + 12hlw(h+w) + 6b^2(l^2 - 2hw) + 2hw(2h^2 + 3hw + 2w^2)}{4(b^3 - 3b^2l - l^3 + 6hlw + 3hw(h+w) + 3b(l^2 - 2hw))}$$
N2	$$\frac{w^2(4(h+l)+w)}{4(3(-b+h+l)^2 + 3(-b+h+l)w + w^2)} + \frac{4b^3 - 3b^2(2(h+l)+w) + (h+l)^2(2(h+l)+3w)}{6(-b+h+l)^2 + 6(-b+h+l)w + 2w^2}$$
O1	$$\frac{8b^3 + h^3 + 4h^2(l+w) + 6h(l+w)^2 + 4(l+w)^3 - 6b^2(h+2(l+w))}{4(3b^2 + h^2 + 3h(l+w) + 3(l+w)^2 - 3b(h+2(l+w)))}$$
P1, P2, P3	$$\frac{1}{4}(3b + h + l + w)$$

Appendix 5C. Hierarchical decomposition procedure leading to 16 different cases

	$b/2 \leq h$							
	$w>b$			$b/2 <w \leq b$			$w \leq b/2$	
	$l>b$	$b/2<l \leq b$	$l \leq b/2$	$l>b$	$b/2<l \leq b$	$l \leq b/2$	$l>b$	$b-w <l \leq b$	$b/2 < l \leq b-w$	$(b/2)-w <l \leq b/2$	$l \leq (b/2)-w$

b/2 > h

w>b			b-h <w ≤ b			w ≤ b-h				
l>b	b-h<l ≤ b	l ≤ b-h	l>b	b-h<l ≤ b	l ≤ b-h	l >b	max{b-w,b-h} <l ≤ b	b-h ≤ l ≤ b-w (if w≤h)	b-w ≤ l ≤ b-h (if h≤w)	b ≤ min{b-w,b-h}

Chapter 6

Optimal Two-Class-Based Storage in a Live-Cube Compact Storage System

6.1. Introduction

Warehouses form vital nodes in any supply chain, decoupling supply from demand. Increased trade has grown the number of warehouses and as a consequence the use of land for warehousing in many regions. Unfortunately, land has become increasingly scarce in many parts of Europe, Asia, and the US, particularly in areas with major customer concentrations. Traditional storage systems, such as automated storage and retrieval (AS/R) systems occupy much space, as they require transport aisle between any two racks. These aisles may consume about 35% of all storage space and contribute to high building cost (Gue, 2006). Shortage of land has driven many companies to search for more compact storage systems.

To solve this land problem, so-called "live-cube" compact storage systems have recently been introduced with growing number of implementations in automated parking systems, warehousing and cross-docking, container handling, and pharmacy automation (e.g. Hyundai Elevator, 2011; Automotion Parking Systems, 2011; Eweco, 2011; Wöhr, 2011; OTDH, 2011; Navstors, 2011; Navpak, 2011; EZ-Indus, 2011; Swisslog, 2011). In such systems, each load is stored on a shuttle that can move autonomously in *x*- and *y*- directions and vertical transport is carried out by lifts. The system is described in chapter 1 (see section 1.2.2).

In live-cube systems, the interfering unit loads on the move path of a requested unit load might slow down the retrieval process. In practice, however, utilizations of not more than 95% are common in systems containing 1000 unit loads or more. This implies there are sufficient empty locations at each level to create a virtual aisle for any desired unit load. By creating a virtual aisle, the requested unit load can freely move to the lift location without interfering with other unit loads. A sufficient condition to create such a virtual aisle is that the number of empty locations on a level equals at least the maximum of the number of rows and the number of columns. Figure 6.1 represents the top view of a five by five, single-level live-cube system. The I/O point is located at the lower-left corner. Figure 6.1(a) shows a situation where a unit load needs to be moved out of a live-cube system. In this case, a virtual aisle can be created by simultaneously moving some interfering unit loads (Figure 6.1(b)). The desired unit load can then be moved to the I/O point without any interference. For a single-level live-cube system with such a condition, the retrieval time of any load at location (x, y), $T(x, y)$, can be approximated by $x+y$ (i.e. $T(x, y) = x+y$), where x and y are the travel times to the I/O point in x- and y- directions, respectively. For a multi-level live-cube system, the retrieval time of any load at location (x, y, z) can be approximated by $\max\{x+y, z\}+z$ (i.e. $T(x, y, z) = \max\{x+y, z\}+z$), where z is the travel time of the lift to level z.
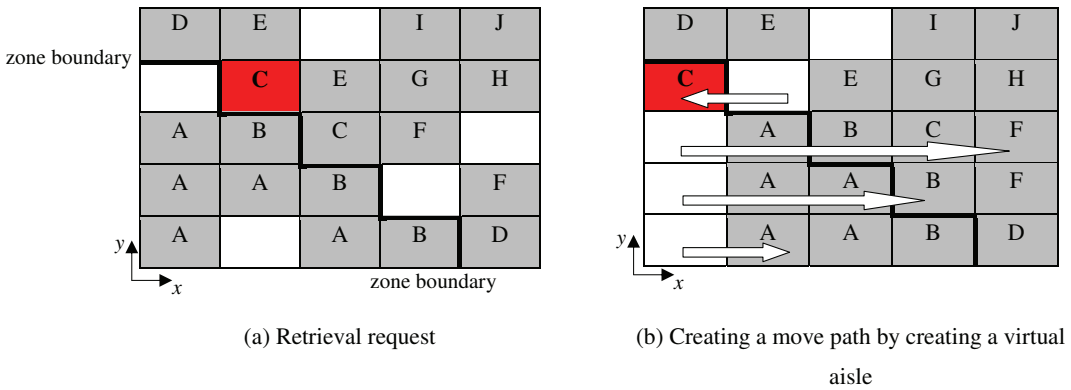
(a) Retrieval request

(b) Creating a move path by creating a virtual aisle

Notes. (1) Requested unit load is in red

(2) Bold line represents first zone boundary

(3) I/O point is located at lower left corner

Figure 6.1. A virtual aisle in a single-level live-cube system

Random storage has been widely used in storage systems due to its simplicity. However, it has been shown that compared to random storage, two-class-based storage can reduce the response time of a

storage system significantly (Hausman et al., 1976; Eynan and Rosenblatt, 1994; Kouvelis and Papanicolaou, 1995; Ruben and Jacobs, 1999; Park, 2006; Yu and De Koster, 2009b). Two-class-based storage can simply be implemented in practice by classifying unit loads in high turnover and low turnover classes. The high-turnover unit loads are then assigned to locations closer to the I/O point. Optimizing the storage zone boundaries (i.e. first zone boundary and system dimensions) of a two-class-based storage system can significantly reduce the response time compared to systems with configurations commonly found in practice (Hausman et al., 1976; Yu and De Koster, 2009b).

In this chapter, we study a live-cube compact storage system where virtual aisles can be created for any requested load. We optimize the system dimensions and the first zone boundary of a two-class system minimizing the response time. The contribution of this chapter is two-fold:

1) we first obtain the optimal boundaries of a two-class live-cube system leading to minimum response times;

2) we extend our model to obtain the optimal boundary of the first storage zone of a two-class live-cube system with a given configuration.

To optimize the boundaries, we propose a mixed-integer nonlinear model. The objective is to minimize the expected retrieval time of an arbitrary unit load. To derive a closed-form formula for the objective function, the system needs to be decomposed in several complementary cases based on the system configuration and zone boundary. Each case corresponds to a different objective function. As it is shown in chapter 5, the system has to be decomposed in 36 cases. This results in a mathematical model with many constraints and also nonlinearity in both objective function and constraints. In addition, as class-based storage is considered, the annual demand of inventoried unit loads (i.e. the skewness of the ABC curve) also affects the optimal solution. Although the model is complex it can still be solved optimally. We first show that some cases do not include the optimal solution. This reduces the solution space without losing any optimality. The remaining cases can then be solved individually to obtain the optimal solution of the model. Although the solution procedure is very tedious, eventually two sets of closed-form solutions for optimal boundaries can be obtained for various ABC curves. The results show that an optimal two-class live-cube system can reduce the response time up to 50% compared to a random storage policy. Moreover, for a system with a given configuration we propose a simple algorithm to obtain the optimal first zone boundary leading to a minimum response time.

Optimizing zone boundaries for class-based storage in traditional automated 2-dimensional (2D) storage systems (e.g. AS/R system) has extensively been studied in the literature. Hausman et al. (1976) derive a travel time formula for a 2D AS/R system with class-based storage, which has been used by

many researchers (Rosenblatt and Eynan, 1989; Park and Webster, 1989; Eynan and Rosenblatt, 1994; Kouvelis and Papanicolaou, 1995; Van den Berg, 1996; Thonemann and Brandeau, 1998; Ruben and Jacobs, 1999; Park, 2006). Researchers have used different methods to obtain the optimal zone boundaries for class-based storage policies. Hausman et al. (1976) use a grid search method to minimize the S/R one-way travel time in a Square-In-Time (SIT) 2D system. Rosenblatt and Eynan (1989) propose a solution method to determine the optimal boundaries for any desired number of zones in a 2D system. They show a relatively small number of zones can lead to the same savings as a full-turnover. Eynan and Rosenblatt (1994) determine the optimal zone boundaries for a Non-Square-In-Time (NSIT) system. Park (2006) determines optimal zone boundaries for a 2D SIT system numerically. He also determines the mean and variance of the travel times for AS/R systems for the two-class NSIT case.

Stadtler (1996), Sari et al. (2005), Gue and Kim (2007), De Koster et al. (2008), Zaerpour et al. (2010) study compact storage systems using different depth handling systems. Stadtler (1996) and Zaerpour et al. (2010) study unit load storage assignment in a satellite-based compact storage system. Sari et al. (2005) study unit load storage assignment and De Koster et al. (2008) study optimal design of a conveyor-based compact storage system. Gue and Kim (2007) study a single-level live-cube storage system, or a so-called puzzle-based storage system. For systems with a single and multiple empty locations, they develop a method to maneuver unit loads to the I/O point yielding short retrieval times. Yu and De Koster (2009b) appear to be the first who study an optimal two-class based storage in a 3D compact storage system. They formulate a mixed-integer non-linear model and develop a decomposition algorithm and one-dimensional search to solve the model leading to optimal zone boundaries.

This chapter extends the results of chapter 4 by considering a class-based storage policy, aiming to shorten response times (chapter 4 considers a random storage policy). We minimize the response time by optimizing both the dimensions of the system and the first zone boundary. Adding the variable representing the first zone boundary increases the complexity of the problem significantly leading to 36 cases compared to 4 cases in the random storage problem. However, solving such a complex problem is still worthwhile since up to 50% reduction in response time can be achieved by using a two-class storage policy versus random storage. In addition, in order to construct the mathematical model, closed-form expressions of the expected retrieval time are required. The closed-form expressions of expected retrieval time of the system with any configuration and zone boundary are obtained in chapter 5. We therefore use these closed-form expressions in this chapter for our mathematical model.

The remainder of this chapter is organized as follows. Section 6.2 proposes the mathematical models and obtains the optimal zone boundaries for single-level and multi-level systems. Section 6.3 extends the

proposed model in various directions and section 6.4 discusses the results. Section 6.5 concludes the chapter.

6.2. General model and optimization

In this section, we propose the mathematical models for single-level and multi-level live-cube systems under a two-class storage policy. The closed-form travel time formulas, each corresponding to a specific configuration (three cases for a single-level system and 36 cases for a multi-level system) obtained in chapter 5, are used for the objective function of the model. Section 6.2.1 gives the mathematical model for a single-level system and obtains the optimal solutions. Section 6.2.2 gives the mathematical model for a multi-level system and solves it optimally.

A continuous space is assumed. This assumption is commonly used in the literature (see Hausman et al. (1976), Bozer and White (1984), Rosenblatt and Eynan (1989), Yu and De Koster (2009b)). A system has length l (shuttle travel time from/to the I/O point to/from the farthest location in x-direction in an empty lane), width or depth w (shuttle travel time from/to the I/O point to/from the farthest location in y-direction in an empty lane) and height h (lift travel time from/to the I/O point to/from the farthest level in z-direction). The first zone boundary includes all the locations with travel time b to the I/O point. For sake of convenience and without loss of generality, we suppose that the length of the system is not less than the width of the system; i.e. $l \geq w$ (see also Bozer and White (1984), Eynan and Rosenblatt (1994) and Yu and De Koster, (2009b)). The system capacity – denoted by A in a single-level system and V in a multi-level system – is constant. G_1 represents the size of the first zone divided by the size of the system. s is the skewness parameter of the ABC curve, and $E[T_i^j]$ represents the expected travel time of an arbitrary load in zone j ($j = 1, 2$) if case i (in a single-level system, $|i| = 3$, and in a multi-level system, $|i| = 36$) is considered.

6.2.1. Optimization of a two-class single-level live-cube system

To optimize the boundaries of a single-level live-cube system with two classes, Model SGM can be built:
Model SGM

$$\min E[T] = \sum_{i=1}^{3} y_i (G_1^{2s/(s+1)} E[T_i^1] + (1 - G_1^{2s/(s+1)}) E[T_i^2]), \qquad (6.1)$$

subject to:

$$l \times w = A, \tag{6.2}$$

$$l - w \geq 0, \tag{6.3}$$

$$\sum_{i=1}^{3} y_i = 1, \tag{6.4}$$

$$\sum_{i=1}^{3} y_i (A_i(b) / A) = G_1, \tag{6.5}$$

$$y_1(w - b) \geq 0, \tag{6.6}$$

$$y_2(b - w) \geq 0, \tag{6.7}$$

$$y_2(l - b) \geq 0, \tag{6.8}$$

$$y_3(b - l) \geq 0, \tag{6.9}$$

$$y_3(l + w - b) \geq 0, \tag{6.10}$$

decision variables: $0 \leq b \leq \max\{l + w\}$, $l > 0$, $w > 0$ and

$y_i \in \{0,1\}$ for $i = 1...3$,

where A_i is a function which gives the area of the first zone for case i (i = 1,2,3). $y_i = 1$ if case i is considered, otherwise, $y_i = 0$. The objective function is minimizing the expected retrieval time of an arbitrary unit load. Constraint (6.2) makes sure the given capacity is achieved. Constraint (6.3) ensures that the length is at least equal to the width of the system. Constraint (6.4) makes sure that only one case is considered. Constraint (6.5) relates any value of boundary b to its corresponding value of G_1. Constraints (6.6)-(6.10) are used to distinguish three different cases. The SGM model is mixed-integer and nonlinear. However, it is possible to find the optimal solutions of the model.

To solve Model SGM, Theorems 1 and 2 are derived, which prove that the cases $b \leq w$ and $w \leq b \leq l$ do not include the optimal solution and their corresponding constraints can be relaxed.

Lemma 1. *In a given system, if there are two candidate shapes of the system that have the same zone area, the system with a shape closer to square has the shorter expected retrieval time.*

Proof. See Appendix 6A.

Theorem 1. *The optimal shape for a two-class live-cube system is square, i.e.*

$$l^* = w^*. \tag{6.11}$$

Proof. Assuming $d = l/w$, since $\dfrac{\partial E[T]}{\partial d} > 0, \forall d \geq 1$, the minimum value of expected retrieval time occurs at

$d=1$(i.e. $l=w$).

Corollary 1. *Case 2 ($w < b \leq l$) does not include the optimal solution of the Model SGM.*

Therefore, $y_2^* = 0$.

Proof. From Theorem 1, $1^* = w^*$ and so the condition of case 2 ($w < b \leq l$) is not met.

Theorem 2. *For a two-class live-cube compact storage system E[T] is an increasing function of boundary b if $l \leq b \leq l + w$.*

Proof. See Appendix 6B.

Corollary 2. *Case 3 ($l < b \leq l + w$) does not include the optimal solution of the Model SGM.*

Therefore, $y_3^* = 0$.

Proof. From Theorem 2, b = l (case 2) leads to a smaller value of *E*[*T*] than $l < b \leq l + w$ (case 3) does.

Corollary 3. *Case 1 ($b \leq w$) includes the optimal solution of the Model SGM.*

Therefore, $y_1^* = 1$.

Proof. From constraint (6.4), as $y_2^* = 0$ and $y_3^* = 0$, then $y_1^* = 1$.

Optimizing zone boundaries for case $b \leq w$

In order to simplify the calculations, the system area is normalized to one. *E*[*T*] for case $b \leq w$ can be calculated by using Equation (6.12) where according to Theorem 1and normalization, $l^* = w^* = 1$,

$$E\left[T_{b\leq w}\right] = \left(\left(\frac{b^2}{2}\right)^{\frac{2s}{s+1}}\right)\left(\frac{2b}{3}\right) + \left(1 - \left(\frac{b^2}{2}\right)^{\frac{2s}{s+1}}\right)\left(\frac{2(-3+b^3)}{3(-2+b^2)}\right). \tag{6.12}$$

The optimal zone boundary *b* can be obtained by solving the first order condition as follows,

$$\frac{\mathrm{d}E[T_{b\leq w}]}{\mathrm{d}b} = \frac{2b^2(6 - 6b + b^3)(1+s) + 4^{\frac{1}{1+s}}(b^2)^{\frac{2s}{1+s}}(-12s + b(2 + 10s + b(-3 + b + 3s - 3bs)))}{3b(-2 + b^2)^2(1+s)} = 0. \tag{6.13}$$

Since solving Equation (6.13) leads to one critical value of *b* for any given *s*, it can easily be shown that the obtained *b* minimizes $E\left[T_{b\leq w}\right]$ for any *s*.

The following table gives the optimal values of l^*, w^*, b^* and G_1^* for some selected skewness parameters (ABC curves). $E[T_{G^*}]$ represents the expected retrieval times of a square shaped live-cube system with an optimal zone size (G_1^*).

Table 6.1. The optimal solutions for single-level system at different skewness parameters

s	ABC curve	l^*	w^*	b^*	G_1^*	$E[T_{G^*}]$	$Impro_{G_1^*}$ (%)
0.065	20%/90%	1	1	0.270	0.036	0.464	53.54
0.139	20%/80%	1	1	0.423	0.089	0.632	36.75
0.22	20%/70%	1	1	0.527	0.139	0.736	26.34
0.32	20%/60%	1	1	0.605	0.183	0.811	18.85
0.43	20%/50%	1	1	0.668	0.223	0.869	13.00
0.57	20%/40%	1	1	0.721	0.260	0.918	8.16
0.75	20%/30%	1	1	0.768	0.295	0.960	3.92
1	20%/20%	1	1	_	/	1	0.00

Note. "_": any value between zero and two; "/": any value between 0 and 1. $Impro_{G_1^*}$ is the reduction of $E[T]$ of a two-class storage policy with an optimal zone size compared to a random storage policy obtained from chapter 4.

A closed-form formula for the optimal boundary b^* (as a function of s) cannot be obtained analytically. To solve this problem, we obtain the optimal boundary as a function of s by fitting the function $b^*(s) = a\,\text{ArcTan}[cs + d] + e$ to optimal values of boundary b for 1000 different s. Equation (6.14) gives the optimal boundary for any given skewness parameter s.

$$b^*(s) = 53725\,\text{ArcTan}[308668s + 57606] - 84390 \tag{6.14}$$

The standard error, t-statistic, and P-value of each parameter are given in Appendix 6C.

Figure 6.2 shows the plotted optimal values of b for 1000 different s values and corresponding fitted function. As Figure 6.2 illustrates, for any value of s the optimal boundary value, b^* is always less than one. This means in an optimal two-class-based single-level system (i.e. square shape), the first zone always occupies less than half of system capacity. Therefore, the optimal shape of the first zone is always like a triangle.
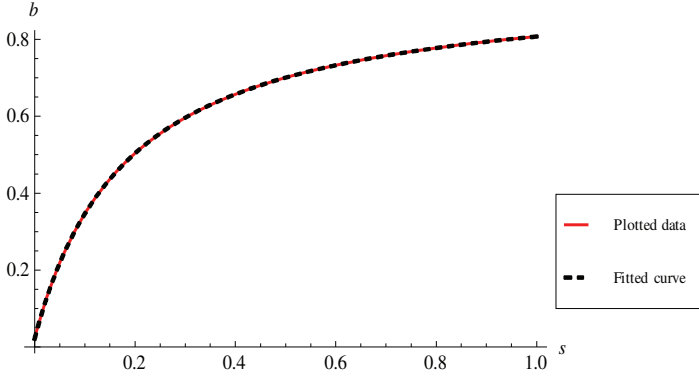
Figure 6.2. Fitted function $b^*(s)$ and the plot of optimal values of b

6.2.2. Optimization of a two-class multi-level live-cube system

To optimize the boundaries of a two-class-based storage system in a multi-level system, Model MGM can be built:

Model MGM

$$\min E[T] = \sum_{i\in\{A1,...,P3\}} y_i (G_1^{2s/(s+1)} E[T_i^1] + (1 - G_1^{2s/(s+1)}) E[T_i^2]),\qquad (6.15)$$

subject to:

$$l \times w \times h = V,\qquad\qquad (6.16)$$

$$l - w \geq 0,\qquad\qquad (6.17)$$

$$\sum_{i\in\{A1,...,P3\}} y_i = 1,\qquad\qquad (6.18)$$

$$\sum_{i\in\{A1,...,P3\}} y_i (V_i(b)/V) = G_1,\qquad\qquad (6.19)$$

$y_{A1}(w-h) \geq 0$, (6.20)	$y_{A1}(2h-b) \geq 0$, (6.21)	$y_{A1}(w-b) \geq 0$, (6.22)
$y_{A2}(h-w) \geq 0$, (6.23)	$y_{A2}(l-h) \geq 0$, (6.24)	$y_{A2}(2h-b) \geq 0$, (6.25)
$y_{A2}(w-b) \geq 0$, (6.26)	$y_{A3}(h-l) \geq 0$, (6.27)	$y_{A3}(l+w-h) \geq 0$, (6.28)
$y_{A3}(2h-b) \geq 0$, (6.29)	$y_{A3}(w-b) \geq 0$, (6.30)	$y_{A4}(h-l-w) \geq 0$, (6.31)
$y_{A4}(2h-b) \geq 0$, (6.32)	$y_{A4}(w-b) \geq 0$, (6.33)	$y_{B1}(w-h) \geq 0$, (6.34)

$y_{B1}(2h - b) \geq 0 \,,$ (6.35) $\quad$ $y_{B1}(b - w) \geq 0 \,,$ (6.36) $\quad$ $y_{B1}(l - b) \geq 0 \,,$ (6.37)

$y_{B2}(h - w) \geq 0 \,,$ (6.38) $\quad$ $y_{B2}(l - h) \geq 0 \,,$ (6.39) $\quad$ $y_{B2}(2w - b) \geq 0 \,,$ (6.40)

$y_{B2}(b - w) \geq 0 \,,$ (6.41) $\quad$ $y_{B2}(l - b) \geq 0 \,,$ (6.42) $\quad$ $y_{B3}(h - l) \geq 0 \,,$ (6.43)

$y_{B3}(l + w - h) \geq 0 \,,$ (6.44) $\quad$ $y_{B3}(2w - b) \geq 0 \,,$ (6.45) $\quad$ $y_{B3}(b - w) \geq 0 \,,$ (6.46)

$y_{B3}(l - b) \geq 0 \,,$ (6.47) $\quad$ $y_{B4}(h - l - w) \geq 0 \,,$ (6.48) $\quad$ $y_{B4}(2w - b) \geq 0 \,,$ (6.49)

$y_{B4}(b - w) \geq 0 \,,$ (6.50) $\quad$ $y_{B4}(l - b) \geq 0 \,,$ (6.51) $\quad$ $y_{C1}(w - h) \geq 0 \,,$ (6.52)

$y_{C1}(2h - b) \geq 0 \,,$ (6.53) $\quad$ $y_{C1}(b - l) \geq 0 \,,$ (6.54) $\quad$ $y_{C2}(h - w) \geq 0 \,,$ (6.55)

$y_{C2}(l - h) \geq 0 \,,$ (6.56) $\quad$ $y_{C2}(2w - b) \geq 0 \,,$ (6.57) $\quad$ $y_{C2}(b - l) \geq 0 \,,$ (6.58)

$y_{C3}(h - l) \geq 0 \,,$ (6.59) $\quad$ $y_{C3}(l + w - h) \geq 0 \,,$ (6.60) $\quad$ $y_{C3}(2w - b) \geq 0 \,,$ (6.61)

$y_{C3}(b - l) \geq 0 \,,$ (6.62) $\quad$ $y_{C4}(h - l - w) \geq 0 \,,$ (6.63) $\quad$ $y_{C4}(2w - b) \geq 0 \,,$ (6.64)

$y_{C4}(b - l) \geq 0 \,,$ (6.65) $\quad$ $y_{D2}(h - w) \geq 0 \,,$ (6.66) $\quad$ $y_{D2}(l - h) \geq 0 \,,$ (6.67)

$y_{D2}(2h - b) \geq 0 \,,$ (6.68) $\quad$ $y_{D2}(b - 2w) \geq 0 \,,$ (6.69) $\quad$ $y_{D2}(l - b) \geq 0 \,,$ (6.70)

$y_{D3}(h - l) \geq 0 \,,$ (6.71) $\quad$ $y_{D3}(l + w - h) \geq 0 \,,$ (6.72) $\quad$ $y_{D3}(2h - b) \geq 0 \,,$ (6.73)

$y_{D3}(b - 2w) \geq 0 \,,$ (6.74) $\quad$ $y_{D3}(l - b) \geq 0 \,,$ (6.75) $\quad$ $y_{D4}(h - l - w) \geq 0 \,,$ (6.76)

$y_{D4}(2h - b) \geq 0 \,,$ (6.77) $\quad$ $y_{D4}(b - 2w) \geq 0 \,,$ (6.78) $\quad$ $y_{D4}(l - b) \geq 0 \,,$ (6.79)

$y_{E2}(h - w) \geq 0 \,,$ (6.80) $\quad$ $y_{E2}(l - h) \geq 0 \,,$ (6.81) $\quad$ $y_{E2}(2h - b) \geq 0 \,,$ (6.82)

$y_{E2}(b - 2w) \geq 0 \,,$ (6.83) $\quad$ $y_{E2}(b - l) \geq 0 \,,$ (6.84) $\quad$ $y_{E2}(l + w - b) \geq 0 \,,$ (6.85)

$y_{E3}(h - l) \geq 0 \,,$ (6.86) $\quad$ $y_{E3}(l + w - h) \geq 0 \,,$ (6.87) $\quad$ $y_{E3}(2h - b) \geq 0 \,,$ (6.88)

$y_{E3}(b - 2w) \geq 0 \,,$ (6.89) $\quad$ $y_{E3}(b - l) \geq 0 \,,$ (6.90) $\quad$ $y_{E3}(l + w - b) \geq 0 \,,$ (6.91)

$y_{E4}(h - l - w) \geq 0 \,,$ (6.92) $\quad$ $y_{E4}(2h - b) \geq 0 \,,$ (6.93) $\quad$ $y_{E4}(b - 2w) \geq 0 \,,$ (6.94)

$y_{E4}(b - l) \geq 0 \,,$ (6.95) $\quad$ $y_{E4}(l + w - b) \geq 0 \,,$ (6.96) $\quad$ $y_{F2}(h - w) \geq 0 \,,$ (6.97)

$y_{F2}(l - h) \geq 0 \,,$ (6.98) $\quad$ $y_{F2}(2h - b) \geq 0 \,,$ (6.99) $\quad$ $y_{F2}(b - l - w) \geq 0 \,,$ (6.100)

$y_{F3}(h - l) \geq 0 \,,$ (6.101) $\quad$ $y_{F3}(l + w - h) \geq 0 \,,$ (6.102) $\quad$ $y_{F3}(b - l - w) \geq 0 \,,$ (6.103)

$y_{F3}(2l - b) \geq 0 \,,$ (6.104) $\quad$ $y_{F4}(h - l - w) \geq 0 \,,$ (6.105) $\quad$ $y_{F4}(b - l - w) \geq 0 \,,$ (6.106)

$y_{F4}(2l - b) \geq 0$, (6.107) $y_{G3}(h - l) \geq 0$, (6.108) $y_{G3}(l + w - h) \geq 0$, (6.109)

$y_{G3}(2l - b) \geq 0$, (6.110) $y_{G3}(b - 2h) \geq 0$, (6.111) $y_{G4}(h - l - w) \geq 0$, (6.112)

$y_{G4}(2l - b) \geq 0$, (6.113) $y_{G4}(b - 2(l + w)) \geq 0$, (6.114) $y_{H4}(h - l - w) \geq 0$, (6.115)

$y_{H4}(b - 2(l + w)) \geq 0$, (6.116) $y_{H4}(2h - b) \geq 0$, (6.117) $y_{I1}(w - h) \geq 0$, (6.118)

$y_{I1}(b - 2h) \geq 0$, (6.119) $y_{I1}(w - b) \geq 0$, (6.120) $y_{J1}(w - h) \geq 0$, (6.121)

$y_{J1}(b - 2h) \geq 0$, (6.122) $y_{J1}(b - w) \geq 0$, (6.123) $y_{J1}(w + h - b) \geq 0$, (6.124)

$y_{J1}(l - b) \geq 0$, (6.125) $y_{K1}(w - h) \geq 0$, (6.126) $y_{K1}(b - 2h) \geq 0$, (6.127)

$y_{K1}(b - l) \geq 0$, (6.128) $y_{K1}(w + h - b) \geq 0$, (6.129) $y_{L1}(w - h) \geq 0$, (6.130)

$y_{L1}(b - w - h) \geq 0$, (6.131) $y_{L1}(l - b) \geq 0$, (6.132) $y_{L2}(h - w) \geq 0$, (6.133)

$y_{L2}(l - h) \geq 0$, (6.134) $y_{L2}(b - 2h) \geq 0$, (6.135) $y_{L2}(l - b) \geq 0$, (6.136)

$y_{M1}(w - h) \geq 0$, (6.137) $y_{M1}(b - w - h) \geq 0$, (6.138) $y_{M1}(b - l) \geq 0$, (6.139)

$y_{M1}(l + h - b) \geq 0$, (6.140) $y_{M2}(h - w) \geq 0$, (6.141) $y_{M2}(l - h) \geq 0$, (6.142)

$y_{M2}(b - 2h) \geq 0$, (6.143) $y_{M2}(b - l) \geq 0$, (6.144) $y_{M2}(l + w - b) \geq 0$, (6.145)

$y_{N2}(h - w) \geq 0$, (6.146) $y_{N2}(l - h) \geq 0$, (6.147) $y_{N2}(b - 2h) \geq 0$, (6.148)

$y_{N2}(b - l - w) \geq 0$, (6.149) $y_{N2}(l + h - b) \geq 0$, (6.150) $y_{O1}(w - h) \geq 0$, (6.151)

$y_{O1}(b - l - h) \geq 0$, (6.152) $y_{O1}(l + w - b) \geq 0$, (6.153) $y_{P1}(w - h) \geq 0$, (6.154)

$y_{P1}(b - l - w) \geq 0$, (6.155) $y_{P1}(l + w + h - b) \geq 0$, (6.156) $y_{P2}(h - w) \geq 0$, (6.157)

$y_{P2}(l - h) \geq 0$, (6.158) $y_{P2}(b - l - h) \geq 0$, (6.159) $y_{P2}(l + w + h - b) \geq 0$, (6.160)

$y_{P3}(h - l) \geq 0$, (6.161) $y_{P3}(l + w - h) \geq 0$, (6.162) $y_{P3}(b - 2h) \geq 0$, (6.163)

$y_{P3}(l + w + h - b) \geq 0$, (6.164)

decision variables: $b \geq 0, l > 0, w > 0, h > 0$ and $y_i \in \{0,1\}$ for $i \in \{A1,...,P3\}$,

where V_i is a function which gives the volume of the first zone of case i ($i \in \{A1,...,P3\}$) and V is the given volume of the system. $y_i = 1$ if case I is considered, otherwise, $y_i = 0$. Equation (6.15) minimizes the expected retrieval time $E[T]$. Constraint (6.16) makes sure that the given capacity is achieved. Constraint (6.17) ensures that the length of the system is at least equal to the width of the system. As the

sub-cases are complementary, constraint (6.18) makes sure that only one sub-case is considered. Constraint (6.19) relates any value of boundary b to its corresponding value of G_1 (G_1 is relative size of the first zone). Constraints (6.20)-(6.164) are used to distinguish 36 different sub-cases. For example, according to Figure 5.6 in chapter 5, case A1 has the following conditions, $b/2 \leq h$, $b \leq w$ and $h \leq w$. Therefore, constraints (6.20)-(6.22) make sure, if case A1 is considered these conditions are met.

In order to obtain the optimal solutions of Model MGM we first give the following theorems.

Lemma 2. *In a given system, if there are two candidate shapes of the system that have the same zone volume and height, the system with a shape closer to square at each level has the shorter expected retrieval time.*

Proof. See Appendix 6D.

Theorem 3. *The optimal system configuration is square for a two-class live-cube system at every level i.e.* $l^* = w^*$. (6.165)

Proof. Assuming $d = l/w$, since $\dfrac{\partial E[T]}{\partial d} > 0, \forall d \geq 1$, the minimum value of expected retrieval time occurs at d=1(i.e. l=w).

Corollary 4. *Sub-cases A2, B2, C2, D2, E2, F2, L2, M2, N2, P2 (i.e. with condition $w \leq h < l$) and sub-cases B1, B3, B4, D3, D4, E3, E4, F3, F4, J1, L1, M1 (i.e. with condition $w \leq b < l$) do not include the optimal solution of the Model MGM and their corresponding constraints can be relaxed in the model.*

Thus, $y_i^* = 0 \ \forall i \in \{A2, B2, C2, D2, E2, F2, L2, M2, N2, P2, B1, B3, B4, D3, D4, E3, E4, F3, F4, J1, L1, M1\}$.

Proof. From Theorem 3, $l^* = w^*$ and so the constraints corresponding to the cases that do not meet this condition can be relaxed.

Theorem 4. *Within each case, the sub-case with condition $h \leq w$ leads to shorter E[T] compared to sub-cases with conditions $l < h \leq l+w$ and $l+w < h$.*

Proof. In order to prove, it only suffices to compare the optimal solutions of sub-cases with condition $l < h \leq l+w$ and $l+w < h$ with the optimal solution of sub-case with condition $h \leq w$ in each case. In Appendix 6E, we show this property holds by comparing two sub-cases and it can be shown for other sub-cases similarly. The optimal solutions of other sub-cases are given in Appendix 6E.

Corollary 5. *Sub-cases A3, A4, C3, C4, and P3 do not include the optimal solution of the Model MGM and their corresponding constraints can be relaxed in the model.*

Therefore, $y_i^* = 0 \ \forall i \in \{A3, A4, C3, C4, P3\}$.

Proof. From Theorem 4, within each case, the sub-case with condition $h \leq w$ leads to shorter $E[T]$ compared to sub-cases with conditions $l < h \leq l + w$ and $l + w < h$ and so the constraints corresponding to the cases with these two conditions can be relaxed.

Theorem 5. *Sub-case C3 compared to sub-case G3, and sub-case C4 compared to sub-cases G4 and H4 lead to shorter E[T]*.
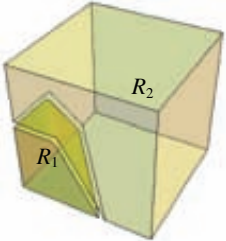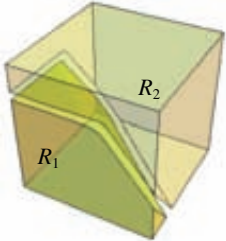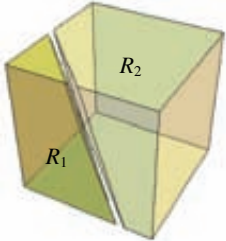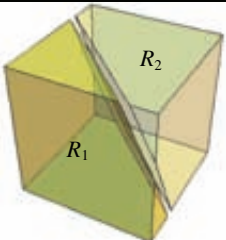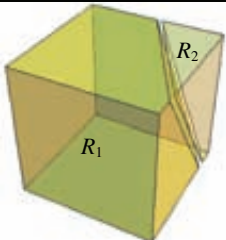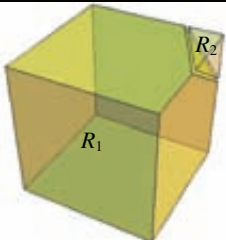
Proof. See Appendix 6F.

Corollary 6. *Sub-cases G3, G4 and H4 do not include the optimal solution of the Model MGM and their corresponding constraints can be relaxed in the model.*

Therefore, $y_i^* = 0 \ \forall i \in \{G3, G4, H4\}$.

Proof. From Theorem 5, Sub-case $C3$ compared to sub-case $G3$, and sub-case $C4$ compared to sub-cases $G4$ and $H4$ lead to shorter $E[T]$ and so the constraints corresponding to the cases $G3$, $G4$ and $H4$ can be relaxed.

Thus, the total 36 sub-cases can be summarized in the following six sub-cases. According to Theorem 3, since $l^* = w^*$, these sub-cases can be simplified by replacing w with l.

(A1) $b/2 \leq h$ & $b \leq l$ & $h \leq l$	**(C1)** $b/2 \leq h$ & $l \leq b \leq 2l$ & $h \leq l$	**(I1)** $b/2 \geq h$ & $b \leq l$ & $h \leq l$

(K1) $b/2 \geq h$ & $l \leq b \leq$	**(O1)** $b/2 \geq h$ & $l+h \leq b$	**(P1)** $b/2 \geq h$ & $2l \leq b \leq$
$l+h$ & $h \leq l$	$\leq 2l$ & $h \leq l$	$2l +h$ & $h \leq l$

Figure 6.3. Sub-cases to be optimized individually

In order to solve Model MGM, we first solve each of six remaining sub-cases individually and obtain the optimal solution in each sub-case. Next, by comparing the optimal solutions obtained from the 6 sub-cases the optimal solution of Model MGM can be found. To simplify the calculations, volume of the system is normalized to one.

Optimizing the dimensions in each of 6 sub-cases individually

The optimization process is explained for sub-cases A1 and C1. For the rest we refer to Appendix 6G.

Sub-case A1. $b/2 \leq h$ & $b \leq l$ & $h \leq l$

V_1, $E[T^1]$ and $E[T^2]$ formulas are given in chapter 5. Hence, by using Equation (5.4) in chapter 5, the objective function in this case is

$$E\left[T_{A1}\right] = G_1^{\frac{2s}{1+s}} \frac{3b}{4} + \left(1 - G_1^{\frac{2s}{1+s}}\right) \frac{21b^4 - 8h\left(h^3 + 12hlw + 12lw\left(l + w\right)\right)}{4\left(7b^3 - 48hlw\right)}. \tag{6.166}$$

However, according to Theorem 3 it is proven in optimal solution $w^* = l^*$. In addition, the volume of the system is normalized to one and so $hl^2 = 1$. Moreover, based on volume formula of the shape of the first zone in this case we have $G_1 = \dfrac{7b^3}{48}$. Therefore, the objective function can be simplified to a two-variable function (b, l) as Equation (6.167),

$$E\left[T_{A1}\right] = \frac{1}{4}\left(\left(\frac{7b^3}{16}\right)^{\frac{2s}{1+s}} 3^{1-\frac{2s}{1+s}} b + \frac{(1 - (\frac{7b^3}{48})^{\frac{2s}{1+s}})(21b^4 - 8(\frac{12}{l^2} + \frac{1}{l^8} + 24l))}{-48 + 7b^3}\right) . \tag{6.167}$$

In order to obtain the optimal value of length of the system (l^*), we solve the following equation,

$$\frac{dE[T_{A1}]}{dl} = \frac{16(-1 + (\frac{7b^3}{48})^{\frac{2s}{1+s}})(-1 - 3l^6 + 3l^9)}{(-48 + 7b^3)l^9} = 0. \tag{6.168}$$

Although $E\left[T_{A1}\right]$ is a function of two variables l and b, solving Equation (6.168) leads to optimal value of l. As only one critical point is obtained by solving Equation (6.168), it only suffices to compare it

with any other feasible solution to ensure the critical point is an absolute minimum. Therefore, the following equation gives the optimal values of l and w,

$$w^* = l^* = \left(\left[-2+\left(\frac{1}{2}\left(11-3\sqrt{13}\right)\right)^{1/3}+\left(\frac{1}{2}\left(11+3\sqrt{13}\right)\right)^{1/3}\right]^{1/3}\right)^{-1/2} = 1.06937 \ . \tag{6.169}$$

Consequently, the following equation gives the optimal value of h, which satisfies the condition $0 < h \le l$,

$$h^* = \left[-2+\left(\frac{1}{2}\left(11-3\sqrt{13}\right)\right)^{1/3}+\left(\frac{1}{2}\left(11+3\sqrt{13}\right)\right)^{1/3}\right]^{1/3} = 0.87446 \ . \tag{6.170}$$

In order to obtain the optimal boundary b following equation should be solved for l^* and any given s,

$$\frac{dE[T_{A1}]}{db} = 0 \, \forall \, 0 < s < 1 \, and \, l = l^* \ . \tag{6.171}$$

b^* can be obtained analytically for any given value of s. Since b^* is the only critical point, it suffices to compare b^* with any other b to make sure b^* is the absolute minimum. However, a closed-form formula for the optimal boundary $b^*(s)$ cannot analytically be obtained. As a result, we analytically obtain optimal value of boundary (b^*) for 1000 different values of s and then we obtain $b^*(s)$ by fitting the function $b^*(s) = a \, \mathrm{ArcTan}[cs+d]+e$ to these optimal values. Equation (6.172) gives the closed-form formula of the optimal boundary as a function of s,

$$b^*(s) = 80854 \, \mathrm{ArcTan}[429284s + 56451] - 127004 \ . \tag{6.172}$$

The standard error, t-statistic, and P-value of each parameter are given in Appendix 6C. However, b is an increasing function of s while according to condition of sub-case A1 we know $b \le l$, therefore, we have to obtain s' in which $b^* = l^*$. s' can be obtained by solving the following equation,

$$b^*(s) = l^* \rightarrow s' = 0.354907. \tag{6.173}$$

Figure 6.4 shows the optimal values of boundary, b and the fitted $b^*(s)$ function for $s \le s'$.
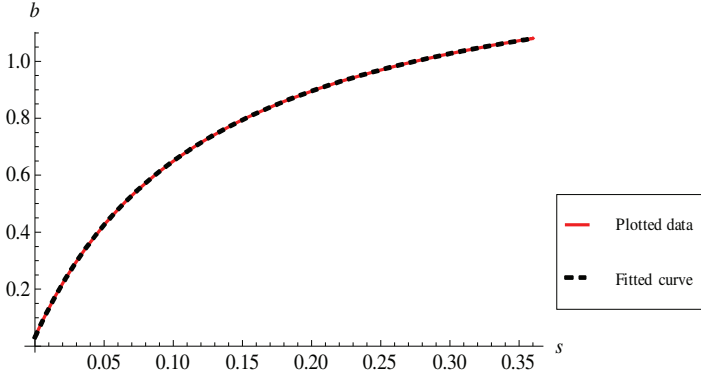
Figure 6.4. Fitted function $b^*(s)$ and the plot of optimal values of b for $s \leq s'$ in sub-case A1

For $s > s'$, the optimal boundary b^* equals the optimal length i.e. $b^* = l^*$ (for the proof see Appendix 6H). Therefore, by replacing b with l, we obtain $E[T_{A1}]$ as a one variable function of l and then l^* can be obtained by solving $\dfrac{dE[T_{A1}]}{dl} = 0$ for any $s > s'$. However, it turns out that the optimal solution of Model MGM for $s > s'$ is obtained from sub-case C1.

Sub-case C1. $b/2 \leq h$ & $l \leq b \leq 2l$ & $h \leq l$

The objective function in this case is,

$$
\begin{aligned}
E[T_{C1}] = G_1^{\frac{2s}{1+s}} \frac{27b^4 - 64b^3(l+w) + 48b^2(l^2+w^2) - 8(l^4+w^4)}{4(9b^3 - 24b^2(l+w) + 24b(l^2+w^2) - 8(l^3+w^3))} \\
+ \left(1 - G_1^{\frac{2s}{1+s}}\right) \frac{27b^4 - 64b^3(l+w) + 48b^2(l^2+w^2) + 8(h^4 - l^4 + 12h^2lw - w^4 + 12hlw(l+w))}{4(9b^3 - 24b^2(l+w) + 24b(l^2+w^2) - 8(l^3 - 6hlw + w^3))}.
\end{aligned}
\tag{6.174}
$$

According to Theorem 3 it is proven in optimal solution $w^* = l^*$. In addition, the volume of the system is normalized to 1 and so $hl^2 = 1$. Moreover, based on volume formula of the shape of the first zone in this case we have $G_1 = \dfrac{1}{48}(-b^3 - 8(b-l)^3 + 24b(b-w)w + 8w^3)$. Therefore, the objective function can be simplified to a two variable function (b, l) as Equation (6.175),

$$E[T_{C1}] = \frac{1}{4}(2304^{-\frac{s}{1+s}}(-9b^3 + 48b^2l - 48bl^2 + 16l^3)^{\frac{-1+s}{1+s}}(-27b^4 + 128b^3l - 96b^2l^2 + 16l^4)$$

$$+ \frac{(1 - (-\frac{3b^3}{16} + b^2l - bl^2 + \frac{l^3}{3})^{\frac{2s}{1+s}})(27b^4 - 128b^3l + 96b^2l^2 + 8(\frac{1}{l^8} + \frac{12}{l^2} + 24l - 2l^4))}{48 + 9b^3 - 48b^2l + 48bl^2 - 16l^3}). \tag{6.175}$$

In order to obtain the optimal value of length of the system (l^*), we solve the following equation,

$$\frac{dE[T_{C1}(l,b)]}{dl} = 0. \tag{6.176}$$

Although Equation (6.176) is a function of two variables l and b, solving $\dfrac{dE[T_{C1}]}{dl} = 0$ leads to the optimal length l^* given by Equation (6.177),

$$l^* = w^* = \left(\left(-2 + \left(\frac{1}{2}\left(11 - 3\sqrt{13}\right)\right)^{1/3} + \left(\frac{1}{2}\left(11 + 3\sqrt{13}\right)\right)^{1/3}\right)^{1/3}\right)^{-\frac{1}{2}} = 1.06937. \tag{6.177}$$

Consequently, the optimal value of height h^*, can be obtained by using the following equation. The optimal dimensions satisfy the condition of case C1 that is $0 < h \le l$,

$$h^* = \left(-2 + \left(\frac{1}{2}\left(11 - 3\sqrt{13}\right)\right)^{1/3} + \left(\frac{1}{2}\left(11 + 3\sqrt{13}\right)\right)^{1/3}\right)^{1/3} = 0.87446. \tag{6.178}$$

In order to obtain the optimal boundary b following equation should be solved for l^* and any given s,

$$\frac{dE[T_{C1}]}{db} = 0 \qquad \forall 0 < s < 1 \text{ and } l = l^*. \tag{6.179}$$

Solving Equation (6.179) leads to $b^*(s) < l^*$ for $s \le s'$ ($s' = 0.354907$). However, according to condition of case C1 we have $l \le b$ and therefore $b^*(s) = l^* = 1.06937$ for $s \le s'$. For $s \le s'$, sub-case C1 leads to longer $E[T]$ compared to optimal solution of sub-case A1. Therefore, it suffices to consider the solution of case C1 for $s > s'$.

b^* can be obtained analytically for any given value of s. Since b^* is the only critical point, it suffices to compare b^* with any other b to make sure b^* is the absolute minimum. However, a closed-form formula for the optimal boundary $b^*(s)$ cannot analytically be obtained. As a result, we analytically obtain optimal value of boundary (b^*) for 1000 different values of s and then we obtain $b^*(s)$ by fitting the function $b^*(s) = a\,\mathrm{ArcTan}[cs + d] + e$ to these optimal values. Equation (6.180) gives the optimal boundary for any given skewness parameter $s > s'$,

$$b^*\left(s\right) = 0.479841\,\mathrm{ArcTan}[3.43086\,s - 0.224308] + 0.691496\,. \tag{6.180}$$

The standard error, t-statistic, and P-value of each parameter are given Appendix 6C. Figure 6.5 shows the optimal values of boundary, b and the fitted $b^*(s)$ function for $s > s'$.
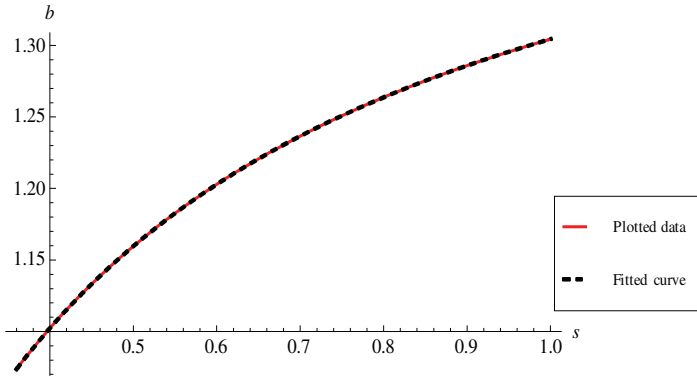
Figure 6.5. Fitted function $b^*(s)$ and the plot of optimal values of b for $s > s'$ in sub-case C1

The optimal solutions of the remaining four cases can be obtained similarly (see Appendix 6G for the optimal solutions of each case). By comparing the optimal solutions of all six sub-cases, it turns on sub-cases A1 and C1 include the overall optimal solutions.

Table 6.2 gives the optimal solution of Model MGM for different values of s. Table 6.2 shows that the skewness of ABC curve does not have any impact on the optimal dimensions of a two-class-based live-cube system. This makes the system very robust to changes in demand patterns of products. The system can optimally be used for different customer demand ABC curves. However, the optimal zone boundary is affected by the skewness of ABC curve leading to different zone shapes and zone sizes.

Table 6.2. Overall optimal solution for different values of s

Sub-case	Skewness parameter (s)	Optimal length (l^*), width (w^*) and height (h^*)	Estimated optimal boundary ($b^*(s)$)

A1. $b/2 \leq h$ & $b \leq l$ & $h \leq l$

$s \leq 0.354907$

$$l^* = w^* = \left(\left(-2 + \left(\frac{1}{2}\left(11 - 3\sqrt{13}\right)\right)^{1/3} + \left(\frac{1}{2}\left(11 + 3\sqrt{13}\right)\right)^{1/3}\right)^{1/3}\right)^{-1/2}$$

$$h^* = \left(-2 + \left(\frac{1}{2}\left(11 - 3\sqrt{13}\right)\right)^{1/3} + \left(\frac{1}{2}\left(11 + 3\sqrt{13}\right)\right)^{1/3}\right)^{1/3}$$

$80854.3\,\mathrm{ArcTan}[429284\,s + 56451] - 127004$

C1. $b/2 \leq h$ & $l \leq b \leq 2l$ & $h \leq l$

$s > 0.354907$

$$l^* = w^* = \left(\left(-2 + \left(\frac{1}{2}\left(11 - 3\sqrt{13}\right)\right)^{1/3} + \left(\frac{1}{2}\left(11 + 3\sqrt{13}\right)\right)^{1/3}\right)^{1/3}\right)^{-1/2}$$

$$h^* = \left(-2 + \left(\frac{1}{2}\left(11 - 3\sqrt{13}\right)\right)^{1/3} + \left(\frac{1}{2}\left(11 + 3\sqrt{13}\right)\right)^{1/3}\right)^{1/3}$$

$0.479841\,\mathrm{ArcTan}[3.43086\,s - 0.224308] + 0.691496$

6.3. Extensions

In this section, we extend our problem in two directions. First, we consider a situation where a live-cube system needs to be installed in a warehouse with fixed building dimensions. The system dimensions and zone boundary minimizing the expected retrieval time can still be obtained (section 6.3.1). Second, we consider an existing live-cube system with fixed dimensions. The expected retrieval time of such a system can still be minimized by optimizing the boundary of the first zone (section 6.3.2).

6.3.1. Constraints on the system dimensions

A live-cube system can be installed either in a new warehouse or in an existing warehouse. In the latter case, the dimensions of the building might prevent the installation of a live-cube system with optimal dimensions. However, the optimal dimensions and zone boundary can still be obtained considering those constraints. We can simplify the problem as follows.

Step 1. Calculate the optimal dimensions using Table 6.2.

Step 2. Identify the number of dimensions that are constrained.

If the number of constrained system dimensions equals zero, no constraints are effective, and the optimal dimensions and boundary are still determined by Table 6.2.

If the number of constrained system dimensions is one or more, we can use these constraints to reduce the number of possible sub-cases to be considered. We then follow an optimization process which is similar but simpler than that of section 6.2. However, in case the height dimension is constrained the optimal dimensions and zone boundary can be obtained even simpler. If the constraint on the height dimension is effective, the dimensions for the *x*- and *y*- directions can be enlarged according to Lemma 2 and Theorem 3 to keep the shape of the system as close to a square as possible at each level.

If the optimal dimensions are obtained, in order to find the optimal zone boundary the algorithm in section 6.3.2 can be followed.

6.3.2. Optimizing zone boundary of an existing live-cube system

The response time of an existing live-cube system with a given configuration can still be minimized by optimizing the boundary of the first zone. In this section, we propose an algorithm to find the optimal first zone boundary for a live-cube system with a given configuration.

Step 1. Find a set of sub-cases, which their conditions can be met given the configuration of the system using Appendix 6I. Within each set, the sub-cases are arranged in an ascending order of *b*. Consider the first sub-case.

Step 2. Replace the given values of *l*, *w*, *h* and *s* in the corresponding closed-form formula of $E[T]$ yielding one variable objective function ($E[T(b)]$).

Step 3. Obtain b^* by solving $\dfrac{d\,E[T]}{d\,b} = 0$. b^* is the optimal boundary if it satisfies the condition of the sub-case. Otherwise, consider the next sub-case in Appendix 6I and go to step 2.

Using the proposed algorithm the expected retrieval time of a two-class live-cube system with a given configuration can be minimized.

6.4. The effectiveness of optimal zone boundaries

In this section, we present numerical results to check the effectiveness of the optimal dimensions and zone boundary. For different values of the ABC curve skewness parameter *s*, optimal system dimensions with optimal zone boundary are compared to optimal dimensions under random storage. For any *p*%/*C(p)*%, *s* can be determined using $C(p) = p^s$. The travel time results for the optimal live-cube system under a random storage policy are obtained from chapter 4. Table 6.3 gives the optimal dimensions of the system, optimal zone boundary, and optimal expected retrieval time for some selected skewness

parameters. $E[T_{G^*}]$ represents the expected retrieval times of a optimal live-cube system with a optimal zone size.

Table 6.3. The optimal solutions for some selected skewness parameters (ABC curve)

s	ABC curve	Sub-case	l^*	h^*	b^*	G^*	$E[T_{G^*}]$	$Impro_{G_1^*}$ (%)
0.065	20%/90%	A1	1.06937	0.87446	0.517	0.020	0.830	45.78
0.139	20%/80%	A1	1.06937	0.87446	0.773	0.067	1.072	30.00
0.22	20%/70%	A1	1.06937	0.87446	0.925	0.116	1.206	21.24
0.32	20%/60%	A1	1.06937	0.87446	1.040	0.164	1.304	14.80
0.43	20%/50%	C1	1.06937	0.87446	1.122	0.206	1.374	10.25
0.57	20%/40%	C1	1.06937	0.87446	1.191	0.246	1.433	6.37
0.75	20%/30%	C1	1.06937	0.87446	1.251	0.283	1.485	3.03
1	20%/20%	_	1.06937	0.87446	_	/	1.531	0.00

Note. "_": any value between 0 and 3.0132 ($\max\{l^*+ w^*, h^*\}+ h^*$); "/": any value between 0 and 1; $Impro_{G_1^*}$ is the reduction of $E[T]$ of a two-class storage policy with an optimal zone size compared to a random storage policy.

From Table 6.3, we make the following observations.

Observation 1. Compared to the random storage policy, the optimal two-class storage policy can bring significant reduction in response time, especially when the ABC curve is very skewed (i.e. small s) and the first zone is relatively small. For example, for a 20%/90% ABC curve, the retrieval time can be decreased more than 45% compared to an optimal random storage policy. However, the reduction becomes insignificant when s is close to one. This is expected since for an increasing skewness parameter s, the beneficial effect of class-based storage disappears. However, skewed ABC curves (e.g. 20%/80%) can commonly be found in practice.

Observation 2. With increasing skewness parameter s, the optimal boundary b^* and the optimal zone size G_1^* increase. However, the optimal dimensions do not change for different skewness parameter values s. This makes it possible to optimally use different ABC curves without any configuration correction.

Observation 3. The results of random storage policy in chapter 4 is a special case of results from this chapter where $G_1 = 1$ or 0 or $s = 1$. This can be verified by calculating the limit values of l^*, w^*, h^*, b^* and $E[T^*]$ for any sub-case at $G_1 = 1$ or 0 or $s = 1$.

6.5. Conclusion

In this chapter, we study a two-class-based live-cube system. We propose a mixed-integer nonlinear mathematical model to optimize the first zone boundary and system dimensions minimizing the response time. Decomposition of the system into 36 complementary sub-cases leads to a model with many constraints. Each sub-case represents a configuration of the system and zone boundary. Due to the complexity of the model, we use some properties of the optimal solution to simplify the mathematical model. The optimal dimensions of a live-cube system together with the optimal first zone boundary can analytically be obtained for any ABC curve. The results show that in a live-cube compact storage system, an optimal two-class-based storage policy can significantly reduce the response time specifically for ABC curves seen in practice (i.e. skewed ABC curves) compared to a random storage policy. For example, for a 20%/90% ABC curve, 45.78% reduction in response time can be obtained. The optimal dimensions of a two-class live-cube system do not change for different ABC curves yielding a robust system for various ABC curves. The problem with a random storage policy is only a special case of our problem. In addition, we extend the chapter in two directions. We optimize the system dimensions and first zone boundary for a system with constraints on the system dimensions. In addition, we minimize the response time of a system with fixed dimensions by optimizing the first zone boundary.

Appendix 6A. Proof of Lemma 1

Let $T(l,w,b)$ represent the retrieval time. Therefore, the objective function can be written as follows,

min $E[T(l, w, b)]$.

Let $d=l/w$ ($d\geq1$), then $E[T]$ function can be reformulated as follows,

min $E[T(d, w, b)]$.

The following illustration shows that $E[T]$ is increasing function of d ($\frac{\partial E[T]}{\partial d} > 0, \forall d \geq 1$). Therefore, the smaller d is (closer to square), the shorter the expected retrieval time will be.

Consider the following figure illustrating two cases of the top-viewed shape of the system, cases A and B with dimensions (l',w') and (l,w), respectively. For the sake of illustration and without loss of generality, we consider a situation where the first zone has a triangular shape. The proof for other shapes of the first zone follows a similar fashion.
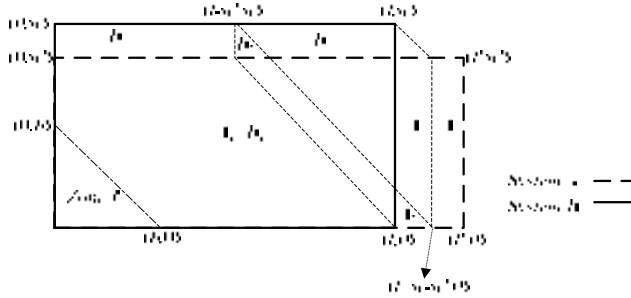
Figure 6.6. Top view of two candidates of the system shape

Case *B* is the system with a shape closer to square (*w'<w<l<l'*). To make a fair comparison we assume both cases have equal area i.e. $S_A=S_B$. Therefore, we can write $l \times w = l' \times w'$ and $(l'-l)w' = (w-w')l$. In addition, as *w'<l*, then $(l'-l)>(w-w')$.

We have to show that $E[T_B]<E[T_A]$. The expected retrieval time of cases *A* and *B* can be written as follows,

$$E[T_A] = G^{\frac{2s}{s+1}} E[T_A^1] + (1 - G^{\frac{2s}{s+1}})E[T_A^2],$$

$$E[T_B] = G^{\frac{2s}{s+1}} E[T_B^1] + (1 - G^{\frac{2s}{s+1}})E[T_B^2].$$

Since the first zone is the same in both cases, $G^{\frac{2s}{s+1}}E[T_A^1]$ and $G^{\frac{2s}{s+1}}E[T_B^1]$ can be removed. $E[T_A^2]$ and $E[T_B^2]$ can be written as follows,

$$E[T_A^2] = \frac{S_{A1}}{S_{ZoneII}} E[T_{A1}^2] + \frac{S_{A2}}{S_{ZoneII}} E[T_{A2}^2] + \frac{S_{A3}}{S_{ZoneII}} E[T_{A3}^2] + \frac{S_{A4}}{S_{ZoneII}} E[T_{A4}^2],$$

$$E[T_B^2] = \frac{S_{B1}}{S_{ZoneII}} E[T_{B1}^2] + \frac{S_{B2}}{S_{ZoneII}} E[T_{B2}^2] + \frac{S_{B3}}{S_{ZoneII}} E[T_{B3}^2] + \frac{S_{B4}}{S_{ZoneII}} E[T_{B4}^2].$$

where S_i is the area of region *i* ($i = A1, A2, A3, A4, B1, B2, B3, B4$) . Comparing each region in Case *B* by its corresponding region in Case *A* shows that Case *A* always has longer total retrieval time compared to Case *B*.

- $E[T_{A1}^2] = E[T_{B1}^2]$: A_1 and B_1 are congruent shapes (two figures are congruent if they have the same shape and size). In addition, any value of retrieval time has the same weight (probability) in both A_1 and B_1 regions.

- $E[T_{A2}^2] = E[T_{B2}^2]$: The comparison is similar to case above (A_1 and B_1).

- $E[T_{A3}^2] > E[T_{B3}^2]$: A_3 and B_3 are also congruent shapes. However, any location in A_3 has longer retrieval time than any location in B_3.

- $E[T_{A4}^2] = E[T_{B4}^2]$: The comparison is similar to case A_1 and B_1.

As a result $E[T_A] - E[T_B] > 0$ and the proof is complete.

Therefore, with increasing d ($=l/w$) the expected retrieval time increases correspondingly ($\frac{\Delta E[T]}{\Delta d} > 0, \forall d \geq 1$).

Appendix 6B. Proof of Theorem 2

For a single-level live-cube system, if $l < b \leq l + w$, the first zone takes up at least half volume of the system. $E[T]$ for this case is $((1 - \frac{(2-b)^2}{2})^{\frac{2s}{s+1}})(\frac{2(1 + (-3 + b)b^2)}{3(2 + (-4 + b)b)}) + (1 - (1 - \frac{(2-b)^2}{2})^{\frac{2s}{s+1}})(\frac{2(1+b)}{3})$. The first derivative of $E[T]$ function over the boundary b is non-negative for all s, $0 < s \leq 1$,

$$\frac{2}{3}\left(1 + \frac{2\left(-1 + 2b - \frac{b^2}{2}\right)^{\frac{2s}{1+s}}}{2 + \left(-4 + b\right)b} - \frac{2\left(-2 + b\right)\left(-1 + 2b\right)\left(-1 + 2b - \frac{b^2}{2}\right)^{\frac{2s}{1+s}}}{\left(2 - 4b + b^2\right)^2} + \frac{4\left(-2 + b\right)\left(-1 + 2b\right)\left(-1 + 2b - \frac{b^2}{2}\right)^{\frac{2s}{1+s}}s}{\left(2 - 4b + b^2\right)^2\left(1 + s\right)}\right) \geq 0, \forall 0 < s \leq 1.$$

$\square$

Appendix 6C. Standard error, t-statistic and P-value of $b^*(s)$ of a single-level system, case A1 in a multi-level system and, case C1 in a multi-level system

Table 6.4. Parameter estimates of function $b^*(s)$ in a single-level system

parameter	Standard error	t-statistic	P-value

a	191.7	280.1	< .0001
c	154.0	2003.5	< .0001
d	210.5	273.6	< .0001
e	301.2	-280.1	< .0001

Table 6.5. Parameter estimates of function $b^*(s)$ for case A1 in a multi-level system

parameter	Standard error	t-statistic	P-value
a	289.0	279.7	< .0001
c	217.2	1975.5	< .0001
d	225.2	250.6	< .0001
e	453.9	-279.7	< .0001

Table 6.6. Parameter estimates of function $b^*(s)$ for case C1 in a multi-level system

parameter	Standard error	t-statistic	P-value
a	0.00224255	213.9	< .0001
c	0.00850802	403.2	< .0001
d	0.00603803	-37.1	< .0001
e	0.00269952	256.1	< .0001

Appendix 6D. Proof of Lemma 2

Let $T(l,w,h,b)$ represent the retrieval time. Therefore, the objective function can be written as follows,

min $E[T(l, w, h, b)]$.

Let $d=l/w$ ($d \geq 1$), then $E[T]$ function can be reformulated as follows,

min $E[T(d, w, h, b)]$.

The following illustration shows that $E[T]$ is increasing function of d ($\frac{\partial E[T]}{\partial d} > 0, \forall d \geq 1$). Therefore, the smaller d is (closer to square), the shorter the expected retrieval time will be.

Consider the following figure illustrating two candidates of the top-viewed shape of the system at any arbitrary level. For the sake of illustration and without loss of generality, we consider a situation where the first zone has a triangular shape. The proof for other shapes of the first zone follows a similar fashion.
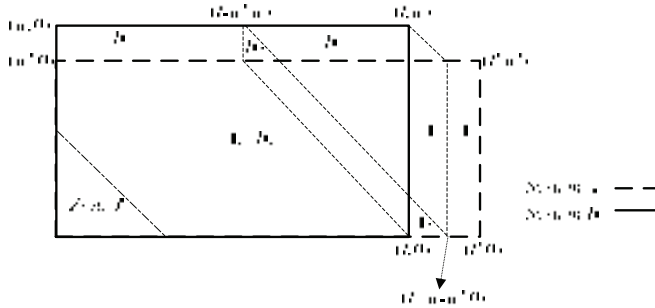
Figure 6.7. Top view of two candidates of the system shape at each level

Case *B* is the system with a shape closer to square at each level (*w'*<*w*<*l*<*l'*). To make a fair comparison we assume both cases have equal area i.e. $V_A=V_B$. Therefore, we can write $l\times w=l'\times w'$ and $(l'-l)w' = (w-w')l$. In addition, as *w'*<*l*, then $(l'-l)>(w-w')$.

We have to show that $E[T_B]<E[T_A]$. The expected retrieval time of cases *A* and *B* can be written as follows,

$$E[T_A] = G^{\frac{2s}{s+1}} E[T_A^1] + (1 - G^{\frac{2s}{s+1}}) E[T_A^2],$$

$$E[T_B] = G^{\frac{2s}{s+1}} E[T_B^1] + (1 - G^{\frac{2s}{s+1}}) E[T_B^2].$$

Since the first zone is the same in both cases, $G^{\frac{2s}{s+1}} E[T_A^1]$ and $G^{\frac{2s}{s+1}} E[T_B^1]$ can be removed. $E[T_A^2]$ and $E[T_B^2]$ can be written as follows,

$$E[T_A^2] = \frac{V_{A1}}{V_{ZoneII}} E[T_{A1}^2] + \frac{V_{A2}}{V_{ZoneII}} E[T_{A2}^2] + \frac{V_{A3}}{V_{ZoneII}} E[T_{A3}^2] + \frac{V_{A4}}{V_{ZoneII}} E[T_{A4}^2],$$

$$E[T_B^2] = \frac{V_{B1}}{V_{ZoneII}} E[T_{B1}^2] + \frac{V_{B2}}{V_{ZoneII}} E[T_{B2}^2] + \frac{V_{B3}}{V_{ZoneII}} E[T_{B3}^2] + \frac{V_{B4}}{V_{ZoneII}} E[T_{B4}^2].$$

where S_i is the area of region i ($i = A1, A2, A3, A4, B1, B2, B3, B4$) . Comparing each region in Case B by its corresponding region in Case A shows that Case A always has longer total retrieval time compared to Case B.

- $E[T_{A1}^2] = E[T_{B1}^2]$: A_1 and B_1 are congruent shapes (two figures are congruent if they have the same shape and size). In addition, any value of retrieval time has the same weight (probability) in both A_1 and B_1 regions.

- $E[T_{A2}^2] = E[T_{B2}^2]$: The comparison is similar to case above (A_1 and B_1).

- $E[T_{A3}^2] > E[T_{B3}^2]$: A_3 and B_3 are also congruent shapes. However, any location in A_3 has longer retrieval time than any location in B_3.

- $E[T_{A4}^2] = E[T_{B4}^2]$: The comparison is similar to case A_1 and B_1.

As a result $E[T_A] - E[T_B] > 0$ and the proof is complete.

Therefore, with increasing d (=l/w) the expected retrieval time increases correspondingly ($\dfrac{\Delta E[T]}{\Delta d} > 0, \forall d \geq 1$).

Appendix 6E. Proof of Theorem 4

Table 6.7 gives the optimal solutions of sub-cases A3, A4, C3, C4 and P3. Comparing these solutions with the optimal solution of sub-case $h \leq w$ in each case shows that these sub-cases can be removed due to longer $E[T]$.

Table 6.7. Optimal solutions of sub-cases A3, A4, C3, C4, P3

Sub-case	s	Optimal length (l^*)	Optimal boundary (b^*)
A3 ($b/2 \leq h$ & $b \leq l$ & $l < h \leq 2\,l$)	$s \leq 0.27457$	1	$121051\,\mathrm{ArcTan}[789183\,s + 86782.2] - 190144$
	$s > 0.27457$	1	1

A4 ($b/2 \leq h$ & $b \leq l$ & $h > 2\,l$)	$s \leq 0.107915$	0.793701	$2.47279\,\mathrm{ArcTan}[19.484\,s + 1.48301] - 2.41888$
	$s > 0.107915$	0.793701	0.793701
C3 ($b/2 \leq h$ & $l \leq b \leq 2l$ & $l < h < 2l$)	$s \leq 0.03042$	0.793701	0.793701
	$0.03042 < s \leq 0.14914$	$14841.2\,\mathrm{ArcTan}[534925\,s + 27162.1] - 23311.3$	$14841.2\,\mathrm{ArcTan}[534925\,s + 27162.1] - 23311.3$
	$0.14914 < s \leq 0.27457$	1	1
	$s > 0.27457$	1	$61669.9\ \mathrm{ArcTan}[250125.0\,s + 51246.3] - 96869.3$

C4 ($b/2 \leq h$ & $l \leq b \leq 2l$ & $h>2l$)	$s \leq 0.03042$	$-26937.4\ \mathrm{ArcTan}[-4.3 \times \mathrm{E6}\,s - 40695.2] - 42312.2$	$-26937.4\ \mathrm{ArcTan}[-4.3 \times \mathrm{E6}\,s - 40695.2] - 42312.2$
	$0.03042 < s \leq 0.107915$	0.793701	0.793701
	$s > 0.107915$	0.793701	$35982.6\,\mathrm{ArcTan}[120589\,s + 25460.7] - 56519.6$
P3 ($2h \leq b \leq 2l + h$ & $h > l$)	$0 < s \leq 1$	1	2

We prove the theorem for case A3. The theorem can be proven for other cases similarly.

Proof for Case A3. $b/2 \leq h$ & $b \leq l$ & $l < h \leq 2\,l$

$E[T^1]$ and $\mathrm{E}[T^2]$ for this case, can be obtained from chapter 5. Hence, the objective function in this case is

$$\mathrm{E}[\mathrm{T}_{A3}] = G^{\frac{2s}{1+s}}\,\frac{3b}{4} + \left(1 - G^{\frac{2s}{1+s}}\right)\frac{21b^4 + 8\left(h^4 + l^4 + 6h^2\left(l-w\right)^2 + w^4 - 4h^3\left(l+w\right) - 4h\left(l+w\right)^3\right)}{4\left(7b^3 - 48hlw\right)}.$$

However, according to Theorem 3 it is proven in optimal solution $w^* = l^*$. In addition, the volume of the system is normalized to one and so $hl^2 = 1$. Moreover, based on volume formula of the shape of the first

zone in this case we have $G = \dfrac{7b^3}{48}$. Therefore, the objective function can be simplified to a two variable function (l, b) as follows where s is skewness parameter ($0<s<1$).

$$\mathrm{E}[T_{A3}] = \frac{1}{4}\left(\left(\frac{7}{16}\right)^{\frac{2s}{1+s}} 3^{1-\frac{2s}{1+s}} b(b^3)^{\frac{2s}{1+s}} + \frac{(1-(\frac{7}{48})^{\frac{2s}{1+s}}(b^3)^{\frac{2s}{1+s}})(21b^4 + 8(\frac{1}{l^8} - \frac{8}{l^5} - 32l + 2l^4))}{-48 + 7b^3}\right).$$

In order to find the optimal values of l and b we solve the following equations,

$$\frac{dE[T_{A3}]}{dl} = 0 \ and \ \frac{dE[T_{A3}]}{db} = 0 \qquad \forall 0 < s < 1.$$

Solving these equations leads to $l^*>1$. However, according to conditions of case A3 it can be shown that $l \leq 1$ and therefore $l^*=1$.

Therefore l can be replaced by its optimal value ($l^*=1$) and so $E[T_{A3}]$ can be written as only one variable function as follows,

$$E[T_{A3}(b)] = \frac{1}{4}\left(\left(\frac{7}{16}\right)^{\frac{2s}{1+s}} 3^{1-\frac{2s}{1+s}} b\left(b^3\right)^{\frac{2s}{1+s}} + \frac{\left(-296 + 21b^4\right)\left(1 - \left(\frac{7}{48}\right)^{\frac{2s}{1+s}}\left(b^3\right)^{\frac{2s}{1+s}}\right)}{-48 + 7b^3}\right).$$

By taking derivative of above equation over b the optimal boundary $b^*(s)$ can be obtained,

$$\frac{dE[T_{A3}(b)]}{db} = \left(\frac{1}{b\left(48 - 7b^3\right)^2\left(1+s\right)}\right)\left(2^{-2-\frac{8s}{1+s}}3^{1-\frac{2s}{1+s}}\left(\begin{array}{c} 29649^{\frac{s}{1+s}}\left(b^3\right)^{\frac{2s}{1+s}}\left(7b^3\left(-1+s\right)-96s\right)+2592^{3+\frac{8s}{1+s}}9^{\frac{s}{1+s}}b^3\left(1+s\right) \\ +492304^{\frac{s}{1+s}}b^7\left(1+s\right)+230449^{\frac{s}{1+s}}b\left(b^3\right)^{\frac{2s}{1+s}}\left(1+7s\right) \\ -672b^4\left[2^{1+\frac{8s}{1+s}}9^{\frac{s}{1+s}}-49^{\frac{s}{1+s}}\left(b^3\right)^{\frac{2s}{1+s}}+2\left(2304^{\frac{s}{1+s}}+49^{\frac{s}{1+s}}\left(b^3\right)^{\frac{2s}{1+s}}\right)s\right] \end{array}\right)\right) = 0.$$

Solving the above equation results in $b^*(s)$ which is an increasing function of s. However, according to condition of case A3, $b \leq l$. Therefore, we have to find an s^* where $b = l = 1$. s^* can be obtained by solving the above equation at $b = l = 1$ which leads to $s^* = 0.27457$. For $s > s^*$, $l^* = b^* = 1$.

For $s \leq s^*$, $b^*(s)$ can be obtained for any given s by solving the above equation. The optimal boundary as a function of s can be obtained by fitting the function $b^*(s) = a\,\mathrm{ArcTan}[cs + d] + e$ to optimal values of boundary b for different s. The estimate, standard error, t-statistic and P-value of each parameter are given in Table 6.8.

Table 6.8. Parameter estimate of function $b^*(s)$

parameter	Estimate	Standard error	t-statistic	P-value
a	121051.0	252.7	478.9	< .0001
c	789183.0	150.8	5233.1	< .0001
d	86782.2	150.9	574.8	< .0001
e	-190144.0	397.0	-478.9	< .0001

Figure 6.8 shows the plotted optimal values of b for 1000 different s and corresponding fitted function.
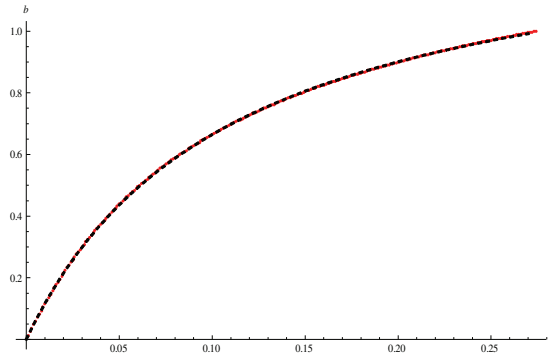
Figure 6.8. Fitted function $b^*(s)$ and the plot of optimal values of b

Comparing the optimal solution of case A3 with the optimal solution of case A1 for any given skewness parameter s shows that case A1 always leads to shorter $E[T]$. □

Appendix 6F. Proof of Theorem 5

We prove the theorem for sub-case $G3$. The proof is analogous for sub-cases $G4$ and $H4$.

If we prove that $E[T]$ for case $G3$ is always larger than $E[T]$ for case $C3$ for any given V_1 then the proof is complete.

For any given V_1 and polytope of case $C3$, polyope of case $G3$ with the same volume V_1 can be obtained as follows: the length (l) of the system should decrease which leads to removing some parts of the first zone. Since we have assumed the volume of the first zone V_1 remains the same, the boundary (b) of the first zone should increase to include locations with longer travel time in the first zone. Therefore, $E[T_{G3}^1] > E[T_{C3}^1]$.

It can be shown that for case $C3$, $l \leq 1.259$, while for case $G3$, $l \leq 0.761$. Since $t < \max\{2h,\ 2l+h\}$ and $\max\limits_{G3} t > \max\limits_{C3} t$, $E[T_{G3}^2] > E[T_{C3}^2]$.

Appendix 6G. Optimal solutions of 4 Sub-cases I1, K1, O1, P1

The summary of optimal solutions of these four sub-cases is given in Table 6.9.

Table 6.9. Optimal solutions of sub-cases I1, K1, O1 and P1

Sub-case	s	Optimal length (l^*)	Optimal boundary (b^*)
I1. $b/2 \geq h$ & $b \leq l$ & $h \leq l$	$s \leq 0.275732$	$(0.5(67986.3\,\mathrm{ArcTan}[663825.0\,s + 50017.7] - 106791.0))^{-1/2}$	$67986.3\,\mathrm{ArcTan}\big[663825.0\,s + 50017.7\big] - 106791.0$
	$s > 0.275732$	1.25992	1.25992
K1.1. $2h \leq b \leq l+h$ & $h \leq l$	$s \leq 0.275732$	$(0.5(39587.7\ \mathrm{ArcTan}[18516.9\,s + 22176.5] - 62181.4))^{-1/2}$	$39587.7\ \mathrm{ArcTan}[18516.9\,s + 22176.5] - 62181.4$
	$s > 0.275732$	1.25992	1.25992
K1.2. $l \leq b \leq l+h$ & $h \leq l$	$s \leq 0.663535$	1.25992	1.25992
	$s > 0.663535$	1.25992	$19.2377\ \mathrm{ArcTan}[63.4077\,s + 19.408] - 28.6456$

O1. $b/2 \geq h$ & $l+h \leq b \leq 2l$ & $h \leq l$	$0 < s \leq 1$	$0.833\ \text{ArcTan}\left[-10.333s - 2.965\right] + 2.315$	$\left(0.833\ \text{ArcTan}\left[-10.333s - 2.965\right] + 2.315\right)$ $+(0.833\ \text{ArcTan}\left[-10.333s - 2.965\right] + 2.315)^{-2}$
P1. $2l \leq b \leq 2l + h$ & $h \leq l$	$s \leq 0.278079$	1	2
	$s > 0.278079$	$3932.9\ \text{ArcTan}\left[32245.0s + 17556.2\right] - 6176.6$	$2(3932.9\ \text{ArcTan}\left[32245.0s + 17556.2\right] - 6176.6)$

Optimization of Sub-cases I1, K1, O1, P1

Case I1. $b/2 \geq h$ & $b \leq l$

$E[T^1]$ and $E[T^2]$ for this case, can be obtained from chapter 5. Hence, the objective function in this case is

$$E[T_{I1}] = G^{\frac{2s}{1+s}} \frac{4b^3 - 3b^2h + h^3}{6b^2 - 6bh + 2h^2} + \left(1 - G^{\frac{2s}{1+s}}\right) \frac{8b^3 - 6b^2h + h^3 - 12hlw - 12lw\left(l + w\right)}{4\left(3b^2 - 3bh + h^2 - 6lw\right)}.$$

However, according to Theorem 3 it is proven in optimal solution $w^* = l^*$. In addition, the volume of the system is normalized to one and so $hl^2 = 1$. Moreover, based on volume formula of the shape of the first zone in this case we have $G = \frac{1}{48}(-b^3 - 8(b - l)^3 + 24b(b - w)w + 8w^3)$. Therefore, the objective function can be simplified to a two variable function (h, b) as follows where s is skewness parameter ($0 < s < 1$),

$$E[T_{I1}] = \frac{6^{-\frac{2s}{1+s}}(h(3b^2 - 3bh + h^2))^{\frac{2s}{1+s}}(4b^3 - 3b^2h + h^3)}{6b^2 - 6bh + 2h^2} - \frac{h(-12 + 8b^3 - 24(\frac{1}{h})^{3/2} - 6b^2h + h^3)(-1 + 6^{-\frac{2s}{1+s}}(h(3b^2}{4(-6 + 3b^2h - 3bh^2 + h^3)}$$

We show that $E[T_{I1}]$ is an increasing function of b and therefore the optimal value of b is at its minimum value. We assume $h = db$ and solve the two following equations to obtain the optimal values of d and b,

$$\frac{dE[T_{I1}]}{db} = 0 \text{ and } \frac{dE[T_{I1}]}{dd} = 0 \qquad \forall 0 < s < 1.$$

It turns out $d^* > 0.5$, $\forall 0 < s < 1$ and so $d^* = 0.5$. Therefore, h can be replaced by b and so $E[T_{I1}]$ can be written as only one variable function as follows,

$$E[T_{I1}(b)] = 3^{1-\frac{2s}{1+s}} 4^{-1-\frac{4s}{1+s}} 49^{\frac{s}{1+s}} b \left(b^3\right)^{\frac{2s}{1+s}} + \frac{\left(384\sqrt{2}\sqrt{\frac{1}{b}} + 96b - 41b^4\right)\left(-1+\left(\frac{7}{48}\right)^{\frac{2s}{1+s}}\left(b^3\right)^{\frac{2s}{1+s}}\right)}{8\left(-48+7b^3\right)}.$$

By taking derivative of above equation over b the optimal boundary $b^*(s)$ can be obtained,

$$\frac{dE[T_{I1}]}{db} = \frac{1}{8}(2^{1-\frac{8s}{1+s}}3^{1-\frac{2s}{1+s}}49^{\frac{s}{1+s}}\left(b^3\right)^{\frac{2s}{1+s}}$$

$$-\frac{4\left(-24+48\sqrt{2}\left(\frac{1}{b}\right)^{3/2}+41b^3\right)\left(-1+\left(\frac{7}{48}\right)^{\frac{2s}{1+s}}\left(b^3\right)^{\frac{2s}{1+s}}\right)}{-48+7b^3}$$

$$+\frac{21b^2\left(-384\sqrt{2}\sqrt{\frac{1}{b}}-96b+41b^4\right)\left(-1+\left(\frac{7}{48}\right)^{\frac{2s}{1+s}}\left(b^3\right)^{\frac{2s}{1+s}}\right)}{\left(48-7b^3\right)^2}$$

$$+\frac{2^{2-\frac{8s}{1+s}}9^{\frac{1}{1+s}}49^{\frac{s}{1+s}}\left(b^3\right)^{\frac{2s}{1+s}}s}{1+s}+\frac{2^{1-\frac{8s}{1+s}}3^{1-\frac{2s}{1+s}}49^{\frac{s}{1+s}}\left(b^3\right)^{\frac{2s}{1+s}}\left(384\sqrt{2}\sqrt{\frac{1}{b}}+96b-41b^4\right)s}{b\left(-48+7b^3\right)\left(1+s\right)}) = 0.$$

Solving the above equation results in $b^*(s)$ which is an increasing function of s. Therefore, $h^*(s) = b^*(s)/2$ is also an increasing function of s and $l^*(s)$ will subsequently be a decreasing function of s. Since the condition of case I1 is $l \geq 2h$ we have to obtain an s_1^* where $l = 2h$. s_1^* can be obtained by solving the above equation at $b = l = 2h = 1.25992$ which is $s_1^* = 0.275732$. For $s_1^* < s$, $l^* = b^* = 1.25992$ and $h^* = 0.62996$.

For $s \leq s_1^*$, $b^*(s) = 2h^*(s)$ which can be obtained for any given s by solving the above equation. The optimal boundary as a function of s can be obtained by fitting the function $b^*(s) = a\,\text{ArcTan}[cs+d] + e$ to

optimal values of boundary b for different s. The estimate, standard error, t-statistic, and P-value of each parameter are given in Table 6.10.

Table 6.10. Parameter estimate of function $b^*(s)$

parameter	Estimate	Standard error	t-statistic	P-value
a	67986.3	1099.5	61.8	< .0001
c	663825.0	446.0	1488.3	< .0001
d	50017.7	749.8	66.7	< .0001
e	-106791.0	1727.1	-61.8	< .0001

Figure 6.9 shows the plotted optimal values of b for 1000 different s and corresponding fitted function.
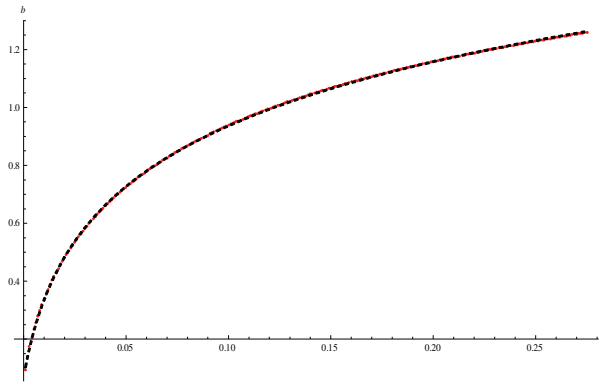
Figure 6.9. Fitted function $b^*(s)$ and the plot of optimal values of b

Case K1. $b/2 \geq h$ & $l \leq b \leq l+h$ & $h \leq l$

$E[T^1]$ and $E[T^2]$ for this case, can be obtained from chapter 5. Hence, the objective function in this case is

$$E[T_{K1}] = G^{\frac{2s}{1+s}} \left[-\frac{6b^4 - 2h^4 - l^4 - w^4 - 8b^3\left(h + l + w\right) + 6b^2\left(h^2 + l^2 + w^2\right)}{4\left(-2b^3 + h^3 + l^3 + w^3 + 3b^2\left(h + l + w\right) - 3b\left(h^2 + l^2 + w^2\right)\right)} \right]$$
$$+ \left(1 - G^{\frac{2s}{1+s}}\right)\left[-\frac{6b^4 - h^4 - l^4 + 12h^2lw - w^4 + 12hlw\left(l + w\right) - 8b^3\left(h + l + w\right) + 6b^2\left(h^2 + l^2 + w^2\right)}{4\left(-2b^3 + h^3 + l^3 - 6hlw + w^3 + 3b^2\left(h + l + w\right) - 3b\left(h^2 + l^2 + w^2\right)\right)} \right].$$

For case K1 two different situations can be realized,

- Case K1.1. $2h > l$,

- Case K1.2. 2h≤l.

Case K1.1. *2h>l*

According to Theorem 3 it is proven in optimal solution $w^* = l^*$. In addition, the volume of the system is normalized to one and so $hl^2 = 1$. Moreover, based on volume formula of the shape of the first zone in this case we have $G = \dfrac{1}{6}(-2b^3 + h^3 + l^3 + l^3 + 3b^2(h+l+l) - 3b(h^2 + l^2 + l^2))$. Therefore, the objective function can be simplified to a two variable function (h, b) as follows where s is skewness parameter $(0 < s < 1)$,

$$E[T_{K1.1}] = \frac{6^{-\frac{2s}{1+s}}\left(h\left(3b^2 - 3bh + h^2\right)\right)^{\frac{2s}{1+s}}\left(4b^3 - 3b^2h + h^3\right)}{4(6b^2 - 6bh + 2h^2)}\left(\begin{array}{l} 6^{-\frac{2s}{1+s}}\left(-2b^3 + 2\left(\frac{1}{h}\right)^{3/2} + h^3 + 3b^2\left(2\sqrt{\frac{1}{h}} + h\right) - \frac{3b\left(2+h^3\right)}{h}\right)^{\frac{-1+s}{1+s}} \\ \left(-6b^4 + 8b^3\left(2\sqrt{\frac{1}{h}} + h\right) - \frac{6b^2\left(2+h^3\right)}{h} + 2\left(\frac{1}{h^2} + h^4\right)\right) \\ \left(6b^4 + 24\sqrt{\frac{1}{h}} - \frac{2}{h^2} + 12h - h^4 - 8b^3\left(2\sqrt{\frac{1}{h}} + h\right) + \frac{6b^2\left(2+h^3\right)}{h}\right) \\ - \frac{\left(1 - 6^{-\frac{2s}{1+s}}\left(-2b^3 + 2\left(\frac{1}{h}\right)^{3/2} + h^3 + 3b^2\left(2\sqrt{\frac{1}{h}} + h\right) - \frac{3b\left(2+h^3\right)}{h}\right)^{\frac{2s}{1+s}}\right)}{-6 - 2b^3 + 2\left(\frac{1}{h}\right)^{3/2} + h^3 + 3b^2\left(2\sqrt{\frac{1}{h}} + h\right) - \frac{3b\left(2+h^3\right)}{h}} \end{array} \right).$$

We show that $E[RT_{K1.1}]$ is an increasing function of b and therefore the optimal value of b is at its minimum value. We assume $h = db$ and solve the two following equations to obtain the optimal values of d and b.

$$\frac{dE[T_{K1.1}]}{db} = 0 \text{ and } \frac{dE[T_{K1.1}]}{dd} = 0 \quad \forall 0 < s \leq 1$$

It turns out $d^* > 0.5$, $\forall 0 < s \leq 1$ and so $d^* = 0.5$. Therefore, h can be replaced by b and so $E[T_{K1.1}]$ can be written as only one variable function as follows,

$$E[T_{K1.1}(b)] = \frac{1}{4}(2304^{-\frac{s}{1+s}}(-96 + \frac{48\sqrt{2}}{(\frac{1}{b})^{3/2}} + 32\sqrt{2}(\frac{1}{b})^{3/2} - 9b^3)^{\frac{-1+s}{1+s}}(\frac{128\sqrt{2}}{(\frac{1}{b})^{5/2}} + \frac{64}{b^2} - 192b - 27b^4)$$

$$- \frac{2^{-1-\frac{2s}{1+s}}9^{\frac{s}{1+s}}(128(-1 - \frac{2\sqrt{2}}{(\frac{1}{b})^{9/2}} + \frac{3\sqrt{2}}{(\frac{1}{b})^{3/2}}) + 480b^3 + 55b^6)(36^{\frac{s}{1+s}} - (-12 + \frac{6\sqrt{2}}{(\frac{1}{b})^{3/2}} + 4\sqrt{2}(\frac{1}{b})^{3/2} - \frac{9b^3}{8})^{\frac{2s}{1+s}})}{b(-144b - 9b^4 + 16\sqrt{2}\sqrt{\frac{1}{b}}(2 + 3b^3))})$$

By taking derivative of above equation over b the optimal boundary $b^*(s)$ can be obtained. Solving the derivative of above equation results in $b^*(s)$ which is an increasing function of s. Therefore, $h^*(s) = b^*(s)/2$ is also an increasing function of s and $l^*(s)$ will subsequently be a decreasing function of s. Since the condition of case K1.1 is $l > 2h$ we have to obtain an s_1^* where $l = 2h$. s_1^* can be obtained by solving the derivative of above equation at $b = l = 2h = 1.25992$ which results in $s_1^* = 0.275732$. For $s_1^* < s$, $l^* = b^* = 1.25992$ and $h^* = 0.62996$.

For $s \leq s_1^*$, $b^*(s) = 2h^*(s)$ which can be obtained for any given s by solving the derivative of above equation. The optimal boundary as a function of s can be obtained by fitting the function $b^*(s) = a\,\text{ArcTan}[cs + d] + e$ to optimal values of boundary b for different s. The estimate, standard error, t-statistic, and P-value of each parameter are given in Table 6.11.

Table 6.11. Parameter estimate of function $b^*(s)$

parameter	Estimate	Standard error	t-statistic	P-value
a	39587.7	31.8	1241.9	< .0001
c	18516.9	184.1	100.5	< .0001
d	22176.5	44.1	502.2	< .0001
e	-62181.4	50.0	-1242.0	< .0001

Figure 6.10 shows the plotted optimal values of b for 1000 different s and corresponding fitted function.
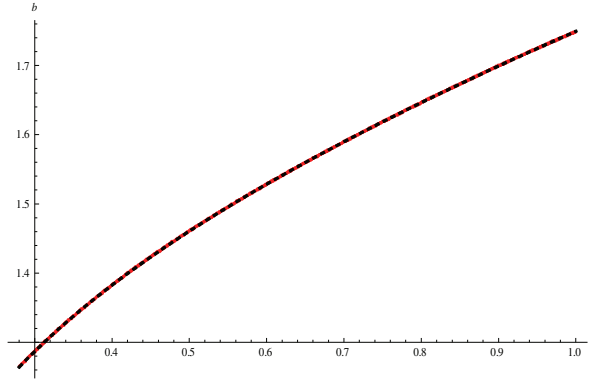
Figure 6.10. Fitted function $b^*(s)$ and the plot of optimal values of b

Case K1.2. 2h<l

According to Theorem 3 it is proven in optimal solution $w^*=l^*$. In addition, the volume of the system is normalized to one and so $hl^2 = 1$. Moreover, based on volume formula of the shape of the first zone in this case we have $G = \dfrac{1}{6}(-2b^3 + h^3 + l^3 + l^3 + 3b^2(h+l+l) - 3b(h^2 + l^2 + l^2))$. Therefore, the objective function can be simplified to a two variable function (l, b) as follows where s is skewness parameter $(0<s<1)$.

$$E[T_{K1.2}] = \frac{1}{4}\left(\begin{array}{c} 6^{-\frac{2s}{1+s}}\left(-2b^3 + \frac{1}{l^6} + 2l^3 + 3b^2\left(\frac{1}{l^2}+2l\right) - 3b\left(\frac{1}{l^4}+2l^2\right)\right)^{\frac{-1+s}{1+s}}\left(-6b^4 + 8b^3\left(\frac{1}{l^2}+2l\right) - 6b^2\left(\frac{1}{l^4}+2l^2\right) + 2\left(\frac{1}{l^8}+l^4\right)\right) \\ -\dfrac{\left(6b^4 - \frac{1}{l^8} + \frac{12}{l^2} + 24l - 2l^4 - 8b^3\left(\frac{1}{l^2}+2l\right) + 6b^2\left(\frac{1}{l^4}+2l^2\right)\right)\left(1 - 6^{-\frac{2s}{1+s}}\left(-2b^3 + \frac{1}{l^6} + 2l^3 + 3b^2\left(\frac{1}{l^2}+2l\right) - 3b\left(\frac{1}{l^4}+2l^2\right)\right)^{\frac{2s}{1+s}}\right)}{-6 - 2b^3 + \frac{1}{l^6} + 2l^3 + 3b^2\left(\frac{1}{l^2}+2l\right) - 3b\left(\frac{1}{l^4}+2l^2\right)} \end{array}\right).$$

According to the condition of case K1.2 it can be shown that $1.25992 \le l \le 1.68665$. By solving the following equation l^* and b^* can be obtained. However, it turns out that the optimal value of l is always less than its minimum possible value and therefore $l^* = 1.25992$, $\forall 0 < s \le 1$. Therefore, l can be replaced by its optimal value at above equation and so $E[T_{K1.2}]$ can be written as only one variable function as follows,

$$\frac{dE[T_{K1.2}]}{db} = 0 \text{ and } \frac{dE[T_{K1.2}]}{dl} = 0 \quad \forall 0 < s \leq 1.$$

$$E[T_{K1.2}(b)] = \frac{1}{4}\Big(576^{-\frac{s}{1+s}}\big(17 - 272^{2/3}b + 302^{1/3}b^2 - 8b^3\big)^{\frac{-1+s}{1+s}}\big(172^{1/3} - 542^{2/3}b^2 + 802^{1/3}b^3 - 24b^4\big)$$

$$+ \frac{4\left(\dfrac{207}{42^{2/3}} + \dfrac{27b^2}{2^{1/3}} - 202^{1/3}b^3 + 6b^4\right)\left(1 - 576^{-\frac{s}{1+s}}\big(17 - 272^{2/3}b + 302^{1/3}b^2 - 8b^3\big)^{\frac{2s}{1+s}}\right)}{7 + 272^{2/3}b - 302^{1/3}b^2 + 8b^3}\Big).$$

By taking derivative of above equation over b the optimal boundary $b^*(s)$ can be obtained,

$$\frac{dE[T_{K1.2}]}{db} = 0.$$

Solving the above equation for $s < s_1^*$ results in $b^* < l^*$ while according to conditions of case K1.2 $b \geq l$.

s_1^* can be obtained by solving the above equation at $b = 1.25992$ which leads to $s_1^* = 0.663535$. Therefore

for $s < s_1^*$, $b^* = l^* = 2h^* = 1.25992$. For $s \geq s_1^*$, $b^*(s)$ can be obtained for any given s by solving Equation

(31). The optimal boundary as a function of s can be obtained by fitting the function

$b^*(s) = a\,\mathrm{ArcTan}[cs + d] + e$ to optimal values of boundary b for different s. The estimate, standard error,

t-statistic, and P-value of each parameter are given in Table 6.12.

Table 6.12. Parameter estimates of function $b^*(s)$

parameter	Estimate	Standard error	t-statistic	P-value
a	19.2377	150.019	0.128235	< .0001
c	63.4077	494.269	0.128286	< .0001
d	19.4080	151.508	0.128099	< .0001
e	-28.6456	235.649	-0.121561	< .0001

Figure 6.11 shows the plotted optimal values of b for 1000 different s and corresponding fitted function.
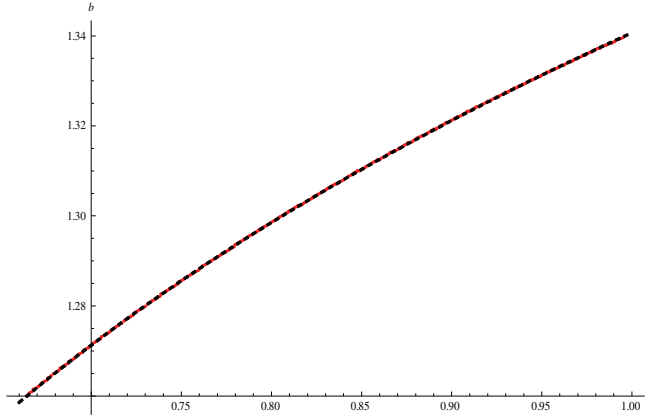
Figure 6.11. Fitted function $b^*(s)$ and the plot of optimal values of b

Case O1. $b/2 \geq h$ & $l+h \leq b \leq 2l$ & $h \leq l$

$E[T^1]$ and $E[T^2]$ for this case, can be obtained from chapter 5. Hence, the objective function in this case is

$$E[T_{O1}] = G^{\frac{2s}{1+s}} \left[\frac{4b^3 + 2h^2(l+w) + 3h(l^2 + w^2) + 2(l^3 + w^3) - 3b^2(h + 2(l+w))}{2(3b^2 + h^2 + 3h(l+w) + 3(l^2 + w^2) - 3b(h + 2(l+w)))} \right]$$

$$+ \left(1 - G^{\frac{2s}{1+s}}\right) \left[\frac{8b^3 + h^3 + 4h^2(l+w) + 6h(l+w)^2 + 4(l+w)^3 - 6b^2(h + 2(l+w))}{4(3b^2 + h^2 + 3h(l+w) + 3(l+w)^2 - 3b(h + 2(l+w)))} \right].$$

However, according to Theorem 3 it is proven in optimal solution $w^* = l^*$. In addition, the volume of the system is normalized to one and so $hl^2 = 1$. Moreover, based on volume formula of the shape of the first zone in this case we have $G = \frac{1}{6}(-2b^3 + h^3 + l^3 + l^3 + 3b^2(h + l + l) - 3b(h^2 + l^2 + l^2))$. Therefore, the objective function can be simplified to a two variable function (l, b) as follows where s is skewness parameter ($0 < s \leq 1$).

$$E[T_{O1}] = \frac{1}{4}\left(\frac{2^{1-\frac{2s}{1+s}}9^{-\frac{s}{1+s}}\left(6 + (-b+2l)^3 - (-b+\frac{1}{l^2}+2l)^3\right)^{\frac{2s}{1+s}}\left(6 + 4b^3 + \frac{4}{l^3} + 4l^3 - 3b^2(\frac{1}{l^2}+4l)\right)}{3b^2 + \frac{1}{l^4} + \frac{6}{l} + 6l^2 - 3b(\frac{1}{l^2}+4l)} \right.$$

$$\left. + \frac{(24 + 8b^3 + \frac{1}{l^6} + \frac{8}{l^3} + 32l^3 - 6b^2(\frac{1}{l^2}+4l))(1 - 6^{-\frac{2s}{1+s}}\left(6 + (-b+2l)^3 - (-b+\frac{1}{l^2}+2l)^3\right)^{\frac{2s}{1+s}})}{3b^2 + \frac{1}{l^4} + \frac{6}{l} + 12l^2 - 3b(\frac{1}{l^2}+4l)} \right).$$

We show that $E[T_{O1}]$ can be optimized for any given s if $b^* = l + h$ by solving the following equation,

$$\frac{dE[T_{O1}]}{db} = 0 \text{ and } \frac{dE[T_{O1}]}{dl} = 0 \qquad \forall 0 < s < 1.$$

Therefore b can be replaced by $l + h$ ($h = 1/l^2$) and so $E[T_{O1}]$ can be written as only one variable function as follows,

$$E[T_{O1}(l)] = (4^{-1-\frac{s}{1+s}}9^{-\frac{s}{1+s}}\left| \frac{2\left(3 - \frac{1}{l^6} + \frac{3}{l^3}\right)^{\frac{2s}{1+s}}\left(-1 + 2l^3 + 9l^6 + 4l^9\right)}{-1 + 3l^3 + 3l^6} + \frac{\left(36^{\frac{s}{1+s}} - \left(3 - \frac{1}{l^6} + \frac{3}{l^3}\right)^{\frac{2s}{1+s}}\right)\left(3 - 4l^3 - 6l^6 + 16l^9\right)}{1 - 3l^3 + 3l^6} \right|) / l^2.$$

By taking derivative of above equation over l the optimal boundary $l^*(s)$ can be obtained,

$$\frac{dE[T_{O1}]}{dl} = 0 .$$

The optimal length as a function of s can be obtained by fitting the function $l^*(s) = a\text{ArcTan}[cs+d]+e$ to optimal values of l for different s. The estimate, standard error, t-statistic, and P-value of each parameter are given in Table 6.13.

Table 6.13. Parameter estimates of function $l^*(s)$

parameter	Estimate	Standard error	t-statistic	P-value
a	0.833	0.002	335.5	< .0001
c	-10.333	0.028	-357.5	< .0001
d	-2.965	0.009	-316.2	< .0001
e	2.315	0.003	594.8	< .0001

Figure 6.12 shows the plotted optimal values of l for 1000 different s and corresponding fitted function.
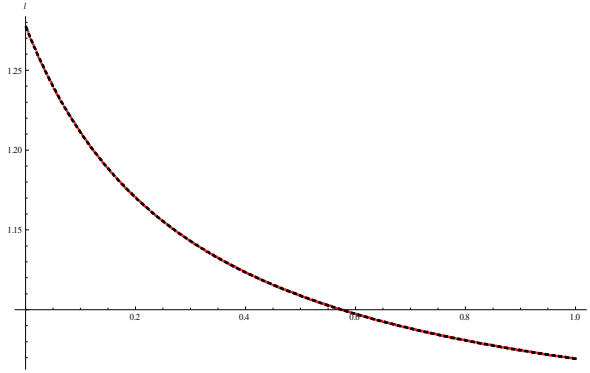

Figure 6.12. Fitted function $l^*(s)$ and the plot of optimal values of l

Case P1. $2l \leq b \leq 2l + h$ **&** $h \leq l$

$E[T^1]$ and $E[T^2]$ for this case, can be obtained from chapter 5. Hence, the objective function in this case is

$$E[T_{P_1}] = G^{\frac{2s}{1+s}} \left[-\frac{3b^4 - 4h^3(l+w) - (l+w)^4 - 8b^3(h+l+w) + 6b^2(h+l+w)^2 - 6h^2(l^2+w^2) - 4h(l^3+w^3)}{4\left(-b^3 + h^3 + 3h^2(l+w) + (l+w)^3 + 3b^2(h+l+w) - 3b(h+l+w)^2 + 3h(l^2+w^2)\right)} \right]$$
$$+ \left(1 - G^{\frac{2s}{1+s}}\right)\left(\frac{1}{4}(3b+h+l+w)\right).$$

However, according to Theorem 3 it is proven in optimal solution $w^*=l^*$. In addition, the volume of the system is normalized to one and so $hl^2 = 1$. Moreover, based on volume formula of the shape of the first zone in this case we have $G = hlw - \frac{1}{6}(-b+h+l+w)^3$. Therefore, the objective function can be simplified to a two variable function (l, b) as follows where s is skewness parameter ($0<s<1$),

$$E[T_{P_1}] = \frac{1}{4}\left[-\frac{\left(1 - \frac{1}{6}\left(-b+\frac{1}{l^2}+2l\right)^3\right)^{\frac{2s}{1+s}}\left(3b^4 - 8b^3\left(\frac{1}{l^2}+2l\right) + 6b^2\left(\frac{1}{l^2}+2l\right)^2 - 4l\left(2+\frac{2}{l^6}+\frac{3}{l^3}+4l^3\right)\right)}{6 - b^3 + \frac{1}{l^6} + \frac{6}{l^3} + 8l^3 + 3b^2\left(\frac{1}{l^2}+2l\right) - 3b\left(\frac{1}{l^2}+2l\right)^2} \right.$$
$$\left. + \left(3b+\frac{1}{l^2}+2l\right)\left(1 - \left(1 - \frac{1}{6}\left(-b+\frac{1}{l^2}+2l\right)^3\right)^{\frac{2s}{1+s}}\right) \right].$$

We show that $E[T_{P1}]$ can be optimized for any given s if $b^* = 2l$ by solving the following equation,

$$\frac{dE[T_{P1}]}{db} = 0 \text{ and } \frac{dE[T_{P1}]}{dl} = 0 \qquad \forall 0 < s \leq 1.$$

Therefore, b can be replaced by $2l$ and so $E[T_{P1}]$ can be written as only one variable function as follows,

$$E[T_{P1}(l)] = \frac{-1 + \left(1 - \frac{1}{6l^6}\right)^{\frac{2s}{1+s}} - 8l^3 + 6\left(1 + \left(1 - \frac{1}{6l^6}\right)^{\frac{2s}{1+s}}\right)l^6 - 24\left(-2 + \left(1 - \frac{1}{6l^6}\right)^{\frac{2s}{1+s}}\right)l^9}{4l^2\left(-1 + 6l^6\right)}.$$

By taking derivative of above equation over l the optimal boundary $l^*(s)$ can be obtained,

$$\frac{dE[RT_{P1}]}{dl} = \frac{1}{2l^3\left(1 - 6l^6\right)^2\left(1 + s\right)} \left(\begin{array}{c} -1 + \left(1 - \frac{1}{6l^6}\right)^{\frac{2s}{1+s}} + \left(-1 + 7\left(1 - \frac{1}{6l^6}\right)^{\frac{2s}{1+s}}\right)s \\ +4l^3\left(1 + s\right) - 36\left(1 + \left(1 - \frac{1}{6l^6}\right)^{\frac{2s}{1+s}}\right)l^{12}\left(1 + s\right) \\ -72\left(-2 + \left(1 - \frac{1}{6l^6}\right)^{\frac{2s}{1+s}}\right)l^{15}\left(1 + s\right) + 12l^6\left(1 - 3\left(1 - \frac{1}{6l^6}\right)^{\frac{2s}{1+s}} + s\right) \\ -12l^9\left(4 - 7\left(1 - \frac{1}{6l^6}\right)^{\frac{2s}{1+s}} + \left(4 + 5\left(1 - \frac{1}{6l^6}\right)^{\frac{2s}{1+s}}\right)s\right) \end{array} \right) = 0.$$

Solving the above equation for $s < s_1^*$ results in $l^* < h^*$ while according to conditions of case P1 $l \geq h$. s_1^* can be obtained by solving the above equation at $l = h = 1$ which leads to $s_1^* = 0.278079$. Therefore for $s < s_1^*$, $l^* = h^* = 1$ and $b^* = 2$. For $s \geq s_1^*$, $l^*(s)$ can be obtained for any given s by solving the above equation. The optimal length as a function of s can be obtained by fitting the function $l^*\left(s\right) = a\text{ArcTan}[cs + d] + e$ to optimal values of l for different s. The estimate, standard error, t-statistic, and P-value of each parameter are given in Table 6.14.

Table 6.14. Parameter estimates of function $l^*(s)$

parameter	Estimate	Standard error	t-statistic	P-value
a	3932.9	1.141	3444.8	< .0001
c	32245.0	3.284	9818.3	< .0001

d	17556.2	5.149	3409.2	< .0001
e	-6176.6	1.793	-3444.2	< .0001

Figure 6.13 shows the plotted optimal values of l for 1000 different s and corresponding fitted function.
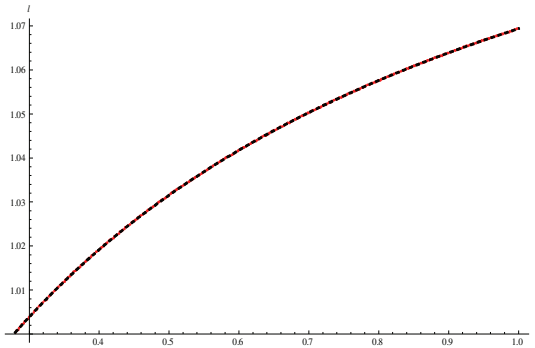

Figure 6.13. Fitted function $l^*(s)$ and the plot of optimal values of l

Appendix 6H. Optimization of case A1 for $s > s^*$

The following is the function of expected retrieval time for this case,

$$E[T_{A1}](l,b) = \frac{1}{4}\left(\left(\frac{7}{16}\right)^{\frac{2s}{1+s}} 3^{1-\frac{2s}{1+s}} b\left(b^3\right)^{\frac{2s}{1+s}} + \frac{\left(1 - \left(\frac{7}{48}\right)^{\frac{2s}{1+s}}\left(b^3\right)^{\frac{2s}{1+s}}\right)\left(21b^4 - \frac{8\left(12 + \frac{1}{l^6} + 24l^3\right)}{l^2}\right)}{-48 + 7b^3}\right).$$

Assuming $l = d\,b$, the theorem can be proven if the optimal $d^* = 1$. Substituting $l = d\,w$ into above equation we obtain the following equation,

$$E[T_{A1}](b,d) = \frac{1}{4}\left(\left(\frac{7}{16}\right)^{\frac{2s}{1+s}} 3^{1-\frac{2s}{1+s}} b\left(b^3\right)^{\frac{2s}{1+s}} + \frac{\left(1 - \left(\frac{7}{48}\right)^{\frac{2s}{1+s}}\left(b^3\right)^{\frac{2s}{1+s}}\right)\left(21b^4 - \frac{8}{b^8 d^8} - \frac{96}{b^2 d^2} - 192bd\right)}{-48 + 7b^3}\right).$$

In order to find the optimal value of d which minimizes the objective function we have to solve the following equation,

$$\frac{dE[T_{A1}]}{dd} = \frac{16(-1+(\frac{7}{48})^{\frac{2s}{1+s}}(b^3)^{\frac{2s}{1+s}})(-1-3b^6d^6+3b^9d^9)}{b^8(-48+7b^3)d^9} = 0.$$

However, since $0<b<l$ none of the optimal values of d satisfies the condition $d \geq 1$. Hence, the optimal value of d places at the boundary if the objective function is a monotonically increasing function of d.

Since, $\frac{dE[T_{A1}]}{dd} \geq 0 \ \ \forall 0 < b \leq l, \ d \geq 1, \ s > s^*$, the optimal d which minimizes the objective function locates at $d^* = 1$. So, $l^* = b^*$ and the proof is complete. □

Since $l^* = b^*$, now we can replace b with l. Thus, the objective function can be written as a function of l,

$$E[T_{A1}](l) = \frac{1}{4}\left(\left(\frac{7}{16}\right)^{\frac{2s}{1+s}} 3^{1-\frac{2s}{1+s}} l \left(l^3\right)^{\frac{2s}{1+s}} + \frac{\left(1-\left(\frac{7}{48}\right)^{\frac{2s}{1+s}}\left(l^3\right)^{\frac{2s}{1+s}}\right)\left(21l^4 - \frac{8\left(12+\frac{1}{l^6}+24l^3\right)}{l^2}\right)}{-48+7l^3}\right).$$

We can obtain the optimal value of l, which minimizes the objective function by solving the first derivative of objective function over l,

$$\frac{dE[T_{A1}]}{dl} = \frac{1}{4}\left(\left(\frac{7}{16}\right)^{\frac{2s}{1+s}} 3^{1-\frac{2s}{1+s}}\left(l^3\right)^{\frac{2s}{1+s}} + \frac{21(-8-96l^6-192l^9+21l^{12})(-1+(\frac{7}{48})^{\frac{2s}{1+s}}(l^3)^{\frac{2s}{1+s}})}{l^6(48-7l^3)^2}\right.$$
$$-\frac{4(16+48l^6-48l^9+21l^{12})(-1+(\frac{7}{48})^{\frac{2s}{1+s}}(l^3)^{\frac{2s}{1+s}})}{l^9(-48+7l^3)}$$
$$\left.+\frac{2^{1-\frac{8s}{1+s}}9^{\frac{1}{1+s}}49^{\frac{s}{1+s}}(l^3)^{\frac{2s}{1+s}}s}{1+s} - \frac{2^{1-\frac{8s}{1+s}}3^{1-\frac{2s}{1+s}}49^{\frac{s}{1+s}}(l^3)^{\frac{2s}{1+s}}(-8-96l^6-192l^9+21l^{12})s}{l^9(-48+7l^3)(1+s)}\right) = 0.$$
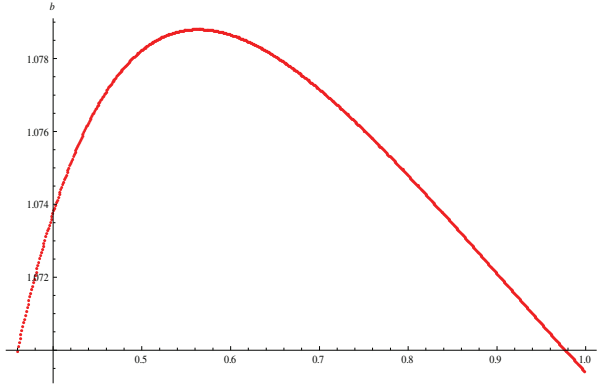
Figure 6.14. Plot of optimal values of b for $s > s^*$

For example for ABC curve 20%/50%, the optimal values of length and boundary will be as follows,

$l^* = b^* = 1.07574$.

Since l^* is the only obtained critical point it suffices to compare the objective value for l^* with any l to make sure l^* is the absolute minimum.

The following equation gives the optimal values of h,

$h^* = 0.86414$.

We have to check whether the optimal values h, l satisfy the condition $0 < h \leq l$. By comparing the values of dimensions, we observe that the condition holds.

Appendix 6I. Set of sub-case possible for any given configuration of the system

Config.1	Sub-config.	Sub-config.	Boundary	Sub-case
$h \leq w$	$w \leq 2h$	$l \leq 2h$	$b \leq w$	A1
			$w \leq b \leq l$	B1
			$l \leq b \leq 2h$	C1
			$2h \leq b \leq w+h$	K1
			$w+h \leq b \leq l+h$	M1
			$l+h \leq b \leq l+w$	O1
			$l+w \leq b \leq l+w+h$	P1
		$2h \leq l \leq w+h$	$b \leq w$	A1

Config.2	Sub-config.	Sub-config.	Boundary	Sub-case
$w \leq h \leq l$	$l+w \geq 2h$	$l \leq 2w$	$b \leq w$	A2
			$w \leq b \leq l$	B2
			$l \leq b \leq 2w$	C2
			$2w \leq b \leq 2h$	E2
			$2h \leq b \leq l+w$	M2
			$l+w \leq b \leq l+h$	N2
			$l+h \leq b \leq l+w+h$	P2
		$2w \leq l \leq 2h$	$b \leq w$	A2

		$w \le b \le 2h$	B1
		$2h \le b \le l$	J1
		$l \le b \le w+h$	K1
		$w+h \le b \le l+h$	M1
		$l+h \le b \le l+w$	O1
		$l+w \le b \le l+w+h$	P1
		$b \le w$	A1
		$w \le b \le 2h$	B1
		$2h \le b \le w+h$	J1
	$w+h \le l \le l+h$	$w+h \le b \le l$	L1
		$l \le b \le l+h$	M1
		$l+h \le b \le l+w$	O1
		$l+w \le b \le l+w+h$	P1
		$b \le 2h$	A1
		$2h \le b \le w$	I1
		$w \le b \le l$	J1
	$2h \le l \le w+h$	$l \le b \le w+h$	K1
		$w+h \le b \le l+h$	M1
		$l+h \le b \le l+w$	O1
		$l+w \le b \le l+w+h$	P1
$w \ge 2h$		$b \le 2h$	A1
		$2h \le b \le w$	I1
		$w \le b \le w+h$	J1
	$w+h \le l \le l+h$	$w+h \le b \le l$	L1
		$l \le b \le l+h$	M1
		$l+h \le b \le l+w$	O1
		$l+w \le b \le l+w+h$	P1

		$w \le b \le 2w$	B2
		$2w \le b \le l$	D2
		$l \le b \le 2h$	E2
		$2h \le b \le l+w$	M2
		$l+w \le b \le l+h$	N2
		$l+h \le b \le l+w+h$	P2
		$b \le w$	A2
		$w \le b \le 2w$	B2
		$2w \le b \le 2h$	D2
	$2h \le l \le l+w$	$2h \le b \le l$	L2
		$l \le b \le l+w$	M2
		$l+w \le b \le l+h$	N2
		$l+h \le b \le l+w+h$	P2
		$b \le w$	A2
		$w \le b \le l$	B2
		$l \le b \le 2w$	C2
	$l \le 2w$	$2w \le b \le l+w$	E2
		$l+w \le b \le 2h$	F2
		$2h \le b \le l+h$	N2
		$l+h \le b \le l+w+h$	P2
$l+w \le 2h$		$b \le w$	A2
		$w \le b \le 2w$	B2
		$2w \le b \le l$	D2
	$2w \le l \le l+w$	$l \le b \le l+w$	E2
		$l+w \le b \le 2h$	F2
		$2h \le b \le l+h$	N2
		$l+h \le b \le l+w+h$	P2

Config.3	Sub-config	Boundary	Sub-case
$l \le h \le l+w$	$l \le 2w$	$b \le w$	A3
		$w \le b \le l$	B3
		$l \le b \le 2w$	C3
		$2w \le b \le l+w$	E3

Config.4	Sub-config	Boundary	Sub-case
$l+w \le h$	$l \le 2w$	$b \le w$	A4
		$w \le b \le l$	B4
		$l \le b \le 2w$	C4
		$2w \le b \le l+w$	E4

		$l+w{\le}b{\le}2l$	F3
		$2l{\le}b{\le}2h$	G3
		$2h{\le}b{\le}l+w+h$	P3
		$b{\le}w$	A3
		$w{\le}b{\le}2w$	B3
		$2w{\le}b{\le}l$	D3
	$l{\ge}2w$	$l{\le}b{\le}l+w$	E3
		$l+w{\le}b{\le}2l$	F3
		$2l{\le}b{\le}2h$	G3
		$2h{\le}b{\le}l+w+h$	P3

		$l+w{\le}b{\le}2l$	F4
		$2l{\le}b{\le}2(l+w)$	G4
		$2(l+w){\le}b{\le}2h$	H4
		$b{\le}w$	A4
		$w{\le}b{\le}2w$	B4
		$2w{\le}b{\le}l$	D4
	$l{\ge}2w$	$l{\le}b{\le}l+w$	E4
		$l+w{\le}b{\le}2l$	F4
		$2l{\le}b{\le}2(l+w)$	G4
		$2(l+w){\le}b{\le}2h$	H4

Chapter 7

Summary and Conclusion

7.1. Summary

Compact storage systems are becoming increasingly popular in practice, as they require a smaller space and less land. One of the key performance measures for such systems, which is also the focus of this study, is response time. Response time of such systems is often measured by the total or average retrieval time of items required for customer orders. In this thesis, we study these systems at two decision-making levels. At the tactical (design) decision level, we focus on the rack-dimensioning problem aiming at short response times. At the operational decision level, we investigate storage assignment and retrieval sequencing problems to shorten the response time.

   In chapter 2, we study the impact of storage policies on the configuration of storage systems. Until now, literature commonly studies the joint impact of the type of storage policy and the system configuration on the average response time. For this purpose, in order to minimize the average response time, the variables representing the system configuration and the storage policy have been considered in one optimization model (Hausman et al., 1976, Yu and De Koster, 2009a). In this chapter, we show that the optimal configuration of a storage system, which minimizes the response time, is independent of the storage policy used. The results of this chapter help the warehouse managers to design optimal storage systems under any storage policy. For any storage policy, a storage system with the minimum average response time can be designed in two consecutive steps. First, the optimal configuration of the system can

be obtained under the assumption of random storage. Second, the optimal values of variables representing the storage policy can be obtained.

In chapter 3, we study temporary storage of fresh produce in a cross-dock center which uses a satellite-based compact storage system. Dedicated storage is commonly used in practice in order to avoid reshuffling. This policy requires additional storage lanes leading to longer response times. This chapter proposes a lane-sharing storage policy aiming at shorter response times. Shared storage is here defined as a storage policy which simultaneously accommodates different products in a multi-deep lane. In order to solve real-size problems a C&I heuristic, based on a greedy construction and an improvement part, is proposed which provides near optimal solutions. Our C&I heuristic results in storage assignment solutions which are virtually insensitive to disturbances in outbound truck schedules. Only when the available information is very uncertain, dedicated storage might result in shorter response times. Warehouse managers often prefer to use dedicated storage in a compact cross-dock system fearing reshuffles imposed by the shared storage. Our chapter shows that the proposed C&I heuristic results in a shared storage policy which generally outperforms dedicated storage even if the available information is uncertain.

Chapters 4, 5, and 6 study live-cube compact storage systems storing and handling unit loads. On each level, shuttles move loads in x- and y- directions and a lift transfer loads across different levels in z-direction. One of the most important performance measures for such systems is the response time.

In chapter 4, we study a live-cube compact storage system where random storage is used and multiple empty locations are available on each level enabling the system to create virtual aisles for any retrieval request. We evaluate the performance using analytical models. First, in order to compare the performance of systems with different configurations, we derive closed-form formulas for the expected retrieval time of an arbitrary unit load. Although the system needs to be decomposed in several cases and sub-cases, eventually four simple closed-form expressions are obtained corresponding to four complementary configurations. Second, we propose and solve a mixed-integer nonlinear model to optimize system dimensions by minimizing the retrieval time. Even though the procedure of finding the optimal configuration of a live-cube storage system is relatively complex, we can derive closed-form expressions which are simple to apply in practice. In addition, our results show that a live-cube system with capability of creating virtual aisles for any requested load can significantly reduce the response time while high system utilization can yet be achieved. Moreover, a cubic-in-time (CIT) system appears to be optimal when minimizing the maximum response time and very close to optimal when minimizing the average response time. This is an interesting outcome as such a configuration can easily be designed in practice.

Our closed-form solutions can be extended for systems with different configurations. For example, our solution shows that a system with a lift at the middle saves 20% of response time compared to a system with a lift at the corner.

In chapter 5, we study a live-cube compact storage system with two storage classes. Two-Class-based storage saves response time compared to random storage while its implementation in practice is quite straightforward. We derive closed-form formulas to calculate the expected retrieval time of a two-class-based live-cube system for any system configuration and zone boundary. In order to evaluate the quality of these closed-form formulas (obtained using a continuous-space approximation), a Monte Carlo simulation is performed based on a real (discrete) application. The results show that the closed-form formulas approximate the expected retrieval time of a discrete system with high precision; errors are usually less than 2%, and below 4% even in extreme cases. With increasing system capacity, skewness parameter, and first zone size, the approximation becomes more precise. Compared to a simulation approach, closed-form formulas can instantly evaluate the performance of a live-cube system with any given configuration and first zone boundary. The closed-form formulas can be used as a reference for further research on live-cube systems such as optimizing system configurations and first zone boundaries.

Chapter 6 extends the previous chapter by optimizing the first zone boundary and system dimensions resulting in minimum average response time. We propose a mixed-integer nonlinear mathematical model for a two-class-based live-cube system. Decomposition of the system into 36 complementary sub-cases leads to a model with many constraints. Each sub-case represents a configuration of the system and zone boundary. Due to the complexity of the model, we use properties of the optimal solution to simplify the mathematical model. The optimal dimensions of a live-cube system together with the optimal first zone boundary can analytically be obtained for any ABC curve. The results show that in a live-cube compact storage system, an optimal two-class-based storage policy can significantly reduce the response time specifically for practical ABC curves (e.g. 20%/70% ABC curve) compared to a random storage policy. For example, for 20%/70% ABC curve, more than 20% reduction is response times can be obtained. The results show that the optimal solution dimensions of a two-class live-cube system are independent of the ABC curves. In addition, we extend the results in two directions. We optimize the system dimensions and first zone boundary for a system with constraints on the system dimensions. The proposed algorithm can be used in situations where a live-cube system needs to be installed in a warehouse with fixed building dimensions. In addition, the response time of a system with fixed dimensions can be reduced by introducing two-class-based storage and by optimizing the first zone boundary. We propose an algorithm to find the optimal first zone boundary for a live-cube system with a given configuration.

7.2. Future outlook

The research on advanced storage systems and specifically on 3D compact storage systems is still in its infancy. In this section, we highlight some potential research questions and briefly picture the future of operations management models in the area of advanced storage systems.

In chapter 3, several research questions regarding use of shared storage in a fresh produce compact cross-dock remain open. While we study decoupled storage and retrieval, some cross-docks have overlapping storage and retrieval processes. It might also be interesting to consider systems with multiple satellites working simultaneously and systems with higher utilizations. While we have studied satellite-based compact storage systems, results for other compact storage system configurations may also prove worthwhile investigating. The problem studied in this chapter is related to bin packing problem. In a bin packing problem objects of different or the same volume must be packed in a minimum number of bins of capacity V. The unit loads can represent the objects of the same size and the storage lanes can represent the bins. Then the question is how to pack objects of the same volume (i.e. unit loads) into finite number of bins (i.e. storage lanes) in a way that the number of bins is minimized and while reshuffling is avoided. If the satellite in depth direction is significantly faster than the S/R machine in horizontal and vertical directions, then minimizing the number of bins (i.e. storage lanes) is equivalent to minimizing the total retrieval time which is the objective of this study. In addition, our problem can be formulated as a parallel machine scheduling problem. In a parallel machine scheduling problem, n jobs with different processing times have to be assigned to m parallel machines. In our problem, unit loads can represent the jobs and storage lanes can represent the machines. The length of overlap for the time windows of each two unit loads defines the length of the additional setup time for the corresponding jobs if they are assigned to the same machine. It might be worthwhile to investigate the existing literature of bin packing and machine scheduling problems in order to find efficient solution algorithms which can be applied to fresh produce cross-docking problems.

In chapter 4, several research questions regarding the live-cube compact storage system remain open. It is interesting to study the impact on makespan of optimally sequencing a group of retrievals. We know from AS/RS literature that savings can be achieved of 20-70% compared to FCFS sequencing (Han et al., 1987, Yu and De Koster, 2012). As shuttles can move unit loads to the lift on different levels simultaneously, improvements might even be larger for live-cube compact storage systems. While we have studied live-cube compact storage systems with lifts, results for other live-cube compact storage

systems with different vertical movement mechanisms may also prove worthwhile investigating. It might be worthwhile to study the impact of the number of empty locations on the response time of the system. It is possible to study the live-cube compact storage system with other storage policies such as full-turnover storage policy and compare the results with the results obtained here in this study.

In Chapter 5, it might be interesting to derive closed-form expressions for average travel time of a three-class-based storage policy or more. In chapter 6, it may be possible to extend results for a two-class-based storage to a three-class-based storage policy. Unfortunately, due to the complexity of the system, analysis of an n-class-based system appears to be extremely difficult.

Performance objectives and evaluation

Advanced storage systems are designed in order to save labor costs and floor space, increase the reliability and reduce error rates, and shorten the response times. Such systems bring many new managerial challenges. At design phase, the challenges include facility layouts (e.g. number and sizes of storage racks, number of cranes, and the position of the depots) aiming at short response times. At the operational phase, the challenges include how to store and retrieve products from storage racks, and how to sequence storage and retrieval jobs to timely satisfy customers orders.

In particular, in 3D compact storage systems, the depth dimension and the variety of different handling systems that can be used in conjunction with other handling systems (e.g. cranes and order pickers) bring many new research challenges in layout design, planning, control, and human operations management aspects. The performance of such systems is often measured by their response times (e.g. cycle time or make-span). Generally, the response time is a good proxy for other important measures to a company such as cost, service level, etc. In order to minimize the response time, modeling and analysis of compact systems depends on many factors. At operational decision level, these factors (and consequential research problems) are: (1) storage policies (where to store which product in multi-deep racks), (2) sequencing (how to sequence multiple storage and retrieval jobs), (3) dwell point strategy (where to stop a idle crane), (4) interleaving policy (how to combine storage jobs with retrieval jobs to reduce the job handling time), (5) combined scheduling (how to schedule machines, order pickers, and depth movement mechanisms simultaneously). At design decision level, the factors include (1) the type of material handling storage systems used (2) the depth movement handling system in warehouses, (3) the dimensions of the multi-deep racks (4) the number and the position of I/O points, (5) the number of cranes, racks/stacks, and their layout in a compact storage facility.

From a methodology point of view, multiple challenges exist in analyzing compact storage systems. First, how to calculate the mean values and variances of the travel time per storage/retrieval job of the crane and the depth movement mechanisms, using different storage and interleaving policies. It is most likely necessary to develop probability distribution functions for the travel time, using probabilistic properties of storage and retrieval load positions. These expressions are situation-dependent and can be used as objectives in optimizing system layout. Second, how to calculate the mean values and variances of order throughput time when orders arrive online. Such an online system can be modeled as a queuing network. Queuing models enable the analysis of such networks. Third, how to sequence the storage and retrieval jobs, and carry them out by scheduling cranes, the depth movement mechanisms, and order pickers. As multiple movements are involved to transport a unit-load in a multi-deep storage facility, the transport time of jobs is sequence dependent, which implies more complex modeling. Fourth, how to check whether theoretical formulations approximately represent real-life systems and improve on them. In order to check the practical applicability of the findings it is required to compare the performance and design approximations with real-life systems, using simulation. Finally, from a more practical perspective, how to compare these systems with traditional storage systems in terms of investment and operational costs, energy consumption and CO_2 emissions, etc.

We now discuss some points of concern regarding automation in material handling systems and the potential impacts on society.

7.3. Impacts on society

Advances in material handling systems help firms to be faster in storing and retrieving items in their warehouses and distribution centers while saving land and space. However, some concerns have always been in the discussions on automation in material handling systems (Business, 2011):

1. The need for more energy efficient and greener material handling systems.
2. The impacts of material handling innovations on the labor force.

Energy and sustainability

Sustainability has been a major concern for the companies in recent years. In the material handling industry, not only are manufacturers changing the internal processes in order to reduce the CO_2 emissions and energy consumption, they are also trying to integrate the concept into the design of material handling systems, enabling warehouses to achieve their own sustainability goals (Tucker, 2011).

Sustainability regulations as an external drive imposed by the governments have moved companies toward CO2 reduction solutions and at the same time performance improvement. In addition, increasing energy costs have driven companies to reduce energy consumption and consequently CO2 emission. Therefore, material handling users are seeking for solutions and systems which can help them to improve their performance and reduce energy costs. Energy consumption is an attractive measure to material handling system users. Reducing energy consumption obviously reduces the operational costs. In addition, a more energy efficient warehouse implies less CO2 emission. Next generation storage systems contribute to a greener environment in two respects. These systems occupy less land and space. This is specifically important to refrigerated distribution centers and freezers as the larger storage space leads to higher energy consumption (see e.g. chapter 3). In addition, such systems are fully automated and the system components are very energy efficient. For instance, as it is shown in chapter 5, live-cube storage systems can reduce the energy consumption and CO2 emission compared to traditional systems significantly. As there are various factors contributing to CO2 emission of warehouses, it might be interesting to study the impact of advanced storage systems on environment. This can be done by using analytical methods including life cycle analysis and empirical methods.

Impacts on labor force

US economy now produces almost more goods and services than it did before the downturn officially began in late 2007. However, this has been done with five million fewer jobs (Rampell, 2012). Apparently, companies have found more productive and faster ways to achieve the same performance mainly by employing higher level of automation in their processes (Modern material handling, 2012). Further automation and technology in material handling systems can help companies to improve their productivity. However, more automation implies fewer jobs. Those jobs that were lost in the economic downturn in distribution centers may not come back and they are going to be replaced by automation. For example, a global clothing retailer and manufacturer was forced to reduce a third of its pickers when its distribution center decided to install an automated order fulfillment system (Napolitano, 2010). Thus, while advanced storage systems are helping companies to improve their productivity, the impacts of these systems on the labor force have to be taken into account. Some points of concern might be looked at more in depth. For example, what are the advantages and disadvantages of automation on the society and in particular labor force? Does automation always negatively influences the labor force? If yes, what are the solutions to alleviate the consequences?

Bibliography

Ashayeri J., R.M. Heuts, M.W.T. Valkenburg, H.C. Veraart, M.R. Wilhelm. 2002. A geometrical approach to computing expected cycle times for zone based storage layouts in AS/RS. *International Journal of Production Research* 40 (17) 4467-4483.

Automotion Parking Systems. 2011. Park, Swipe, Leave Systems, available online at: http://www.automotionparking.com/index.php

Bartholdi, J.J., K.R. Gue. 2000. Reducing labor costs in an LTL cross-docking terminal. *Operations Research* 48 823-832.

Bartholdi, J.J., K.R. Gue. 2004. The best shape for a cross-dock. *Transportation Science* 38 235-244.

Boysen, N., M. Fliedner. 2010. Cross dock scheduling: Classification, literature review and research agenda. *Omega* 38 413-422.

Bozer, Y.A., J.A. White. 1984. Travel-time models for automated storage/retrieval systems. *IIE Transactions* 16(4) 329-338.

Bozer, Y.A., H. Carlo. 2008. Optimizing inbound and outbound door assignments in less-than-truckload cross-docks. *IIE Transactions* 40 1007-1018.

Bureau of Labor Statistics (BLS) report. 2004. Available online at: http://useconomy.about.com/od/supply/p/Aging_Workers.htm

Business. 2011. Material Handling Equipment News and Trends. Available online at: http://www.business.com/guides/material-handling-equipment-news-and-trends-24848/

Chen, J.F. 2007. A hybrid heuristic for the uncapacited single allocation hub location problem. *Omega* 35 211-220.

Chen, L., A. Langevin, D. Riopel. 2010. The storage location assignment and interleaving problem in an automated storage/retrieval system with shared storage. *International Journal of Production Research* 48(4) 991-1011.

De Koster, M.B.M. 1996. Ontwerp van een eenvoudig magazijn. In: J.P. Duijker et al. (Eds.), *Praktijkboek Magazijnen/Distributiecentra* 3.10A.01-3.10A.20 Deventer: Kluwer.

De Koster, M.B.M, T. Le-Duc, and K.J. Roodbergen. 2007. Design and Control of Warehouse Order Picking: A Literature Review. *European Journal of Operational Research* 182 (2) 481–501.

De Koster, M.B.M, B.M. Balk. 2008. Benchmarking and monitoring international warehouse operations in Europe. *Production and Operations Management* 17(2) 175-183.

De Koster, M.B.M., T. Le-Duc, Y. Yu. 2008. Optimal storage rack design for a 3-dimensional compact AS/RS. *International Journal of Production Research* 46(6) 1495-1514.

Drury, J. 1988. Towards more efficient order picking, IMM Monograph No. 1. *Report*, The Institute of Materials Management, Cranfield, U.K.

Eweco. 2011. Space parking optimization technology (SPOT), available online at: http://www.eweco.eu/spot/ (more videos of SPOT at: http://www.youtube.com/watch?v=eu7pRjI6APM and http://www.youtube.com/watch?v=9P-WOl8fu-M).

Eynan, A., M.J. Rosenblatt (1994) Establishing zones in single-command class-based rectangular AS/RS. *IIE Transactions* 26 (1) 38-46.

EZ-Indus. 2011. UCW container storage system, available online at: http://www.ezindus.com

Fisher, M.L. 1981. The Lagrangian relaxation method for solving integer programming problems. Management Science 27(1) 1-18.

Foley, R.D., S.T. Hackman, B.C. Park. 2004. Back-of-the-envelope miniload throughput bounds and approximations. *IIE Transactions* 36(3) 279-285.

Francis, R.L., F. McGinnis, J.A. White. 1991. *Facility Layout and Location: An Analytical Approach,* 2nd ed., Prentice Hall.

Fukunari, M. and Malmborg, C. J., 2007. An efficient cycle time model for autonomous vehicle storage and retrieval Systems. *International Journal of Production Research* 46(12) 3167-3184.

Garey, M.R., D.S. Johnson. 1979. *Computers and Intractability: A Guide to the Theory of NP-Completeness*, W. H. Freeman.

Goetschalckx, M. and J. Ashayeri. 1989. Classification and design of order picking systems. *Logistics World* 99-106.

Goetschalckx, M., H.D. Ratliff. 1990. Shared storage policies based on the duration stay of unit loads. *Management Science* 36(9) 1120-1132.

Graves, S.C., W.H. Hausman, L.B. Schwarz. 1977. Storage-retrieval interleaving in automatic warehousing systems. *Management Science* 23(9) 935-945.

Gue, K.R. 1999. The effect of trailer scheduling on the layout of freight terminals. *Transportation Science* 33 419-428.

Gue, K.R. 2006. Very high-density storage systems. *IIE Transactions* 38(1) 79-90.

Gue, K.R., B.S. Kim. 2007. Puzzle-based storage systems. *Naval Research Logistics* 54(5), 556-567.

Han, M.H., L.F. McGinnis, J.S. Shieh, J.A. White. 1987. On sequencing retrievals in an automated storage/retrieval system. *IIE Transactions* 19(1) 56-66.

Hausman, W.H., L.B. Schwarz, S.C. Graves. 1976. Optimal storage assignment in automatic warehousing systems. *Management Science* 22(6) 629-638.

Heskett, J.L. 1963. Cube-per-order index – A key to warehouse stock location. *Transport and Distribution Management* 3 27-31.

Hu, Y.H., S.Y. Huang, C. Chen, W.J. Hsu, A.C. Toh, C.K. Loh, T. Song. 2005. Travel time analysis of a new automated storage and retrieval system. *Computers & Operations Research* 32(6) 1515-1544.

Hyundai Elevator Co. Ltd. 2011. Hyundai Integrated Parking System (HIP), available online at: http://hyundaielevator.co.kr/eng/parking/car/automobile.jsp.

Johnson, M.E., M.L. Brandeau. 1996. Stochastic modeling for automated material handling system design and control. *Transportation Science* 30(4) 330–350.

Keserla, A., B.A. Peters. 1994. Analysis of dual-shuttle automated storage/retrieval systems. *Journal of Manufacturing Systems* 13(6) 424-434.

Kim, J., A. Seidmann. 1990. A framework for the exact evaluation of expected cycle times in automated storage systems with full-turnover item allocation and random service requests. *Computers and Industrial Engineering* 18(4) 601-612.

Klose, A., A. Drexl. 2005. Facility location models for distribution system design. *European Journal of Operational Research* 162 4-29.

Kouvelis, P., V. Papanicolaou. 1995. Expected travel time and optimal boundary formulas for a two-class-based automated storage/retrieval system. *International Journal of Production Research* 33(10) 2889-2905.

Kulturel, S., N.E. Ozdemirel, C. Sepil, Z. Bozkurt. 1999. Experimental investigation of shared storage assignment policies in automated storage/ retrieval systems. *IIE Transactions* 31 739-749.

Kuo, P.H., A. Krishnamurthy, C.J. Malmborg. 2007. Design models for unit load storage and retrieval systems using autonomous vehicle technology and resource conserving storage and dwell point policies. *Applied Mathematical Modeling* 31 2332-2346.

Lee, M.K., E.A. Elsayed. 2005. Optimization of warehouse storage capacity under a dedicated storage policy. *International Journal of Production Research*. 43(9) 1785-1805.

Lee, Y.H., J.W. Jung, K.M. Lee. 2006. Vehicle routing scheduling for cross-docking in supply chain. *Computers & Industrial Engineering* 51 247-256.

Lim, A., Z. Miao, B. Rodrigues, Z. Xu. 2005. Transshipment through cross-docks with inventory and time windows. *Naval Research Logistics* 52 724-733.

Malmborg, C.J. 1996. Storage assignment policy tradeoffs. *International Journal of Production Research* 34(2) 363-378.

Malmborg, C.J. 2000. Interleaving models for the analysis of twin shuttle automated storage and retrieval systems. *International Journal of Production Research* 38(18) 4599-4610.

Malmborg, C.J., 2002. Conceptualizing tools for autonomous vehicle storage and retrieval systems. *International Journal of Production Research* 40(8) 1807-1822.

Manicore. 2011. available online at:
 http://www.manicore.com/anglais/missions_a/carbon_inventory.html.

Miao, Z., A. Lim, H. Ma. 2009. Truck dock assignment with operational time constraint within cross-docks. *European Journal of Operational Research* 192 105-115.

Modern material handling. 2012. Available online at: http://www.mmh.com/

Montulet, P., A. Langevin, D. Riopel. 1998. Minimising the peak load: an alternate objective for dedicated storage policies. *International Journal of Production Research* 36(5) 1369-1385.

Munkres, J. 1957. Algorithms for the assignment and transportation problems. *Journal of the Society of Industrial and Applied Mathematics* 5(1) 32-38.

Napolitano, M. 2010. Warehouse/DC Equipment & Technology: Materials Handling Trends and Future Spending Plans. Available online at: http://www.logisticsmgmt.com/article/spending_gets_a_lift/

Navpak. 2011. Shipboard package handling system, available online at: http://www.agilesystems.com/navpak%20frame.htm.

Navstors. 2011. Naval automatic stowage and retrieval system, available online at: http://www.agilesystems.com/navstors_frame.htm.

OTDH. 2011. Magic black box, available online at: http://www.odth.be/solutions.php.

Park, B.C. 2001. An optimal dwell point policy for automated storage/ retrieval systems with uniformly distributed, rectangular racks. *International Journal of Production Research* 39(7) 1469-1480.

Park, B.C. 2006. Performance of automated storage/retrieval systems with non-square-in-time racks and two-class storage. *International Journal of Production Research* 44(6) 1107-1123.

Park, B.C., R.D. Foley, J.A. White, E.H. Frazelle. 2003. Dual command travel times and miniload system throughput with turnover-based storage. *IIE Transactions* 35(4) 343-355.

Park, Y.H., D.B. Webster. 1989a. Modeling of three-dimensional warehouse systems. *International Journal of Production Research* 27(6) 985-1003.

Park, Y.H., D.B. Webster. 1989b. Design of class-based storage racks for minimizing travel time in a three-dimensional storage system. *International Journal of Production Research* 27(9) 1589-1601.

Rampell, C. 2012. Hiring Picks Up in July, but Data Gives No Clear Signal. Available online at: http://www.nytimes.com/2012/08/04/business/economy/us-added-163000-jobs-in-july-jobless-rate-ticked-up.html?_r=3&ref=global-home&

Roodbergen, K.J., I.F.A. Vis. 2009. A survey of literature on automated storage and retrieval systems. *European Journal of Operational Research* 194(2) 343-362.

Rosenblatt, M.J., A. Eynan. 1989. Deriving the optimal boundaries for class-based automatic storage/retrieval systems. *Management Science* 35 (12) 1519-1524.

Ruben, R.A., F.R. Jacobs. 1999. Batch construction heuristics and storage assignment strategies for walk/ride and pick systems. *Management Science* 45(4) 575–596.

Sari, Z., C. Saygin, N. Ghouali. 2005. Travel-time models for flow-rack automated storage and retrieval systems. *International Journal of Advanced Manufacturing Technology* 25 979-987.

Sarker, B.R., A. Sabapathy, A.M. Lal, M.H. Ha. 1991. Performance evaluation of a double shuttle automated storage and retrieval system. *Production Planning and Control* 2(3) 207-213.

Slocum, J., D. Sonneveld. 2006. *The 15 Puzzle book*. Slocum Puzzle Foundation.

Stadtler, H. 1996. An operational planning concept for deep lane storage systems. *Production and Operations Management* 5 266-282.

Swisslog. 2011. Pharmacy automation systems, available online at: http://www.swisslog.com/index/hcs-index/hcs-pharmacy.htm.

Thonemann, U.W., and M.L. Brandeau. 1998. Optimal Storage Assignment Policies for Automated Storage and Retrieval Systems with Stochastic Demands. *Management Science* 44 (1) 142-148.

Tompkins, J.A., J.A. White, Y.A. Bozer, J.M.A. Tanchoco. 2010. *Facilities Planning* 4th ed., John Wiley & Sons.

Tsui, L.Y., C.H. Chang. 1992. An optimal solution to dock door assignment problem. *Computers and Industrial Engineering* 23 283-286.

Tucker, R. 2011. Going Green: Sustainability Best Practices in the Material Handling Industry. *Frost & Sullivan*. Available online at: http://www.frost.com/sublib/display-market-insight-top.do?id=224027985

Van den Berg, J.P. 1996. Class-based storage allocation in a single command warehouse with space requirement constraints. *International Journal of Industrial Engineering* 3 (1) 21-28.

Van den Berg, J.P., A.J.R.M. Gademann. 2000. Simulation study of an automated storage/retrieval system. *International Journal of Production Research* 38 (6) 1339-1356.

Wohr. 2011. Wohr Parksafe, available online at:
 http://www.woehr.de/de/projekte/liverpool_p583/index.htm.

Yu, Y., M.B.M. de Koster. 2009a. Designing an optimal turnover based storage rack for a 3D compact AS/RS. *International Journal of Production Research* 47(6), 1551-1571.

Yu, Y., M.B.M. de Koster. 2009b. Optimal zone boundaries for two-class-based compact three-dimensional automated storage and retrieval systems. *IIE Transactions* 41 (3) 194-208.

Yu, Y., H. Chen, F. Chu. 2008. A new model and hybrid approach for large scale inventory routing problems. *European Journal of Operational Research* 189(3) 1022-1040.

Yu, Y., M.B.M. de Koster. 2012. Sequencing heuristics for storing and retrieving unit loads in 3D compact storage and retrieval systems. *IIE Transactions* 44(2) 69-87.

Yu, Y., M.B.M. de Koster. 2012. On the suboptimality of full turnover-based storage. *International Journal of Production Research,* to appear.

Zaerpour, N., Y. Yu, M.B.M. de Koster. 2010. Storing fresh produce for fast retrieval in an automated compact cross-dock system, working paper, Rotterdam School of Management, Erasmus University, Rotterdam, the Netherlands.

Zaerpour, N., Y. Yu, M.B.M. de Koster. 2011. Optimal configuration of a live-cube compact storage system in service industries, working paper, Rotterdam School of Management, Erasmus University, Rotterdam, the Netherlands.

Zaerpour, N., Y. Yu, M.B.M. de Koster. 2012a. Response time analysis of a live-cube compact storage system with two classes, working paper, Rotterdam School of Management, Erasmus University, Rotterdam, the Netherlands.

Zaerpour, N., Y. Yu, M.B.M. de Koster. 2012b. Optimal two-class-based storage in a live-cube compact storage system, working paper, Rotterdam School of Management, Erasmus University, Rotterdam, the Netherlands.

Zaerpour, N., M.B.M. de Koster, Y. Yu. 2012c. Storage policies and optimal shape of a storage system, working paper, Rotterdam School of Management, Erasmus University, Rotterdam, the Netherlands.

Summary

Warehouses are important nodes in supply chains. They decouple supply from demand in time, assortment, quantity, and space. By doing so, economies of scale can be achieved in transport, as warehouses allow to regroup transport flows leading to lower cost. They also allow postponement of value addition, increasing service levels at lower inventory levels. Warehouses are particularly needed in densely populated areas, close to where demand is generated and where the labor is available. Warehouses require much space to realize economies of scale. Warehouse buildings are often quite large, more than 10,000 m^2 built space is common (De Koster and Balk, 2008), and much infrastructure outside the building is needed. Unfortunately, in many of the urbanized areas, space for such large facilities has become short. In order to address this issue, enterprises are moving toward next generation storage systems, namely "three-dimensional (3D) compact storage systems". These systems are designed in order to save floor space and labor costs, and increase the reliability of the order picking process. The following figure illustrates that 3D compact systems require less footprint compared to two-dimensional (2D) traditional systems. Several types of 3D compact storage systems exist with different handling systems (like S/R machines, conveyors, shuttles, or elevators) taking care of the horizontal, vertical and depth movements. This dissertation focuses on new types of 3D compact storage systems, in particular live-cube storage systems, where each unit load rests on a shuttle which can move in horizontal and depth directions, in cooperation with shuttles of other unit loads. In such a system, at least one empty storage slot per level is required.
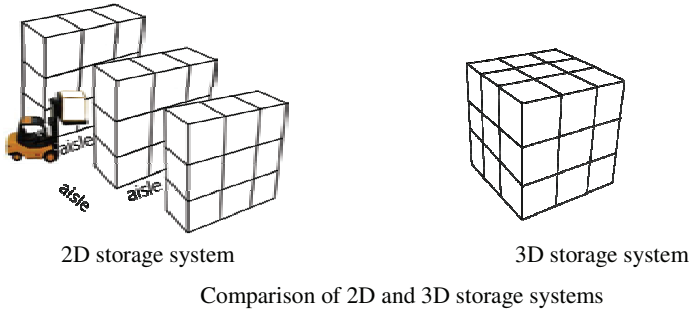
2D storage system   3D storage system

Comparison of 2D and 3D storage systems

One of the key performance measures for compact storage systems, which is also the focus of this dissertation, is response time. We analyze these systems at two decision-making levels. At the tactical (design) decision level, we focus on the rack-dimensioning problem aiming at short response times. At the operational decision level, we investigate storage assignment and retrieval sequencing problems to shorten the response time.

In chapter 2, we study the impact of storage policies on the configuration (length/width/height ratio) of automated storage systems. We show that the optimal configuration of a storage system, which minimizes the response time, is independent of the storage policy used. The result of this chapter significantly simplifies finding optimal dimensions of a storage system, as random storage can be assumed. In chapter 3, we study temporary storage of fresh produce in a cross-dock center which uses a satellite-based compact storage system. This chapter proposes a lane-sharing storage policy aiming at shorter response times than dedicated storage. Warehouse managers often prefer to use dedicated storage in a compact cross-dock system fearing reshuffles imposed by the shared storage. This chapter shows that the proposed C&I heuristic results in a shared storage policy which generally outperforms dedicated storage even if the available information is uncertain. Chapters 4, 5, and 6 study live-cube compact storage systems. In chapter 4, we study a live-cube compact storage system where random storage is used and multiple empty locations are available on each level enabling the system to create virtual aisles for any retrieval request. First, we derive closed-form formulas for the expected retrieval time of an arbitrary unit load. Second, we propose and solve a mixed-integer nonlinear model to optimize system dimensions by minimizing the retrieval time. We derive closed-form expressions which are simple to apply in practice. In chapter 5, we study a live-cube compact storage system with two storage classes. Two-Class-based storage saves response time compared to random storage while its implementation in practice is quite straightforward. We derive closed-form formulas to calculate the expected retrieval time of a two-

class-based live-cube system for any system configuration and zone boundary. In order to evaluate the quality of these closed-form formulas (obtained using a continuous-space approximation), a Monte Carlo simulation is performed based on a real (discrete) application. The results show that the closed-form formulas approximate the expected retrieval time of a discrete system with high precision; errors are usually less than 2%, and below 4% even in extreme cases. Chapter 6 extends the previous chapter by optimizing the first zone boundary and system dimensions resulting in minimum average response time. We propose a mixed-integer nonlinear mathematical model for a two-class-based live-cube system. Decomposition of the system into 36 complementary sub-cases leads to a model with many constraints. Still, the optimal dimensions of a live-cube system and the optimal first zone boundary can analytically be obtained for any ABC demand curve. The results show that in a live-cube compact storage system, an optimal two-class-based storage policy can significantly reduce the response time specifically for practical ABC demand curves (e.g. 20%/70% ABC curve) compared to a random storage policy.

Samenvatting

Magazijnen zijn belangrijke knooppunten in de supply chain. Met hun voorraden ontkoppelen ze vraag en aanbod in de tijd, hoeveelheid en ruimte en in assortiment. Hierdoor kunnen schaalvoordelen behaald worden in transport: het hercombineren van ingaande en uitgaande transportstromen leidt tot lagere kosten vergeleken met directe leveringen. Magazijnen zijn ook de plekken waar waarde aan producten wordt toegevoegd middels klantspecifieke processen als labelen, verpakken en assemblage. Magazijnen zijn in het bijzonder nodig in dichtbevolkte gebieden, dichtbij de vraag en beschikbaarheid van arbeid. Magazijnen vragen veel ruimte om schaalvoordelen te realiseren, wat leidt tot grote gebouwen; magazijngebouwen groter dan 10.000 m2 zijn geen uitzondering (De Koster en Balk, 2008), en er is veel infrastructuur buiten het gebouw nodig. Helaas, in veel verstedelijkte gebieden is er een tekort aan ruimte voor zulke grote gebouwen. Een gedeeltelijk antwoord op deze problemen kan gegeven worden door een volgende generatie opslagsystemen, zogenaamde "driedimensionale (3D) compacte opslagsystemen". Deze systemen zijn ontworpen om vloeroppervlak en arbeidskosten te besparen, en om de betrouwbaarheid van het orderverzamelproces te vergroten. De onderstaande figuren illustreren dat 3D compacte systemen minder ruimte nodig hebben vergeleken met traditionele tweedimensionale (2D) systemen, doordat ze geen of minder transportgangen hebben. Er bestaan verschillende typen 3D compacte opslagsystemen met verschillende interne transportsystemen (zoals S/R machines, transportbanden, shuttles, en liften) welke horizontale, verticale en dieptebewegingen verzorgen. Dit proefschrift focust op nieuwe typen 3D compacte opslagsystemen, in het bijzonder de "live-cube storage systemen", waar elke ladingdrager steunt op een shuttle die in twee richtingen horizontaal kan bewegen, in samenwerking met andere shuttles (met andere ladingen). In zo'n systeem, is minimaal één lege locatie per niveau nodig.

2D opslagsysteem   3D opslagsysteem

Vergelijking van 2D en 3D opslagsystemen
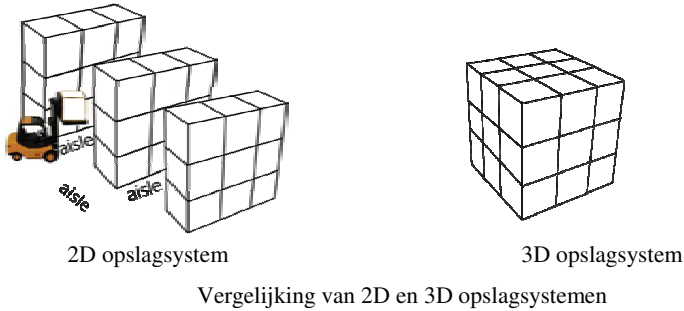
Een belangrijk prestatiecriterium van compacte opslagsystemen, en ook de focus van dit proefschrift, is de reactietijd (of uitslagtijd): de tijd die nodig is om een gewenste lading op het juiste afzetpunt te krijgen. We analyseren deze systemen op twee verschillende beslissingsniveaus. Op het tactische (of ontwerp) beslissingsniveau focussen we op het optimaliseren van de systeemafmetingen teneinde de reactietijd te minimaliseren. Op het operationele beslissingsniveau berekenen we de speltijden voor inslag- en uitslagopdrachten bij een gegeven systeemconfiguratie en zonegrenzen voor klassegeorienteerde opslag.

In hoofdstuk 2 onderzoeken we de impact van opslagstrategieën op de configuratie (hoogte en breedte ratio) van geautomatiseerde opslagsystemen. We laten zien dat de optimale configuratie van een opslagsysteem, welke de reactietijd minimaliseert, onafhankelijk is van de opslagstrategie die gehanteerd wordt. Het resultaat van dit hoofdstuk versimpelt het vinden van optimale afmetingsverhoudingen van opslagsystemen, omdat een random opslagstrategie verondersteld mag worden. In hoofdstuk 3 bestuderen we de tijdelijke opslag van versproducten in een crossdock centrum dat een compact opslagsysteem gebruikt met satellietkranen. In dit hoofdstuk wordt een "lane-sharing" gemengde opslagstrategie geïntroduceerd, waarbij meerder producten een multidiepe opslaglane kunnen delen, teneinde een korte uitslagtijd te realiseren. Een dergelijke strategie geeft kortere uitslagtijden dan een strategie met slechts één product per lane. Magazijnmanagers prefereren echter vaak een strategie met één product per lane in een compact opslagsysteem omdat een gemengde strategie kan leiden tot extra verplaatsingen. Dit hoofdstuk laat zien dat gemengde opslag, gebruikmakend van de voorgestelde C&I heuristiek, over het algemeen beter presteert dan een strategie met één product per lane, zelfs als de beschikbare uitslaginformatie onzeker is. Hoofdstukken 4, 5 en 6 bestuderen "live-cube" compacte opslagsystemen. In hoofdstuk 4 bestuderen we een "live-cube" compact opslagsysteem waar random opslag wordt gebruikt

en meerdere lege locaties beschikbaar zijn op elk niveau, wat het mogelijk maakt om virtuele gangpaden te creëren in het systeem voor elke uitslagopdracht.

Eerst leiden we gesloten formules af voor de verwachte uitslagtijd van een willekeurige eenheidslading. Daarna formuleren we een mixed-integer nietlinear model om de systeemdimensies te optimaliseren door de uitslagtijd te minimaliseren. Dit model kan opgelost worden en leidt tot gesloten formules voor de systeemdimensies welke gemakkelijk in de praktijk toegepast kunnen worden. In hoofdstuk 5 bestuderen we een live-cube compact opslagsysteem met twee opslagklassen. Opslag, gebaseerd op twee productklassen met verschillende omloopsnelheden (snellopers versus langzaamlopers) (ofwel two-class-based), bespaart uitslagtijd vergeleken met random opslag, terwijl de implementatie in de praktijk redelijk eenvoudig is.
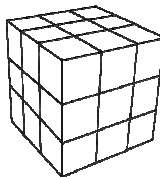
We leiden gesloten formules af voor de verwachte uitslagtijd van een live-cube systeem met twee opslagklassen voor elke systeemconfiguratie en klasse-zonegrens. De kwaliteit van deze gesloten formules (verkregen door het gebruik van een continue-ruimte benadering), wordt gecontroleerd middels een Monte Carlo simulatie, gebaseerd op een echte (discrete) applicatie. De resultaten laten zien dat de gesloten formules de verwachte uitslagtijd benaderen van een discreet systeem met hoge precisie; fouten zijn gewoonlijk minder dan 2%, en zelfs onder de 4% in extreme gevallen. Hoofdstuk 6 gaat verder in op het vorige hoofdstuk door de zonegrens van de eerste opslagklasse te optimaliseren en systeemdimensies met minimale gemiddelde uitslagtijden te ontwikkelen. We formuleren een mixed-integer nietlineair mathematisch model voor een live-cube systeem met twee opslagklassen. Om het model op te lossen dienen 36 complementaire verschillende gevallen onderscheiden te moeten worden. Echter, de optimale afmeting van een live-cube systeem en de optimale eerste zonegrens kan analytisch afgeleid worden voor elke ABC vraagcurve. De resultaten laten zien dat in een live-cube compact opslagsysteem met twee opslagklassen en optimale klassegrenzen de uitslagtijd significant kan verminderen vergeleken met random opslag, speciaal voor veel voorkomende ABC vraag curven (bijv. een 20%/70% ABC curve).

چکیده(Summary in Farsi)

انبارها و مراکز توزیع بخش مهمی از زنجیره تامین را تشکیل می‌دهند. انبارها در واقع عرضه را از تقاضا در بعد زمان، کمیت، تنوع، و مکان جدا می‌کنند. بنابراین، حمل و نقل مقرون به صرفه خواهد شد با توجه به این که حمل‌ونقل‌های متعدد و در حجم کم جای خود را به حمل‌ونقل در حجم زیاد و در دفعات کمتر خواهند داد. همچنین، انبارها افزایش سطح خدمت‌دهی به مشتری و کاهش هزینه‌های موجودی را میسـر مـی‌-سازند. انبارها به ویژه درنزدیکی مکان‌های پرجمعیت مورد نیاز هستند، چرا که تقاضا در شهرهای پرجمعیت بیشتر بوده و نیروی کـار نیـز بـه وفور یافت می‌شود. انبارها فضای بسیار وسیعی را اشغال می‌کنند. انبارهایی با مساحت بـیش از ۱۰۰۰۰ مترمربـع بـه تعـدد یافـت مـی‌شـوند. متاسفانه، در بسیاری از محیط‌های شهری، فضای کافی برای احداث چنین سازه‌هایی در دسترس نیست. به منظور پاسـخ بـه چنـین معضـلی، سازمان‌ها در حال سوق به سمت استفاده از نسل نوین انبارها هستند: "سیستم‌های انبارش فشرده یا سه‌بعدی". ایـن سیسـتم‌هـا بـه منظـور کاهش مساحت زمین مورد نیاز و کاهش هزینه نیروی انسانی، و همچنین افزایش پایایی فرایند پاسخدهی به سفارشات مشتری طراحی شـده‌-اند. با توجه به شکل ذیل، واضح است که سیستم‌های انبارش فشرده (سه بعدی) در مقایسه با سیستم‌هـای سـنتی (دوبعـدی) بـه مسـاحت و فضای کمتری نیازمند هستند. این پژوهش بر روی نوآوری‌های اخیر در زمینه سیستم‌های انبارش فشرده و بـه طـور ویـژه بـر روی "سیسـتم انبارش فشرده مکعب متحرک" تمرکز می‌نماید. در سیستم انبارش مکعب متحرک هر محصول (به عنوان نمونه، پالت، کارتون، اتوموبیل،...) بـر روی یک شاتل قرار گرفته و شاتل، محصول را در سطح افقی جابجا می‌کند. مکانیسم حرکتی این سیستم با بـازی "پـازل پـانزده‌تـایی" قابـل قیاس است. در چنین سیستمی، حداقل یک مکان خالی در هر طبقه از سیستم مورد نیاز است.
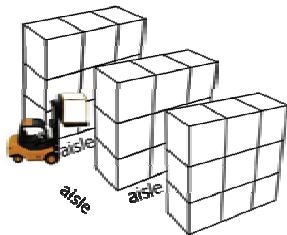
سیستم‌های انبارش فشرده (سه‌بعدی)   سیستم‌های انبارش سنتی (دوبعدی)

مقایسه سیستم‌های انبارش سنتی و فشرده

یکی از شاخص‌های اندازه‌گیری عملکرد سیستم‌های انبارش فشرده، که در واقع مورد توجه این پژوهش نیز می‌باشد، زمان پاسخگویی بـه مشتری می‌باشد. این سیستم‌ها در دو سطح مختلف تصمیم‌گیری قابل ارزیابی هستند. در سطح تصمیم‌گیری استراتژیک، تمرکز بر روی یافتن ابعاد بهینه این سیستم‌ها با هدف کاهش زمان پاسخگویی می‌باشد. در سطح تصمیم‌گیری عملیاتی، مسائلی از قبیل نحوه تخصیص مکـان‌هـای انبارش به محصولات مورد بررسی قرار می‌گیرد.

در فصل ۲، تاثیر استراتژی‌های انبارش بر ابعاد بهینه یک سیستم انبارش مورد مطالعه قرار می‌گیرد. بر اساس نتایج این فصل، ابعاد بهینه یک سیستم انبارش که زمان پاسخگویی را کمینه می‌سازد، از استراتژی انبارش مورد استفاده مستقل است. نتایج این فصل به طرز قابل توجهی یافتن ابعاد بهینه یک سیستم انبارش را تسهیل می‌سازد، با توجه به این که همواره کافی است استراتژی انبارش "تصادفی" را در نظر گرفـت. در فصل ۳، انبارش موقتی محصولات فاسدشدنی (اعم از میوه‌جات و صیفی‌جات) در یک مرکز توزیع مورد مطالعه قـرار گرفتـه اسـت. در ایـن فصل، یک الگوریتم ابتکاری با هدف کاهش زمان پاسخگویی به مشتری ارائه شده است. بر اساس نتایج این فصل، این الگوریتم ابتکـاری منجـر به کاهش چشمگیر زمان پاسخگویی به مشتری در مقایسه با الگوریتم‌های حال حاضر در این گونه مراکز توزیع می‌گردد. فصـول ۴، ۵، و ۶ بـر روی سیستم‌های انبارش فشرده مکعب متحرک متمرکز است. در فصل ۴، یک سیستم انبارش فشرده بـا اسـتراتژی انبـارش تصـادفی در نظر گرفته شده است. در این فصل در ابتدا، عبارات ریاضی به منظور تخمین میانگین زمان پاسخگویی به مشتری بـه دسـت مـی‌آیـد. سـپس، بـا استفاده از یک مدل غیرخطی و عدد صحیح، ابعاد بهینه چنین سیستمی که منجر به کمینه‌سازی زمان پاسخگویی می‌شود، یافت می‌گردد. در فصل ۵ یک سیستم انبارش فشرده با استراتژی انبارش "کلاس‌بندی" مورد مطالعه قرار می‌گیرد. استراتژی انبارش با دو کلاس، زمان پاسـخ‌-گویی به مشتری را به طرز چشمگیری در مقایسه با استراتژی انبارش تصادفی کاهش می‌دهد. این در حالی است که نسبت به استراتژی تصادفی، این استراتژی به سادگی در واقعیت قابل پیاده‌سازی می‌باشد. فصل ۵، عبارات ریاضی به منظور تخمین میانگین زمان پاسخگویی به مشتری در یک سیستم انبارش فشرده با دو کلاس به دست می‌دهد. به منظور ارزیابی دقت این عبارات ریاضی، از شبیه‌سازی مونـت‌کـارلو اسـتفاده شـده

است. نتایج شبیه‌سازی نشان می‌دهد که خطای عبارات ریاضی در تخمین میانگین زمان پاسخگویی در اغلب مـوارد کمتــر از ۲ درصـد اسـت.

فصل ۶ بر روی یافتن ابعاد بهینه یک سیستم انبارش فشرده با دو کلاس متمرکز است. بدین منظور، یک مدل غیرخطی و عدد صحیح پیشنهاد

گردیده‌است. اگرچه در مقایسه با استراتژی انبارش تصادفی، مدل پیشنهادی بسیار پیچیده‌تر است، نتایج نشان می‌دهد که کاهشی تا سقف ۵۰

درصد در میانگین زمان پاسخگویی به مشتری قابل حصول است.

About the author

Nima Zaerpour (1983) received his B.Sc. in Industrial Engineering from Sharif University of Technology in 2005 and his M.Sc. in Industrial Engineering from University of Tehran in 2008 both in Tehran, Iran. In September 2008, he joined Rotterdam School of Management, Erasmus University Rotterdam. His research interests are next generation storage systems, e-commerce order fulfillment systems, sustainable warehouse operations, facility logistics, distribution logistics, etc. In 2012, he was a visiting scholar at School of Industrial and Systems Engineering at Georgia Tech, where he attended Global Supply Chain Scholars Program. Moreover, in 2011, he was a visiting scholar in the Department of Information Management and Decision Science, University of Science and Technology of China. His research findings has been presented in many international conferences including INFORMS Annual Meetings (2009, 2010, 2011, 2012), POMS (2012) and EURO (2009, 2010). He is currently a Postdoctoral fellow at Rotterdam School of Management, Erasmus University Rotterdam.

ERIM PH.D. SERIES RESEARCH IN MANAGEMENT

The ERIM PhD Series contains PhD dissertations in the field of Research in Management defended at Erasmus University Rotterdam and supervised by senior researchers affiliated to the Erasmus Research Institute of Management (ERIM). All dissertations in the ERIM PhD Series are available in full text through the ERIM Electronic Series Portal: http://hdl.handle.net/1765/1 ERIM is the joint research institute of the Rotterdam School of Management (RSM) and the Erasmus School of Economics at the Erasmus University Rotterdam (EUR).

DISSERTATIONS LAST FIVE YEARS

Acciaro, M., *Bundling Strategies in Global Supply Chains.* Promoter(s): Prof.dr. H.E. Haralambides, EPS-2010-197-LIS, http://hdl.handle.net/1765/19742

Agatz, N.A.H., *Demand Management in E-Fulfillment*. Promoter(s): Prof.dr.ir. J.A.E.E. van Nunen, EPS-2009-163-LIS, http://hdl.handle.net/1765/15425

Alexiev, A., *Exploratory Innovation: The Role of Organizational and Top Management Team Social Capital.* Promoter(s): Prof.dr. F.A.J. van den Bosch & Prof.dr. H.W. Volberda, EPS-2010-208-STR, http://hdl.handle.net/1765/20632

Asperen, E. van, *Essays on Port, Container, and Bulk Chemical Logistics Optimization*. Promoter(s): Prof.dr.ir. R. Dekker, EPS-2009-181-LIS, http://hdl.handle.net/1765/17626

Benning, T.M., *A Consumer Perspective on Flexibility in Health Care: Priority Access Pricing and Customized Care*, Promoter(s): Prof.dr.ir. B.G.C. Dellaert, EPS-2011-241-MKT, http://hdl.handle.net/1765/23670

Betancourt, N.E., *Typical Atypicality: Formal and Informal Institutional Conformity, Deviance, and Dynamics*, Promoter(s): Prof.dr. B. Krug, EPS-2012-262-ORG, http://hdl.handle.net/1765/32345

Bezemer, P.J., *Diffusion of Corporate Governance Beliefs: Board Independence and the Emergence of a Shareholder Value Orientation in the Netherlands.* Promoter(s): Prof.dr.ing. F.A.J. van den Bosch & Prof.dr. H.W. Volberda, EPS-2009-192-STR, http://hdl.handle.net/1765/18458

Binken, J.L.G., *System Markets: Indirect Network Effects in Action, or Inaction,* Promoter(s): Prof.dr. S. Stremersch, EPS-2010-213-MKT, http://hdl.handle.net/1765/21186

Blitz, D.C., *Benchmarking Benchmarks,* Promoter(s): Prof.dr. A.G.Z. Kemna & Prof.dr. W.F.C. Verschoor, EPS-2011-225-F&A, http://hdl.handle.net/1765/22624

Borst, W.A.M., *Understanding Crowdsourcing: Effects of Motivation and Rewards on Participation and Performance in Voluntary Online Activities,* Promoter(s): Prof.dr.ir. J.C.M. van den Ende & Prof.dr.ir. H.W.G.M. van Heck, EPS-2010-221-LIS, http://hdl.handle.net/1765/ 21914

Budiono, D.P., *The Analysis of Mutual Fund Performance: Evidence from U.S. Equity Mutual Funds,* Promoter(s): Prof.dr. M.J.C.M. Verbeek, EPS-2010-185-F&A, http://hdl.handle.net/1765/18126

Burger, M.J., *Structure and Cooptition in Urban Networks*, Promoter(s): Prof.dr. G.A. van der Knaap & Prof.dr. H.R. Commandeur, EPS-2011-243-ORG, http://hdl.handle.net/1765/26178

Camacho, N.M., *Health and Marketing; Essays on Physician and Patient Decision-making*, Promoter(s): Prof.dr. S. Stremersch, EPS-2011-237-MKT, http://hdl.handle.net/1765/23604

Carvalho de Mesquita Ferreira, L., *Attention Mosaics: Studies of Organizational Attention*, Promoter(s): Prof.dr. P.M.A.R. Heugens & Prof.dr. J. van Oosterhout, EPS-2010-205-ORG, http://hdl.handle.net/1765/19882

Chen, C.-M., *Evaluation and Design of Supply Chain Operations Using DEA*, Promoter(s): Prof.dr. J.A.E.E. van Nunen, EPS-2009-172-LIS, http://hdl.handle.net/1765/16181

Defilippi Angeldonis, E.F., *Access Regulation for Naturally Monopolistic Port Terminals: Lessons from Regulated Network Industries,* Promoter(s): Prof.dr. H.E. Haralambides, EPS-2010-204-LIS, http://hdl.handle.net/1765/19881

Deichmann, D., *Idea Management: Perspectives from Leadership, Learning, and Network Theory*, Promoter(s): Prof.dr.ir. J.C.M. van den Ende, EPS-2012-255-ORG, http://hdl.handle.net/1765/ 31174

Desmet, P.T.M., *In Money we Trust? Trust Repair and the Psychology of Financial Compensations*, Promoter(s): Prof.dr. D. De Cremer & Prof.dr. E. van Dijk, EPS-2011-232-ORG, http://hdl.handle.net/1765/23268

Diepen, M. van, *Dynamics and Competition in Charitable Giving*, Promoter(s): Prof.dr. Ph.H.B.F. Franses, EPS-2009-159-MKT, http://hdl.handle.net/1765/14526

Dietvorst, R.C., *Neural Mechanisms Underlying Social Intelligence and Their Relationship with the Performance of Sales Managers,* Promoter(s): Prof.dr. W.J.M.I. Verbeke, EPS-2010-215-MKT, http://hdl.handle.net/1765/21188

Dietz, H.M.S., *Managing (Sales)People towards Performance: HR Strategy, Leadership & Teamwork*, Promoter(s): Prof.dr. G.W.J. Hendrikse, EPS-2009-168-ORG, http://hdl.handle.net/1765/16081

Dollevoet, T.A.B., *Delay Management and Dispatching in Railways*, Promoter(s): Prof.dr. A.P.M. Wagelmans, EPS-2013-272-LIS, http://hdl.handle.net/1765/1

Doorn, S. van, *Managing Entrepreneurial Orientation*, Promoter(s): Prof.dr. J.J.P. Jansen, Prof.dr.ing. F.A.J. van den Bosch & Prof.dr. H.W. Volberda, EPS-2012-258-STR, http://hdl.handle.net/1765/32166

Douwens-Zonneveld, M.G., *Animal Spirits and Extreme Confidence: No Guts, No Glory*, Promoter(s): Prof.dr. W.F.C. Verschoor, EPS-2012-257-F&A, http://hdl.handle.net/1765/31914

Duca, E., *The Impact of Investor Demand on Security Offerings*, Promoter(s): Prof.dr. A. de Jong, EPS-2011-240-F&A, http://hdl.handle.net/1765/26041

Eck, N.J. van, *Methodological Advances in Bibliometric Mapping of Science*, Promoter(s): Prof.dr.ir. R. Dekker, EPS-2011-247-LIS, http://hdl.handle.net/1765/26509

Eijk, A.R. van der, *Behind Networks: Knowledge Transfer, Favor Exchange and Performance*, Promoter(s): Prof.dr. S.L. van de Velde & Prof.dr.drs. W.A. Dolfsma, EPS-2009-161-LIS, http://hdl.handle.net/1765/14613

Essen, M. van, *An Institution-Based View of Ownership*, Promoter(s): Prof.dr. J. van Oosterhout & Prof.dr. G.M.H. Mertens, EPS-2011-226-ORG, http://hdl.handle.net/1765/22643

Feng, L., *Motivation, Coordination and Cognition in Cooperatives,* Promoter(s): Prof.dr. G.W.J. Hendrikse, EPS-2010-220-ORG, http://hdl.handle.net/1765/21680

Gertsen, H.F.M., *Riding a Tiger without Being Eaten: How Companies and Analysts Tame Financial Restatements and Influence Corporate Reputation*, Promoter(s): Prof.dr. C.B.M. van Riel, EPS-2009-171-ORG, http://hdl.handle.net/1765/16098

Gharehgozli, A.H., *Developing New Methods for Efficient Container Stacking Operations*, Promoter(s): Prof.dr.ir. M.B.M. de Koster, EPS-2012-269-LIS, http://hdl.handle.net/1765/ 37779

Gijsbers, G.W., *Agricultural Innovation in Asia: Drivers, Paradigms and Performance,* Promoter(s): Prof.dr. R.J.M. van Tulder, EPS-2009-156-ORG, http://hdl.handle.net/1765/14524

Gils, S. van, *Morality in Interactions: On the Display of Moral Behavior by Leaders and Employees*, Promoter(s): Prof.dr. D.L. van Knippenberg, EPS-2012-270-ORG, http://hdl.handle.net/1765/ 38028

Ginkel-Bieshaar, M.N.G. van, *The Impact of Abstract versus Concrete Product Communications on Consumer Decision-making Processes*, Promoter(s): Prof.dr.ir. B.G.C. Dellaert, EPS-2012-256-MKT, http://hdl.handle.net/1765/31913

Gkougkousi, X., *Empirical Studies in Financial Accounting*, Promoter(s): Prof.dr. G.M.H. Mertens & Prof.dr. E. Peek, EPS-2012-264-F&A, http://hdl.handle.net/1765/37170

Gong, Y., *Stochastic Modelling and Analysis of Warehouse Operations*, Promoter(s): Prof.dr. M.B.M. de Koster & Prof.dr. S.L. van de Velde, EPS-2009-180-LIS, http://hdl.handle.net/1765/16724

Greeven, M.J., *Innovation in an Uncertain Institutional Environment: Private Software Entrepreneurs in Hangzhou, China*, Promoter(s): Prof.dr. B. Krug, EPS-2009-164-ORG, http://hdl.handle.net/1765/15426

Hakimi, N.A, *Leader Empowering Behaviour: The Leader's Perspective: Understanding the Motivation behind Leader Empowering Behaviour*, Promoter(s): Prof.dr. D.L. van Knippenberg, EPS-2010-184-ORG, http://hdl.handle.net/1765/17701

Hensmans, M., *A Republican Settlement Theory of the Firm: Applied to Retail Banks in England and the Netherlands (1830-2007)*, Promoter(s): Prof.dr. A. Jolink & Prof.dr. S.J. Magala, EPS-2010-193-ORG, http://hdl.handle.net/1765/19494

Hernandez Mireles, C., *Marketing Modeling for New Products,* Promoter(s): Prof.dr. P.H. Franses, EPS-2010-202-MKT, http://hdl.handle.net/1765/19878

Heyden, M.L.M., *Essays on Upper Echelons & Strategic Renewal: A Multilevel Contingency Approach*, Promoter(s): Prof.dr. F.A.J. van den Bosch & Prof.dr. H.W. Volberda, EPS-2012-259-STR, http://hdl.handle.net/1765/32167

Hoever, I.J., *Diversity and Creativity: In Search of Synergy*, Promoter(s): Prof.dr. D.L. van Knippenberg, EPS-2012-267-ORG, http://hdl.handle.net/1765/37392

Hoogendoorn, B., *Social Entrepreneurship in the Modern Economy: Warm Glow, Cold Feet*, Promoter(s): Prof.dr. H.P.G. Pennings & Prof.dr. A.R. Thurik, EPS-2011-246-STR, http://hdl.handle.net/1765/26447

Hoogervorst, N., *On The Psychology of Displaying Ethical Leadership: A Behavioral Ethics Approach*, Promoter(s): Prof.dr. D. De Cremer & Dr. M. van Dijke, EPS-2011-244-ORG, http://hdl.handle.net/1765/26228

Huang, X., *An Analysis of Occupational Pension Provision: From Evaluation to Redesign,* Promoter(s): Prof.dr. M.J.C.M. Verbeek & Prof.dr. R.J. Mahieu, EPS-2010-196-F&A, http://hdl.handle.net/1765/19674

Hytönen, K.A. *Context Effects in Valuation, Judgment and Choice*, Promoter(s): Prof.dr.ir. A. Smidts, EPS-2011-252-MKT, http://hdl.handle.net/1765/30668

Jalil, M.N., *Customer Information Driven After Sales Service Management: Lessons from Spare Parts Logistics,* Promoter(s): Prof.dr. L.G. Kroon, EPS-2011-222-LIS, http://hdl.handle.net/1765/22156

Jaspers, F.P.H., *Organizing Systemic Innovation*, Promoter(s): Prof.dr.ir. J.C.M. van den Ende, EPS-2009-160-ORG, http://hdl.handle.net/1765/14974

Jiang, T., *Capital Structure Determinants and Governance Structure Variety in Franchising*, Promoter(s): Prof.dr. G. Hendrikse & Prof.dr. A. de Jong, EPS-2009-158-F&A, http://hdl.handle.net/1765/14975

Jiao, T., *Essays in Financial Accounting*, Promoter(s): Prof.dr. G.M.H. Mertens, EPS-2009-176-F&A, http://hdl.handle.net/1765/16097

Kaa, G. van, *Standard Battles for Complex Systems: Empirical Research on the Home Network,* Promoter(s): Prof.dr.ir. J. van den Ende & Prof.dr.ir. H.W.G.M. van Heck, EPS-2009-166-ORG, http://hdl.handle.net/1765/16011

Kagie, M., *Advances in Online Shopping Interfaces: Product Catalog Maps and Recommender Systems,* Promoter(s): Prof.dr. P.J.F. Groenen, EPS-2010-195-MKT, http://hdl.handle.net/1765/19532

Kappe, E.R., *The Effectiveness of Pharmaceutical Marketing*, Promoter(s): Prof.dr. S. Stremersch, EPS-2011-239-MKT, http://hdl.handle.net/1765/23610

Karreman, B., *Financial Services and Emerging Markets,* Promoter(s): Prof.dr. G.A. van der Knaap & Prof.dr. H.P.G. Pennings, EPS-2011-223-ORG, http://hdl.handle.net/1765/ 22280

Kwee, Z., *Investigating Three Key Principles of Sustained Strategic Renewal: A Longitudinal Study of Long-Lived Firms,* Promoter(s): Prof.dr.ir. F.A.J. Van den Bosch & Prof.dr. H.W. Volberda, EPS-2009-174-STR, http://hdl.handle.net/1765/16207

Lam, K.Y., *Reliability and Rankings*, Promoter(s): Prof.dr. P.H.B.F. Franses, EPS-2011-230-MKT, http://hdl.handle.net/1765/22977

Lander, M.W., *Profits or Professionalism? On Designing Professional Service Firms*, Promoter(s): Prof.dr. J. van Oosterhout & Prof.dr. P.P.M.A.R. Heugens, EPS-2012-253-ORG, http://hdl.handle.net/1765/30682

Langhe, B. de, *Contingencies: Learning Numerical and Emotional Associations in an Uncertain World*, Promoter(s): Prof.dr.ir. B. Wierenga & Prof.dr. S.M.J. van Osselaer, EPS-2011-236-MKT, http://hdl.handle.net/1765/23504

Larco Martinelli, J.A., *Incorporating Worker-Specific Factors in Operations Management Models,* Promoter(s): Prof.dr.ir. J. Dul & Prof.dr. M.B.M. de Koster, EPS-2010-217-LIS, http://hdl.handle.net/1765/21527

Li, T., *Informedness and Customer-Centric Revenue Management,* Promoter(s): Prof.dr. P.H.M. Vervest & Prof.dr.ir. H.W.G.M. van Heck, EPS-2009-146-LIS, http://hdl.handle.net/1765/14525

Lovric, M., *Behavioral Finance and Agent-Based Artificial Markets*, Promoter(s): Prof.dr. J. Spronk & Prof.dr.ir. U. Kaymak, EPS-2011-229-F&A, http://hdl.handle.net/1765/ 22814

Maas, K.E.G., *Corporate Social Performance: From Output Measurement to Impact Measurement,* Promoter(s): Prof.dr. H.R. Commandeur, EPS-2009-182-STR, http://hdl.handle.net/1765/17627

Markwat, T.D., *Extreme Dependence in Asset Markets Around the Globe*, Promoter(s): Prof.dr. D.J.C. van Dijk, EPS-2011-227-F&A, http://hdl.handle.net/1765/22744

Mees, H., *Changing Fortunes: How China's Boom Caused the Financial Crisis*, Promoter(s): Prof.dr. Ph.H.B.F. Franses, EPS-2012-266-MKT, http://hdl.handle.net/1765/34930

Meuer, J., *Configurations of Inter-Firm Relations in Management Innovation: A Study in China's Biopharmaceutical Industry*, Promoter(s): Prof.dr. B. Krug, EPS-2011-228-ORG, http://hdl.handle.net/1765/22745

Mihalache, O.R., *Stimulating Firm Innovativeness: Probing the Interrelations between Managerial and Organizational Determinants*, Promoter(s): Prof.dr. J.J.P. Jansen, Prof.dr.ing. F.A.J. van den Bosch & Prof.dr. H.W. Volberda, EPS-2012-260-S&E, http://hdl.handle.net/1765/32343

Moonen, J.M., *Multi-Agent Systems for Transportation Planning and Coordination*, Promoter(s): Prof.dr. J. van Hillegersberg & Prof.dr. S.L. van de Velde, EPS-2009-177-LIS, http://hdl.handle.net/1765/16208

Nederveen Pieterse, A., *Goal Orientation in Teams: The Role of Diversity*, Promoter(s): Prof.dr. D.L. van Knippenberg, EPS-2009-162-ORG, http://hdl.handle.net/1765/15240

Nielsen, L.K., *Rolling Stock Rescheduling in Passenger Railways: Applications in Short-term Planning and in Disruption Management*, Promoter(s): Prof.dr. L.G. Kroon, EPS-2011-224-LIS, http://hdl.handle.net/1765/22444

Niesten, E.M.M.I., *Regulation, Governance and Adaptation: Governance Transformations in the Dutch and French Liberalizing Electricity Industries*, Promoter(s): Prof.dr. A. Jolink & Prof.dr. J.P.M. Groenewegen, EPS-2009-170-ORG, http://hdl.handle.net/1765/16096

Nijdam, M.H., *Leader Firms: The Value of Companies for the Competitiveness of the Rotterdam Seaport Cluster,* Promoter(s): Prof.dr. R.J.M. van Tulder, EPS-2010-216-ORG, http://hdl.handle.net/1765/21405

Noordegraaf-Eelens, L.H.J., *Contested Communication: A Critical Analysis of Central Bank Speech,* Promoter(s): Prof.dr. Ph.H.B.F. Franses, EPS-2010-209-MKT, http://hdl.handle.net/1765/21061

Nuijten, A.L.P., *Deaf Effect for Risk Warnings: A Causal Examination applied to Information Systems Projects*, Promoter(s): Prof.dr. G. van der Pijl & Prof.dr. H. Commandeur & Prof.dr. M. Keil, EPS-2012-263-S&E, http://hdl.handle.net/1765/34928

Nuijten, I., *Servant Leadership: Paradox or Diamond in the Rough? A Multidimensional Measure and Empirical Evidence*, Promoter(s): Prof.dr. D.L. van Knippenberg, EPS-2009-183-ORG, http://hdl.handle.net/1765/21405

Oosterhout, M., van, *Business Agility and Information Technology in Service Organizations,* Promoter(s): Prof,dr.ir. H.W.G.M. van Heck, EPS-2010-198-LIS, http://hdl.handle.net/1765/19805

Oostrum, J.M., van, *Applying Mathematical Models to Surgical Patient Planning*, Promoter(s): Prof.dr. A.P.M. Wagelmans, EPS-2009-179-LIS, http://hdl.handle.net/1765/16728

Osadchiy, S.E., *The Dynamics of Formal Organization: Essays on Bureaucracy and Formal Rules*, Promoter(s): Prof.dr. P.P.M.A.R. Heugens, EPS-2011-231-ORG, http://hdl.handle.net/1765/23250

Otgaar, A.H.J., *Industrial Tourism: Where the Public Meets the Private,* Promoter(s): Prof.dr. L. van den Berg, EPS-2010-219-ORG, http://hdl.handle.net/1765/21585

Ozdemir, M.N., *Project-level Governance, Monetary Incentives and Performance in Strategic R&D Alliances*, Promoter(s): Prof.dr.ir. J.C.M. van den Ende, EPS-2011-235-LIS, http://hdl.handle.net/1765/23550

Peers, Y., *Econometric Advances in Diffusion Models*, Promoter(s): Prof.dr. Ph.H.B.F. Franses, EPS-2011-251-MKT, http://hdl.handle.net/1765/ 30586

Pince, C., *Advances in Inventory Management: Dynamic Models,* Promoter(s): Prof.dr.ir. R. Dekker, EPS-2010-199-LIS, http://hdl.handle.net/1765/19867

Porras Prado, M., *The Long and Short Side of Real Estate, Real Estate Stocks, and Equity*, Promoter(s): Prof.dr. M.J.C.M. Verbeek, EPS-2012-254-F&A, http://hdl.handle.net/1765/30848

Potthoff, D., *Railway Crew Rescheduling: Novel Approaches and Extensions,* Promoter(s): Prof.dr. A.P.M. Wagelmans & Prof.dr. L.G. Kroon, EPS-2010-210-LIS, http://hdl.handle.net/1765/21084

Poruthiyil, P.V., *Steering Through: How Organizations Negotiate Permanent Uncertainty and Unresolvable Choices*, Promoter(s): Prof.dr. P.P.M.A.R. Heugens & Prof.dr. S. Magala, EPS-2011-245-ORG, http://hdl.handle.net/1765/26392

Pourakbar, M. *End-of-Life Inventory Decisions of Service Parts*, Promoter(s): Prof.dr.ir. R. Dekker, EPS-2011-249-LIS, http://hdl.handle.net/1765/30584

Rijsenbilt, J.A., *CEO Narcissism; Measurement and Impact*, Promoter(s): Prof.dr. A.G.Z. Kemna & Prof.dr. H.R. Commandeur, EPS-2011-238-STR, http://hdl.handle.net/1765/ 23554

Roelofsen, E.M., *The Role of Analyst Conference Calls in Capital Markets*, Promoter(s): Prof.dr. G.M.H. Mertens & Prof.dr. L.G. van der Tas RA, EPS-2010-190-F&A, http://hdl.handle.net/1765/18013

Rosmalen, J. van, *Segmentation and Dimension Reduction: Exploratory and Model-Based Approaches*, Promoter(s): Prof.dr. P.J.F. Groenen, EPS-2009-165-MKT, http://hdl.handle.net/1765/15536

Roza, M.W., *The Relationship between Offshoring Strategies and Firm Performance: Impact of Innovation, Absorptive Capacity and Firm Size,* Promoter(s): Prof.dr. H.W. Volberda & Prof.dr.ing. F.A.J. van den Bosch, EPS-2011-214-STR, http://hdl.handle.net/1765/22155

Rus, D., *The Dark Side of Leadership: Exploring the Psychology of Leader Self-serving Behavior*, Promoter(s): Prof.dr. D.L. van Knippenberg, EPS-2009-178-ORG, http://hdl.handle.net/1765/16726

Schellekens, G.A.C., *Language Abstraction in Word of Mouth,* Promoter(s): Prof.dr.ir. A. Smidts, EPS-2010-218-MKT, ISBN: 978-90-5892-252-6, http://hdl.handle.net/1765/21580

Sotgiu, F., *Not All Promotions are Made Equal: From the Effects of a Price War to Cross-chain Cannibalization,* Promoter(s): Prof.dr. M.G. Dekimpe & Prof.dr.ir. B. Wierenga, EPS-2010-203-MKT, http://hdl.handle.net/1765/19714

Srour, F.J., *Dissecting Drayage: An Examination of Structure, Information, and Control in Drayage Operations*, Promoter(s): Prof.dr. S.L. van de Velde, EPS-2010-186-LIS, http://hdl.handle.net/1765/18231

Sweldens, S.T.L.R., *Evaluative Conditioning 2.0: Direct versus Associative Transfer of Affect to Brands,* Promoter(s): Prof.dr. S.M.J. van Osselaer, EPS-2009-167-MKT, http://hdl.handle.net/1765/16012

Teixeira de Vasconcelos, M., *Agency Costs, Firm Value, and Corporate Investment*, Promoter(s): Prof.dr. P.G.J. Roosenboom, EPS-2012-265-F&A, http://hdl.handle.net/1765/37265

Tempelaar, M.P., *Organizing for Ambidexterity: Studies on the Pursuit of Exploration and Exploitation through Differentiation, Integration, Contextual and Individual Attributes,* Promoter(s): Prof.dr.ing. F.A.J. van den Bosch & Prof.dr. H.W. Volberda, EPS-2010-191-STR, http://hdl.handle.net/1765/18457

Tiwari, V., *Transition Process and Performance in IT Outsourcing: Evidence from a Field Study and Laboratory Experiments,* Promoter(s): Prof.dr.ir. H.W.G.M. van Heck & Prof.dr. P.H.M. Vervest, EPS-2010-201-LIS, http://hdl.handle.net/1765/19868

Tröster, C., *Nationality Heterogeneity and Interpersonal Relationships at Work*, Promoter(s): Prof.dr. D.L. van Knippenberg, EPS-2011-233-ORG, http://hdl.handle.net/1765/23298

Tsekouras, D., *No Pain No Gain: The Beneficial Role of Consumer Effort in Decision Making*, Promoter(s): Prof.dr.ir. B.G.C. Dellaert, EPS-2012-268-MKT, http://hdl.handle.net/1765/ 37542

Tzioti, S., *Let Me Give You a Piece of Advice: Empirical Papers about Advice Taking in Marketing,* Promoter(s): Prof.dr. S.M.J. van Osselaer & Prof.dr.ir. B. Wierenga, EPS-2010-211-MKT, hdl.handle.net/1765/21149

Vaccaro, I.G., *Management Innovation: Studies on the Role of Internal Change Agents,* Promoter(s): Prof.dr. F.A.J. van den Bosch & Prof.dr. H.W. Volberda, EPS-2010-212-STR, hdl.handle.net/1765/21150

Verheijen, H.J.J., *Vendor-Buyer Coordination in Supply Chains,* Promoter(s): Prof.dr.ir. J.A.E.E. van Nunen, EPS-2010-194-LIS, http://hdl.handle.net/1765/19594

Verwijmeren, P., *Empirical Essays on Debt, Equity, and Convertible Securities*, Promoter(s): Prof.dr. A. de Jong & Prof.dr. M.J.C.M. Verbeek, EPS-2009-154-F&A, http://hdl.handle.net/1765/14312

Vlam, A.J., *Customer First? The Relationship between Advisors and Consumers of Financial Products*, Promoter(s): Prof.dr. Ph.H.B.F. Franses, EPS-2011-250-MKT, http://hdl.handle.net/1765/30585

Waard, E.J. de, *Engaging Environmental Turbulence: Organizational Determinants for Repetitive Quick and Adequate Responses*, Promoter(s): Prof.dr. H.W. Volberda & Prof.dr. J. Soeters, EPS-2010-189-STR, http://hdl.handle.net/1765/18012

Wall, R.S., *Netscape: Cities and Global Corporate Networks,* Promoter(s): Prof.dr. G.A. van der Knaap, EPS-2009-169-ORG, http://hdl.handle.net/1765/16013

Waltman, L., *Computational and Game-Theoretic Approaches for Modeling Bounded Rationality*, Promoter(s): Prof.dr.ir. R. Dekker & Prof.dr.ir. U. Kaymak, EPS-2011-248-LIS, http://hdl.handle.net/1765/26564

Wang, Y., *Information Content of Mutual Fund Portfolio Disclosure*, Promoter(s): Prof.dr. M.J.C.M. Verbeek, EPS-2011-242-F&A, http://hdl.handle.net/1765/26066

Weerdt, N.P. van der, *Organizational Flexibility for Hypercompetitive Markets: Empirical Evidence of the Composition and Context Specificity of Dynamic Capabilities and Organization Design Parameters,* Promoter(s): Prof.dr. H.W. Volberda, EPS-2009-173-STR, http://hdl.handle.net/1765/16182

Wubben, M.J.J., *Social Functions of Emotions in Social Dilemmas*, Promoter(s): Prof.dr. D. De Cremer & Prof.dr. E. van Dijk, EPS-2009-187-ORG, http://hdl.handle.net/1765/18228

Xu, Y., *Empirical Essays on the Stock Returns, Risk Management, and Liquidity Creation of Banks*, Promoter(s): Prof.dr. M.J.C.M. Verbeek, EPS-2010-188-F&A, http://hdl.handle.net/1765/18125

Yang, J., *Towards the Restructuring and Co-ordination Mechanisms for the Architecture of Chinese Transport Logistics*, Promoter(s): Prof.dr. H.E. Harlambides, EPS-2009-157-LIS, http://hdl.handle.net/1765/14527

Zhang, D., *Essays in Executive Compensation*, Promoter(s): Prof.dr. I. Dittmann, EPS-2012-261-F&A, http://hdl.handle.net/1765/32344

Zhang, X., *Scheduling with Time Lags,* Promoter(s): Prof.dr. S.L. van de Velde, EPS-2010-206-LIS, http://hdl.handle.net/1765/19928

Zhou, H., *Knowledge, Entrepreneurship and Performance: Evidence from Country-level and Firm-level Studies,* Promoter(s): Prof.dr. A.R. Thurik & Prof.dr. L.M. Uhlaner, EPS-2010-207-ORG, http://hdl.handle.net/1765/20634

Zwan, P.W. van der, *The Entrepreneurial Process: An International Analysis of Entry and Exit*, Promoter(s): Prof.dr. A.R. Thurik & Prof.dr. P.J.F. Groenen, EPS-2011-234-ORG, http://hdl.handle.net/1765/23422

EFFICIENT MANAGEMENT OF COMPACT STORAGE SYSTEMS

   Warehouses are important nodes in supply chains. They decouple supply from demand in time, assortment, quantity, and space. By doing so, economies of scale can be achieved in transport, as warehouses allow to regroup transport flows leading to lower cost. Warehouses are particularly needed in densely populated areas, close to where demand is generated and where the labor is available. Warehouses require much space to realize economies of scale. Warehouse buildings are often quite large, more than 10,000 m2 built space is common. Unfortunately, in many of the urbanized areas, space for such large facilities has become short. In order to address this issue, enterprises are moving toward next generation storage systems, namely "three-dimensional (3D) compact storage systems". These systems are designed in order to save floor space and labor costs, and increase the reliability of the order picking process. 3D compact systems require less footprint compared to two-dimensional (2D) traditional systems. Several types of compact storage systems exist with different handling systems (like S/R machines, conveyors, shuttles, or elevators) taking care of the horizontal, vertical and depth movements. This dissertation focuses on new types of compact storage systems, in particular live-cube storage systems, where each unit load rests on a shuttle which can move in horizontal and depth directions, in cooperation with shuttles of other unit loads comparable to solving a Sam Loyd's sliding puzzle. One of the key performance measures for compact storage systems, which is also the focus of this dissertation, is response time. We analyze these systems at two decision-making levels. At the tactical (design) decision level, we focus on the rack-dimensioning problem aiming at short response times. At the operational decision level, we investigate storage assignment and retrieval sequencing problems to shorten the response time.

E R i M

   The Erasmus Research Institute of Management (ERIM) is the Research School (Onder-zoekschool) in the field of management of the Erasmus University Rotterdam. The founding participants of ERIM are the Rotterdam School of Management (RSM), and the Erasmus School of Economics (ESE). ERIM was founded in 1999 and is officially accredited by the Royal Netherlands Academy of Arts and Sciences (KNAW). The research undertaken by ERIM is focused on the management of the firm in its environment, its intra- and interfirm relations, and its business processes in their interdependent connections.

   The objective of ERIM is to carry out first rate research in management, and to offer an advanced doctoral programme in Research in Management. Within ERIM, over three hundred senior researchers and PhD candidates are active in the different research programmes. From a variety of academic backgrounds and expertises, the ERIM community is united in striving for excellence and working at the forefront of creating new business knowledge.

Erasmus Research Institute of Management - ERiM

ERIM PhD Series
Research in Management